



The University of
Nottingham

UNITED KINGDOM • CHINA • MALAYSIA

**Hierarchical Energy Management
System for Controlling Distributed
Energy Resources in a Community
Microgrid**

Mahmoud Elkazaz, BSc. , MSc.

Thesis submitted to the University of Nottingham for the degree of Doctoral of Philosophy

May 2021

Abstract

Community Energy Systems (CES) can be used to unlock the potential of Distributed Energy Resources (DERs), maximize the local consumption of Renewable Energy Resources (RES) at the lowest level of electricity grid, and offer collective benefits to the end-users involved. If different electricity producers and consumers (prosumers) are connected to form a CES, the economic behaviour of the system needs to be fully understood. Therefore, a high priority in this important area is the development of a novel design procedure which allows the comprehensive and analytical investigation of the CES using integrating control, management strategies, optimal planning and scheduling and sizing procedures.

This thesis presents novel centralized and decentralized hierarchical Community Energy Management Systems (CEMSs) which facilitate energy trading between prosumers in the CES by coordinating the operation of energy resources such as distributed or centralized battery energy storage and shiftable home appliances (located in each house) to achieve a further reduction in the daily household energy costs for each house, compared to being operated individually (i.e. not a part of the CES).

The hierarchical CEMS represents an optimization-based real-time interactive algorithm which uses a combination of a Peer-to-Peer (P2P) energy trading scheme and a hierarchical optimization and control framework. This hierarchical CEMS reduces energy costs for end-users, maximizes self-consumption of locally generated energy, reduces the dependency of the CES on the main electrical grid, and reshapes the consumption profile of the CES to reduce peak consumption, while taking into account the battery degradation costs and the use of Demand Side Management (DSM) techniques. The novel structure of the hierarchical CEMS enables the algorithm to deal with frequent changes in the system using a short sample time.

Detailed analysis of the performance of the household energy system using a real historic data of several UK households was performed to compare between end-users acting individually or as members of a CES. The performance of the household energy system is also assessed using different factors such as the overnight charging level, forecasting uncertainty, control sample time and tariff policies.

Finally, a novel sizing methodology (in terms of energy and power rating) for a Community Battery Energy Storage System (CBESS) to provide Community Bill Management service plus addition ancillary services for the electricity/energy markets is presented. This includes an economic study to investigate if addition revenue could be obtained if the CBESS is used to provide more than one service.

The results show the importance of participation in energy trading systems and the advantages of being a member of a CES, the need for using a centralized or a decentralized CEMS in coordination with energy trading systems to tackle the technical problems that may arise, and the importance of participation of the CES in the electricity market to achieve an appropriate return on investment.

List of publications extracted from this thesis

Journal papers:

- [1] **M. Elkazaz**, M. Sumner, D. Thomas, "A Hierarchical and Decentralized Energy Management System for Peer-to-Peer Energy Trading", Applied Energy journal, 2021, Vol. 291, 116766 [**Q1-IF 8.84- Published**].
- [2] **M. Elkazaz**, M. Sumner, E. Naghiyev, S. Pholboon, R. Davis, D. Thomas, "A Hierarchical Two-Stage Energy Management for a Home Microgrid Using Model Predictive and Real-Time Controllers", Applied Energy journal, 2020, Vol. 269, 115118. [**Q1-IF 8.84- Published**].
- [3] **M. Elkazaz**, M. Sumner, D. Thomas, "Energy management system for hybrid PV-wind-battery microgrid using convex programming, model predictive and rolling horizon predictive control with experimental validation", International Journal of Electrical Power & Energy Systems, Volume 115, 2020. [**Q1-IF 3.58- Published**].
- [4] **M. Elkazaz**, M. Sumner, E. Naghiyev, Z. Hua, D. Thomas, "Techno-Economic Sizing of a Community Battery to Provide Community Energy Billing and Additional Ancillary Services ", Sustainable Energy, Grids and Networks, 2021 [**Q1-IF 2.5 - Published**].
- [5] **M. Elkazaz**, M. Sumner, S. Pholboon, R. Davis, D. Thomas, "Performance Assessment of an Energy Management System for a Home Microgrid with PV Generation", Energies, 2020, 13, 3436. [**Q2-IF 2.7 - Published**].
- [6] **M. Elkazaz**, M. Sumner, D. Thomas, "Real-Time Energy Management for a Small Scale PV-Battery Microgrid: Modeling, Design, and Experimental Verification", Energies, 2019, 12(14), 2712. [**Q2-IF 2.7 - Published**].

Conference Papers:

- [1] **M. Elkazaz**, M. Sumner and D. Thomas, "Sizing Community Energy Storage Systems — Used for Bill Management compared to Use in Capacity and Firm Frequency Response Markets," 2020 IEEE Power & Energy Society Innovative Smart Grid Technologies Conference (ISGT), Washington DC, USA, 2020, pp. 1-6.

- [2] **M. Elkazaz**, M. Sumner, R. Davies, S. Pholboon and D. Thomas, "Optimization based Real-Time Home Energy Management in the Presence of Renewable Energy and Battery Energy Storage," IEEE 2019 International Conference on Smart Energy Systems and Technologies (SEST), Porto, Portugal, 2019, pp. 1-6.
- [3] **M. Elkazaz**, M. Sumner, S. Pholboon and D. Thomas, "Microgrid Energy Management Using a Two Stage Rolling Horizon Technique for Controlling an Energy Storage System," IEEE 2018 7th International Conference on Renewable Energy Research and Applications (ICRERA), Paris, 2018, pp. 324-329.
- [4] **M. Elkazaz**, M. Sumner and D. Thomas, "A Hierarchical Centralized Community Energy Management System Using a Model Predictive Controller," 2020 International Conference on Smart Grids and Energy Systems (SGES), Perth, Australia, 2020, pp. 801-806.
- [5] **M. Elkazaz**, M. Sumner, S. Pholboon and D. Thomas, "A Peer to Peer Energy Management System for Community Microgrids in The Presence of Renewable Energy and Storage Systems" The 10th International Conference on Power Electronics, Machines and Drives (PEMD), 2020.
- [6] Z. Hua, **M. Elkazaz**, M. Sumner and D. Thomas, "An Investigation of a Domestic Battery Energy Storage System, Focussing on Payback Time," 2020 International Conference on Smart Grids and Energy Systems (SGES), Perth, Australia, 2020, pp. 940-945.

Acknowledgement

I am beholden to a number of people, who supported me to carry out this work. First and foremost, my heartily profound thanks, gratitude and appreciation are to my supervisors: Prof. Mark Sumner and Prof. David Thomas for their encouragement, help and kind support. Their invaluable technical and editorial advice, suggestions, discussions and guidance were a real support to complete this research.

Very special thanks to my family for their patience, understanding and encouragement during the different phases of my work.

I would also like to thank all the colleges at the FlexElec laboratory that I had the pleasure to work with. In particular I would like to thank Dr. Seksak Pholboon, Dr. Eldar Naghiyev, and Dr. Richard Davies for all the help and support.

Acronyms and Nomenclature

Acronym	Description
AI	Artificial intelligence
ANN	Artificial Neural Networks
ANFIS	Adaptive neuro-fuzzy inference system
BESS	Battery energy storage system
CAN	Controller area network
CAPEX	Capital expenditure
CBESS	Community battery energy storage system
CES	Community energy system
CEBM	Community energy bill management
CEMS	Community energy management system
CM	Capacity market
CREST	Centre for renewable energy systems technology
DERs	Distributed energy resources
DFFR	Dynamic firm frequency response
DOD	Depth of discharge
DSM	Demand-side management
DSML	Demand-side management level
DUOS	Distribution use of system
E7 tariff	Economy 7 tariff
EM	Energy management
EMS	Energy management system
EV	Electric vehicle
GA	Genetic algorithm
GCP	Grid connection point
HBSS	Home battery storage system
HEM	Home energy management
HEMS	Home energy management system
IRR	Internal rate of return

MAPE	Mean average percentage error
MG	Microgrid
MILP	Mixed integer linear programming
MPC	Model predictive control
NPV	Net present value
OPEX	Operating expenditure
P2P	Peer-to-Peer
P2PEML	Peer-to-Peer energy management level
PV	Photovoltaic
RES	Renewable energy resources
RTC	Real-time controller
RTP tariff	Real-time pricing tariff
SC	Standing charge
SHEML	Single-home energy management level
SHR	Smart home rig
SOC	State of charge
STEF	Short term energy forecasting
TNUOS	Transmission network use of system
TOU tariff	Time of use tariff

Contents

Abstract	I
List of publications extracted from this thesis	III
Acknowledgement.....	V
Acronyms and Nomenclature	VI
Contents.....	VIII
List of Figures	XV
List of Tables	XX
Chapter 1: Introduction	1
1.1 Introduction	1
1.2 Motivation	2
1.3 Project aims and objectives.....	5
1.4 Thesis Contributions	6
1.5 Thesis organization	10
Chapter 2: Background and Literature Review	13
2.1 Introduction	13
2.2 Moving Towards Community Energy Systems	14
2.3 Battery Energy Storage Systems	16
2.4 Energy Management Systems and Control Framework Review	21

2.4.1	Energy Management Systems for communities.....	22
2.4.2	Home Energy Management Systems	28
2.4.3	Hierarchical Energy Management Systems	30
2.4.4	Centralized vs. Decentralized Hierarchical Energy Management System Frameworks	32
2.5	Sizing Community Energy Storage System.....	35
2.6	The Aim of this Thesis in the Context of the Literature Review	38
Chapter 3: Data Resources, Forecasting and Performance indices.....		41
3.1	Introduction	41
3.2	Household/Community Consumption Data.....	42
3.3	PV Generation Data	43
3.4	Shiftable Loads	45
3.5	The Electricity Tariff Schemes.....	45
3.6	Battery Energy Storage System.....	48
3.7	Forecasting Methods	49
3.8	Performance Indices and Metrics	52
3.9	Summary.....	55
Chapter 4: Home Energy Management System (HEMS)		56
4.1	Introduction	56
4.2	Case study.....	57
4.3	Real-Time Controller-based Single Layer HEMS.....	59
4.3.1	Operating Algorithm.....	59

4.3.2	Adjustment of the overnight charging level	62
4.3.3	Results	64
4.3.4	Limitations of the RTC based-single layer HEMS	71
4.4	Model Predictive Controller-based Single Layer HEMS	73
4.4.1	Model Predictive Control theory	73
4.4.2	Operating Algorithm	74
4.4.3	System Modeling and Constraints	75
4.4.3.1	HBSS Model	75
4.4.3.2	Battery degradation model	78
4.4.3.3	Shiftable appliances model	79
4.4.3.4	Imported/exported power model	81
4.4.3.5	System Constraints	83
4.4.4	Formulation of the Mixed Integer Linear Programming Optimization problem	83
4.4.5	Simulation procedure	85
4.4.6	Results	86
4.4.7	The effect of the sample time on the operation of MPC	89
4.4.8	The effect of forecasting uncertainties on the operation of MPC	93
4.4.9	The effect of changing purchasing tariff policy	96
4.4.10	Limitations of the MPC-based single layer HEMS	99
4.5	Hierarchical Two-Layer Home Energy Management System.....	101
4.5.1	Structure of the Two-Layer Home Energy Management System.....	102
4.5.1.1	The Upper Layer.....	102
4.5.1.2	The Lower Layer.....	104
4.5.2	Results	107
4.5.3	Limitations of the two-layer HEMS.....	113
4.6	Summary and Conclusion.....	113

Chapter 5: Distributed and Centralized Community Energy Management System....	119
5.1 Introduction	119
5.2 Architecture of the Community Energy System	120
5.3 Distributed Community Energy Management System.....	122
5.3.1 Structure of the Distributed Community Energy Management System.....	122
5.3.1.1 The Home Energy Management Level	122
5.3.1.2 The P2P Energy Management Level	124
5.3.1.3 The Selection level	125
5.3.2 Formulation of the joint optimization problem	127
5.3.3 Results and Discussion	131
5.3.4 Limitations of the Distributed Community Energy Management System	141
5.4 Centralized Community Energy Management System.....	141
5.4.1 Structure of the Centralized Community Energy Management System.....	142
5.4.1.1 The Community level	144
5.4.1.2 The Home Energy Management level	145
5.4.2 Formulation of the optimization problem	145
5.4.3 Results	148
5.4.4 Limitations of the Centralized CEMS	156
5.5 Summary and Conclusion.....	156
Chapter 6: A Hierarchical Community Energy Management System Using a Centralized Battery Store and Demand-Side Management.....	160
6.1 Introduction	160
6.2 Structure of the Hierarchical Community Energy Management System	161
6.2.1 Community Level	163

6.2.2	CBESS Control Level	163
6.2.3	Demand-Side Management Level	164
6.3	Formulation of the optimization problem	165
6.4	Experimental Test.....	169
6.4.1	Laboratory-based Microgrid Rig Architecture	169
6.4.2	Experimental procedure.....	172
6.4.3	Experimental results.....	173
6.5	Simulation Results	177
6.6	Sensitivity Analysis and Selection of Key Parameters	180
6.6.1	Load Shift Coefficient versus Grid Maximum Power Limit	180
6.6.2	Load Shift Coefficient versus Capacity of the Central CBESS	183
6.6.3	Changing the Size of the Battery's Power Converter	184
6.7	Summary and Conclusion.....	186
Chapter 7: Sizing of a Community Battery to Provide Energy Management Services		189
7.1	Introduction	189
7.2	The Architecture of the Community Energy System.....	190
7.3	The Techno-Economic Sizing Methodology	191
7.4	CBESS Sizing to Provide a CEBM Service	192
7.4.1	Formulating the Optimization Problem and its Constraints	193
7.4.2	Economic analysis	196
7.4.3	Results	199
7.4.4	The Effect of the CBESS size on the IRR while Providing a CEBM Service.....	200
7.5	CBESS for Capacity Market Service in the UK.....	202

7.5.1	Operating steps and annual revenue calculations	202
7.5.2	Results	204
7.5.3	The Effect of the CBESS Size on the IRR while Providing a CM Service.....	205
7.6	CBESS for Dynamic Firm Frequency Response Service in the UK	206
7.6.1	Operating algorithm and annual revenue calculations.....	208
7.6.2	Results	209
7.6.3	The effect of the CBESS size on the IRR while providing a DFFR service	211
7.7	CBESS Sizing to Provide Multiple Services	213
7.7.1	Providing multiple services with only one service per year	216
7.7.2	Providing multiple services with more than one service per day	218
7.8	Conclusion.....	220
Chapter 8: Overall Conclusions, Recommendations and Future Work		223
8.1	Overall Conclusion.....	223
8.2	Recommendations.....	227
8.3	Future work.....	228
Appendices.....		247
Appendix A - Details of the four houses used in this study.....		247
Appendix B -Load forecasting using Adaptive Neuro-Fuzzy Inference System (ANFIS) technique		248
Appendix C- Experimental Verification for the Hierarchical Two-Layer HEMS		253
Appendix D- The daily operation of the four houses using the distributed CEMS		257
Appendix E- The daily operation of the four houses using centralized CEMS.....		258

Appendix F- The LABVIEW program used in the experiment test of the Hierarchical centralized community energy management system	259
Appendix G - Calculations used to obtain the cumulative cash flow results from providing Community Bill Management service.....	262
Appendix H- Calculations used to obtain the cumulative cash flow results from providing Capacity Market service	263
Appendix I- Calculations used to obtain the cumulative cash flow results from providing Dynamic Firm Frequency Response service	264

List of Figures

Fig. 2. 1. Lithium-ion battery prices over 20 years	17
Fig. 2. 2. Services which can provided by the BESS to the three stakeholder groups.	18
Fig. 3. 1. Annual load profile for house no. 1 for one year	42
Fig. 3. 2. Daily load profile for house no. 1 on weekday- summer day- 24/06/2009.....	43
Fig. 3. 3. Annual PV generation for the 3.8 kW rooftop PV station	44
Fig. 3. 4. The daily PV generation profile for the 3.8 kW rooftop PV station on winter day- 18/01/2015.	44
Fig. 3. 5. Values of the purchasing tariff schemes used in this research	47
Fig. 3. 6. Examples of Tesla battery storage systems	49
Fig. 4. 1. Household electrical network.....	58
Fig. 4.2. The rule-based control algorithm of the RTC based-single layer HEMS.	61
Fig. 4. 3. The performance of the RTC based-single layer HEMS for two consecutive days using cases 1, 2 and 3 respectively	65
Fig. 4. 4. The performance of the RTC based-single layer HEMS for two consecutive days using cases 4, 5 and 6 respectively	68
Fig. 4. 5. Annual household energy costs and PV self-consumption ratio using different adjustment cases for the overnight charging level.....	69
Fig. 4. 6. The annual household energy costs and the annual PV self-consumption ratio using different overnight charging levels for the yearly optimized case (case 2).	70
Fig. 4. 7. The operating algorithm of the MPC-based single layer HEMS.	75

Fig. 4. 8. The operation of the household system, using the MPC-based single layer HEMS, for one day	87
Fig. 4. 9. (a) The requested and the actual operating time of the shiftable washing machine, (b) the actual household power consumption after the operation of the washing machine at 20:30.	89
Fig. 4. 10. The effect of using a 60 minute sample time versus a two minute sample time for MPC operation.....	90
Fig. 4. 11. Annual average MAPE values of the forecasted load demand and the forecasted PV generation profiles for the next day using the forecasting methods listed in chapter 3	94
Fig. 4. 12. The effect of forecasting uncertainty for both the load demand and PV generation on (a) the annual household energy cost increment ratio, and (b) the annual energy wastage ratio using TOU purchasing tariff scheme and a two minute sample time.....	95
Fig. 4. 13. The daily performance of the MPC using RTP, TOU, and E7 purchasing tariff scheme respectively	97
Fig. 4. 14. The annual household energy costs for the three purchasing tariff schemes.	98
Fig. 4. 15. The hierarchical scheme of the two-layer HEMS.	103
Fig. 4. 16. The rule-based control algorithm when using control mode 1 for the operation of the two layer HEMS.	105
Fig. 4. 17. The rule-based control algorithm when using control mode 2 for the operation of the two-layer HEMS.	106
Fig. 4. 18. The daily operation of the household system using the two-layer HEMS (Control mode 1).....	107

Fig. 4. 19. The daily operation of the household system, using the two-layer HEMS (Control mode 2) and RTP tariff	111
Fig. 5. 1. The architecture of the CES.	120
Fig. 5. 2. The hierarchical Distributed CEMS.	123
Fig. 5. 3. The optimal settings obtained from the distributed CEMS for the daily operation of the best pair (house no. 1 and house no. 2).....	135
Fig. 5. 4. The operation of the house no. 1 as a part of the community using distributed CEMS (P2P), versus being operated individually (single).....	138
Fig. 5. 5. Hierarchical centralized CEMS.....	143
Fig. 5. 6. The operation of the whole community for one day using the centralized CEMS	150
Fig. 5. 7. The optimal settings obtained for the daily operation of house no. 1 and house no. 2 using the centralized CEMS	152
Fig. 5. 8. Operation of house no. 1 as a part of the community using centralized CEMS, versus being individually (single operation).....	154
Fig. 6. 1. Architecture of the hierarchical central CES in the presence of central CBESS.	162
Fig. 6. 2. The rule-based algorithm used in the CBESS control level.....	165
Fig. 6. 3. MG used in the experiment at the University of Nottingham Laboratory.	170
Fig. 6. 4. Architecture of the MG at the University of Nottingham Laboratory.	171

Fig. 6. 5. Experimental results for the daily operation of the community MG using the hierarchical CEMS.....	174
Fig. 6. 6. Time required for measuring, computing and communicating by (a) the MPC level, (b) the central CBESS level, and (c) the DSM level.	176
Fig. 7. 1. Architecture of the CES.....	191
Fig. 7. 2. Effect of changing the CBESS size on the initial investment cost, operating cost, and the total project cost when used to provide CEBM services.	193
Fig. 7. 3. Cumulative cash flow over 20 years for using a 1000kWh/250kW CBESS to provide CEBM services.	200
Fig. 7. 4. Effect of changing the size of the CBESS (the rated capacity and the rated power) on the IRR while providing a CEBM service.	201
Fig. 7. 5. Cumulative cash flow over 20 years for using a 1000kWh/250kW CBESS to provide CM services.	205
Fig. 7. 6. Effect of changing the size of the CBESS (the rated capacity and the rated power) on the IRR over 20 years while providing a CM service.	206
Fig. 7. 7. Available frequency response services by the UK National Grid [214].	207
Fig. 7. 8. Dynamic Firm Frequency Response sub-services	208
Fig. 7. 9. Cumulative cash flow over 20 years for using a 1000kWh/250kW CBESS to provide DFFR services.	210
Fig. 7. 10. Effect of changing the size of the CBESS (the rated capacity and the rated power) on the IRR over a 20 year period while providing a DFFR service.	212

Fig. 7. 11. (a) Effect of changing the size of the CBESS (the rated capacity and the rated power) on the IRR while providing CEBM, CM and DFFR services over a 20 year period215

Fig. 7. 12. Selection criteria of the most profitable service in which the 1000 kWh/500 kW CBESS should participate in each year.217

List of Tables

Table 4. 1. Data and parameters of the household.....	58
Table 4. 2. The effect of using different sample times on the annual household energy costs, annual energy wastage ratio, and MPC Computation time.	91
Table 4. 3. The annual results for the household energy costs, energy wastage ratio, and the computation time using the two-layer HEMS versus using single layer HEMS.....	109
Table 4. 4. The annual results for household energy costs, energy wastage ratio, and the computation time using the two-layer HEMS (control mode 2) versus using single-layer HEMS, while considering the use of RTP tariff and ideal forecasting.	113
Table 5. 1. Data and parameters of the four houses.....	121
Table 5. 2. Results of the selection process of the promising paired houses using the P2P optimization process.	133
Table 5. 3. The daily household energy costs of the four houses when being operated as a part of CES using distributed CEMS (P2P operation), compared to being operated individually.....	133
Table 5. 4. The annual household energy costs of the four houses when being operated as a part of the community using the P2P operating algorithm, compared to being operated individually.....	139
Table 5. 5. The daily energy costs of the four houses when being operated as a part of the CES using the centralized CEMS, compared to being operated individually.	149

Table 5. 6. The annual household energy costs of the four houses when being operated as a part of the community using centralized CEMS, compared to being operated individually.....	155
Table 6. 1. Annual household energy costs of the four houses when being operated as a part of a community using the hierarchical CEMS, compared to operated individually....	178
Table 6. 2. The reduction percentage in the annual energy costs of the community using different load shift coefficients and different grid maximum power limit	181
Table 6. 3. The reduction percentage in the annual energy costs of the community using different load shift coefficients and different capacities of the central CBESS	184
Table 6. 4. The reduction percentage in the annual energy costs for the community using different sizes of the battery’s power converter while using 85% of the rated sized of the CBESS, load shift coefficient of 15%, and grid maximum power limit of 55%, compared to using the rated CBESS size, the rated grids’ power limit and zero load shift coefficient.	185
Table 7. 1. Values used in the simulation process for the participation of the CBESS in the CEBM, CM and DFFR services.....	198
Table 7. 2. Economic revenue over a 20 year period of the investment in a 1000 kWh/500 kW CBESS if used to provide any of the CEBM, CM, or DFFR services.	216
Table 7. 3. IRR of the investment in the 1000 kWh/500 kW CBESS if used to provide both DFFR and CEBM services in the same day, compared to being used to provide only DFFR or CEBM service for the whole day.	219

Chapter 1

Introduction

1.1 Introduction

The depletion of oil and gas resources alongside the rapid growth of renewable generation, and the move towards electrification of transport and heating has pushed researchers towards introducing a new vision for the transmission and distribution of electricity [1]. The future electrical grid should be smarter and more efficient. Centralized fossil-fired generation should be replaced by smaller localized renewable generation with zero carbon emissions wherever possible. The capability for integrating different kinds of Distributed Energy Resources (DERs), such as renewable energy and energy storage systems, will improve the sustainability and efficiency of the overall system. However, increasing the complexity and variability of generation sources usually comes with challenges for the overall system control and management, such as power balance, power quality, system stability and sustainability, as well as the cost implications [2]. The realization of future grids relies not only on good planning and design, but also on efficient and intelligent operation of the system's components making sure that practical considerations are respected.

By 2050, a legally binding target arising from the 2008 Climate Change Act states that greenhouse gas emissions should be reduced by at least 80% below the 1990 baseline [3]. Currently, the UK stands at a reduced emission of 43% compared to the 1990 baseline [4], most of which is contributed by the power sector. One of the most significant aspects to minimize our greenhouse gas emission footprint and address sustainable development is the transformation of the current structure of the electrical power grid. The Committee of Climate Change in the UK has put forward recommendations to the government, based on the learnings of the last decade, to support low-cost options such as onshore wind and PV

installations, and increased efficiency in buildings [5]. Besides the gradual transformation of energy to renewable sources, a further contribution towards increasing the security of supply and reducing the greenhouse gas emissions is expected to occur in the UK in the near future.

According to the National Grid's estimates of future energy scenarios in the UK, electricity annual demand could potentially reach 375 TWh/year by 2035/36 with residential energy consumption corresponding to about 33% of the total electricity demand [6]. Also, an analysis by the Department of Energy and Climate Change showed that the UK's electricity demand between 2015 and 2035 will increase by nearly 20% [7]. According to this analysis, renewable generation will represent 53% of the installed capacity and will provide 50% of the generated energy with wind and PV contributing almost 46% of the supply mix. Another mandatory target for European governments, driven by the Kyoto Protocol established in 1997, calls for 27% of the EU's overall community energy consumption to be produced from renewable sources by 2030 [8].

1.2 Motivation

Momentum is developing in the field of Community Energy Systems (CESs) [9] to understand its philosophy, define its challenges and try to introduce solutions to the technical and regulatory challenges. The term 'Community Energy' can be defined as any energy project that is wholly or partly owned or controlled by a community group [10]. A CES can be a group of neighbouring domestic dwellings, from which some of them have their own generation such as PV and battery storage systems and are able to trade the excess power in a hierarchical way: first, within the community, next with the Community Battery Energy Storage System (CBESS) and only finally export it to the main electricity grid [11]. When different prosumers are connected to form a CES, the behaviour of the system is unpredictable. Furthermore, when multiple resources are available for generation and storage

with different constraints on each resource, the management of these options to obtain the best economic behaviour of the system is not well understood. Therefore, the main motivations for this research are summarized as follows:

- **Increasing attention towards CESs and the pressing need for maximizing the consumption of Renewable Energy Resources (RES) at the lowest level of electricity grid.** In order to efficiently manage the available resources and load demand, a shift from individual energy users towards community energy operation should take place, whereby energy is generated, purchased, and managed collectively by a group of residential and/or commercial establishments. Although more than 300 communities in the UK have taken part in community energy initiatives in the last 5 years [10], the sector is still small and needs more innovation, compared to countries such as Denmark and Germany which have long since adopted a sustainable approach to combat the energy crisis [12].
- **Battery prices are reducing.** In recent years, Home Battery Storage Systems (HBSSs) in combination with solar PV energy production systems have become commercially available and more affordable [13]. The price of a Lithium-ion batteries pack has fallen 85% from 2010 to 2018, reaching an average of \$176/kWh [14]. Also, BloombergNEF's 2019 Battery Price Survey predicts that the prices will fall below \$100/kWh by 2024 [15]. These HBSS are presented as an ideal solution for households to minimize the cost of import energy through capturing and storing surplus locally generated renewable energy during the high generation periods and using it during periods of low or no renewable generation with high demand. Working together with communities and other partners can help understand how customers' energy bills can be reduced by capturing energy from PV panels and delaying its use with a storage device such as a battery.
- **The force of present-day energy tariff schemes,** Energy Services Companies (ESCOs), aided by the advent of affordable smart meters, can be a driving force in energy shifting

through HBSS by providing different energy tariff schemes. These tariff schemes incentivise battery charging during off-peak hours using cheap electricity tariffs (p/kWh), and by including an expensive peak-period, which encourages users to meet load demand from previously stored cheap electricity or surplus PV rather than from the grid. The HBSS in this case needs to be equipped with intelligent controllers that respond to the energy tariff signal to lower energy bills and increase the system's efficiency. From the other side, utility companies nowadays are lowering feed-in tariff rates to encourage microgeneration system owners to maximize the usage of the generated energy locally (in the lowest level of the electricity grid, i.e. end user level) [16].

- **Availability of second hand batteries.** The need to dispose of millions of Electric Vehicle (EV) batteries in the future has already led to the emergence of recycling and reuse industries [17]. These new industries are creating value pools that align profit with efficient resource use and enable the integration of renewable power into our grids. Lithium-ion batteries used in EVs, usually designed to be useful for a decade, degrade significantly during the first five years of operation. But even after 10 years of use, an EV battery can be reused in markets that need stationary energy storage requiring less frequent cycling. It is expected that by 2030, the rapid rise of EVs could supply a storage application market with a global value exceeding \$30 billion [18], since “second-life” batteries removed from EVs will be suitable to meet several storage applications.
- **Individual versus community behaviour.** There is a great need to gather, study and analyse real-life data from households belonging to real existing energy communities across the UK containing dispatchable energy resources, e.g. HBSS and control schemes to get a better understanding of whether the HBSSs can provide additional benefits for the electricity end-users if they operate as a community (i.e. aggregated energy sources) rather than being operated for individual uses. Furthermore, the importance of

behavioural change from electricity users needs to be addressed to derive maximum benefits from energy shifting.

1.3 Project aims and objectives

The aim of this project is to investigate how the cooperation between the prosumers in an energy community can help in reducing electricity costs for community members, i.e. in particular how the control of HBSSs and household shiftable loads by central community energy controllers provide greater benefits compared to being controlled as an individual household. As part of this work, additional aims were to understand how a Community Battery Energy Storage System (CBESS) (i.e. aggregated or central) could be sized to meet community energy needs, and how it should be controlled to exploit local generation and current tariffs schemes.

In order to achieve these aims, a number of key objectives had to be developed and tested:

- 1) To create a novel optimization-based real-time interactive Energy Management System (EMS) which can economically exploit HBSSs and Demand-Side Management (DSM) techniques to minimize daily energy costs and maximize the local-consumption of RES for the household level.
- 2) To investigate the effect of different factors such as the overnight charging level, forecasting uncertainty, control sample time and tariff policy on the household energy system and systems efficiency. This investigation can be considered an aid for decision makers to select an appropriate controller for each PV-battery system.
- 3) To develop a novel Hierarchical centralized and decentralized Community Energy Management System (CEMS) which facilitates the energy trading between prosumers in the CES by coordinating the operation of the distributed HBSSs and any appropriate shiftable home appliances (located in each house) either in a centralized or a decentralized

way. The shiftable loads such as washing machines, dishwashers, dryers, charging of EVs, etc. can be shifted in time to avoid operating them at high-peak tariff periods. This shifting process helps in reducing the imported energy from the main electricity grid at high prices. These loads are shifted to operate at the low tariff periods or at the period when there is a surplus PV generation.

- 4) To analyse economically how the networked operation of houses in the local community energy systems can provide extra benefit compared to single house operation.
- 5) To develop a hierarchical community energy management algorithm which ensures better performance, provides greater flexibility and needs lower computational times when applied to large communities (with a large number of houses). It is also important to investigate how the networked operation of houses in the community reduces the need for an overly large CBESS, leaves more transformer and feeder capacity and achieves a further reduction in the annual energy costs for the community.
- 6) To develop a novel methodology for sizing a CBESS to achieve the aforementioned objectives and at the same time, provide additional ancillary services for grid operators.

1.4 Thesis Contributions

The main contributions of this work are:

- **The first contribution** is the development of a novel design procedure which allows the comprehensive and analytical investigation of the energy systems considered in this thesis using integrated control and management strategies and optimal planning, scheduling and sizing procedures. A comprehensive, analytical and detailed design and development procedure can function as a catalyst that transforms technological innovation to systems operation and can potentially help the wider spread of CES through

valuable information, guidance and a suitable framework for the actual project/system implementation.

- **The second contribution** is the development of a novel hierarchical EMS which represents an optimization-based real-time interactive algorithm. The hierarchical EMS combines the use of an optimization layer and a control layer and highlights the differences between the ideal scheme and the real operation with a user-interactive control algorithm. This hierarchical EMS reduces energy costs for end-users and energy wastage, maximizes self-consumption of locally generated energy, reduces the dependency of the CES on the main electrical grid, and reshapes the consumption profile of the CES to reduce peak consumption, while taking into account the battery degradation costs and the use of DSM techniques. The novel structure of the hierarchical EMS enables the algorithm to deal with frequent changes in the system by using a short sample time. This short sample time enables the proposed EMS to observe and respond to the small changes in load and generation throughout the day.
- **The third contribution is in** introducing novel hierarchical centralized and decentralized CEMSs which facilitate the energy trading between prosumers in the CES by coordinating the operation of the distributed HBSSs and the shiftable home appliances (located in each house) within the CES either in a centralized or decentralized way to achieve a further reduction in the daily household energy costs for each house, compared to being operated individually (not being a part of the CES). The proposed CEMSs use a combination of a Peer-to-Peer (P2P) energy trading scheme and a hierarchical control and management framework. The novelty of the proposed centralized and decentralized hierarchical EMSs relies on combining the following points: (a) system coordination of both the day-ahead scheduling and the actual operating stages to appropriately consider the influence of uncertainty in RES and consumption, (b) the use of a HBSS control in

both the day-ahead and the actual operation stages, (c) the system links the multiple controllable household appliances with the real-time control of the HBSS to maximize the self-consumption of the RES and compensates for uncertainties, (d) the approaches are computationally efficient.

- **The fourth contribution** of this thesis is the analytical and detailed analysis of the performance of the household energy system using real historic data from several UK households while considering different factors such as the overnight charging level, forecasting uncertainty, control sample time and tariff policies. This analysis of the performance also includes an assessment of the system's financial sensitivity to these parameters.
- **The fifth contribution** of this work is based on the capability of making comparisons when the end-users act individually and when they are members of a CES as this study provides design and management recommendations for the CES level and the single house applications. The comparisons between the single house application and the CES can concern: the financial benefits of people working together rather than individually, the difference on the household incomes when different management algorithms are implemented, etc. As the CES concept has not yet flourished, this study could be evidence of its potential feasibility and profitability, and could influence the spread of CESs across the UK.
- **The final contribution** of this study is providing a novel sizing methodology (in terms of energy and power rating) for a CBESS to provide a Community Energy Bill Management (CEBM) service considering the economic performance over a 20 year lifetime. Also, a sizing methodology is developed to accurately optimize the size of the CBESS to be able to provide additional ancillary services for the electricity/energy markets. This includes an investigation of the potential revenue achieved when the

CBESS participates in National Grid services such as the Capacity Market (CM) and Dynamic Firm Frequency Response (DFFR) market.

- **List of publications extracted from this thesis**

Journal papers:

- [1] **M. Elkazaz**, M. Sumner, D. Thomas, "A Hierarchical and Decentralized Energy Management System for Peer-to-Peer Energy Trading", Applied Energy journal, 2021, Vol. 291, 116766 [**Q1-IF 8.84- Published**].
- [2] **M. Elkazaz**, M. Sumner, E. Naghiyev, S. Pholboon, R. Davis, D. Thomas, "A Hierarchical Two-Stage Energy Management for a Home Microgrid Using Model Predictive and Real-Time Controllers", Applied Energy journal, 2020, Vol. 269, 115118. [**Q1-IF 8.84- Published**].
- [3] **M. Elkazaz**, M. Sumner, D. Thomas, "Energy management system for hybrid PV-wind-battery microgrid using convex programming, model predictive and rolling horizon predictive control with experimental validation", International Journal of Electrical Power & Energy Systems, Volume 115, 2020. [**Q1-IF 3.58- Published**].
- [4] **M. Elkazaz**, M. Sumner, E. Naghiyev, Z. Hua, D. Thomas, "Techno-Economic Sizing of a Community Battery to Provide Community Energy Billing and Additional Ancillary Services ", Sustainable Energy, Grids and Networks, 2021 [**Q1-IF 2.5 - Published**].
- [5] **M. Elkazaz**, M. Sumner, S. Pholboon, R. Davis, D. Thomas, "Performance Assessment of an Energy Management System for a Home Microgrid with PV Generation", Energies, 2020, 13, 3436. [**Q2-IF 2.7 - Published**].
- [6] **M. Elkazaz**, M. Sumner, D. Thomas, "Real-Time Energy Management for a Small Scale PV-Battery Microgrid: Modeling, Design, and Experimental Verification", Energies, 2019, 12(14), 2712. [**Q2-IF 2.7 - Published**].

Conference Papers:

- [7] **M. Elkazaz**, M. Sumner and D. Thomas, "Sizing Community Energy Storage Systems — Used for Bill Management compared to Use in Capacity and Firm Frequency Response Markets," 2020 IEEE Power & Energy Society Innovative Smart Grid Technologies Conference (ISGT), Washington DC, USA, 2020, pp. 1-6.

- [8] **M. Elkazaz**, M. Sumner, R. Davies, S. Pholboon and D. Thomas, "Optimization based Real-Time Home Energy Management in the Presence of Renewable Energy and Battery Energy Storage," IEEE 2019 International Conference on Smart Energy Systems and Technologies (SEST), Porto, Portugal, 2019, pp. 1-6.
- [9] **M. Elkazaz**, M. Sumner, S. Pholboon and D. Thomas, "Microgrid Energy Management Using a Two Stage Rolling Horizon Technique for Controlling an Energy Storage System," IEEE 2018 7th International Conference on Renewable Energy Research and Applications (ICRERA), Paris, 2018, pp. 324-329.
- [10] **M. Elkazaz**, M. Sumner and D. Thomas, "A Hierarchical Centralized Community Energy Management System Using a Model Predictive Controller," 2020 International Conference on Smart Grids and Energy Systems (SGES), Perth, Australia, 2020, pp. 801-806.
- [11] **M. Elkazaz**, M. Sumner, S. Pholboon and D. Thomas, "A Peer to Peer Energy Management System for Community Microgrids in The Presence of Renewable Energy and Storage Systems" The 10th International Conference on Power Electronics, Machines and Drives (PEMD), 2020.
- [12] Z. Hua, **M. Elkazaz**, M. Sumner and D. Thomas, "An Investigation of a Domestic Battery Energy Storage System, Focussing on Payback Time," 2020 International Conference on Smart Grids and Energy Systems (SGES), Perth, Australia, 2020, pp. 940-945.

1.5 Thesis organization

In addition to chapter one, which is the introduction of this thesis, including motivation, objectives and the main contributions of this research, the thesis comprises another seven chapters that are organized as follows:

CHAPTER 2 presents a literature review, which addresses the need for hierarchical energy management systems in modern CESs and discusses previous works and solutions provided to address the barriers for integration of RES and the energy storage systems. This chapter presents also the available community management systems and control techniques and a review for CBESS sizing techniques.

In **CHAPTER 3**, the data resources that have been used in this thesis are introduced, including the annual real life household load consumption profiles, annual PV generation profiles, energy tariff schemes, and data for real battery storage. This chapter introduces also the next day load demand and PV generation forecasting methods, i.e. these methods are required in this thesis, and the indices used to assess the performance of the proposed EMS.

A novel optimization-based real-time interactive hierarchical HEMS has been created in **CHAPTER 4** to economically exploit the HBSS and the DSM techniques for the household level. It was important to examine first the operation of the proposed hierarchical HEMS on the household level to be used as a cornerstone for making a comparison between when end-users act individually and when they are members of a CES. Also, **CHAPTER 4** examines the performance of the household energy system using Real-Time Control (RTC) and Model Predictive Control (MPC)-based management strategies and investigates the effect of different factors on the systems' performance.

Simulation results for the operation of the system are presented in this chapter to consider the effect of different seasons (i.e. all four seasons), different overnight charging level, different tariff schemes on the annual energy costs, annual PV self-consumption ratio and annual energy saving. In addition, experimental test has been implemented to ensure that the proposed hierarchical two-layer HEMS can be applied for a real system without any difficulties. This chapter practically addresses objectives (1) and (2) listed in section 1.3.

CHAPTER 5 introduces two types of Community Energy Management Systems : (a) distributed CEMS, and (b) centralized CEMS, which facilitates the energy trading between prosumers in the CES by coordinating the operation of distributed HBSSs and shiftable home appliances (located in each house) within the CES either in a centralized or decentralized way. Both CEMSs achieve a further reduction in the daily household energy costs for each house,

compared to being operated individually. This chapter demonstrates that additional financial benefits could be achieved for members working together within the CES instead of individually. This chapter practically addresses objectives (3) and (4) listed in section 1.3.

In **CHAPTER 6**, the hierarchical centralized CEMS, presented in chapter 5, has been developed to provide greater flexibility, ensure that the optimization process is faster and more robust to communications, and be applied to larger communities (with a large number of houses). Furthermore, this chapter investigates how the networked operation of houses in the community reduces the need for overly large CBESS, lowers investment costs, and leaves more transformer and feeder capacity besides achieving a reduction in the annual energy costs for the community. Also in **CHAPTER 6**, the complete hierarchical CEMS has been implemented experimentally in real-time, using an emulation MG at the University of Nottingham FlexElec Laboratory, to ensure that the proposed CEMS can be applied in a real system. This chapter practically addresses objective (5) listed in section 1.3.

CHAPTER 7 provide a novel methodology for sizing a CBESS (in terms of energy and power rating) to either provide CEBM service, or to participate in the ancillary services considering the economic performance over a 20-year lifetime. This includes an investigation of the potential revenue when the CBESS participates in the UK National Grid to provide CM or DFFR services. This chapter practically addresses objective (6) listed in section 1.3.

All the conclusions made from different stages of this project in addition to the recommendations and the future work are presented in **CHAPTER 8**.

Chapter 2

Background and Literature Review

2.1 Introduction

The current trend in Community Energy Systems (CES) is oriented towards encouraging local consumption of the energy generated by local RES instead of exporting surplus electrical energy to the main grid [10], [19]. This trend has received more attention following: (a) the appearance of the CES concept, in which the cooperation between householders as part of a wider community can achieve many benefits including a reduction in the exported power to the main electricity grid, a reduction in the daily operating costs of the CES, and a reduction in the need for massive Battery Energy Storage Systems (BESSs), (b) the recent rapid growth of utility-scale photovoltaic (PV) deployment, and (c) the reducing costs of energy storage technologies have stimulated interest in combining PV with energy storage to provide dispatchable energy (i.e., energy on demand) and reliable capacity (i.e., grid stability) [1].

This chapter introduces the concept of CES and the importance of moving towards CES in Section 2.2. Section 2.3 emphasises the importance of the BESSs as a central tool for enabling the effective integration of the RES and unlocking the benefits of the local generation through future smart grids. Section 2.4 introduces a review for the available energy management systems and control framework for today's smart grids. This includes the hierarchical EMS for community system and for household level (as the cellular structure of the community system). Section 2.5 presents a literature survey of different sizing techniques for the CBESS and the participation of the CBESS in both capacity and energy markets. Finally, the areas to be covered by this thesis will be presented in the content of gaps seen in the literature survey.

2.2 Moving Towards Community Energy Systems

CES are seen as an auspicious topic which can unlock the potential of DERs and at the same time promote specific locations and offer collective benefits to the end-users involved. The term ‘Community Energy’ can be defined as any energy project that is wholly or partly owned or controlled by a community group [10], [9]. A CES can be a group of neighbouring domestic dwellings, from which some of them have their own generation such as PV and battery storage systems and are able to trade the excess power in a hierarchical way: first, within the community, next with the CBESSs and only finally export it to the main electricity grid [11]. The CES can be connected to the main electricity grid (grid-connected) or can be stand-alone (islanded system). Also, it can be connected or not to a CBESS and/or to central RES such as stand-alone PV solar stations, community wind turbines, communal hydro, heat pumps, etc. The CES considered in this study, can be described as a group of local neighbour dwellings which are acting either as consumers or as prosumers (i.e. prosumers are the dwellings capable of producing energy through, for example, PV solar systems installed on their roof and using innovative equipment and technologies such as BESSs, EVs and DSM techniques to interact with the energy market through different pricing mechanisms [20]) and they are targeting to reduce their electricity cost by optimally using the power flow within the community.

CESs have grown gradually in the UK over the past two decades since the UK government has encouraged individuals to work as a group. More than 300 community led projects have been sprouting across the UK, within the last 5 years, as a significant proportion of consumers expressed desire to get involved in a CES [10]. Moreover, a survey from the UK’s Energy and Climate Change department at 2014 showed that more than 50% of citizens expressed their interest in getting involved in CESs if they could potentially reduce their electricity cost [21]. A recent UK study forecasted that by 2050, 44% of the UK energy will

be generated by prosumers [22], and the energy generated by CES will provide 0.3-1.4% of the UK's electricity consumption [23].

Since 2010, the UK government has been encouraging households to install PV panels by offering the Feed-in Tariff (FIT) scheme. This has resulted in significant growth of PV installations at a domestic level from a 7MW peak power in 2010 to over 13248 MW in mid 2019 [24]. This rapid growth of the PV generation has encouraged a lot of people towards maximizing local consumption of PV energy instead it being injected into the grid [25]. Due to this reason, the concept of CES is gaining more and more ground within the energy market as multiple prosumers produce domestic electricity [26].

The advantages of being part of a CES are being more likely to be allowed access to a Time of Use (TOU) tariff, can benefit from economies of scale for energy storage and control equipment, increase community self-consumption and also will have a chance to be a part of community Microgrids (MGs) [27]. Besides achieving benefits for community's residents, these communities offer the opportunity to adjust main electricity network demand/generation through the use of RES such as PV panels and wind turbines, DSM techniques, and battery energy storage [28].

Although at high-level such CES sound straightforward, in practice there are a number of issues to be solved [11]. These include selecting a proper Energy Management (EM) and control strategy, sizing issues, the system layout, scalability and adaptability [29]. Selecting a proper EM strategy which guides the power flow between the decentralized generation units, the main electricity power grid, and the consumption loads is critical for a smooth and proper operation of CES [30]. In this thesis, multiple points will be studied for the CES examined such as: (a) selecting a proper EMS for the CES, (b) optimizing the power circulation (by controlling and monitoring the energy and power flow), (c) managing energy (balancing local

supply and demand instantly with the ‘cheaper’ available energy source), (d) collective trading among community members, (e) optimizing and coordinate the operation of the distributed BESSs within the community, and (f) determining the optimal size for the central community energy storage to provide bill management and capacity/energy markets services.

2.3 Battery Energy Storage Systems

The storage systems will play a key role in the management of future electric grids [31]. BESSs are rising as a central tool for enabling the effective integration of the RES and unlocking the benefits of the local generation [32]. Most grid operators are encouraging the use of BESS to address the increasing peak demand for electrical energy and congestion in the electricity grid [33]. The importance of merging the BESS into the electricity grid system in the UK started from 2006, when the Microgeneration Strategy from the Department of Energy and Climate Change in the UK was released. The Microgeneration Strategy promoted the importance of micro-generation as a realistic alternative energy generation source for end-user, communities, MGs and small businesses [21]. Afterwards, the Low Carbon Building Programme which started in 2006 provided grant support for the investment in the renewable technologies including PV generation, solar hot water, micro-wind, micro-generation, and heat pumps [34]. Also, during this period, the first Feed-In-Tariff scheme was launched in the UK in 2010, paying the microgeneration system owners for their renewable generation exported to the power grid [35]. These led to the increase in capacity of PV generation in the electric grid, i.e. the PV installed capacity in the UK reached 13 GW by 2019 [24].

Furthermore, lower feed-in tariff rates are offered nowadays to encourage the microgeneration system owners to maximize the usage of the generated energy in the lowest level of the electricity grid (i.e. end users level) [16]. Domestic BESSs are considered as the best solution to incorporate small roof mounted PV energy systems to the electrical network,

at the low voltage level especially, and a number of studies [13], [36] revolve around the economic viability of such solutions.

Encouraging stakeholders to maximize the usage of locally generated energy in the lowest level of the electricity grid (especially behind the meter level) has been widely accepted as the prices of the BESSs have fallen dramatically in the recent years. In December 2018, BloombergNEF published the results of its ninth Battery Price Survey. The annual price survey has become an important benchmark in the industry and the fall in prices has been nothing short of remarkable. The price of a Lithium-ion batteries pack fell 85% from 2010 to 2018, reaching an average of \$176/kWh [14], see Fig. 2. 1. From the observed historical values, BloombergNEF calculated a learning rate of around 18%. This means that for every doubling of cumulative volume, they observe an 18% reduction in price. Based on this observation, and the battery demand forecast, they expect the price of an average battery pack to be around \$94/kWh by 2024 and \$62/kWh by 2030. Also, BloombergNEF’s 2020 Battery Price Survey observed that the Battery Pack Prices Cited Below \$100/kWh for the First Time in 2020 [15]. Also BloombergNEF predicts that prices will fall below \$100/kWh by 2030 [15].

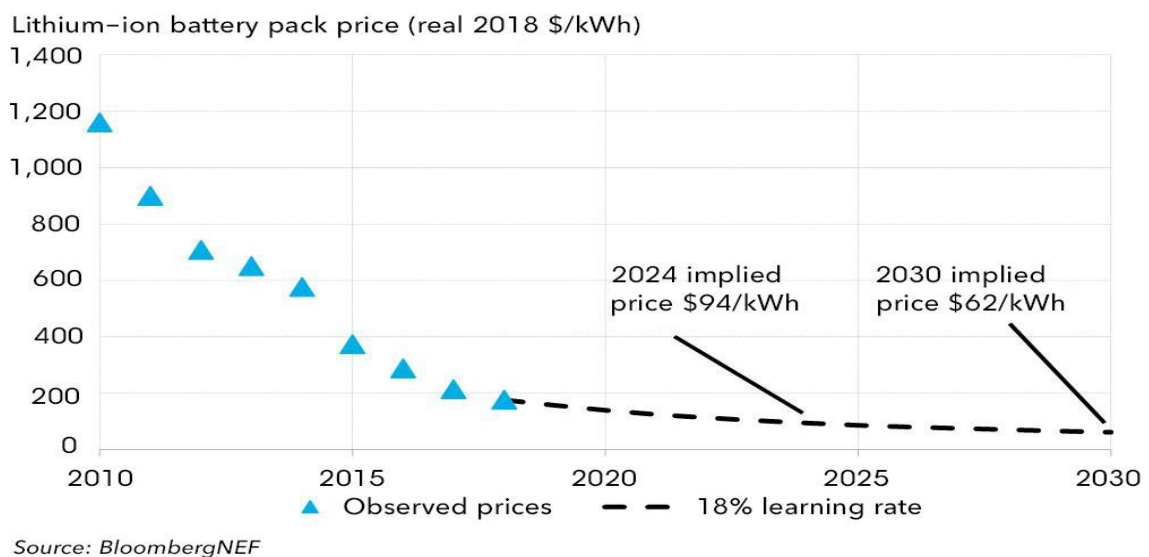
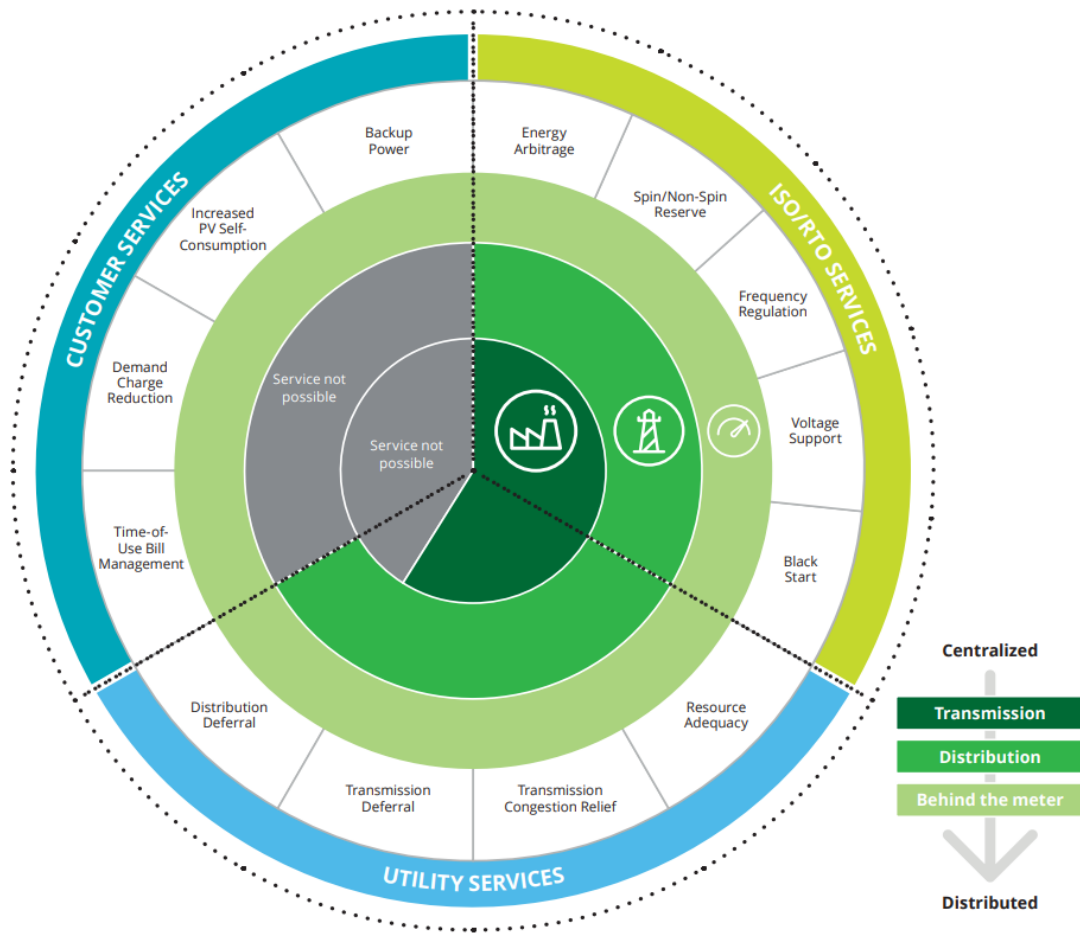


Fig. 2. 1. Lithium-ion battery prices over 20 years [14].

The massive decrease in the battery costs encourages people who are concerned with the energy market to increase their investment in BESS for either behind the meter uses or at grid scale [37]. In 2015, there were 27 installed energy storage projects in the UK, with a total capacity of around 33 GWh as detailed in [38]. This number is increasing every year due to the fast decrease in the BESS costs. Also, it is worth noting that the value proposition of the investment in the BESS changes significantly depending on where it is installed in the electricity grid, i.e. the BESS can be deployed at either Transmission Level, Distribution Level, or Behind the Meter Level of the electricity grid to provide value to the electricity system [39]. Fig. 2. 2. shows the 13 services that can be provided by the BESS to the three stakeholder groups [38].



Source: Mandel and Morris, "The Economics of Battery Storage", Rocky Mountain Institute

11

Fig. 2. 2. Services which can provided by the BESS to the three stakeholder groups [38].

The trend for CES towards encouraging local consumption of energy generated from RES at the lowest levels of the grid surplus is receiving increasing attention with the development of domestic energy storage technologies (i.e. HBSS) (<20kWh) as well as large scale BESSs (>1MWh) and techniques for incorporating these battery systems into CES architectures [40]. Furthermore, over recent years, small HBSS in combination with solar PV systems have become commercially available and more affordable. Currently commercially available HBSS provided by a number of well-known manufacturers (e.g. LGChem [41], Tesla [42], MOXIXA [43]) are promoted as being the ideal combination to have with residential solar PV generation systems in order to maximize PV self-consumption by storing the excess energy during the high generation periods and using it during the night or during the peak tariff periods [44]. In this way, the HBSS owners can save money on their energy bills and minimize their dependence on the energy provider utility. Moreover, through proper management and control techniques, appropriate modelling and suitable energy pricing and policies, HBSSs can unlock their full capabilities and maximize their returns (financial, environmental and social) [45].

Aggregation of behind-the-meter batteries started to be developed recently as an emerging topic for CES [46]. Virtual aggregation of distributed HBSS allowing CESs to provide grid services and compete in energy markets. The HBSSs have been aggregated to facilitate the integration of the RES, optimize system operation, minimize utility bills, improve power quality, maintain system stability and provide capacity and energy market services [47]. The importance of HBSS aggregation is summarized as follows:

- **Facilitate integration of the RES:** One of the major drawbacks of RES is the fluctuation of power output, which results in a variable power source for the MG [48]. Using HBSS can compensate for this fluctuation by storing the extra energy during surplus times and use it later on during a shortage time to provide a stable and reliable power source.

Integration of the RES with the HBSS in the lowest energy level means fewer and cheaper electricity transmission and distribution system upgrades are required.

- **Optimize system's operation:** Aggregated HBSSs can be used to optimize the operation of the CES by playing the role of compensator in coordination with the other microsources [49], providing a smooth transient in case of microsource failure or outage and compensating for the peak times to provide economic saving. Also, aggregated HBSSs technologies could decrease the need to invest in new conventional generation capacity, resulting in financial savings and reduced emissions especially from electricity generation.
- **Improve power quality:** Aggregated HBSSs play an important role in improving the power quality of the system [50]. They are used to inject/absorb active and reactive power to maintain certain output specifications for customers especially in transient cases. Also, they can be used to compensate energy shortage to avoid voltage and frequency fluctuations.
- **Maintain system stability:** System stability is a very important issue. Keeping the voltage and frequency within limits during transient and transfer times has become a real challenge. In recent years, aggregated HBSSs play an important role in providing a smooth transition between grid-connected and islanded mode for the MGs, compensating for energy shortage and sudden outage or failure of any unit [51].
- **An effective economic solution for CES.** The aggregated HBSSs are now one of the key players in achieving an economical solution for CES [52]. BESS can economically store energy for hours or days by purchasing power from the grid at off peak times to use it later on to feed the load at peak demand. The aggregated BHSSs can participate in capacity and energy markets, providing extra financial revenue for the system operators.

2.4 Energy Management Systems and Control Framework Review

EM is one of the most important fields that appears associated with the idea of MGs and automated control of the electric grids [53]. A lot of research focuses on this as a promising field with plenty of challenges which require investigation and solutions. The literature provides many definitions of EM. Based on the definitions given in [54], an EMS is a control software which can optimally manage (i.e. optimal means determining the best possible operating scenario for the system to maximize the revenue from the system components and minimize the operating costs) the power flow among different decentralized generation units, consumption loads and system components (such as BESS) by monitoring the operation of the energy system and by following a certain control structure.

The cooperation between the EMS and the optimization techniques can have a great influence on the operation of CESs to achieve the desired power quality at minimum costs. Various optimization techniques have been used by researchers to optimize and solve the EM properly in MGs [55], and to optimize the performance and the operation of any part of the MG. Examples include generation control such as maximum power point tracking control systems, distribution control, optimization of power quality, cost control, decision making algorithms and control of power dispatch.

This research focuses on EM problems and tries to find solutions that can help to enhance the performance of our electric grid. To do this, we should first make a survey of what has been accomplished in this area and the latest research results. Some examples of state of art in control and management will be listed. Also, attention will be paid to the connections between optimization and control theory as many researchers are focusing on applying optimization algorithms to optimal control [56].

2.4.1 Energy Management Systems for communities

The EMS is required to achieve interactive operation of the RES and the other community components (such as decentralized generation units and BESS) [57]. Management and control strategies for MG have been studied in literature (e.g. [58], [59]). Most EMSs reported in the literature are based on optimal controllers [58]. Loads and renewable energy resources must be predicted in advance, making the effectiveness of optimal approaches dependent mainly on the accuracy of the prediction models. Computation times can also be significantly longer for these optimal EMS, particularly when using many constraints and shorter sample times [60]. Also, researchers used optimization based Model Predictive Control (MPC) as a promising type for EM studies to tackle the problem of uncertainty with the forecasted energy consumption/generated, and keep updating certain parameters [61].

When the behaviour of the system cannot be captured by the prediction models or cannot be implemented in real-time, controllers with real-time decision-making capabilities are used. These can be based on instantaneous power measurements and “rule-based” control rather than prediction profiles as in [62], [63], [64]. For this type of EMS, the aim is usually to reduce energy costs by efficient use of a battery and maximizing the use of renewable energy to satisfy local demand, while maintaining the reliability of the electrical system [62]. They do not require a detailed model of the system and can respond quickly to changes in the system. However, they are not guaranteed to be optimal and can lead to inefficient energy usage.

Study [65] developed a control strategy for optimal use of a BESS in order to integrate the dispatchable intermittent renewable energy sources. The study considered a rule-based control scheme which suggested as the solution to the optimal control problem defined without violating any BESS operating constraints such as SOC limits, charging/discharging

current limits and lifetime. It is observed that the battery was not charged overnight. Furthermore, it was found that a large battery size - about 15-20% of the solar PV power (in MW) - is needed in order to have an effective hourly dispatch. Using a rule-base controller in [65], which controls the battery taking into account the current situation only without estimating the changes in the system through the next time periods, may lead to inaccurate results.

On the other hand, there is much research focusing on the management of MGs using optimal controllers, particularly in optimizing system behaviour [66], [67]. Daniel & Erlon [68] present a mathematical model for the EM problem of a MG by means of a Mixed Integer Linear Programming (MILP) approach. The objective is to minimize the operating costs subject to economical and technical constraints over a planning horizon through determining a generation and a controllable load demand policy. The model has wind generators, PV generators, micro-turbines, fuel cells and a battery bank all forming the MG and connected to the main grid. [69] introduces a power demand scheduling policy that minimizes the MG operational costs over a fixed time horizon. The cost is a convex function of total instantaneous power consumption. Numerical results demonstrate the benefit of the proposed approaches compared to the default policy of serving demands.

In [70], Carlos et al. introduce an iterative algorithm that manages energy flows to obtain the minimum energy cost for a smart energy system based on the availability of resources, prices and the expected demand. Eight scenarios of an energy system under different conditions have been simulated. However, the forecasting uncertainties of renewable sources, tariff prices and the expected demand are not considered. The authors in [71] described a technology platform for energy monitoring within a community energy scheme. The monitoring scheme helps to optimize the multifaceted system and to provide feedback to residents to visualize and control their energy consumption and encourage reductions in

demand. However, the effect of delaying or loss of data on the EM of the community system has not been studied. [72] present an energy management strategy based on a low complexity Fuzzy Logic Control for grid power profile smoothing of a residential grid-connected MG including RES and BESS. Although the proposed strategy shows good results, the effect of the proposed EMS on the battery lifetime and battery state of health has not been considered.

In [73], the authors developed an algorithm that decomposes and solves the online problem in a distributed manner and proves that the distributed online solution is asymptotically optimal. The problem is shown to be convex and can be solved with a centralized online algorithm. The authors in [74] applied an MPC approach to the problem of efficiently optimizing MG operation while satisfying a time-varying request and operating constraints. The results show a significant improvement in the quality of the solution and the computational burden. However, the effect of battery's degradation and the effect of using a shorter sample time on the computation costs have not been considered in this study.

In [75], Mohsen et al. introduce two dispatch-optimizers for a centralized EMS as a universal tool. Scheduling the unit commitment and economic dispatch of MG units has been achieved using an improved real-coded Genetic Algorithm (GA) and an enhanced MILP based method. This approach achieved good results, but the uncertainty of both generation and demand was not addressed, and the effect of inaccurate forecasting for load demand and generation on the EM results was not considered. The authors in [76] present a Smart Hybrid Energy System aiming towards significantly reducing the amount of fuel needed and minimizing transportation logistics while meeting camp energy demands. All components are controlled by an energy management system that prioritizes output and switches between different power generators, ensuring operation at optimum efficiencies. However forecasting uncertainties, energy trading capabilities and variable energy prices have not been considered in this research.

In [77], a day-ahead Economic Load Dispatch was performed for a MG with intermittent DERs and a BESS; it was adjusted every 15 minutes to ensure that the voltages were kept within acceptable limits, trying to maintain the dispatch of units as close as possible to the predetermined values. Akomeno et al. [78] analyse the economic and environmental impacts of distributed energy systems at the neighbourhood scale in comparison to conventional centralized energy generation systems by creating a MILP model for the design of a distributed energy system. This design aims to meet the electricity and heating demands of a cluster of commercial and residential buildings while minimizing annual investment and operating cost.

The authors in [79] focus on the development of optimization-based scheduling strategies for the coordination of MGs. Simultaneous management of energy demand and energy production are used within a reactive scheduling approach to solve the problem of uncertainty associated with generation and consumption. The proposed approach has proven the advantages of managing the energy demand by optimizing the management of the microgrid, which allows enhancing its flexibility and autonomy. However, the effect of the DSM techniques and the overnight charging level of the battery have not been examined. Martin et al. [80] presented an EMS prototype for an isolated renewable-based MG which consists of two stages: a deterministic management model is formulated in the first stage followed by integration into a rolling horizon control strategy. The advantage in this proposal considers the management of energy sources in addition to including the possibility of flexible timing of energy consumptions (i.e. DSM) by modelling shiftable and non-shiftable loads. However, battery degradation costs and modelling of weather or demand uncertainties are not presented in this research.

The authors in [81] applied a real-time EMS for smart grids which minimized the energy cost and carbon dioxide emissions of the smart grid while maximizing the power of the

available RES using a GA technique. Minimizing carbon dioxide emissions of a smart grid is achieved by maximizing the dependence on the energy storage technology, Demand-side management techniques, renewable energy resources (PV/Wind) and Fuel cells, while in the same time minimizing the dependence on the conventional generation units (i.e. diesel generation units) and microturbines.

In [82], the design and experimental validation of an adaptable EMS implemented in an online scheme is presented. In this case, the author aims to minimize the operating costs and the load disconnections by proposing an architecture that allows the interaction of forecasting, measurement and optimization modules, in which a generic generation-side mathematical problem is modelled. Study [83] investigated the power flow management for grid-connected PV-BESS. The objective of the study was to promote intensive penetration of PV production into the power grid by proposing peak shaving services at the lowest cost. The structure of a power supervisor based on an optimal predictive power scheduling algorithm was proposed and the optimization problem was performed by dynamic programming. The particularity of the study considers the ‘day-ahead’ approach of power management. However, the ESS sizing was not considered in the study, as it only focused on the system management for a pre-defined battery capacity and power converter rating.

Study [84] proposed an optimal battery management model for stationary applications connected at distribution grids. The purpose of the management model was to maximize the utilization of the distributed renewable energy resources, preventing situations of reverse power flow in the distribution transformer. The management model requires predictions of residual distribution grid demand and electricity curves. Although this study presented good results, the BESS SOC limits had not been considered, the BESS was used only for storing excess power of the wind turbine and did not charge overnight, the sample resolution of the dataset used was one hour and no sizing considered.

[85] investigated the battery control policy which minimizes the total discounted cost by extensive numerical experiments. By using a real time pricing which varied every one hour, the financial returns offered by different battery sizes were quantified. However, it was found that the cost is the same for both the communal battery and individual ones. This can be explained by the fact that the prices were the same for all the end-users and thus, irrespective to the size of the battery, the behaviour of the optimal policy is primarily influenced by the common pricing signal, eliminating the potential benefits of pooling. In addition, the battery was not charged overnight.

From this section, it is observed that the EMS is important to achieve interactive operation of the DERs and the other MG components. Most EMSs reported in the literature are based on optimal controllers due to their effectiveness, compared to the rule-based controllers. However, the effectiveness of optimal approaches dependent mainly on the accuracy of the prediction models because the loads and energy resources must be predicted in advance. It is observed that the uncertainty in RES and load demand in addition to long computation times, particularly when using many constraints and shorter sample times, and the need for an accurate model for the system are the main barriers for using optimization-based EMS.

Limited studies have focused on presenting EMS, for energy communities, which introduce cost effective solutions, i.e. effective for both the community residents and the grid operators, in addition of considering the special characteristics of the energy communities such as sharp changes in demand profiles over a short period [11] and the aggregation nature of DERs. Furthermore, it is observed that the development of battery control policies/techniques in coordination with the current tariff policies is important to ensure an effective EMS for energy communities.

2.4.2 Home Energy Management Systems

With the increasing penetration of domestic solar panels and the impending move to EVs and the electrification of heating, there is a real need to understand how Home Battery Storage Systems (HBSS), Home Energy Management Systems (HEMS), Demand Side Management (DSM) techniques and real-time-pricing schemes are considered to help defer the grid reinforcement costs [86], [87].

HEMS is a technology platform comprised of both hardware and software that allows the user to monitor energy usage and production and to economically manage/control the use of energy within a household [87]. A HEMS can reduce household utility bills and ensure an overall reduction in peak energy demand as demonstrated in [88]. A HEMS can also play an important role in encouraging local consumption of the energy generated by RES (such as PV systems) in homes rather than exporting the surplus electric energy to the main distribution grid, this can be achieved by moving loads in time (i.e. DSM) or by incorporating HBSS into homes to capture surplus PV or off-peak (low cost) grid energy and use it at peak times [89].

In recent years, there has been much research into exploiting energy market real-time-pricing schemes to develop and enhance the use of HEMS to manage home electricity consumption economically [90]. For example, an optimal energy management model to minimize fuel and battery wear costs is presented in [91], which finds the optimal power flow, taking into account the available PV power. The authors in [92] introduced a smart HEMS to support the grid. The system uses RES such as PV as an alternate power source which helps in reducing the dependence of the home on the grid.

Many researchers have focused on optimizing home energy management (HEM) using approaches such as optimal controllers or real-time decision-making controllers. Using optimal controllers, researchers presented HEM problem as an optimization problem with

multiple variables and multiple constraints, where the variables are both discrete and continuous [93], [94]. Different optimization/control approaches such as MILP, MPC and dynamic programming have been used to optimize the HEM [95], [96].

The authors in [97] used MILP optimization to determine the optimal operation of a home with a HBSS, a PV system, and an EV with a “vehicle to home” option. Several test cases were examined considering the impacts of PV and battery availability as well as shiftable load controllability. However, the effect of battery’s degradation and the capability of engaging in a community management system has not been studied. To study dynamic pricing and peak power limiting based DSM strategy, a MILP model of the HEM structure was established in [94] with an EV and an energy storage system. Although the authors claim using a 15-minute sampling time for the optimization process, all the results obtained are of one hour sample time. A MILP model of a HEMS, as well as an Artificial Neural Network (ANN) for forecasting of residential loads, is described in [98]. However, the EMS and the ANN forecasting model used a sample time of one hour for the forecasted load profiles of the home: this is a very crude indication of the home’s load profile as these profiles vary at a much faster rate.

[99] developed an optimization strategy to efficiently consider price-based demand response techniques for HEMS, a control framework was constructed for the management of various home appliances, considered given the price information, in order to support DSM using an EMS in a single smart home. Another energy management scheme which integrates RES, electrical battery storage, and vehicle to grid was proposed in [100]. The authors claim accurate results, but run the algorithm only once every day and use a time slot of one hour for management which leads to inaccurate results due to the uncertainty of RES and load demand.

However, many researchers have focused on optimizing HEM using optimal controllers, most of them (e.g. [101], [102]) have narrowly considered the economic effects of the HBSS operation under forecasting uncertainties and different sample time resolutions or have assumed no degradation costs for battery operation [103], [104]. The impact of using load shifting capabilities is not well addressed in [105] and the impact of using intelligent overnight battery charging techniques is not considered in [85]. Furthermore, it is observed that no research has considered, in the same study, the effect of control and management strategies, the tariffs schemes, the overnight charging level techniques, and the effect of uncertainties and battery degradation on the performance of the HEMS.

2.4.3 Hierarchical Energy Management Systems

The hierarchical control scheme was proposed for different disciplines such as manufacturing, power systems, process systems, and for large complex systems [106]. Dedicated control algorithms are placed in different layers with necessary information/signal exchange between them, but with decoupled behaviours [107]. The use of a hierarchical control scheme has been proposed for MGs to manage objectives in different time scales, technical fields, and with different priorities [108].

The authors in [109] focused on introducing a two-stage stochastic EMS to minimize the operational cost of a MG with various types of distributed energy resources. A scenario reduction method based on MILP optimization was used to obtain the set of reduced scenarios. The authors took the uncertainty of price, load, wind speed and solar radiation into account to obtain more realistic results. Use of a scenario reduction method based on MILP optimization is often used offline, which restricts the use of this methodology for real-time applications especially when dealing with DSM.

[110] discusses the community power flow concept in designing a hierarchical control structure for optimal dispatch of DERs within different levels of the distribution network and optimizing the operation of flexible resources at the community cell level. A bottom-up approach is taken to control the hierarchical structure which contains the cell community level, the cluster of community cells intermediate level and the distribution network clusters top level. The simulation results show the effectiveness of the load and storage dispatch in meeting the objective function of maintaining community's power flow below a pre-specified threshold. Similarly, in [111], a two-stage demand response scheduling was proposed to integrate renewable energy into power systems.

An EMS based on a two-stage rolling horizon strategy for a renewable-based MG is proposed in [112] and implemented for a MG in which a MILP optimization problem based on forecasting is solved for each decision step. Furthermore, based on a DSM technique, the EMS provides online set points for each generation unit and signals for consumers. The authors used economic load dispatch with a sample time of 5 minutes in the rolling horizon stage. However, the coordination between the operation of the two stages which have different priorities, different sample time has not well presented in this study. In addition, the daily operation of the system has not been presented and discussed.

In [113], the benefits of optimal management of the BESS via multi-stage optimization are estimated to be a 5% reduction in the operating cost. However, this result strongly depends on the particular size and efficiency of the BESS considered, and the cost characteristics of the MG generators.

It is observed, from this section, that most multi-stage EMSs suffer from the mis-coordination between the operation of different layers which have different priorities, different sample time, and specially when considering real-time application such as DSM.

Furthermore, it is observed that most studies have used datasets (with long sample time) which result in errors in the system design and sizing, as sharp and rapid power changes were not taken into account. This requires the introduction of a novel EMS which integrates both the planning layer and the real-time operation to enable the whole EMS to operate accurately and efficiently.

2.4.4 Centralized vs. Decentralized Hierarchical Energy Management System Frameworks

The hierarchical EMS control can broadly be divided into central and decentral (distributed). Centralized supervisory systems are hierarchical systems, where the central controller resides on the highest level of the hierarchy pyramid and acts as an overall system manager. The central controller is responsible for both the technical system operation (i.e. satisfying instant load demand) and the economic system operation (i.e. choosing the cheapest available energy source) [114]. The lower level controllers gather operational data and send them to the main controller which after processing them, takes the final decisions and sends out operation commands to the lower controllers. The main advantage of the centralized energy system control is the minimization of conflicts during system operation since everything is decided at the highest level. However, as the system becomes bigger in size and more complex, the server's computational power needs to be on par with the calculation effort in order to perform the management and control tasks in real time. This can lead to the need for bigger and more powerful master servers able to handle the huge amount of data and communications, which will result to higher costs and inflexible systems. Moreover, any change of the configuration of the energy system (newly installed DERs, more loads, topology, etc.) will result in updates of the network design, and in many occasions, re-designing the whole system from the beginning [115]. Also, it is hard to maintain data security in this system.

On the other hand, the decentralized architecture is based on a network of autonomous local controllers, each responsible for a component of the system, without depending on a single main controller [116]. Each system component must be equipped with a local control unit, and the controllers can communicate and negotiate directly between each other to achieve goals, without a central influence. One of the main advantages of the decentralized control is the high reliability of the system; in case of a failure or a maintenance break, the rest of the system can still operate and the failure does not affect the whole system performance [117]. Despite its benefits, switching from centralized to decentralized control, requires new infrastructures to be installed, which results to increased costs for upgrading the existing control, management and communication facilities.

In [118], a two-level architecture for the DERs management for multiple MGs using multi-agent systems with BESSs is developed. The developed mechanism allows the pool members such as generation agents, load agents, auction agents, and storage agents to participate in the energy market. The authors claim the agent-based management is economically effective in resource management among multiple microgrids. However, the uncertainty of load demand, RES generation and energy market prices have not been considered in this study. Colson and Nehrir [119] proposed also a decentralized control architecture for MGs for ongoing investigations in real-time and agent-based decision-making, demonstrating the viability and capability of decentralized agent-based control for MGs.

A convex programming problem was formulated to minimize electricity payment costs and the optimization process executing time under real-time pricing for a multi-agent system in [120]. However, even though accurate results have been obtained, the algorithm still depends heavily on the communication between different agents to determine the optimal

home appliances settings, the accuracy of the obtained results will be affected badly if data is delayed or lost.

Study [121] focused on high peak powers, which can be reasonably buffered by battery systems. Two exemplary battery storage systems including power electronics were presented. The main outcome was that the battery size impacts on the function of power converter and its operational power, and hence on the overall ESS operation and system efficiency. However, the application of this study included wind farms and EVs applications, and not focusing on the domestic PV sector. Hence, it was not taken into consideration control and management nor TOU tariffs and overnight charging. Furthermore, despite that utilities are generally curious to test the capabilities of the behind-the-meter BESS aggregation, there is still a huge amount of uncertainty around this newly proposed technology [122], such as complicated networks of independent system operators, difficulties in defining a suitable management and control for the BESS which suits both the end-users and the utilities.

[123] which provides a review on decentralized energy planning and focusing on modelling, concluded that there is little existing literature on the feasibility of decentralized energy planning at district level. Also, it highlighted that applications of models for matching the projected energy demand with energy sources at the decentralized level are limited.

It is observed from this literature that the coordination between the day-ahead scheduling and the actual operation stages while considering the influence of uncertainty in RES and consumption is not well studied. Furthermore, it is observed that the computational effectiveness of most listed approaches in the literature is not measured and analysed, which limits the application of these approaches to the small applications only. In addition, limited studies have considered the comparison between the centralized and the decentralized CEMS to quantify the techno-economic benefits that could be obtained in each case.

2.5 Sizing Community Energy Storage System

The complete design of an energy system must include the proper sizing of the system components in addition to the system control and management. The sizing of the electric BESSs components (in terms of energy and power rating) is among the most challenging and important calculations of the community/MG design [124]. In recent years there has been much research into sizing approaches for BESSs. Several algorithms for optimal BESS placement and sizing are proposed in the literature (e.g. [125], [126]).

Community storage can encompass a wide range of storage technologies, including batteries, thermal storage, as well as EVs. Meanwhile, many algorithms were applied for optimal sizing of BESSs. [126] proposed an improved evolutionary algorithm to achieve lowest cost and developing corrective strategies. In [127], an optimal sizing algorithm is presented for the pumped hydro storage in a stand-alone Wind-PV hybrid renewable energy system. [128] explored a large-scale battery application which provides ancillary services in an electricity market, while [129] presents the design and testing of a community BESS composed of used EV or plug-in hybrid EV battery packs.

According to [130], efficient and economic component sizing should meet all the system requirements with the minimum operating cost. A grid-connected system with PV and battery were presented in [131], analyzing the relationship between electricity market and the battery capacity. Moreover, the optimal sizing of a BESS, determined in [132], compared some possible combinations of systems with PV, wind turbine and battery capacity. Focusing on economic benefit of accurate battery storage's sizing, [133] presented the technical feasibility and the economic profitability of a system with PV and battery energy storage. With a TOU tariff, [134] investigated the impact of the demand response on BESS optimal sizing. Also,

[135] examined various technologies for BESS and assesses their economic viability and impacts on power systems.

In view of the loss of the power supply probability and economical costs, a different approach for optimizing battery sizing is researched [136]. An analytical approach to determine the size of a backup storage unit in a power system, considering reliability requirements is proposed in [137]. In [138] a sensitivity analysis of a variety of BESS sizes and technologies in an isolated wind-diesel MG is performed, in which BESS is used to improve the penetration of renewable energy sources to MGs.

[139] presented a method to determine battery capacity for a grid-connected PV storage system with respect the best scheduling of the battery. Optimization of the energy dispatch schedule and the battery sizing were decoupled. Two time-varying pricing structures were used as pricing scenarios and the battery was fully charged every night during the off-peak tariff. This study did not use any intelligent overnight charging control algorithm, simply the battery was fully charged overnight. Furthermore, the study ignored the probability of partition of the battery in the energy/capacity market services.

The authors in [140] designed a method to obtain the optimum BESS operation for a community system. The method evaluated the optimum performance, levelized cost, the internal rate of return and the levelized value of suitable community BESS technologies, and the optimum community BESS size was calculated as a function of the community size. As two different scenarios were considered (2020 and zero carbon year), the renewable penetration within the community was fixed and for the former was taken to be 7.6% and for the latter 57%. Hence, the PV sizing/penetration within the community was not investigated and the power converter rating limits were not taken into account into the sizing analysis. Furthermore, the community battery was fully charged overnight for all the examined sizes

without considering intelligent charging techniques. Moreover, this study did not apply excess energy trading within the community members and any power flow management.

Efficient BESS are essential for providing ancillary services, and lithium is chosen material, considering safety, lifespan and reliability [141]. Connecting the BESS to the main electricity grid, where it can participate in joint Energy and Ancillary Services was mentioned in [142]. [143] pointed out that BESS can discharge at peak hours to get benefits, based on price arbitrage. Also, they predicted high revenues from spot market price arbitrage. With the integration of renewables, the potential and significance of participation of BESS in electricity market is strengthened in [144].

Also, the authors in [145] mentioned the participation of the BESSs in the Frequency Response Service, as a part of energy market services. Furthermore, based on the studies of the Germany and Netherlands Markets, [146] pointed out the role of profitability and feasibility of BESSs in frequency response services, and mentioned that the power and capacity of energy storage is significant for ensuring contract services. [147] investigated the sizing of battery storage based on power and energy for frequency response. In [135], a virtual energy storage system is modelled by combining demand response of domestic refrigerators and flywheels, which have a significant cost reduction. [126] highlights that although there is a vast body of research on MG management, little attention has been paid to the influence of BESS sizing, especially the BESS for “behind-the-meter” application, on both operation management and economical revenue of energy systems

From this section, it is concluded that each study has limitations on either the system modelling (battery and/or power converter representation) or on the system design (management and control were not considered while applying the sizing methodology) or have not examined the partition of the BESS in different electricity markets in great detail or

have ignored important factors such as energy prices increase rate, inflation rate and return on investment over a long term. Furthermore, the provision of providing multiple services for both the capacity and the energy market simultaneously is not well analyzed. In addition, it is observed that sizing of the BESS to participate in community bill management and to provide additional ancillary service while taking into account battery operation and degradation costs, return on investment over a long term and sizing reliability in face of the frequent changes of market prices, is rarely addressed in the literature.

2.6 The Aim of this Thesis in the Context of the Literature

Review

At present, the operation and management of a smart community still face some challenges that should be addressed if efficient energy management is required. [148] stated that a disconnection remains in the literature across highly technical (engineering based), social (social science based) and applied (planning and policy based) studies and little attempt has yet been made to incorporate new communities into system planning. Therefore, this project aims to investigate how the cooperation between the prosumers in an energy community can help in reducing electricity costs for community members.

There is a gap in knowledge for designing an EMS for a CES derived from the analysis of real load and generation data of the electricity prosumers and the community. The current literature is found to include many studies which examine hybrid systems under invalid assumptions concerning the BESS model (idealistic models which can lead to significant misinformation for the system financial analysis) and/or imported datasets (with a long sample time) which result in errors in the system design and sizing, as sharp and rapid power changes are not taken into account. Unlike large interconnected systems or islands, the electrical load profiles of the CES suffer from sharp changes over a short period [11], i.e. the

aggregation or smoothing effect is reduced and the uncertainty is increased as the size of the CES gets smaller. For this reason, EMS used for CES should be characterized by having a short sampling time to observe and respond to small changes in the load and generation throughout the day [31, 149]. In addition, the literature review shows that a deep understanding is still required to investigate the effect of different factors such as sample time, tariff values, different seasons, centralized versus decentralized frameworks, and battery overnight charging level on the performance of the EMS for CES. This investigation can be considered an aid for decision-makers to select an appropriate controller for each PV-battery system.

This thesis, therefore, attempts to fill this gap in the literature by developing a novel hierarchical centralized and decentralized CEMS which facilitates the energy trading between prosumers in the CES by coordinating the operation of the distributed HBSSs and the shiftable home appliances in a hierarchical way. Traditionally, in order to suggest the most suitable energy flow and best operation of an energy system, a two-level sequential approach was applied; firstly the process was designed and then the control was deployed for its efficient operation and management [150]. The aforementioned stages (design and management /control) should not be seen individually, but be integrated into one mathematical framework which would provide the most beneficial operation and smooth function of each energy system. In this context, this thesis aims to create a novel optimization-based real-time interactive EMS which can economically exploit local generation, BESSs, current tariffs schemes and DSM techniques to minimize the daily energy costs and to maximize the local-consumption of RES for both the household and the local community energy levels. The EMS should overcome the drawbacks of the EMS listed in literature and integrates both the day-ahead energy scheduling layer and the real-time operation and load shifting to enable the EMS to operate more accurately and efficiently. In addition, this thesis is deriving all presented

analysis and design based only on real energy data (consumption and generation) collected from different prosumers across the UK. Experimental verification is required to ensure that these EMS operate efficiently in real environment in the presence of a real-time interactive system.

In the context of designing CES and battery sizing, it is important for the CBESS, either as a single central battery or aggregated from small batteries, to be able to provide different services for the community and also participate in the electricity market. The BESS located at both household level and local community energy level can be aggregated to provide extra benefits and be more appealing as an investment. Therefore, the operation of aggregated HBSS as a single controllable unit is important [11], [151]. This requires the introduction of a novel EMS which integrates both the planning layer and the real-time operation layer to ensure efficient operation. [152] pointed out that more effective installations with less waste in terms of investment costs and energy usage during the life of the BESSs will be achieved by having a deep understanding of the specifications and requirements of the overall energy system. Therefore, a reliable sizing design requires building in a proper designing analysis to understand how a community BESS (i.e. aggregated or central) could be sized to meet community energy needs and in addition, provide ancillary services for the electricity/energy markets considering the economic performance over a long lifetime. This includes an investigation of the potential revenue achieved when the community BESS participates in different electricity markets and provides more than one service simultaneously.

Chapter 3

Data Resources, Forecasting and Performance indices

3.1 Introduction

This chapter introduces the data resources that have been used in this thesis, the forecasting methods used for next day load demand and PV generation forecasting, and the performance indices.

The data used in this thesis is actual data from different resources for annual household load consumption profiles, PV generation profiles, energy tariff schemes, and the HBSSs. The data for household consumption is real life, high resolution data measured from UK based houses. The annual PV generation profiles used are measured from a UK based PV generation station. The data for the community system is obtained by adding the data of multiple houses together. For tariff schemes, data resources from UK based energy companies has been used. Also, data resources from the UK National Grid for the participation of the BESS in capacity and energy markets has been used in this thesis.

These data resources have been used to test and examine the performance of the energy management systems (EMS) introduced in this thesis. It is important to examine the proposed EMS using real data through experimental tests or simulation process to obtain a real indication for the performance of the EMS and analyse the effect of different variables on the daily and the annual performance of the EMS.

3.2 Household/Community Consumption Data

The data used for household consumption is real, high resolution data measured from 22 houses based in Milton Keynes, UK for one year (from 01/01/2009 until 31/12/2009) and of one minute resolution [153]. Examples of the annual load profile as well as the daily load profile for one of the houses (i.e. house no. 1) are shown in Fig. 3. 1. and Fig. 3. 2. respectively. It is observed from the figure that the period between 14th and 28th of August has a reduced load consumption due to the absence of residents from the house for a holiday, i.e. only the mandatory home appliances, e.g. the fridge, are in operation. Additional details such as the appliances used in houses and the number of residences in each house, and details of heating system and thermal insulation of each house have been presented in appendix A. Finally, the consumption profiles for multiple houses are added directly together to create the overall consumption profile of the community.

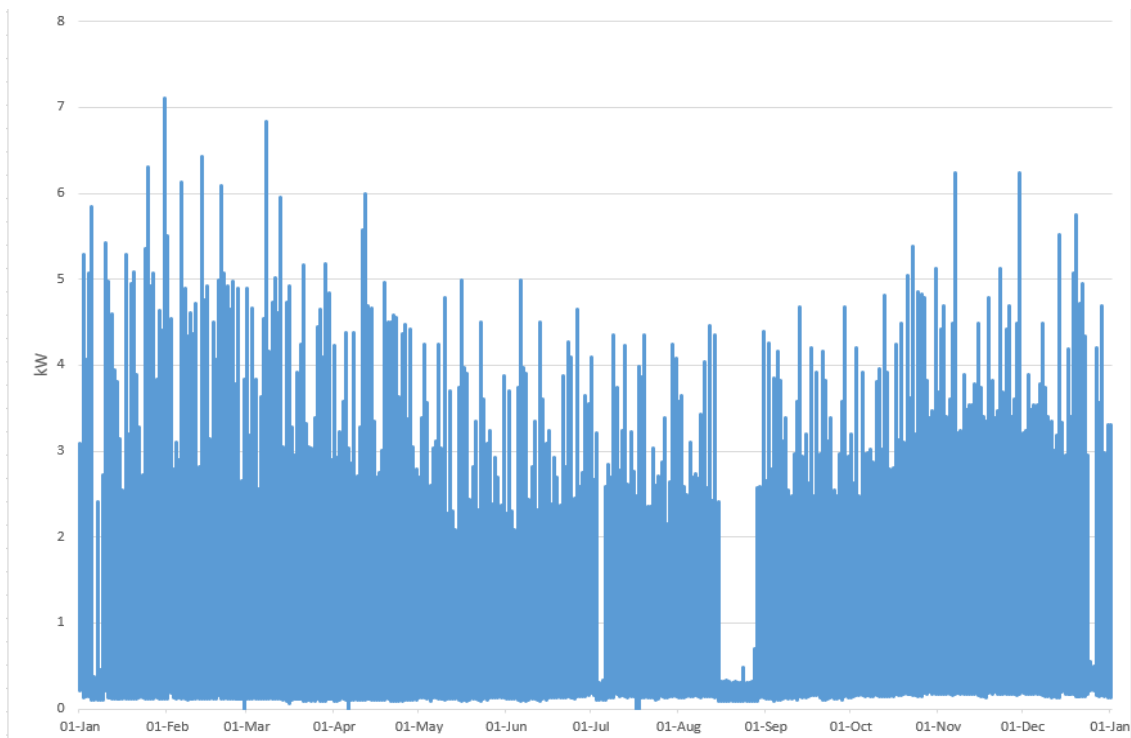


Fig. 3. 1. Annual load profile for house no. 1 for one year (from 01/01/2009 until 31/12/2009)

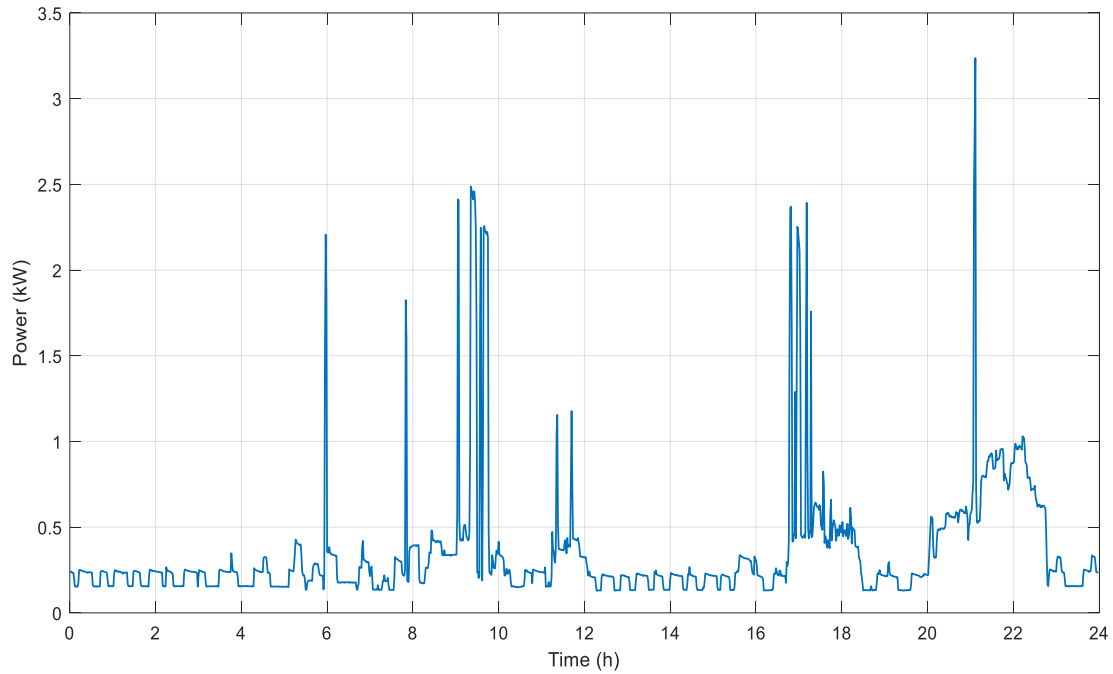


Fig. 3. 2. Daily load profile for house no. 1 on weekday- summer day- 24/06/2009

3.3 PV Generation Data

Real data available at the PVOutput.org website [154] for the generation profile of a 3.8 kW rooftop PV system located in Nottingham, UK has been used as the primary source of data for the PV generation profiles. The data is for one year (from 01/01/2015 until 31/12/2015) and of one minute resolution. The PV generation profiles are then scaled up or down to be equivalent to the PV generation assumption for each house or for the community. The PVOutput.org website is a free organisation for sharing, comparing and monitoring live solar PV data. The system uses 20 Schüco 190 MS 05 panels of 190 W peak each and an SMA Sunny Boy SB 4000 TL inverter with a rated power of 4 kW and maximum efficiency of 97%. Fig. 3. 3. shows the annual PV generation profile for the 3.8 kW rooftop PV station. Also, Fig. 3. 4. shows an example for the daily PV generation profile of this PV station.

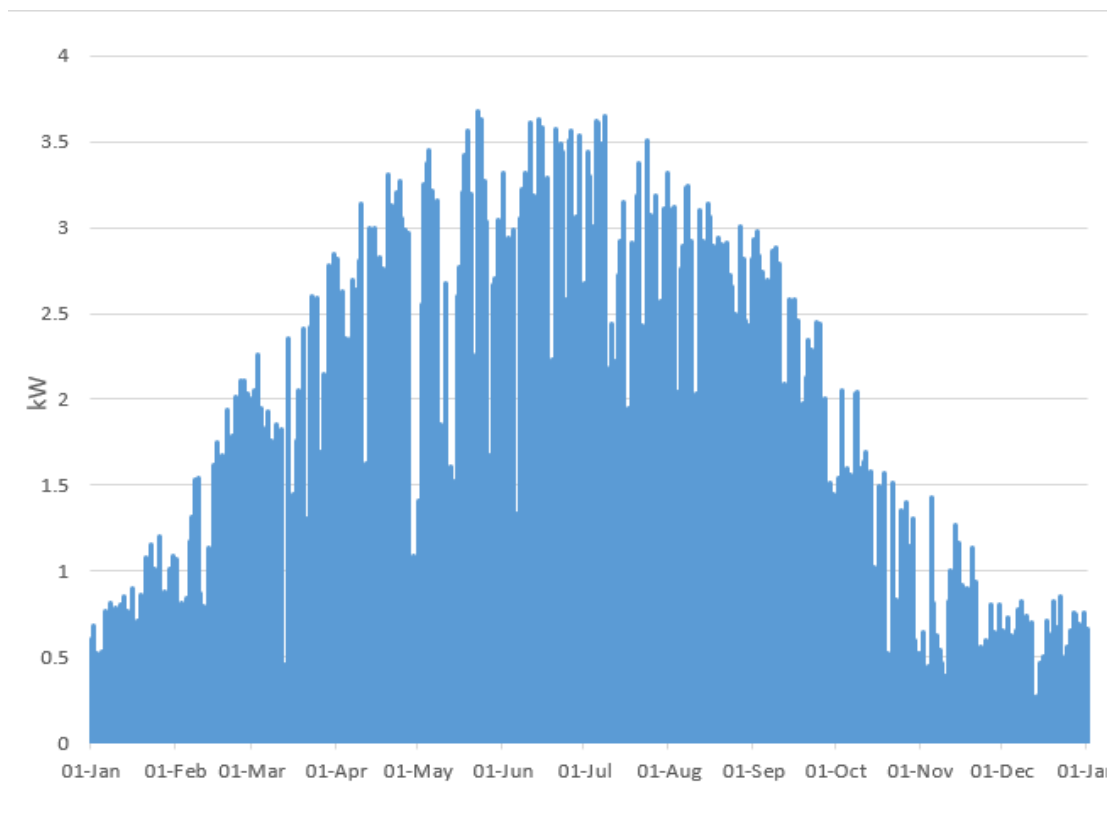


Fig. 3. 3. Annual PV generation for the 3.8 kW rooftop PV station

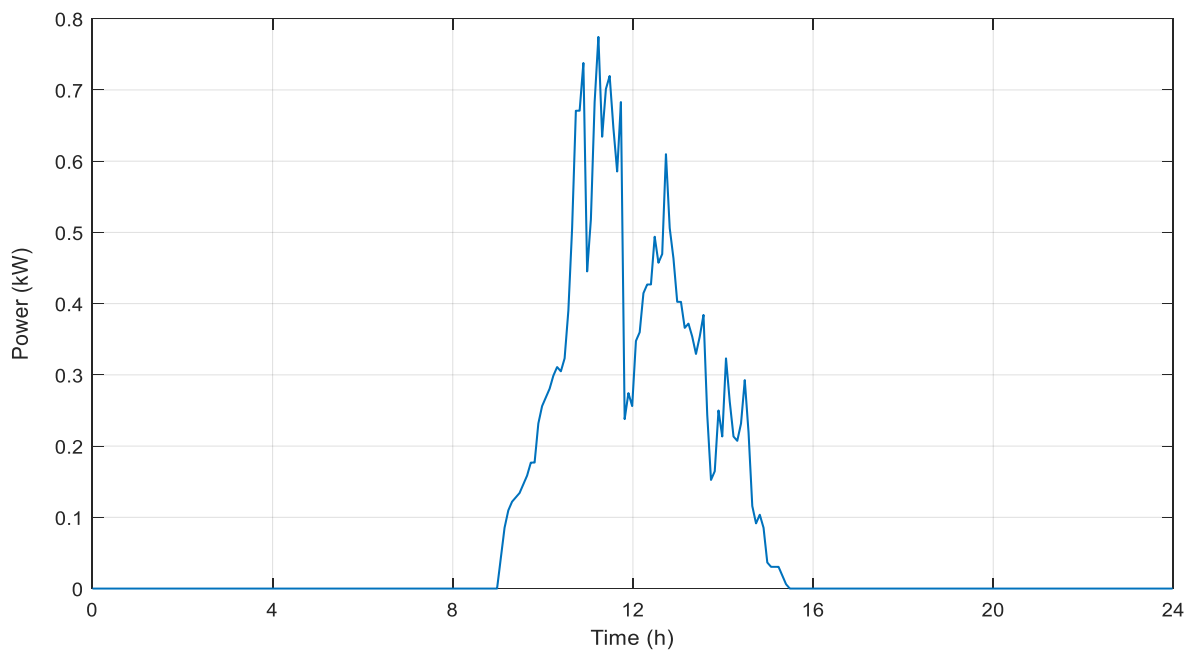


Fig. 3. 4. The daily PV generation profile for the 3.8 kW rooftop PV station on winter day-18/01/2015.

3.4 Shiftable Loads

It is assumed that the houses have shiftable loads. The shiftable loads such as washing machines, dishwashers, dryers, charging of EVs, etc. can be shifted in time to avoid operating them at high-peak tariff periods. The shiftable loads are key players in achieving lower energy costs for householders/community. They can help in reducing the energy cost under the condition of dynamic electricity pricing. In this thesis, it is assumed that the user sends a switch ON signal to the EMS to enable the start of a specific appliance - the switch ON signal is simulated by generating a random number within a pre-defined time period. The EMS receives the ON switch signal, for that appliance, and schedule for its operation as soon as possible based on an economic decision.

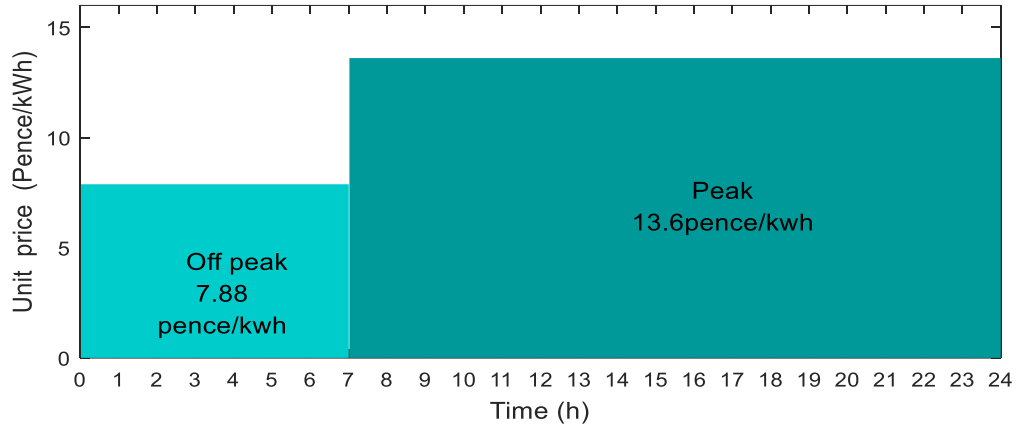
3.5 The Electricity Tariff Schemes

Purchasing and selling energy between a household (or a community) from one side and the main electricity grid from the other side is subjected to certain tariff schemes. This section presents the various tariff schemes that have been used in this thesis as follows: Economy 7 (E7), Time of Use (TOU), and Real-Time Pricing (RTP).

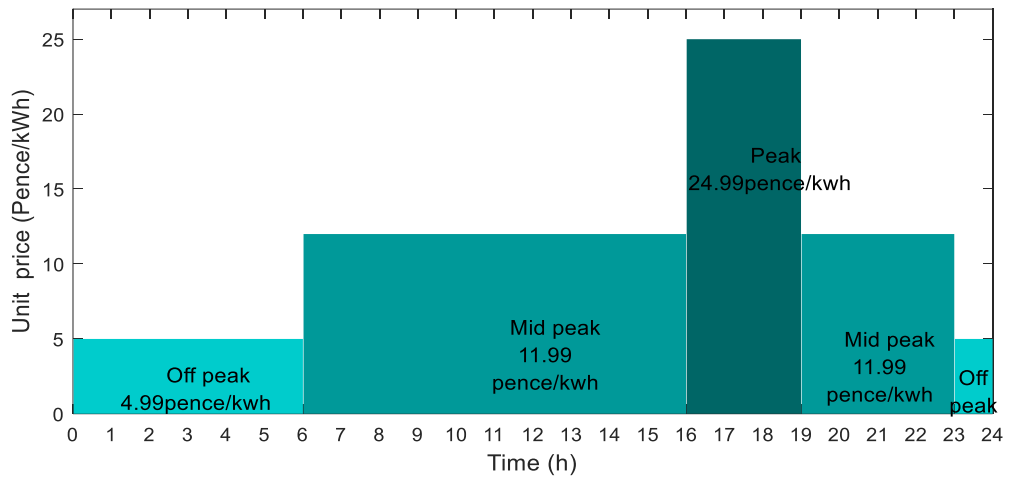
- The E7 tariff has been introduced in the UK electric power system in the 1970s and can be defined as an incentive from the power companies to enforce the consumers to use electricity during non-peak hours [155]. So, the price per kWh is different for peak and off-peak hours. A recent UK survey estimated that 13%-21% of British electricity consumers are currently on an E7 tariff [156]. The majority of the houses in the UK, which are not using the single rate tariffs are using the E7 pricing scheme [157] as it is available from almost all the electricity supply companies. An E7 meter records the electricity usage on two rates; from 00:00-07:00 an off-peak rate is applied, whereas, for the rest of the day, a peak price tariff is used. The exact rate pricing varies depending on

the supplier, the location of the property and the contract duration. In this thesis, the used E7 purchasing tariff is RobinHood Energy Nottingham E7 V7. This tariff is obtained from the RobinHood Energy Company, UK for the year 2017 [158]. Fig. 3. 5.a shows the values of the E7 tariff for each hour.

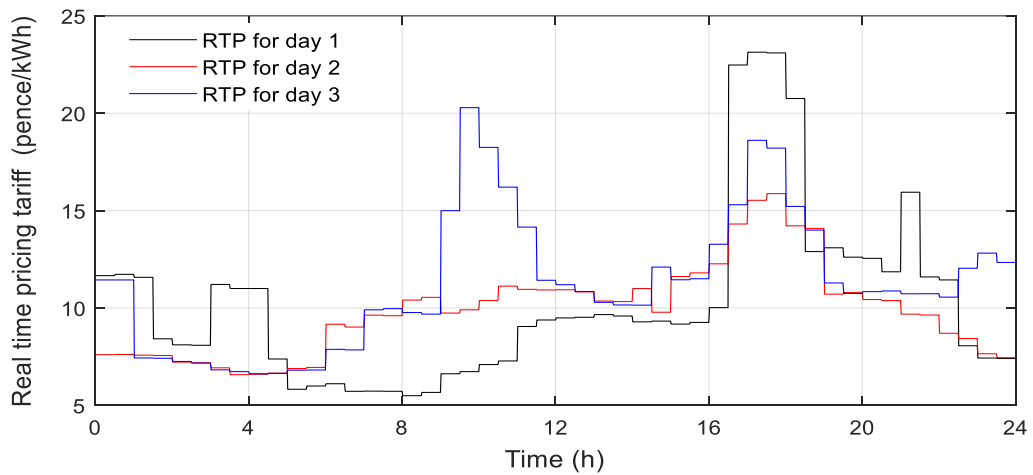
- The TOU tariff is a new concept, designed to incentivise customers to use more energy at off-peak times, in order to balance demand. TOU tariff provides electricity at three different rates depending on the time of day – with the lowest rate offered during the night, while higher prices are placed during daytime [159]. Even though the TOU tariff is similar to the E7 tariffs, the cost structure is a bit more complicated using TOU tariff. In this thesis, the TOU purchasing tariff values are obtained from the Green Energy Company, UK, for the year 2017, see Fig. 3. 5.b [160], [161]. The customers are charged at three different rates: a low rate between 23:00 and 06:00, a medium rate from 06:00 to 16:00 and from 19:00 to 23:00, and a much higher peak rate between 16:00 and 19:00. The value of the TOU tariff is fixed all the year or all of the contract period.
- Under RTP tariff, electricity prices vary over short time intervals, typically hourly or every 30 minutes, and are quoted one day or less in advance to reflect contemporaneous marginal supply costs [162]. RTP tariff requires the installation of an electricity smart meter that can send and receive information about electricity costs and give consumers more information about their own usage. In this thesis, the values of the RTP tariff are obtained from a dataset based on the UK electricity consumption. This dataset can be found from New Electricity Trading Arrangements (NETA) for the year 2017 [163]. The data shows the energy price divided into half hour blocks. Fig. 3. 5.c shows an example for RTP tariff for three consecutive days. Changing the values of the RTP tariff every day depends on many reasons such as, weekday or weekend, the weather, international events, the overall expected consumption.



(a) Economy 7 (E7) Purchasing tariff scheme, year 2017



(b) Time of Use (TOU) Purchasing tariff scheme, year 2017



(c) Real-Time Pricing (RTP) purchasing tariff scheme for three consecutive days, year 2017

Fig. 3. 5. Values of the purchasing tariff schemes used in this research

For all kinds of purchasing tariff schemes, the householders also have to pay a fixed monthly standing charge along with each electricity purchasing tariff scheme to pay for Transmission Network Use of System (TNUOS) and Distribution Use of System (DUOS) [164]. A standing charge value of 21.9 pence/day from year 2017 has been used in this thesis.

When the householders have excess electric energy from the PV generation after charging the HBSS and satisfying the load demands, this surplus energy could be exported to the main electricity grid for extra income or exported to the neighbour houses (when being a part of CES). When exporting the surplus energy to the main electricity grid, a fixed feed-in tariff value of 3.79 pence/kWh is used. The feed-in tariff values are obtained from the Ofgem website for feed-in tariffs in the UK [165].

3.6 Battery Energy Storage System

In this thesis, two types of BESS have been used: (a) a HBSS for domestic applications (houses), and (b) a large central community BESS.

For household application, Tesla Powerwall HBSS has been used [166]. The Powerwall are rechargeable stationary lithium-ion battery products manufactured by Tesla. The Powerwall batteries are intended to be used for home energy storage and stores electricity for PV self-consumption, time of use load shifting, and backup power applications. In this thesis, the HBSS used are “Powerwall 1 battery” (6.4 kWh) with a 2.5 kW power converter, and a “Powerwall 2 battery” (13.5 kWh) with 5 kW power converter [42], [167]. Fig. 3. 6.a. shows Tesla Powerwall 1 battery.

For community use, the larger Tesla Powerpack BESS has been used. The Powerpack is intended for commercial or electric utility grid use and can be used for peak shaving, load shifting, backup power, demand response, MGs, renewable power integration, frequency regulation, and voltage control [168]. In this thesis, the used Powerpack BESS are 1MWh

battery with a 250 kW power converter, and a 1MWh battery with 500 kW power converter.

Fig. 3. 7.b. shows an example for 1 MWh Tesla battery.



(a) Tesla Powerwall 1 battery

(b) 1 MWh Tesla battery

Fig. 3. 8. Examples of the Tesla battery storage systems

The full details of the BESSs for the household or communal use will be presented in the chapters where they are used. In this thesis the BESS has been used to minimize the annual energy costs for a household or a CES, maximize the PV self-consumption, time of use load shifting, minimize the exported energy to the main electricity grid, demand response application, and participate in additional ancillary/energy market services.

3.7 Forecasting Methods

Next day load demand and PV generation forecasting are essential for the operation of the EMS either for the household level or for the community level. The EMS needs the household consumption profile and the PV generation profile for the next 24 hours to perform the optimization process to determine the optimal power flow and the best operation scenario for the system.

There are several forecasting methods that could be used to forecast the household consumption and the PV generation for the next day [169], [170]. In this thesis, two main

types of forecasting methods have been used: (a) simple forecasting methods, and (b) complex forecasting methods. The simple forecasting methods depend only on the historical data sets such as the data of the past week or the past day to forecast the expected energy pattern in the next day. However, the complex forecasting methods use the historical data sets, the forecasted meteorological data and algorithms based on Artificial Intelligence (AI) to forecast the expected energy pattern in the next day. The use of the simple forecasting methods which depends only on the historical data for household consumption and PV generation minimizes the dependence on external communication technologies (i.e. no need for complex forecasting packages that require additional meteorological data), which makes these forecasting method a reasonable solution for remote areas which suffer from a bad communication environment.

The forecasting methods have been used in this thesis to measure its effect on the EMS's performance and on the results obtained. Furthermore, it is important to analysis the effect of forecasting techniques on the performance of the EMS using actual data so as to be able to select the most proper forecasting method that suits the householders or the community.

The following forecasting methods are used in this research:

For Load forecasting, four forecasting methods are used to forecast the household consumption for the next day:

- Using the previous day's load profile (L-PD), where L means load and PD means the previous day
- Using the previous week, same day load profile (L-PWSD), where L means load and PWSD means the previous week same day.
- Using the average load profile of the previous week (L-AV), where L means load and AV means the average.

- Using one of the load demand forecasting packages (L-FP) [169], [170], where L means load and FP means the forecasting package. E.g., ANN, Adaptive Neuro-Fuzzy Inference System (ANFIS), or Autoregressive Integrated Moving Average plus ANN which show better results for demand forecasting.

For PV forecasting, three forecasting methods are used to forecast the PV generation for the next day:

- Using the previous day's PV generation profile (PV-PD), where PV means photovoltaic and PD means the previous day.
- Using the average PV generation profile of the previous week (PV-AV), where PV means photovoltaic and PD means the average.
- Using the next day weather prediction data plus a PV forecasting package (PV-FP) to determine accurately the forecasted PV pattern for the next day [171], where PV means photovoltaic and FP means the forecasting package. The forecasted PV pattern for the next day can be received and updated every sample time (ΔT) (e.g. 15 minutes or 2 minutes) depending on the type of application and the required accuracy. This forecasting method needs continuous internet access to download the weather forecast data for the next day, i.e. this service could be available from the Utility Company or the retail agent for an extra price.

In this research, the historical dataset has been used to determine the forecasted load demand and PV generation profiles of the next day for the L-PD, L-PWSD, L-AV, PV-PD, and PV-AV forecasting methods. The ANFIS forecasting technique has been used to forecast the next day load demand for L-FP forecasting method [172], see appendix B for more details about ANFIS forecasting technique. PV-FP forecasting method uses the actual PV generation profile for the next day, after adding Gaussian noise, to generate the next day's forecasted PV

pattern; i.e. this is possible as we are using the historical database. The Gaussian noise represents the forecasting uncertainty associated with the forecasted PV generation. In this case, the forecasting uncertainty is assumed based on the results available from [173] for day ahead PV generation forecasting.

3.8 Performance Indices and Metrics

To assess the performance of the EMS and the techno-economic techniques, the following performance indicators have been used:

- **Household/community energy cost:** the household/community electrical energy cost include the cost of electricity purchased from the main electricity grid to feed the load demand and charge the BESS, and the incomes from the surplus energy exported to the main electricity grid, i.e. the surplus electricity produced by the PV generation after charging the BESS and satisfying the load consumptions. In some sections, this cost includes also the battery's degradation cost.
- **Household energy cost increment ratio:** the household energy cost increment ratio, shown in (3.1), is the ratio between the actual household energy costs and the household energy costs that would be achieved in the ideal case (i.e. ideal forecasting). The ideal case is the case in which the actual PV generation and load demand profiles are assumed (instead of the forecasted profiles), and the minimum sample time is used for the operation of the HEMS. If the value of the household energy cost increment ratio is 0%, this means the system has ideal performance. As this value increases, higher energy costs and poorer system performance will be observed. This term has been used to give an indication of the performance of the system (away from the ideal case) after using the forecasted load demand and PV generation profiles and/or longer sample time for the operation of the EMS.

Household energy cost increment ratio

$$= \left(\frac{\text{Actual household energy costs}}{\text{Household energy costs (ideal case)}} - 1 \right) \times 100 \quad (3.1)$$

- **The PV self-consumption ratio index:** The PV self-consumption ratio is used to measure the amount of PV energy consumed in the home/community either by direct consumption or by storing in the BESS and used later [174]. This ratio is calculated by dividing the PV energy consumed inside the home by the total generated PV energy, (3.2). 100% PV self-consumption ratio means that all the generated PV energy is consumed by the home; i.e. no exported energy to the main electricity grid is observed.

$$\text{PV self consumption ratio} = \left(1 - \frac{E_{PVgen}^{export}}{E_{PVgen}^{total}} \right) \times 100 \quad (3.2)$$

where E_{PVgen}^{total} is the total daily generated PV energy, E_{PVgen}^{export} is the daily exported energy from the PV generation system during the day.

- **Energy wastage ratio index:** The wastage energy is the unwanted feed-in energy to the main electricity grid [175], resulting from (a) the forecasting uncertainties or the sample time accuracy which leads to inaccurate power settings for the HBSS, and/or (b) poor estimation of the required overnight charging level of the battery. This may result in the battery incorrectly being fully charged such that excess PV energy cannot be stored. The energy wastage ratio is calculated by dividing the total energy exported to the main electricity grid by the total generated PV energy, see (3.3). The wastage energy should be saved in the battery to be used at the correct time instead of being fed into the utility for no or low reward. The energy wastage ratio index counts for both the unwanted feed-in energy to the main electricity grid from the HBSS (results from inaccurate power settings of the BESS) and from the PV generation system, compared to using the

complementary of the PV-self consumption ratio which counts only for the exported energy from the PV generation system during the day. When the energy wastage ratio equals 0%, no lost energy will be observed. As this value increases, more energy wastage will be observed, which therefore leads to more household energy costs and poorer system performance.

$$\text{Energy wastage ratio} = \frac{E^{\text{export}}}{E_{PV\text{gen}}^{\text{total}}} \times 100 \quad (3.3)$$

where $E_{PV\text{gen}}^{\text{total}}$ is the total daily generated PV energy. E^{export} is the total daily exported energy to the main electricity grid.

The Internal Rate of Return (IRR): The IRR is a metric used in capital budgeting to estimate the revenue of potential investment over a fixed time period [176]. The IRR, (3.4a), is a discount rate that makes the net present value (NPV) of all cash flows from a particular project equals to zero [177]. The NPV is used to calculate today's value of a future stream of payments. IRR is used to evaluate the attractiveness of a project or investment. If the IRR of a new project exceeds a company's required rate of return, that project is desirable. However, if IRR falls below the required rate of return, the project should be rejected; i.e. the higher a project's IRR, the more desirable it is to undertake. Generally speaking, if the IRR value is more than zero, this means that investment in this project will achieve profits. However, if the IRR value is negative, this means that the project will achieves losses.

$$0 = NPV = \sum_{Yr=1}^{\text{year } 20} \frac{Cash_{Yr}}{(1 + IRR)^{Yr}} - Cash_0 \quad (3.4a)$$

where NPV is the net present value. $Cash_{Yr}$ is the net cash inflow during the period Yr. Yr is the number of time periods (year). $Cash_0$ is the initial investment costs. IRR is the internal rate of return, year N is the estimated project lifetime (years).

- **Mean Absolute Percentage Error (MAPE) metric:** The accuracy of the forecasting methods for next day load demand or PV generation patterns is assessed using the MAPE metric [171]. The MAPE metric is formulated as (3.5) [178].

$$M.A.P.E = \frac{1}{N} \sum_{t=t_0}^{t_0+24h} \left| \frac{A_t - F_t}{A_t} \right| \times 100 \quad (3.5)$$

where A_t is the actual point, F_t is the forecasted point and N is the number of observation points.

3.9 Summary

This chapter presented the data resources that have been used in this thesis. Actual data for annual household load consumption profiles, PV generation profiles, energy tariff schemes, and the HBSSs parameters has been presented. It was mandatory to show clearly the data resources that have been used in this thesis as these resources have been used to test and examine the performance of the EMS and to obtain a real indication for the system's performance.

Also, this chapter presented the different forecasting methods used for next day load demand and PV generation forecasting. The forecasting methods presented have been used in this thesis to complete the operation of the proposed EMS.

Different performance indicators have been presented in this chapter as they have been used in this thesis to assess the performance of the proposed EMSs and to quantify their economic revenues.

Chapter 4

Home Energy Management System (HEMS)

4.1 Introduction

HEMSs are a key technology for lowering household energy costs, maximizing local PV self-consumption, and enabling houses to participate in community energy schemes. HEMSs are considered the cell structure of the Community Energy Management System (CEMS). Therefore, a HEMS for a domestic residence is developed and analysed first, before studying how several houses could participate in CEMS. This study of a stand-alone HEMS can then be used as a benchmark for studies into participation in a CEMS.

This chapter introduces a HEMS which aims to (a) minimize the daily household energy costs and energy wastage, (b) maximize the local PV self-consumption, (c) compensate for RES power fluctuations, (d) smooth the fluctuations of the electric power exchanges at the point of common coupling with the main electricity grid, and (e) compensate for the effect of forecast uncertainties and the effect of sample time, while considering the computational overhead, the battery degradation costs, and the possibility of load shifting.

Three types of real-time interactive HEMS have been presented and examined. (a) A Real-Time Controller (RTC)-based Single-Layer HEMS, (b) a Model Predictive Controller (MPC)-based Single-Layer HEMS, and (c) a Hierarchical Two-Layer HEMS. For each HEMS, the proposed control algorithm is introduced, the performance of the HEMS is assessed, the results obtained are discussed and analysed, and the limitations are presented.

Simulation results for the operation of the HEMSs are presented to consider the effect of different seasons (i.e. all four seasons), different overnight charging levels, and different tariff schemes on the annual energy costs and the annual PV self-consumption ratio and energy

saving. The simulation process for one year is important because the proposed HEMS should be tested for the whole year to verify that a significant annual improvement (reduction) in the operation costs can be achieved in the presence of seasonal variations

In addition, an experimental test has been implemented to ensure that the proposed hierarchical two-layer HEMS can be applied for a real system without any difficulties. The experimental test has been implemented using the “Smart Home Rig” located at the University of Nottingham’s FlexElec Laboratory.

4.2 Case study

The case study used in this chapter is for a UK based house which consists of common home appliances, a rooftop PV generation system, a HBSS, and shiftable home appliances. Also, the house is connected to the grid to import any further required energy and export any excess PV energy. Fig. 4. 1. shows the electrical network of the house under study. The annual load consumption, the annual PV generation, the rated power of the PV generation system, the size and the cost of the HBSS, and the details of the shiftable loads used in this house are presented in Table 4. 1.

The household load profiles are obtained from the data set described in section 3.2 for one of the houses (i.e. the real consumption data for house no. 1 for a whole year with a one-minute resolution). The annual consumption of the house is 4104 kWh and this value is close to the UK average of 4200 kWh for medium type users [179]. This data was combined with the real PV generation profile, presented in section 3.3. The PV generation profiles were scaled down to be equivalent to the PV generation of 1.4 kW peak system, which was assumed to be suitable for the house under study. The size of the PV system (1.4 kW peak system) is assumed based on a survey for the PV systems used in 33 houses in meadows area, Nottingham. The PV 1.4 kW peak system is acceptable for detached and semi-detached

houses because they have a limited roof space [180]. Again data for a full year with one-minute sample time is used.

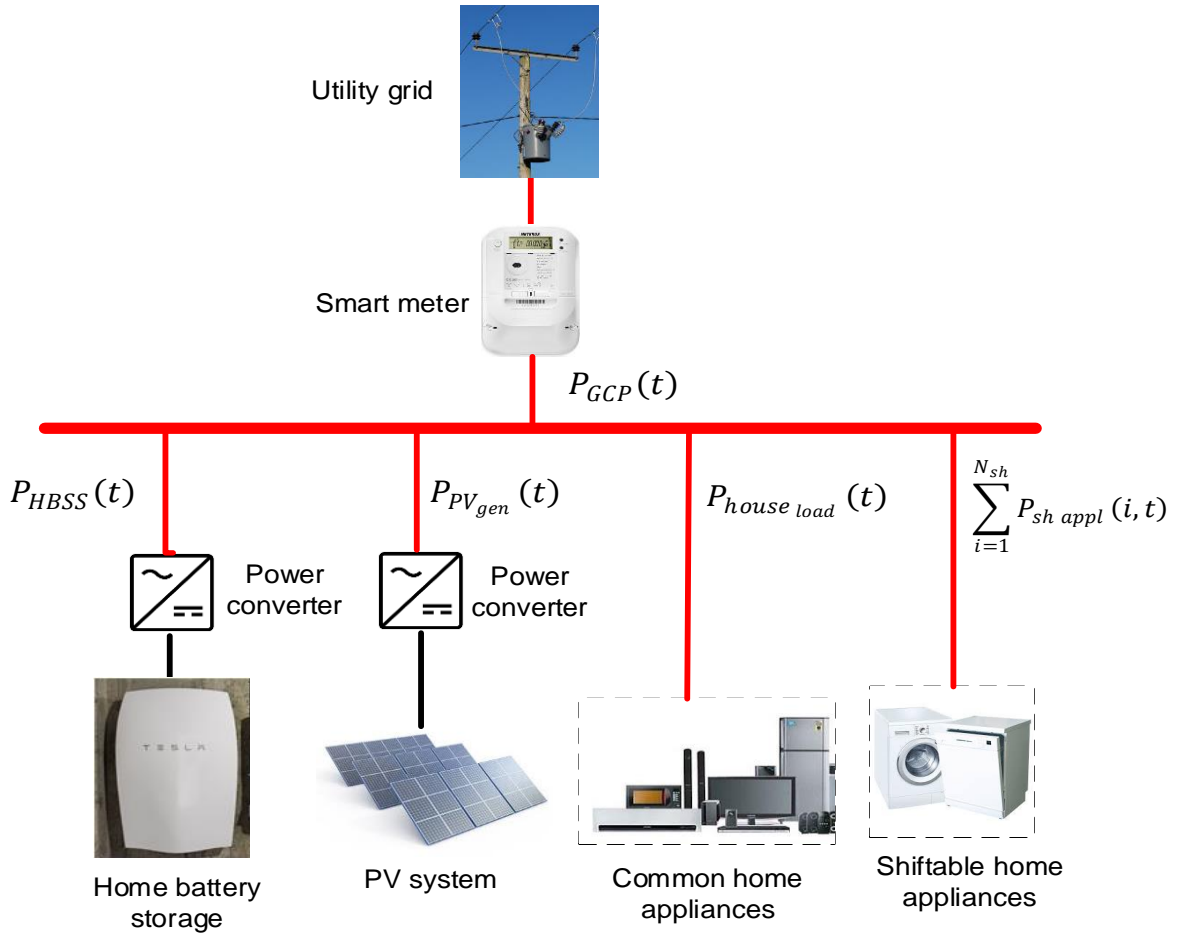


Fig. 4. 1. Household electrical network.

Table 4. 1. Data and parameters of the household

Parameter	Value	Parameter	Value
Annual household consumption	4104 kWh	Shiftable load (Washing machine)	1 kW
PV generation system	1.4 kW peak	Capital cost of the HBSS system (CC_{bat}) [42]	£3000
Annual PV generation	1358 kWh	Number of life cycles of the battery (N_{cycle}) [42]	5000
Battery storage system [42] (Capacity & efficiency)	6.4 kWh, 92%	Battery's power converter rating [167]	2.5 kW (η_{conv} 96%)

4.3 Real-Time Controller-based Single Layer HEMS

The RTC based-single layer HEMS is a fast controller which uses a developed rule-based control algorithm to achieve HEM. The RTC based-single layer HEMS does not require any system modelling or optimization process for its operation. It depends on instantaneous power measurements and does not require any load predictions. The RTC-based-single layer HEMS aims to reduce the daily household energy costs, maximize PV self-consumption and minimize energy wastage by controlling a HBSS.

4.3.1 Operating Algorithm

The RTC based-single layer HEMS uses a developed rule-based control algorithm to control the HBSS. The rule-based control algorithm is built to minimize the daily household energy costs and maximize PV self-consumption. The daily household energy costs “ C_{house} ”, that need to be minimized, can be formulated in terms of payments and incomes as (4.1). The payments include the cost of electricity purchased from the main electricity grid (4.2), while the incomes are the revenue from the energy exported to the main electricity grid (4.3), i.e. the surplus electricity produced by the PV generation after charging the HBSS and satisfying the house consumptions.

$$C_{house} = C_{house\ import} + C_{house\ export} \quad (4.1)$$

$$C_{house\ import} = \sum_{t=t_0}^{t_0+24h} \Delta T \times f_{import}(t) \times P_{GCP}(t) \quad , \text{at } P_{GCP}(t) > 0 \quad (4.2)$$

$$C_{house\ export} = \sum_{t=t_0}^{t_0+24h} \Delta T \times f_{export}(t) \times P_{GCP}(t) \quad , \text{at } P_{GCP}(t) < 0 \quad (4.3)$$

$$P_{GCP}(t) = P_{house\ load}(t) - P_{PV\ gen}(t) - P_{HBSS}(t) \quad (4.4)$$

where C_{house} is the daily household electrical energy cost (£), $C_{\text{house_import}}$ is the cost of the daily electrical energy purchased from the main electricity grid (£), $C_{\text{house_export}}$ is the cost of the daily exported electrical energy to the main electricity grid (£), ΔT is the sample time (h), $P_{\text{GCP}}(t)$ is the electrical power (kW) measured at the grid connection point (GCP) at time t ; a positive value means that the house is importing power from the main electricity grid while a negative value means exporting, $f_{\text{import}}(t)$ is the electricity purchase tariff at time t (£/kWh), $f_{\text{export}}(t)$ is the electricity sale tariff (i.e. feed in tariff) at time t (£/kWh), $P_{\text{house_load}}(t)$ is the household electrical load demand at time t (kW), $P_{\text{PVgen}}(t)$ is the electrical power generated by the household PV system at time t (kW), $P_{\text{HBSS}}(t)$ is the charge/discharge power from the HBSS at time t (kW); where a negative value means the HBSS is charging, while a positive value means the HBSS is discharging.

During the off-peak tariff period (i.e. night period), the controller charges the HBSS up to a pre-adjusted overnight charging level. During the rest of the day (i.e. peak tariff period), the controller discharges the HBSS or charge if surplus PV generation is available - it compares the power at the GCP and tries to make this power equal to zero. Fig. 4.2. summarizes the rule-based control algorithm of the RTC based-single layer HEMS. The control decision of the controller is based on instantaneous power measurements. The rule-based control algorithm is built assuming the use of the E7 tariff scheme for purchasing electric energy from the main electricity grid.

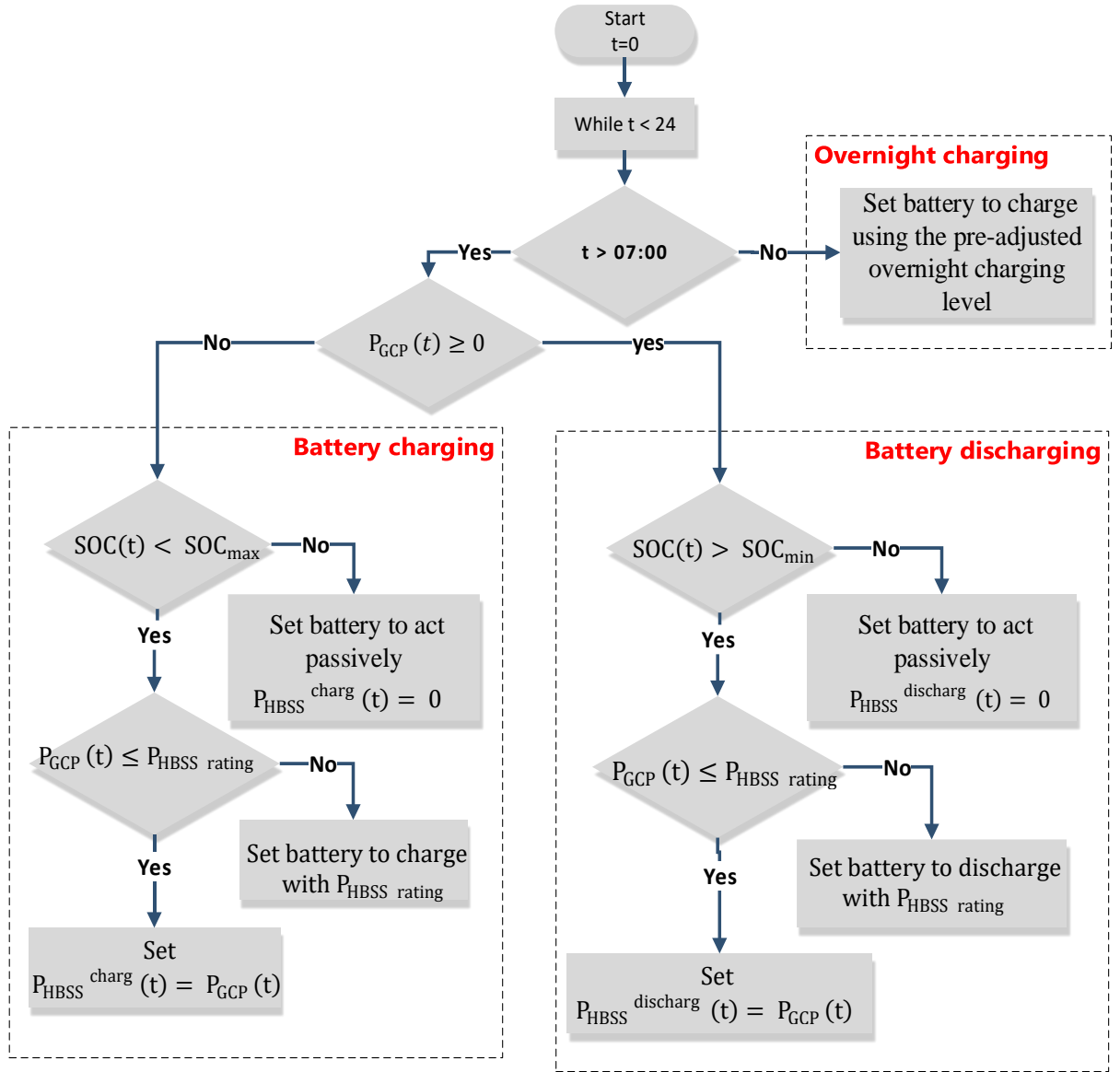


Fig. 4.2. The rule-based control algorithm of the RTC based-single layer HEMS.

where $SOC(t)$ is the state of charge (SOC) of the battery at time t , SOC_{max} and SOC_{min} are the maximum and the minimum allowable SOC limit of the battery; the SOC limits of the lithium-ion battery, considered in this research, are restricted to a range between 20 and 90 % of the nominal battery capacity; minimum and maximum SOC limits are used to avoid overcharging or deep discharging the HBSS, as that can significantly reduce the battery lifetime [181]. These constraints are recommended by the IEEE [182] and are critical to the battery operation. $P_{HBSS\ rating}$ is the rated charge/discharge power (kW) of the HBSS; i.e. the

rated power of the converter, $P_{\text{HBSS}}^{\text{disch}}(t)$ and $P_{\text{HBSS}}^{\text{charg}}(t)$ are the discharge and charge power (kW) of the HBSS at time t respectively; $P_{\text{HBSS}}^{\text{disch}}(t)$ is always a positive value while $P_{\text{HBSS}}^{\text{charg}}(t)$ is always a negative value.

4.3.2 Adjustment of the overnight charging level

The RTC based-single layer HEMS charges the HBSS overnight when the purchasing energy tariff from the main electricity grid is low and uses the stored energy to feed the loads at high peak tariff periods. The overnight charging level should be adjusted accurately. For example, if the overnight charge level is high and the day ahead is sunny, then the battery will be completely charged overnight and hence any surplus PV energy must be exported to the main electricity grid (for no or low reward). On the other hand, if the day ahead is cloudy and the battery is not sufficiently charged at night, then the battery might be completely discharged before the end of the day and hence electric energy at peak tariff prices may need to be purchased.

Five cases for adjusting the overnight charging level of the HBSS will now be discussed:

- **Case 1: Constant Full Overnight Charging:** The battery charges fully during the off-peak tariff (i.e. night period from 00:00 to 07:00). There is no requirement to access the previous power profiles for load demand or PV generation. No weather forecasts (which need internet access and additional cost for the forecasting package) nor calendar timers are used in this type [183].
- **Case 2: Yearly Optimized Overnight Charging:** In this case, the battery is charged overnight to an optimized pre-set level (fixed throughout the year) which depends on the battery capacity and the PV system size. This type should give better results compared to the previous type since the battery is not fully charged overnight, which leaves capacity for the battery to be charged by the surplus PV generation through the day.

- **Case 3: Seasonal Optimized Overnight Charging**: Each season, the overnight charging level is adjusted to a certain value. This value is selected based on the nature of the season and the PV and battery sizes. It is assumed that the HBSS contains a calendar timer to adjust the charging level at the beginning of each season. For example, for summer, the lowest charging level will be selected to capture most available PV generation during the current day. However, for winter, the maximum overnight charging level should be selected.
- **Case 4: Previous Day Modification**: The overnight charging level is adjusted based on the charging pattern for the previous day. For example, the overnight charging level increases by 10 % for the current day, if peak energy was purchased during the previous day. whereas the overnight charge level for the current day decreases by 10% if surplus PV energy was exported to the power grid the day before.
- **Case 5: Next day PV generation forecasting** (i.e. Weather prediction for the next day): A weather forecast data for the next day is used to adjust the overnight charging level of the battery which leaves capacity for the battery to be charged by the expected PV generation on the next day. The weather forecast data is used to generate a forecasted PV generation pattern for the next day, then (4.5) is used to adjust the overnight charging level.

$$\text{Overnight charging level} = 1 - \frac{(1 - C_{PV}) \times E_{PVgen}^{expect}}{B_{Capacity}} \quad (4.5)$$

where C_{PV} is annual average PV self-consumption ratio without using the HBSS; this value is obtained by simulating the system for one year without using the HBSS; Also, this value is assumed fixed for the whole year, $B_{Capacity}$ is the capacity of the battery (kWh), E_{PVgen}^{expect} is the expected PV generated energy for the next day, i.e. this value is obtained using the forecasted PV generation pattern for the next day.

Adjusting the overnight charging level using the weather prediction case minimizes exports and minimizes the amount of peak tariff energy purchased since the battery is topped up using all the available surplus PV energy. It is worth mentioning that this case needs internet access to download the weather forecast data for the next day, and a PV forecasting model to predict the PV energy.

4.3.3 Results

The operation of the RTC based-single layer HEMS has been simulated for two consecutive days in spring, as shown in Fig. 4. 3. and Fig. 4. 4, using the five cases for adjusting the overnight charging level of the HBSS. The simulation process determines both the annual household energy costs and the annual PV self-consumption ratio when using different cases for overnight charging level adjustment. The simulation process has been performed to study the daily performance of the rule-based controller, and the effect of using the different adjustment cases for the overnight charging level. This simulation process has used the real household consumption and PV generation profiles (mentioned in chapter 3), the rule-based control algorithm (shown in Fig. 4.2.), the E7 purchasing electricity tariff, the fixed feed-in tariff for the selling surplus PV energy, and equations (4.1 - 4.5).

In case 1, it is clear from Fig. 4. 3. (b)-case 1 that, for each of the two days, the HBSS is charged up to its maximum limit (90%) during the night while the following days were sunny, so most of the surplus PV energy has been fed into the grid, without being stored in the HBSS as shown in Fig. 4. 3.(c)-case 1. The household energy costs and the PV self-consumption ratio for the 2 days are £0.977 and 62 % respectively.

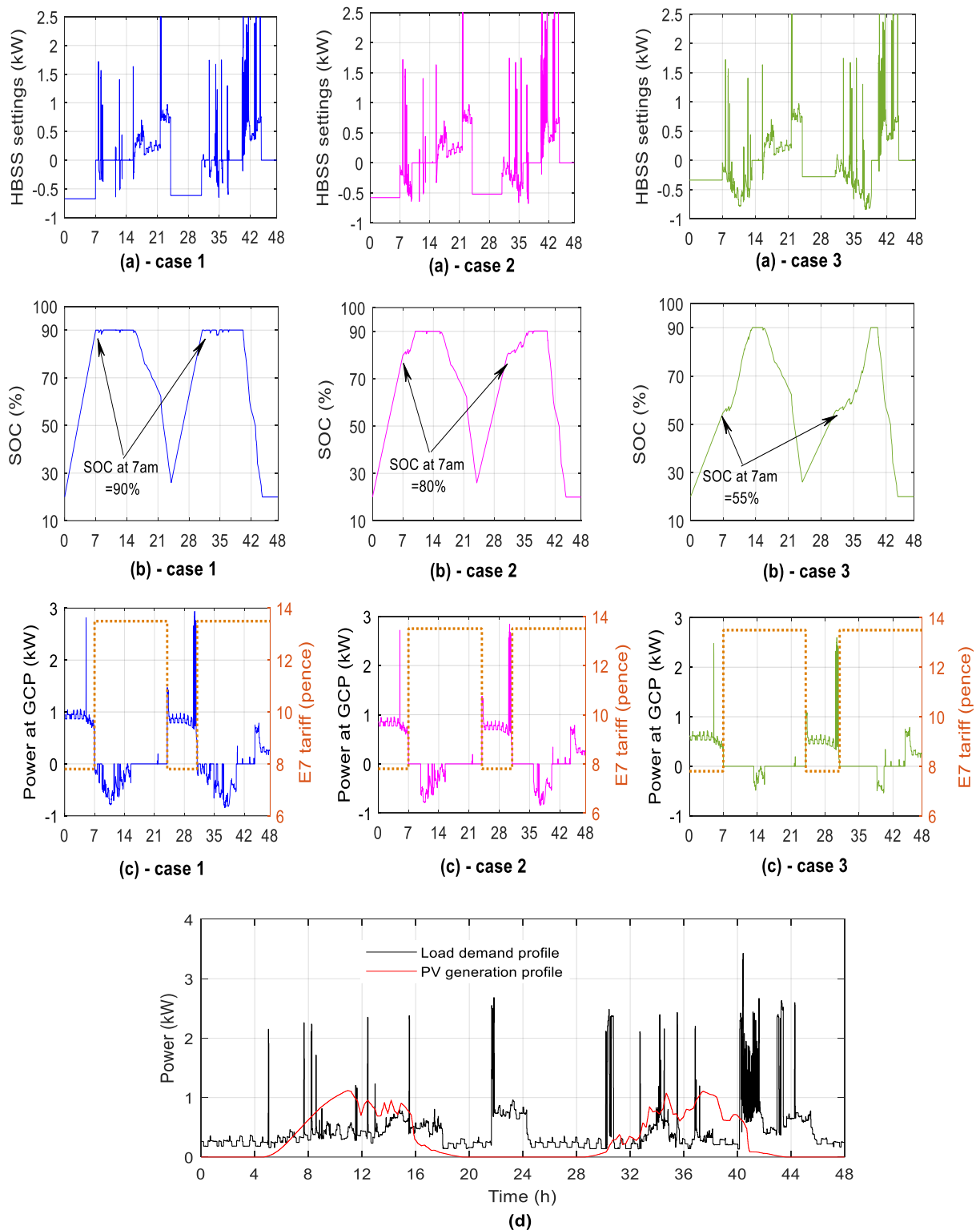


Fig. 4. 3. The performance of the RTC based-single layer HEMS for two consecutive days using cases 1, 2 and 3 respectively, (a) the HBSS power settings obtained from the RTC, i.e. a positive value means that the HBSS is discharging, while a negative value means that the HBSS is charging, (b) the SOC curve of the HBSS, (c) the resultant power at the GCP, i.e. a positive value means the house is importing power from the main electricity grid, and a negative value means exporting, and the corresponding E7 tariff values, (d) the actual household consumption and PV generation profiles for two consecutive days.

In case 2, a yearly optimized overnight SOC level is selected (i.e. 80% - Fig. 4. 6 will discuss how this value is being selected). Fig. 4. 3. (b)-case 2 shows that the HBSS is charged up to 80% overnight and then topped up with the surplus PV generation available during the day. The household energy costs and the PV self-consumption ratio, for the 2 days, are £0.922 and 70.8 % respectively, compared to £0.977 and 62% in case 1. It is clear from the results that using an adjustment for the overnight charging level improves the PV self-consumption ratio and reduces the household energy costs.

In case 3, selecting a seasonal overnight charging setting gives the chance for the HBSS to be topped up with the surplus PV energy through the day. This achieves lower household energy costs (£0.78) and a greater PV self-consumption ratio (92.8%), compared to case 1 and case 2. It is clear from Fig. 4. 3. (c)-case 3, that the exported energy to the main electricity grid decreases, compared to Fig. 4. 3. (c)-case 1 and to Fig. 4. 3. (c)-case 2, which means higher PV self-consumption ratio. Generally speaking, for summer, the best overnight charging level should be the minimum one to maximize the PV self-consumption ratio, whereas for winter the larger one. However, for batteries with a small capacity, the most beneficial charging level for all the seasons was found to be the maximum available one, due to their restricted capacity. These settings ensure less household energy costs and more PV self-consumption ratio. Overall, as the battery capacity and PV size increases, the optimal overnight charging level should decrease for all seasons.

In Case 4, it is assumed that the overnight charging level for the first day is 60% as can be observed from Fig. 4. 4. (b)-case 4. The first day was sunny and surplus PV energy has been fed into the grid as is clear from Fig. 4. 4. (c)-case 4. As surplus PV energy has been fed into the grid during the first day, the RTC decreases the overnight charging level for the second day to 50% (i.e. decrease by 10%) to minimize the exported PV energy in the second

day. The household energy costs and the PV self-consumption ratio, for these 2 days, are found to be £0.79 and 92.5% respectively.

In case 5, The forecasted PV generation profile for the next day is used to accurately adjust the overnight charging level. The forecasted PV generation profile for the next day has been assumed to be the actual PV generation profile for the next day after adding Gaussian noise; i.e. this is possible as we are using the historical database. The Gaussian noise represents the forecasting uncertainty associated with the forecasted PV generation. In this case, MAPE of 14% is assumed to represent the forecasting uncertainty. The forecasting uncertainty is assumed based on the results available from [173] for the day ahead PV generation forecasting.

For the case under study, it is observed that 53% of the total generated PV energy is directly consumed through the household consumption without any HBSS. (4.5) has been used to adjust the overnight charging level for each day. The overnight charging levels for the 2 days are 48% and 52.5% respectively as can be seen in Fig. 4. 4. (b)-case 5. The household energy costs and the PV self-consumption ratio are found to be £0.71 and 96.7% for these 2 days. It is clear from Fig. 4. 4. (c)-case 5 that accurately adjusting the overnight charging level for each day minimizes the exported excess PV energy and maximizes the PV self-consumption ratio.

A new case, case 6 (Ideal case), has been created to be used as a reference case. Case 6 is similar to case 5, the only difference is that the forecasted PV generation in case 6 is assumed ideal, i.e. zero forecasting error, by using the data available.

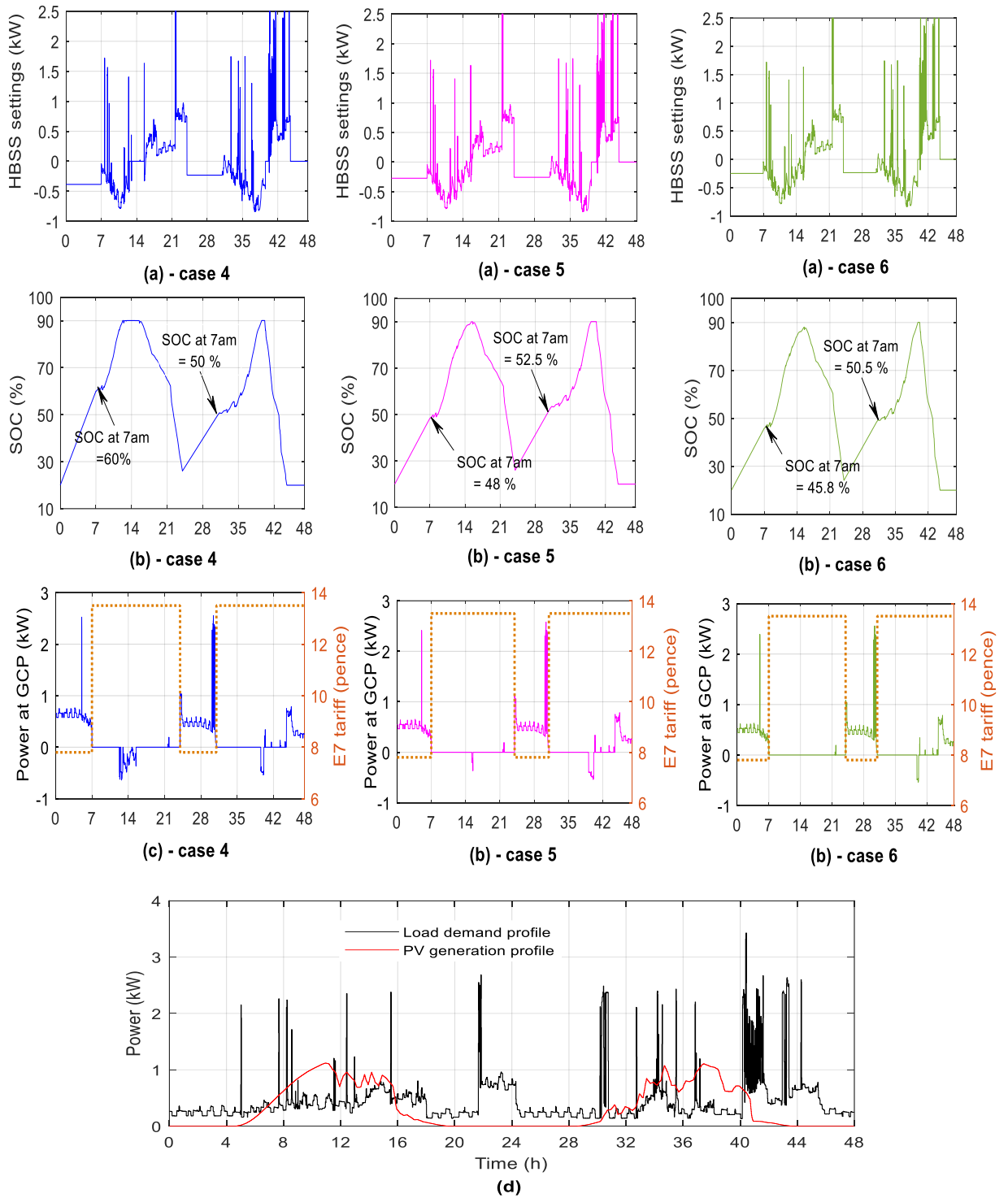


Fig. 4. 4. The performance of the RTC based-single layer HEMS for two consecutive days using cases 4, 5 and 6 respectively, (a) the HBSS power settings obtained from the RTC, i.e. a positive value means that the HBSS is discharging, while a negative value means that the HBSS is charging, (b) the SOC curve of the HBSS, (c) the resultant power at the GCP, i.e. a positive value means the house is importing power from the main electricity grid, and a negative value means exporting, and the corresponding E7 tariff values, (d) the actual household consumption and PV generation profiles for two consecutive days.

In case 6, Ideal case, it is assumed that the ideal PV generation for the next day has been used to accurately adjust the overnight charging level. This case is used as a reference case. The household energy costs and the PV self-consumption ratio, in this case, are found to be £0.68 and 97.8% respectively.

The operation of the RTC-based single layer HEMS has been simulated for one year to consider the effect of different seasons (i.e. all four seasons) and to assess fairly the effect of using different overnight charging level adjustment cases. Fig. 4. 5. shows the annual household energy costs and the annual PV self-consumption ratio when using different cases for overnight charging level adjustment. This simulation uses the annual household consumption and PV generation profiles (mentioned in chapter 3).

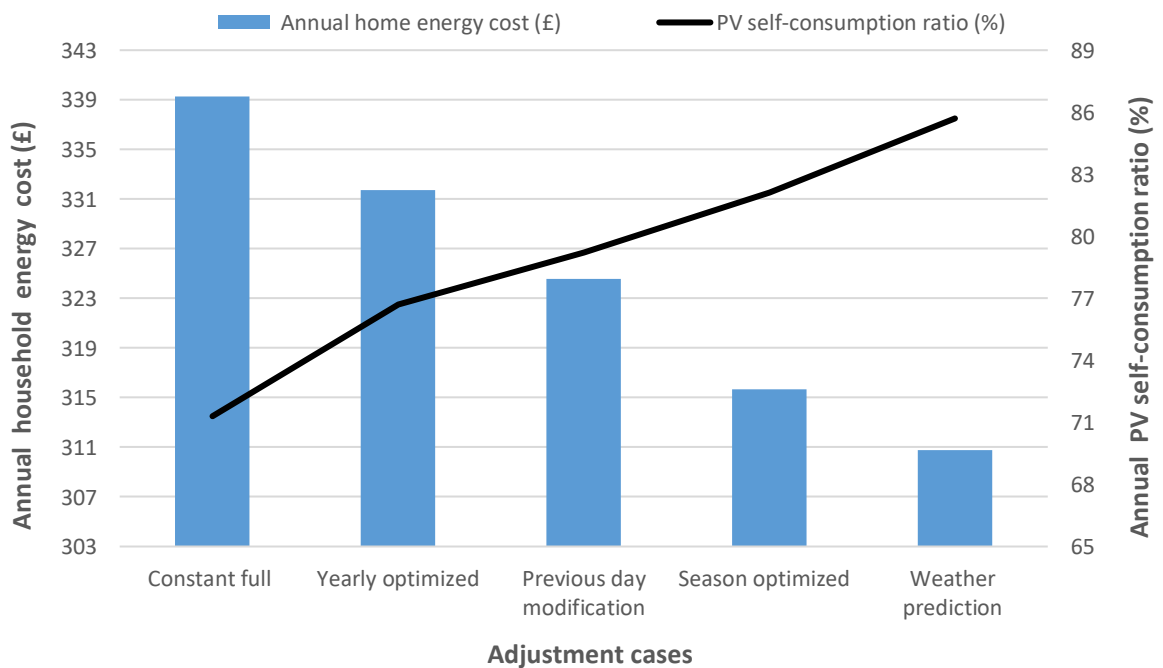


Fig. 4. 5. Annual household energy costs and PV self-consumption ratio using different adjustment cases for the overnight charging level.

It can be observed from Fig. 4. 5 that accurate adjustment of the overnight charging level for the HBSS is very important and affects both the annual household energy costs and the annual PV self-consumption ratio. If the overnight charging level is selected properly

according to each season (i.e. as in case 3), lower household energy costs and higher PV self-consumption ratio are achieved compared to the other cases (case 1, 2, and 4). It is observed that case 5 (i.e. weather prediction for the next day), achieves the lowest annual household energy costs compared to the other cases (case 1-4). It is also worth noting that in case 5, a continuous connection to the internet is required to download the weather forecast for the next day to be able to determine the overnight charging level of the HBSS. Additional costs may be added to make a contract for a proper forecasting package that updates the system with the up to date weather prediction data.

To determine the optimal overnight charging level for the yearly optimized case (case 2) or season optimized case (case 3), the operation of the system has to be simulated using different values of the overnight charging levels for one year to determine the minimum annual household energy costs and the maximum annual PV self-consumption ratio, see Fig. 4. 6.

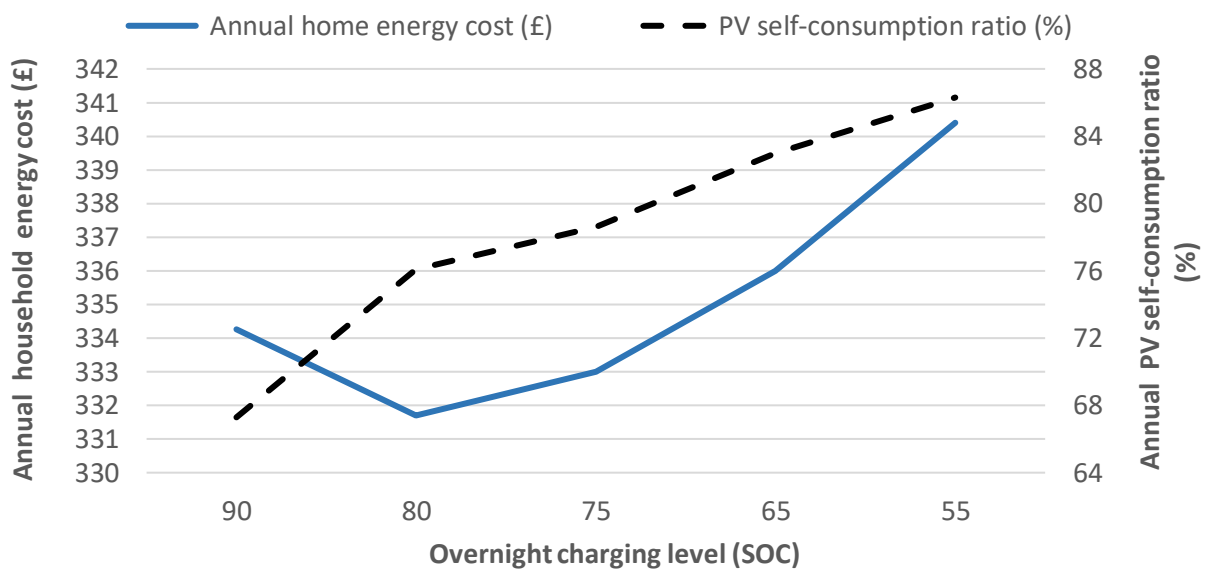


Fig. 4. 6. The annual household energy costs and the annual PV self-consumption ratio using different overnight charging levels for the yearly optimized case (case 2).

It is observed from Fig. 4. 6. that as the overnight charging level decreases, the annual PV self-consumption ratio increases. This is because the lower overnight charging level means more available capacity in the HBSS to store the surplus PV energy. It is observed that the annual household energy cost decreases as the overnight charging level decreases until a certain point (i.e. 80% in this case), after this point, the annual household energy cost increases as the overnight charge level decreases. This is because the overnight charging level is being fixed all the year. For example, if the overnight charging level for the yearly optimized case was selected to be 55%, in the winter, no surplus PV energy is available most of the days. Therefore, the HBSS will not be topped up during the daytimes and hence, it will not be able to feed the majority of the load at peak tariff periods as it will drain quickly, leads to increase of imported energy from the main electricity grid at high prices (i.e. at peak tariff times), which increases the total annual household energy costs. As can be seen from Fig. 4. 6., the point which achieves minimum annual household energy costs is at 80% overnight charging level. This point is selected to be the yearly optimized Overnight charging level for the case under study.

By using the same procedure followed in case 2 (to determine the optimal overnight charging level), the optimal overnight charging levels of the season optimized case (case 3), are found to be 90%, 63%, 55%, 30% for winter, autumn, spring, and summer respectively.

4.3.4 Limitations of the RTC based-single layer HEMS

The limitations of using RTC based-single layer HEMS are:

- It takes control decisions based on the instantaneous power measurements only, without taking into account any future changes. These control decisions are not guaranteed to be optimal and can lead to inefficient energy usage due to a lack of foresight (i.e. prediction

of the system's performance for the next 24 hour). Also, using this control technique will fail to manage the shiftable home appliances or EV charging, due to lack of foresight.

- It needs accurate adjustment for the overnight charging level to guarantee cost effective system operation. This adjustment is time consuming since it depends on the simulation of the system for many times until the accurate settings are determined. This simulation process needs the yearly consumption and PV generation profiles for the household under study. Also, the settings obtained may not be accurate if the behaviour of householders changes.
- It does not take into account the battery degradation costs while determining the HBSS power settings.
- It does not guarantee efficient system operation when applying the TOU tariff scheme, i.e. when applying the TOU tariff scheme, the energy stored in the HBSS should be divided into parts, each part should be used during a certain time period. For example, if the household consumption increases in the mid-peak period (from 06:00 to 16:00), the current RTC will discharge most of (or all) the stored energy in the HBSS during this period, leaving insufficient or no stored energy in the HBSS to be used in the peak-tariff period. Therefore the house will import all the additional required energy from the main electricity grid at high prices (peak tariff prices), which increases the daily household energy costs and leads to inefficient energy usage.
- The RTC cannot be used when applying RTP tariff schemes since the RTP tariff needs a controller which compares the rational effect of the tariff's value at a time t with the remaining values at the rest of the daytime, i.e. in other word, it needs a controller that takes the effect of predicted values rather than instantaneous values.

The previous limitations of the RTC based-single layer HEMS push us towards predictive controllers. Predictive controllers optimize the system for the current sample while keeping

account of future changes that will happen. The new version of the HEMS system should overcome the drawbacks of RTC and be able to control shiftable home appliances and EV chargers if they exist, in addition to using the HBSS. Also, the HEMS should be able to deal with tariff schemes such as TOU and RTP.

4.4 Model Predictive Controller-based Single Layer HEMS

This section presents a MPC based single layer HEMS. The HEMS presented minimizes the household energy costs and maximizes the PV self-consumption ratio, while taking into account the battery degradation costs and the possibility of load shifting. The HEMS comprises an MPC which optimizes household energy usage using a Mixed Integer Linear Programming (MILP) optimization. The MPC controls the operation of the HBSS and the controllable home appliances to guarantee the cost effective use of electrical energy in the home.

In this section: (a) The operating algorithm of the MPC-based single layer HEMS will be introduced, including the formulation of the optimization cost function and system modelling. (b) The effect of forecasting uncertainty, sample time, and using different tariff policies on the performance of the HEMS will be studied. (c) The importance of designing a HEMS being able to respond to changes in the system (i.e. changing of loads and PV generation) that happen in a short sample time (i.e. two minutes) and its impact on the annual energy costs and the annual energy wastage ratio will be studied.

4.4.1 Model Predictive Control theory

MPC is an advanced method of process control. MPC has a long history in the field of control engineering where it has been used in chemical plants and oil refineries since 1980 [184]. Recently, it has also been used in power system applications and management [185]. Almost all control systems are enclosed by constraints due to technical, physical, economic

and environmental limits on system operation. MPC strategies are characterized by systematic handling of constraints which give it a significant performance improvement over conventional control methodologies. Through our research, MPC is used as a powerful technique to optimize the performance of constrained systems [186], [187].

MPC performs an optimization process at each time step for a finite control horizon to optimize the operation of a certain plant [56]. At each time step (t), a finite horizon optimal control sequence is computed and an optimal solution is obtained for this period of time. However, only the first step of the control action is applied. At the next time step ($t + 1$), new measurements of the variables are requested, and with these updates, the optimal control settings are recalculated for the next periods. The main advantage of MPC is optimizing the system for the current sample while keeping account of future changes that will happen.

4.4.2 Operating Algorithm

Every sample time, the MPC-based single layer HEMS (1) requests the forecasted household consumption and PV generation profiles for the next 24 hours. It also requests the real-time measurements of the SOC of the HBSS to update the control model, (2) A MILP optimization process is performed to determine the 24-hour profiles for: (a) the optimal HBSS power settings, required for optimal battery operation, and (b) appliance scheduling, required for controlling the shiftable appliances; Only the first step of these profiles is sent directly from the MPC to the HBSS and the shiftable appliances. (3) This procedure is repeated every sample time using a rolling horizon approach to update the input variables and obtain new updated settings. These settings will guarantee the best economic use of electrical energy in the home. Fig. 4. 7. shows the operating algorithm of the MPC-based single layer HEMS.

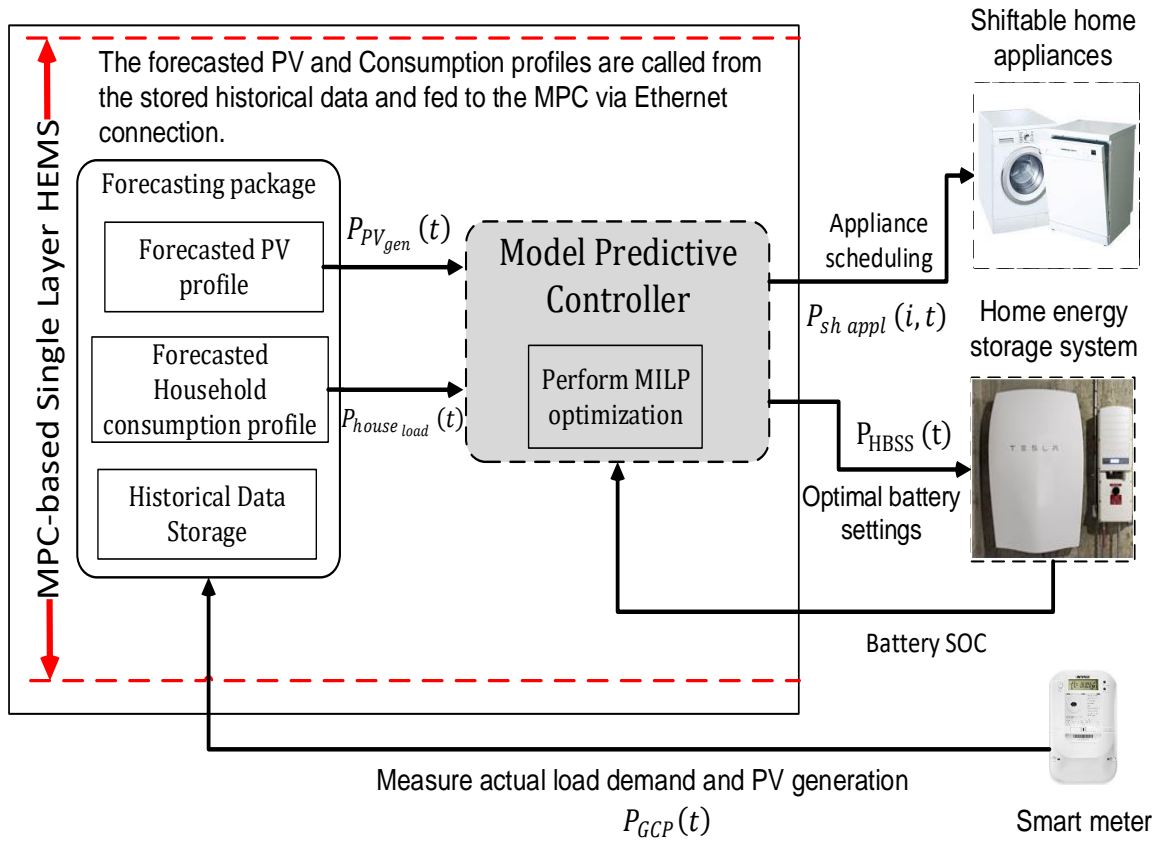


Fig. 4. 7. The operating algorithm of the MPC-based single layer HEMS.

4.4.3 System Modeling and Constraints

The first step to optimize the operation of the house is to create the model of the system that needs to be optimized, and all the constraints that affect the system's operation. The house model includes: (a) the model of the HBSS, (b) the shiftable appliances model, (c) the battery degradation model, and (d) imported/exported power model. Also, all the constraints that affect the system's operation are formulated.

4.4.3.1 HBSS Model

The model of the HBSS is represented as follows:

The stored energy in the battery, every time (t), can be formulated as a discrete time equation (4.6).

$$E(t) = E(t - \Delta T) - \frac{\Delta T \times P_{HBSS}^{disch}(t)}{\eta_d} - \Delta T \times \eta_c \times P_{HBSS}^{charg}(t) \quad (4.6)$$

where $E(t)$ and $E(t - \Delta T)$ are the stored energy (kWh) in the HBSS at times t and $t - \Delta T$ respectively, $P_{HBSS}^{disch}(t)$ and $P_{HBSS}^{charg}(t)$ are respectively the HBSS discharge and charge powers at sample time t (kW); $P_{HBSS}^{disch}(t)$ is always a positive value while $P_{HBSS}^{charg}(t)$ is always a negative value, η_d, η_c are the battery discharging and charging efficiencies respectively (%); the battery efficiencies are assumed to be constant values, neglecting the variation of the efficiency for different values of charging or discharging power.

The status of the stored energy of a battery every sample time is defined as SOC, see (4.7):

$$SOC(t) = \frac{E(t)}{B_{capacity}} \times 100 \quad (4.7)$$

where $B_{Capacity}$ is the battery capacity (kWh).

Minimum and maximum SOC level constraints (4.8), are used to avoid overcharging or deep discharging the HBSS, as that can significantly reduce the battery lifetime [181]. These constraints are recommended by the IEEE [182] and are critical to the HBSS operation. The SOC limits of the lithium-ion battery, considered in this research, are restricted to a range between 20 and 90 % of the nominal battery capacity.

$$SOC_{min} \leq SOC(t) \leq SOC_{max} \quad (4.8)$$

where SOC_{max} and SOC_{min} are the maximum and minimum allowable SOC limit (%) respectively.

The model of the battery power converter is represented by (4.9). The battery power converter acts as an interface between the battery and the HEMS and is used to control the battery.

$$P_{HBSS}(t) = P_{HBSS}^{disch}(t) \times \eta_{Conv} + \frac{P_{HBSS}^{charg}(t)}{\eta_{Conv}} \quad (4.9)$$

where $P_{HBSS}(t)$ is the charge/discharge power from the HBSS at time t (kW); where a negative value means the HBSS is charging, while a positive value means the HBSS is discharging, η_{Conv} is the efficiency of the power converter (%); the efficiency of the power converter is assumed constant in this research.

The HBSS power output constraint (4.10), reflects the operating limits of the HBSS and defines the maximum power that can be discharged/charged by the HBSS.

$$-P_{HBSS\ rating} \leq P_{HBSS}(t) \leq P_{HBSS\ rating} \quad (4.10)$$

where $P_{HBSS\ rating}$ is the rated (maximum allowable) HBSS charge/discharge power (kW), i.e. rated converter power.

Two binary variables $\delta_{B\ disch}(t)$ and $\delta_{B\ charg}(t)$ are introduced to create a link restriction to ensure the battery is not charged and discharged at the same time, i.e. battery power flows in one direction at any given time, see (4.11- 4.13):

$$\delta_{B\ disch}(t) + \delta_{B\ charg}(t) \leq 1 \quad (4.11)$$

$$\delta_{B\ disch}(t) = \begin{cases} 1 & , P_{HBSS}(t) \geq 0 \\ 0 & , P_{HBSS}(t) < 0 \end{cases} \quad (4.12)$$

$$\delta_{B\ charg}(t) = \begin{cases} 1 & , P_{HBSS}(t) < 0 \\ 0 & , P_{HBSS}(t) > 0 \end{cases} \quad (4.13)$$

where $\delta_{B\ disch}(t)$ equals 1 if the battery is discharging and equals 0 otherwise, $\delta_{B\ charg}(t)$ equals 1 if the battery is charging and 0 otherwise.

Constraints (4.14, 4.15) are used to create a link between the battery power and the binary variables $\delta_{B \text{ disch}}(t)$ and $\delta_{B \text{ charg}}(t)$.

$$P_{HBSS}^{disch}(t) \leq \delta_{B \text{ disch}}(t) \times (P_{HBSS \text{ rating}}) \quad (4.14)$$

$$P_{HBSS}^{charg}(t) \geq \delta_{B \text{ charg}}(t) \times (-P_{HBSS \text{ rating}}) \quad (4.15)$$

4.4.3.2 Battery degradation model

In order to simultaneously optimize energy cost and battery lifetime, the estimated equivalent costs of battery degradation are defined in terms of battery lifetime reduction. [188] divided the battery degradation cost into three parts: SOC related degradation, temperature related degradation, and the depth of discharge (DOD) related degradation. The temperature related degradation is caused by the fluctuations in charging or discharging power. It is negligible for the HBSS since their discharging/charging current and voltage are usually stable. The DOD related degradation is considered the capacity fade resulting from the daily minimum SOC level achieved during battery operation [189]. The manufacturers of the batteries quantify the life of the battery (i.e. the number of cycles until the end of life) as a function of the DOD. The lifetime throughput can be calculated using the charts available in the battery specification sheet [190]. For HBSS, the HEMS keeps the DOD (i.e. minimum SOC level) of the battery within certain limits to maximize the lifetime of the battery. The SOC related degradation is considered as a function of the daily number of the charging and discharging cycles. In this research, the daily cost of battery degradation (C_{HBSS_d}) due to the number of charging and discharging cycles is defined as (4.16, 14.7) [188], [191].

$$C_{HBSS_d} = C C_{bat} \times \frac{\Delta L}{N_{cycle}} \quad (4.16a)$$

$$\Delta L = \sum_{t=t_0}^{t_0+24h} \left(\frac{\eta_{Conv} \times \eta_c \times \Delta T \times P_{HBSS}^{charg}(t)}{B_{capacity} \times 2} + \frac{\Delta T \times P_{HBSS}^{disch}(t)}{B_{capacity} \times \eta_{Conv} \times \eta_d \times 2} \right) \quad (4.16b)$$

where C_{HBSS_d} is the battery degradation cost (£) due to charging and discharging cycles, CC_{bat} is the capital cost of the battery (£), ΔT counts for the number of charging and discharging cycles undergone by the battery in 24 hours period. N_{cycle} is the number of typical life cycles of the battery.

$$C_{HBSS_d} = \sum_{t=t_0}^{t_0+24h} \left(\frac{CC_{bat} \times \eta_{Conv} \times \eta_c \times \Delta T \times P_{HBSS}^{charg}(t)}{B_{capacity} \times 2 \times N_{cycle}} + \frac{CC_{bat} \times \Delta T \times P_{HBSS}^{disch}(t)}{B_{capacity} \times \eta_{Conv} \times \eta_d \times 2 \times N_{cycle}} \right) \quad (4.17)$$

4.4.3.3 Shiftable appliances model

In this section, the model of the shiftable home appliances is presented. Operation of some home appliances, such as washing machines, dishwashers, dryers, etc. can be shifted in time to avoid operating them at high-peak tariff periods. The HEMS determines the best scheduling of the home appliances to achieve the lowest energy costs for householders. It is assumed that the user sends a switch ON signal to the HEMS to enable the start of an appliance 'i'. The HEMS receives the ON switch signal, for appliance 'i', and schedules its operation as soon as possible based on a certain criteria. The HEMS shifts the appliance from operating at peak-tariff periods to either operate at off-peak tariff period to minimize the household energy costs, or to operate at surplus PV generation periods to maximize PV-self consumption. The time consumed between the receiving of the ON switch signal and actual operation of the appliance is called the waiting time. The maximum allowable waiting time can be adjusted by householders based on their requirements, i.e. zero waiting time means the immediate start of the device when a switch ON signal is received. If no choice is made, it is assumed to be 4 hours to keep a high comfort level for householders. A high comfort level is met when the HEMS manages to operate the household appliances in a way which meets the

householders preferences (i.e. desired way of operation of appliances which is defined by each householder), and vice versa. The comfort level or the maximum permissible waiting time for the shiftable appliances) is determined by analysing a survey data of appliances usage to characterize the patterns of appliance usage, which includes the mean power consumption, usual start time, and duration of time [192]. For some houses, the householders can set their comfort preference for each appliance. For example, the clothes dryer must finish its operation be midnight, the EV must be fully charged by 7am, etc.

(4.18) defines the waiting time constraints for each appliance ‘i’.

$$\Delta T \times \sum_{t=Tstart_{signal}(i)}^{Tstart_{signal}(i)+24h} logic\ NOT(\mathfrak{b}_{appl}(i,t)) \leq T_{max\ wait}(i) \quad (4.18)$$

where $T_{max\ wait}(i)$ is the maximum waiting time of appliance ‘i’ (h) (i.e. defined by the users, or 4 hours otherwise), $Tstart_{signal}(i)$ is the time at which the HEMS receives an ON switch signal for appliance ‘i’ (h), ΔT is the sample time (h), $\mathfrak{b}_{appl}(i,t)$ is a binary variable represents the operation status of a shiftable appliance ‘i’ at time t, (4.19).

$$\mathfrak{b}_{appl}(i,t) = \begin{cases} 1, & \text{if ON} \\ 0, & \text{if OFF} \end{cases} \quad (4.19)$$

A new binary variable $\mathfrak{b}_{startup}(i,t)$ is introduced to indicate the starting up of an appliance ‘i’; $\mathfrak{b}_{startup}(i,t)$ equals 1 when the status of an appliance ‘i’ has changed from OFF to ON and equal 0 otherwise, (4.20).

$$\mathfrak{b}_{appl}(i,t+1) - \mathfrak{b}_{appl}(i,t) - \mathfrak{b}_{startup}(i,t) \leq 0 \quad (4.20)$$

Constraint (4.21) is used to keep the appliance ‘i’ in continuous operation for the complete operation cycle without being switched OFF, see (4.21).

$$\Delta T \times \sum_{t=Tstart_{signal}(i)}^{Tend(i)} \mathfrak{b}_{appl}(i,t) = T_{cycle}(i) \quad (4.21)$$

where $T_{\text{cycle}}(i)$ is the time needed (h) for an appliance 'i' to complete a full operating cycle, $T_{\text{end}}(i)$ is the end time of operation.

To avoid starting any appliance without a request from the user, and also to ensure the appliance is switched OFF after completing its operation cycle, the appliance status $\delta_{\text{appl}}(i, t)$ is set to 0 before the HEMS receives the start signal for appliance 'i', and after finishing the operation cycle, see (4.22).

$$\delta_{\text{appl}}(i, t) = 0 \quad \text{at } t < T_{\text{start_signal}}(i), \quad t > T_{\text{end}}(i) \quad (4.22)$$

Finally, the power drawn by shiftable home appliance 'i' at any time period can be represented by (4.23).

$$P_{\text{sh_appl}}(i, t) = P_{\text{rate_appl}}(i) \times \delta_{\text{appl}}(i, t) \quad (4.23)$$

Where $P_{\text{sh_appl}}(i, t)$ is the electric power drawn by the controllable (shiftable) appliance 'i' at time t (kW), $P_{\text{rate_appl}}(i)$ is the rated electrical power (kW) of appliance 'i'.

4.4.3.4 Imported/exported power model

The house imports energy from the main electricity grid to feed the household consumption and charges the HBSS. Also, the house exports the surplus PV energy (if it exists) to the main grid after satisfying the household demands and charging the HBSS. Two binary variables $\Phi_{\text{import}}(t)$ and $\Phi_{\text{export}}(t)$ are introduced to create a link restriction to ensure the house is only importing or exporting power at a certain time t, i.e. power at GCP flows in one direction at any given time, (4.24-4.26):

$$\Phi_{\text{import}}(t) + \Phi_{\text{export}}(t) \leq 1 \quad (4.24)$$

$$\Phi_{\text{import}}(t) = \begin{cases} 1 & , P_{\text{Grid}}(t) \geq 0 \\ 0 & , P_{\text{Grid}}(t) < 0 \end{cases} \quad (4.25)$$

$$\Phi_{export}(t) = \begin{cases} 1 & , P_{Grid}(t) < 0 \\ 0 & , P_{Grid}(t) > 0 \end{cases} \quad (4.26)$$

where $\Phi_{import}(t)$ equals 1 if the house is importing power from the main electricity grid at time t and equals 0 otherwise, $\Phi_{export}(t)$ equals 1 if the house is exporting power to the main electricity grid at time t and 0 otherwise, $P_{Grid}(t)$ is the power imported/exported by the house from the main electricity grid at time t (kW); i.e. a positive value means the house is importing power from the main electricity grid, and a negative value means exporting.

Constraints (4.27, 4.28) are used to create a link between the grid power and the binary variables $\Phi_{import}(t)$ and $\Phi_{export}(t)$

$$P_{Grid}^{import}(t) \leq \Phi_{import}(t) \times P_{Grid}^{max\ import} \quad (4.27)$$

$$P_{Grid}^{export}(t) \leq \Phi_{export}(t) \times P_{Grid}^{max\ export} \quad (4.28)$$

where $P_{Grid}^{import}(t)$ is the power imported from the main electricity grid at time t , $P_{Grid}^{export}(t)$ is the power exported to the main electricity grid at time t , $P_{Grid}^{max\ import}$ is the limit of the imported power from the main electricity grid, i.e. this value is used to control the maximum imported power (by the house) from the main electricity grid at time t . This value is assumed infinity unless specified by the electricity company. $P_{Grid}^{max\ export}$ is the limit for the exported power to the main electricity grid, i.e. this value is used also to control the maximum exported power to the main electricity grid at a time t . This value is assumed infinite, unless specified by the electricity company. Some electricity companies added a penalty to the electricity bill if the exported power to the main electricity grid increases over a certain limit.

The term $P_{GCP}(t)$ will be used to refer to the power imported/exported at a time t , (4.29), where $P_{GCP}(t)$ is the power at the GCP between the house and the main electricity grid; a

positive value means that the house is importing power from the main electricity grid while a negative value means exporting.

$$P_{GCP}(t) = P_{Grid}^{import}(t) - P_{Grid}^{export}(t) \quad (4.29)$$

4.4.3.5 System Constraints

The total active power balance equation of the household system is represented by (4.30).

$$P_{GCP}(t) + P_{HBSS}(t) = P_{houseload}(t) + \sum_{i=1}^{N_{sh}} P_{sh\ appl}(i, t) - P_{PVgen}(t) \quad (4.30)$$

where $P_{houseload}(t)$ is the household electrical load demand at time t (kW), $P_{PVgen}(t)$ is the electrical power generated by the household PV system at time t (kW), N_{sh} is the total number of the shiftable appliances in the house.

Constraint (4.31) is used to introduce an interlock between the discharging of the HBSS and exporting power to the main electricity grid. This constraint forces the HBSS to discharge power to feed the household consumption only without exporting power to the grid, thus the exported power to the main electricity grid is from only the surplus PV generation, after feeding the load demands and charging the HBSS.

$$\sigma_{B\ disch}(t) + \Phi_{export}(t) \leq 1 \quad (4.31)$$

4.4.4 Formulation of the Mixed Integer Linear Programming Optimization problem

MILP is a mathematical optimization used to solve constrained optimization problems which contain a set of variables, an objective function and a set of constraints [193], [194]. The role of the optimization is to find the best solution for the objective function in the set of solutions that satisfy the constraints (constraints can be equations, inequalities or linear

restrictions on the type of a variable). The mathematical formulation of the MILP problem is expressed as follows:

$$\text{Objective:} \quad \text{minimize} = Cx$$

$$\text{Constraints:} \quad A \cdot x \leq b$$

$$x_{min} \leq x \leq x_{max}$$

where $x \in Z^n$ C, b are vectors and A is a matrix,

A solution that satisfies all constraints is called a feasible solution. Feasible solutions that achieve the best objective function value are called optimal solutions.

The daily household energy costs C_{house} , (4.32), which need to be minimized, must be reformulated in terms of payments, incomes and battery degradation costs, i.e. instead of (4.1).

$$C_{house} = C_{house \text{ import}} + C_{house \text{ export}} + C_{HBSS_d} \quad (4.32)$$

The daily household energy cost function, C_{house} , is formulated as a MILP optimization problem, in which: (a) the HBSS model is fed into the power calculations of the MILP optimization problem, i.e. $P_{HBSS}(t)$ in (4.30), and the constraints of the HBSS model (4.6-4.15) are considered as a MILP optimization constraints, (b) The shiftable appliances' model is fed into the power calculations of the MILP optimization problem, i.e. $P_{sh \text{ appl}}(i, t)$ in (4.30), and the constraints (4.18-4.22) are considered as a MILP optimization constraints, (c) The battery degradation model is fed into the cost function equation, i.e. C_{HBSS_d} in (4.32), to count for the battery degradation costs into the optimization problem.

There are three different approaches for solving MILP problem, namely, Branch and Bound, Cutting Plane and Feasibility Pump. MILP problems are generally solved using a branch-and-bound algorithm [195]. Basic linear programming (LP)-based branch and bound algorithms (Known as Tree search) can be discussed as follows. Start with the original mixed

integer linear problem and remove all restrictions, the resulting problem is called “linear programming relaxation” of the original problem, which is solved using the tree search algorithm. The tree is built using three main steps. Branch: pick a variable and divide the problem in two sub problems at this variable. Bound: solves the LP-relaxation to determine the best possible objective value for the node. Prune: prune the branch of the tree, i.e. the tree will not develop any further in this node if the sub problem is infeasible [195].

For example, to optimize the cost function formulated in eq. (4.32). First, the problem is solved without any constraints and a list of initial variables and solutions are obtained. Second, the constraints are applied over the obtained solutions and the infeasible ones are removed. Third, the variables which give a feasible solution are then used to generate more variables and the problem is solved again with those variables until the optimal solution is obtained.

4.4.5 Simulation procedure

The MPC-based single layer HEMS was implemented in a simulation environment such that at each sample time (i.e. two minutes in this simulation): (1) The forecasted household consumption profile, as well as the forecasted PV generation profile, for the next 24 hours is obtained from the historical data; the forecasted household consumption profile for the next day is assumed to be the same as the previous week (same day) household consumption profile (L-PWSD). This is introduced in section 3.7, and can be justified as consumption patterns follow a weakly profile, e.g. reading a book on Tuesday, shopping on Wednesday. The forecasted PV generation profile for the next day is assumed to be the same as the previous day PV generation profile (PV-PD) - the simplest way to predict sunshine tomorrow is to assume it is similar to today, (2) The values of the actual SOC level of the HBSS are updated every sample time, (3) the MILP optimization process is performed using a MATLAB script

to determine (a) the HBSS optimal power setting profile for the next 24 hours, and (b) the appliance scheduling (i.e. ON/OFF status of the shiftable appliances) for the next 24 hours; Only the appliance scheduling obtained for the next sample time ($t+1$) is sent to each appliance. Also, only the HBSS optimal power setting obtained for the next sample time ($t+1$) is sent directly to the battery power converter, (6) the previous steps are repeated every sample time to update the input variables and obtained new settings for the appliance scheduling and the HBSS.

A two minute sample time was used in this simulation, i.e. this means that the input data are scanned and the optimal HBSS power settings and appliance scheduling are updated using a two minute sample time. Using a short sample time for MPC operation enables the single-layer HEMS to respond to any changes in the system, i.e. changing of loads, PV generation, battery status, and battery SOC level, that happen in a short time. Also, a TOU tariff for purchasing electricity from the main electricity grid and a fixed feed in tariff for exported energy have been used in this simulation.

4.4.6 Results

Fig. 4. 8. shows the operation of the household system, using the MPC-based single layer HEMS, for one day in winter. Fig. 4. 8.a and Fig. 4. 8.b show that the MPC-based single layer HEMS feeds the household demands at the peak-time hours (from 16:00 to 19:00) using the HBSS, instead of importing energy from the utility during the peak tariff period (i.e. when the purchasing tariff value is high, 24.99 pence/kWh). The unwanted imported and/or exported power spikes (positive and negative values of the black profiles start from 07:00) that are observed in Fig. 4. 8.b are because of inaccurate forecasting for the load demand and PV generation, time delays between the spike occurring and the HBSS reacting, and the battery power being limited to 2.5 kW, so cannot respond to the spikes greater than that, which

therefore affects the HBSS settings leading to these spikes. These spikes are the main reason for energy wastage. The daily energy wastage ratio, due to these spikes, is calculated to be 22.3%. This value is not a good value since nearly one quarter of the generated PV energy is exported to the main electricity grid with low reward. The wastage energy should be stored in the HBSS to be used at the correct times. The daily household energy cost for this day, using the MPC-based single-layer HEMS, is £1.13.

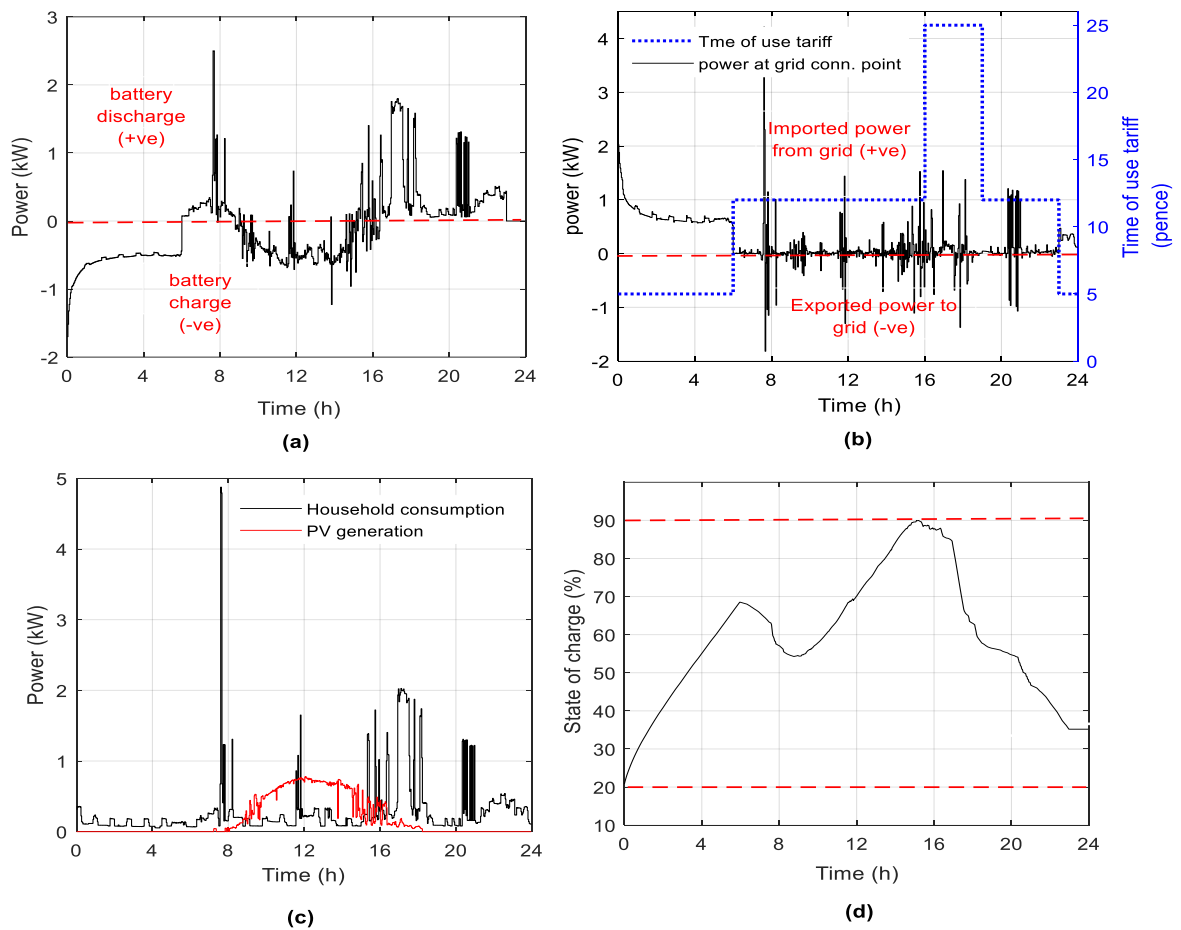


Fig. 4. 8. The operation of the household system, using the MPC-based single layer HEMS, for one day, (a) the optimal power settings delivered to the HBSS, (b) actual power measured at the GCP, and the corresponding TOU tariff, (c) the actual household demand and PV generation for the current day, (d) the daily actual SOC of the HBSS.

It is observed from Fig. 4. 8.d that the HEMS charges the HBSS during the night (from 12:00 to 06:00) up to 68% and not up to its maximum limit (i.e. 90%) because it is the optimal overnight charging level. The optimization process determines the optimal overnight charging level to enable the battery to be topped-up by the forecasted surplus PV generation during the following day, and at the same time, feed the forecasted load demand during the morning period, i.e. aim not to purchase energy from the main utility from 6:00 to 10:00.

It is worth noting that the last state point of each horizon in MPC (i.e. the last point of the SOC of the HBSS) is kept free (i.e. no constraint is set on the SOC of the battery at the end of the day) to give more flexibility to the MPC to take actions. For example, if there is a constraint over the last point of SOC of the HBSS, the HEMS will be forced to export energy to the utility (at no or low revenue) to keep the SOC of the battery at the end of the day within the set limit. Also, if the actual PV generation was more than the predicted PV generation, the MPC will not store the excess PV energy in the HBSS and export it to the utility (at no or low revenue) to keep the SOC of the battery at the end of the day as constrained. This actually decreases the PV self-consumption ratio and does not ensure the best economic use of electrical energy in the house.

For the shiftable loads (i.e. washing machine in this simulation), it is assumed that the user requested to operate the washing machine at 16:30. The single layer HEMS shifted the washing machine to operate at 20:30 (mid-peak tariff period) instead of 16:30 (peak tariff period) to reduce the cost of the energy imported from the utility, this is clear from Fig. 4. 9. The HEMS has not shifted the washing machine to operate at 23:00 (i.e. at off-peak tariff period) because the maximum waiting time for each appliance is 4 hours.

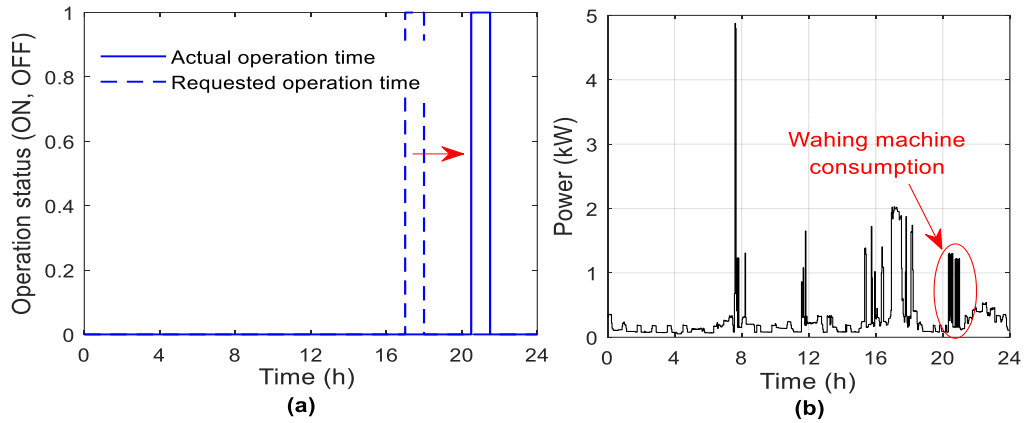


Fig. 4. 9. (a) The requested and the actual operating time of the shiftable washing machine, (b) the actual household power consumption after the operation of the washing machine at 20:30.

4.4.7 The effect of the sample time on the operation of MPC

Selecting a proper sample time is important for MPC operation. For example, selecting a 60 minute sample time for MPC operation means that the HBSS optimal power settings obtained, from the MPC optimization process, will remain constant for 60 minutes. Consequently, any change in load demand and/or PV generation during this 60 minute period will be compensated from the main electricity grid based on the balance equation of the total active power in the house (see 4.30), which may affect the overall energy costs.

On the other hand, using a two minute sample time for MPC operation, enables the MPC to respond to small changes in load demand and PV generation by updating the HBSS power settings every two minutes in a way that works for minimizing the overall energy costs and minimizing energy wastage.

Fig. 4. 10, shows the effect of using a 60 minute sample time versus a two minute sample time for MPC operation. It is clear from Fig. 4. 10.a that when using a 60 minute sample time for MPC operation, the HBSS power settings obtained remain fixed for 60 minutes. Consequently, the changes in load demand and PV generation are compensated from the main electricity grid as shown in Fig. 4. 10.b (red line). Fig. 4. 10.b shows that using 60 minute-sample time leads to purchasing energy from the main electricity grid at peak-tariff period

(i.e. from 16:30 to 17:15) at high cost. Also, unwanted exported energy is fed into the grid during the period 16:00 to 16:45 however, this energy could be stored in the HBSS to be used later instead of selling it with a low price.

When using a two minute sample time, Fig. 4. 10.a shows that the MPC updates the HBSS power settings (blue line) every two minutes to respond to load and PV generation changes (i.e. Fig. 4. 10.c) to avoid buying or selling energy from/to the utility at wrong time periods as shown in Fig. 4. 10. (blue line).

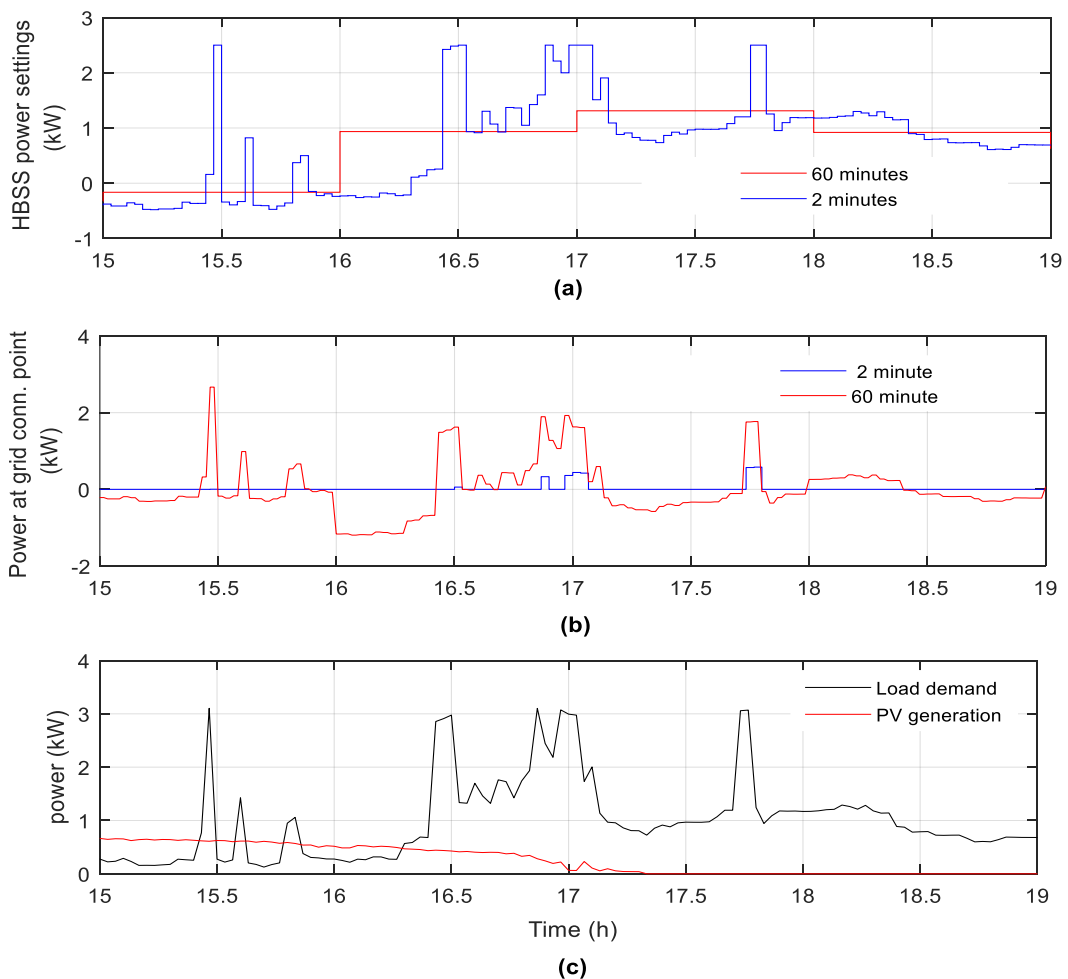


Fig. 4. 10. The effect of using a 60 minute sample time versus a two minute sample time for MPC operation. (a) The HBSS optimal power settings when using a 60 minute (red settings) and when using a two minute (blue settings), (b) the resultant power at the GCP when using a 60 minute sample time (red settings) and a two minute (blue settings), (c) load demand and PV generation profile of a two minute sample time.

To accurately show the effect of using different sample times on the operation of the MPC, the operation of the system has been simulated, using five different sample times, for one year to consider the effect of all four seasons, see Table 4. 2. The proposed MPC-based single layer HEMS has been used to manage the operation of the household system. The forecasted load demand and PV generation profiles used in this simulation are assumed ideal (i.e. zero forecasting error) to clearly study the effect of sample time only.

Table 4. 2. shows the effect of using different sample times, for MPC operation, on the annual household energy costs and the daily energy wastage ratio. It can be seen from Table 4. 2. that as long as a shorter sample time is used, a lower household energy costs and a lower energy wastage ratio are achieved. However, more computation time is needed for the MPC optimization process. Using a longer sample time (60 minutes), for MPC operation, increases the annual household energy cost by 23.2 % compared to using lower sample time (two minutes).

Table 4. 2. The effect of using different sample times on the annual household energy costs, annual energy wastage ratio, and MPC Computation time.

Sample time (minutes)	Household energy costs (£)	Energy wastage ratio	MPC Computation time* (s)
60	315.1	30.4 %	5.16
30	293	27.6 %	6.31
15	281	23.9 %	7.53
5	265	16.7 %	16.3
2	255.7	5.9 %	104

* The MPC computation time is obtained from Matlab optimization software, the optimization process is performed on a PC: Core i3-7100 CPU, 3.91 GHz

It can be seen from Table 4. 2. that the energy wastage ratio reaches up to 30.4 % in the case of using a 60 minute sample time. This means that one third of the generated PV energy is exported to the grid for no or low reward. This energy should be saved in the battery to be used at the correct times. The annual energy wastage ratio decreases from 30.4% to 5.9 % after using a shorter sampling time (two minutes). Using a short scanning and responding time of two minutes, gives a chance for the MPC controller to respond to the changes in load and generation that occur at a short sample time, therefore guarantee better performance and more reduction in costs for the householders.

It is observed from Table 4. 2. that the computation time increases exponentially as a shorter sample time is used. Using a shorter sample time increases the number of sample points in the optimization process, which means more coordination between points is required to obtain the optimal solution, which consumes more time, needs a more powerful computing platform and a larger memory. For example, if the sample time is 15 minutes, the number of sample points in the optimization process is: 96 (for 24 hour control horizon) multiplied by the number of variables, e.g. HBSS charging/discharging profile, load profile, PV profile, shiftable appliance's control profile, etc. However, if the sample time is 2 two minutes, the number of points for a 24 hour optimization process is: 720, which is then multiplied by the number of variables.

Using short sample times, for MPC operation, may conflict at some points with the computational time of the optimization process. For example, if a one minute sample time is used, and a rolling step of one minute is assumed for MPC operation, the MPC will take 5.62 minutes to perform the optimization process only (i.e. more computation time than the rolling step assumed), which makes the use of this one minute sample time infeasible. Also, the computation time of the optimization process may be longer if a more complicated system with more constraints and variables is used.

On the other hand, using a very short sample time (i.e. less than one minute) assumes using a special processing platform that computes the optimization process in less than one minute, will force the controller to respond to each change (fluctuations) that the renewable PV generation or load can have. This leads to unsmooth controller actions and may affect the HBSS lifetime since charging and discharging the HBSS, for example every one second, will expose the battery to high stress in operation.

4.4.8 The effect of forecasting uncertainties on the operation of MPC

In this section, the effect of forecasting uncertainties of both the load demand and PV generation on the annual household energy costs and the annual energy wastage ratio have been tested. The system has been simulated for one year using the forecasting methods, listed in chapter 3, for the load demand and the PV generation forecasting. TOU purchasing tariff scheme and a two minute sample time have been used in this simulation. The lowest possible sample time (two minutes) has been used to focus on studying the effect of the forecasting uncertainties only without the effect of using a long sample time. The “annual household energy cost increment ratio” index has been used in this part to show the percentage of the increment in the household energy costs when using forecasting method, compared to using ideal forecasting.

Fig. 4. 11. in the next page shows the annual average MAPE of the forecasted load demand and the forecasted PV generation profiles for the next day, using the forecasting methods listed in section 3.7. It is clear from Fig. 4. 11. that the L-FP forecasting method achieves the lowest MAPE value, compared to all the other load demand forecasting methods. However, the L-AV forecasting method achieves the highest value. It observed that there is a small difference in the MAPE value when using L-FP and L-PWSD forecasting method. This is a preliminary indication that using the simple forecasting method (L-PWSD) may achieve

a similar economic result if compared to using the complex forecasting methods (L-FP). For PV forecasting, it is observed that the PV-FP forecasting method achieves the lowest MAPE value, compared to all the other PV forecasting methods. The PV-FP forecasting method uses the forecasted meteorological data for the next day to provide an accurate forecasting for the expected PV generation.

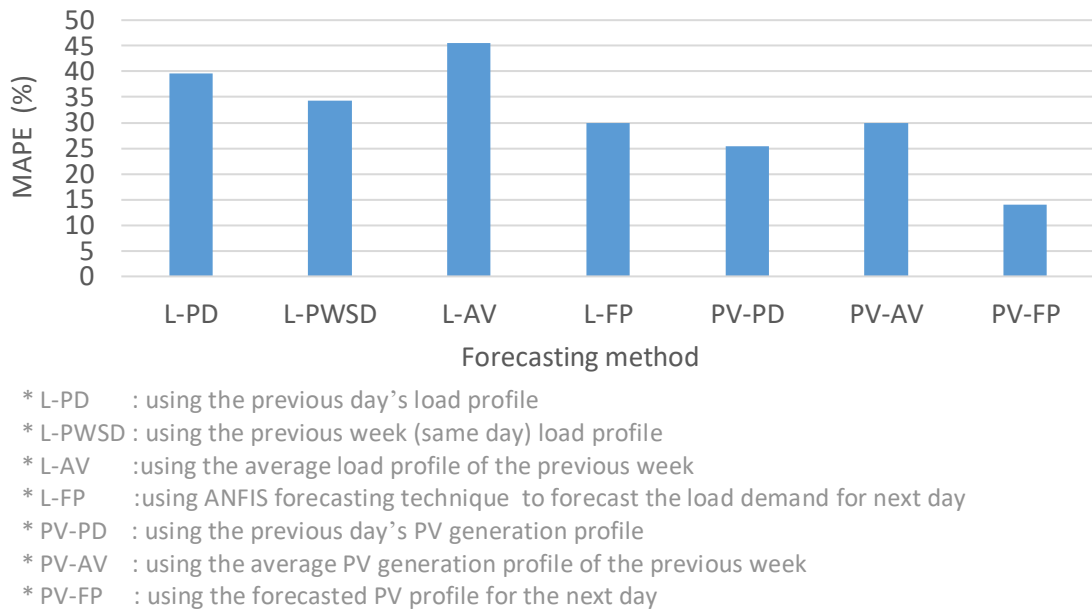
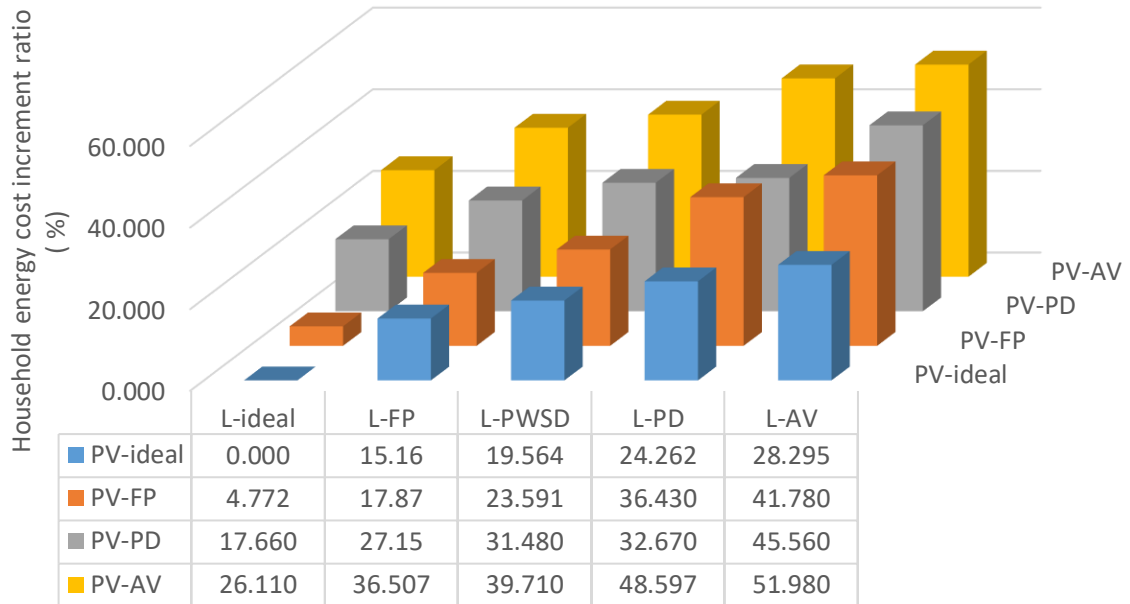
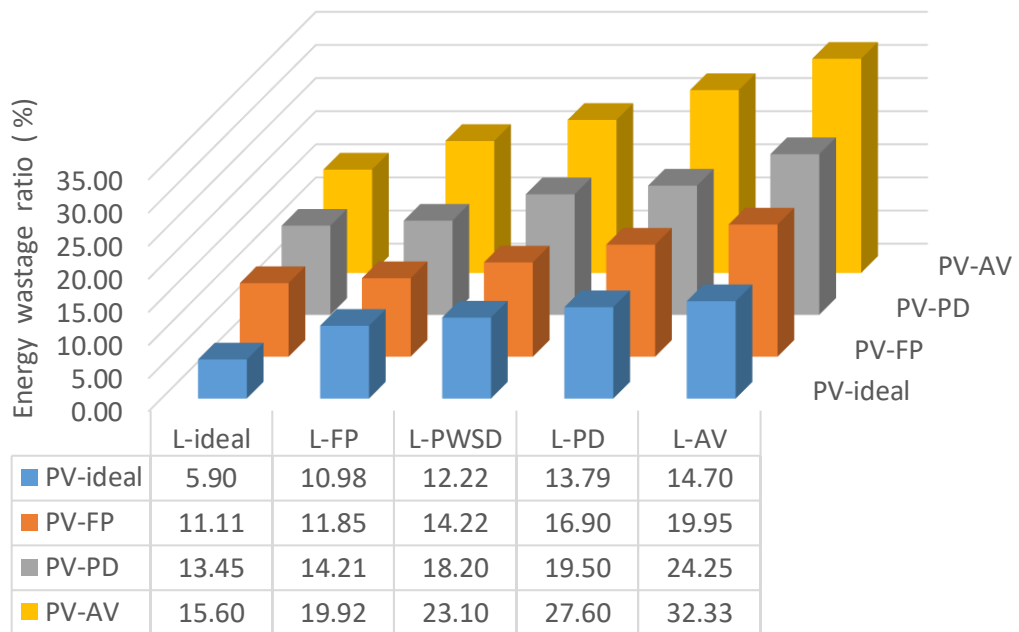


Fig. 4. 11. Annual average MAPE values of the forecasted load demand and the forecasted PV generation profiles for the next day using the forecasting methods listed in chapter 3

Fig. 4. 12. shows the effect of forecasting uncertainty for both the load demand and PV generation on the annual household energy cost increment ratio, and the annual energy wastage ratio using different forecasting methods. It is clear from Fig. 4. 12. that the forecasting uncertainty of next day load demand and PV generation greatly affect the household energy costs and the energy wastage ratio. Using the L-FP and PV-FP forecasting methods achieves a low household energy cost increment ratio (17.87%) and a low energy wastage ratio (11.85 %), compared to the using of the other forecasting methods.



(a)



(b)

Fig. 4. 12. The effect of forecasting uncertainty for both the load demand and PV generation on (a) the annual household energy cost increment ratio, and (b) the annual energy wastage ratio using TOU purchasing tariff scheme and a two minute sample time.

It is observed from Fig. 4. 12. that the household energy cost increment ratio and the energy wastage ratio reach 51.98 % and 32.33 % respectively when using the L-AV and PV-AV forecasting methods - these values are high. The wastage energy should be saved in the

HBSS to be used at the correct times instead of being exported to the main electricity grid for no or low reward. Also, it is worth noting that the actual household energy cost increment ratio and energy wastage ratio will be higher than the values obtained in Fig. 4. 12. when a longer sample time for MPC operation is used.

It can be seen from the results that MPC-based single layer HEMS is greatly affected by the forecasting uncertainty. The reason is the direct control of the HBSS using the optimal power settings obtained from the MILP optimization process. Since the MILP optimization process depends mainly on the forecasted load demand and PV generation profiles to determine the optimal HBSS settings, so as long as the forecasted load demand or PV generation profiles has high forecasting uncertainty, the obtained HBSS settings will be away from optimal, see (4.30), which leads to higher household energy costs and a higher energy wastage ratio.

4.4.9 The effect of changing purchasing tariff policy

This section studies the effect of changing the purchasing tariff policy on the performance of the MPC, and on the annual household energy costs. The sample time used in this section is two minutes. Also, ideal forecasting is assumed for both the load demand and PV generation. The daily performance of the MPC has been tested by applying the three purchasing tariff schemes: Real-Time Pricing (RTP), Time of Use (TOU), and Economy 7 (E7) respectively, see Fig. 4. 13.

It is clear from Fig. 4. 13.a that the MPC managed to control the HBSS and delivered different settings to the HBSS after using different tariff schemes. When using the RTP tariff, the MPC charged the HBSS during the period which has the lowest tariff value over the day (between 4:00 and 5:00) and used a part of the stored energy to feed the morning load (5:00 to 8:00). Also, the MPC managed to discharge the HBSS to feed the load at peak tariff value

(16:00 to 19:00). The overall performance of the MPC in this case is observed as: charging the HBSS, as much as possible, at low tariff periods and discharging it at peak tariff periods to avoid purchasing energy from the main grid at high prices. The daily household energy cost in this case is £1.38.

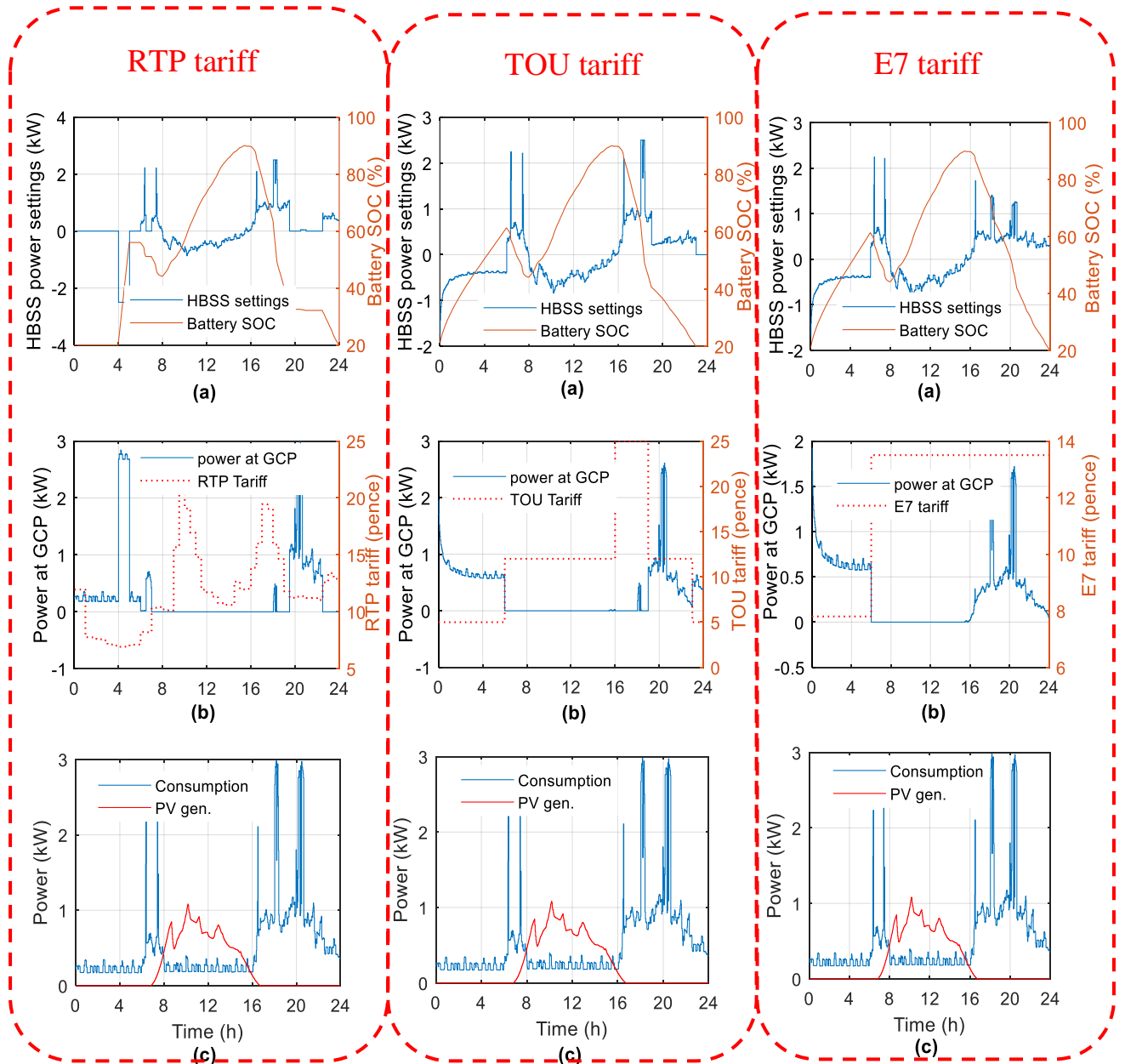


Fig. 4. 13. The daily performance of the MPC using RTP, TOU, and E7 purchasing tariff scheme respectively, (a) the optimal power settings delivered to the HBSS, and the daily SOC curve, (b) actual power measured at the GCP; a positive value means the house is importing power from the utility, and a negative value means exporting, and the corresponding purchasing tariff scheme, (c) the actual household demand and PV generation.

When using the TOU tariff scheme, the MPC managed to control the HBSS to feed the load (i.e. load less than 2.5 kW) during the peak-tariff period (between 16:00 and 19:00), to avoid buying energy from the main electricity grid at a high price during this period. The MPC charges the HBSS during the off-peak tariff period (night period in this case, from 23:00 to 6:00). The daily household energy cost in this case is £1.26.

When using the E7 tariff scheme, the MPC discharged the HBSS starting from 16:00 to 00:00, unlike the TOU tariff case, which prioritized feeding the loads at peak tariff periods only (16:00 to 19:00), i.e. see Fig. 4. 13b. when using TOU and E7 tariff respectively. The daily household energy cost when using E7 tariff scheme is £1.46.

The operation of the system has been simulated for one year to clearly quantify the effect of using different purchasing tariff schemes on the annual household energy costs and to consider the effect of all seasons. Fig. 4. 14. shows the annual household energy costs using the three purchasing tariff schemes.

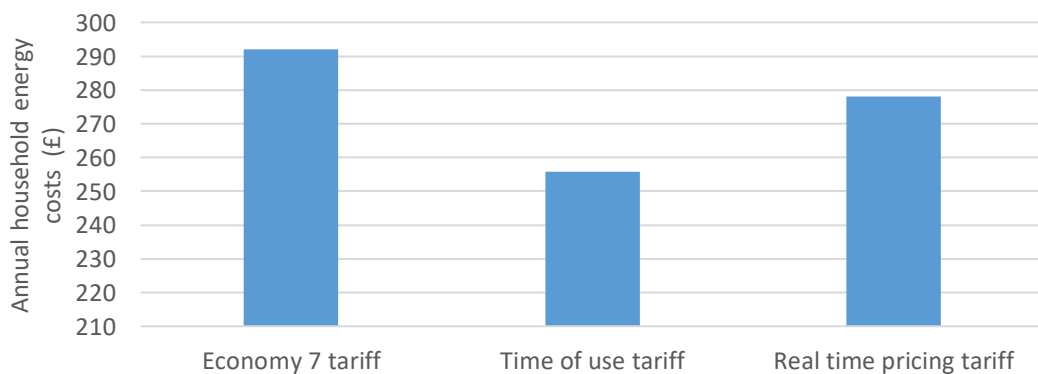


Fig. 4. 14. The annual household energy costs for the three purchasing tariff schemes.

It can be seen from Fig. 4. 14. that using the TOU tariff achieves lower household energy costs compared to using the E7 and RTP tariffs. This is because: (a) the TOU tariff offers lower energy prices during off-peak periods (i.e. 4.99 pence/kWh), compared to the E7 tariff which offers 7.8 pence/kWh for the same off-peak period, see tariff values in Fig. 4. 13b; i.e. lower energy prices during off-peak periods give the HBSS a chance to store as much energy as needed at low cost to cover the household demands through the day; (b) the TOU tariff offers lower prices at night, which give a chance to the HBSS to store as much energy as needed to cover the household demands through the day with low cost, compared to RTP tariff which may offer high prices at night. Using high tariff prices at night when RTC tariff forces the HEMS to postpone the charging of the HBSS until lower prices period, which affect the overall household energy costs, see Fig. 4. 13b. Note: the RTP tariff profile is changed every day; (c) The TOU tariff offers less tariff values at mid-peak periods (from 6:00 to 16:00 and from 19:00 to 23:00), compared to E7 tariff, which offer higher values for the same periods. This means that, when using TOU tariff, if the MPC managed to feed the loads at the peak tariff periods (from 16:00 to 19:00) from the HBSS or shift these loads to the mid-peak tariff periods, a great reduction in household costs will be achieved. Generally speaking, using TOU tariff with a PV- battery system achieves more reduction in household energy costs compared to the other purchasing tariff such as E7 or RTP.

4.4.10 Limitations of the MPC-based single layer HEMS

The limitations of the MPC-based single layer HEMS are:

- It is greatly affected by the sample time selection, i.e. using a two minute sample time enables the HEMS to respond faster to the changes in load demand and PV generation, but may conflict with the computation time of the optimization process. While, using a

60 minute sample time makes the response of the HEMS to changes in the system slower, which affects the overall energy costs and increases energy wastage.

- It is greatly affected by the forecasting uncertainties since they directly lead to inaccurate HBSS power settings and unwanted imported and/or exported power spikes that are observed in Fig. 4. 8.b.
- It fails to minimize the energy wastage, compensate for RES power fluctuations, or smooth the fluctuations of the electric power exchanges at the point of common coupling with the grid.
- Slow response for the changes in load demand and PV generation: the MPC-based single layer HEMS takes time to call the forecasted data, measure the current SOC of the battery, perform the optimization process and deliver the optimal settings to the battery.

Due to these limitations, it is mandatory to develop a more advanced HEMS to overcome the limitations of the MPC-based single layer HEMS and ensure high efficiency. The Two-Layer HEMS is considered an improvement over the MPC-based single layer HEMS because the two-layer HEMS: (a) will use a longer sample time (i.e. 15 minutes), in the upper layer to avoid the long computation time, and (b) will use a fast responding layer (lower layer) to determine the optimal power settings of the HBSS in real-time, every one minute, under the supervision of the upper layer. This is instead of directly controlling the HBSS using the upper layer only, as in MPC-based single layer HEMS, which is greatly affected by forecasting errors, sampling time and delay of signals, (c) The fast responding layer (lower layer) will minimize the energy wastage which results from forecasting errors and sample time, minimize the RES power fluctuations, smooth the fluctuations of the electric power exchanges at the point of common coupling with the grid, through determining the optimal power settings for the HBSS in real-time while taking into account the limits of the required energy stored in the HBSS every sample time period (i.e. obtained from the upper MPC layer), (d) The two-layer

HEMS ensures no direct coupling between the forecasted power of the load demand and PV generation and the battery power settings. Instead, the upper layer will focus on energy scheduling and ensuring the best economic use of electrical energy in the home, while the lower layer focuses on power balance of the system.

4.5 Hierarchical Two-Layer Home Energy Management System

This section presents a hierarchical two-layer HEMS which minimizes (a) the household energy costs and energy wastage, (b) maximizes the PV self-consumption, (c) minimizes the effect of RES power fluctuations, and (d) smooths the fluctuations of the electric power exchanges at the point of common coupling with the main electricity grid, while taking into account the battery degradation costs and the possibility of load shifting. The proposed hierarchical two-layer HEMS combines the optimization layer and control layer and points out the gap between the planned scheme and the real operation through an interactive control algorithm.

The hierarchical HEMS consists of two layers: (a) The upper layer (MPC layer) and, (b) the lower layer (RTC layer), and the two layers are combined together using an interactive control algorithm. The upper layer comprises an MPC which optimizes household energy usage using a MILP optimization. The upper layer focuses on the energy scheduling, ensuring the best economic use of electrical energy in the home, and controlling the operation of the lower layer using an interactive control algorithm. The lower layer consists of a RTC which controls the HBSS in real-time. The lower layer compensates for the effect of forecast uncertainties and sample time, minimizes energy wastage and RES power fluctuations, smooths the fluctuations of the electric power exchanges at the point of common coupling with the main electricity grid, and keeps the upper layer updated with the actual SOC of the

HBSS and any disturbance that may appear by sending feedback. The upper layer uses this feedback (every sample time) to update the initial SOC of the battery, which is essential to perform the following optimization process (new energy scheduling).

The proposed hierarchical HEMS provides two control modes: (a) control mode 1 is appropriate for the houses that only use E7 or TOU tariff schemes, or the houses that operate alone without engaging in a CES, while (b) control mode 2 is appropriate for the houses that use any type of tariff schemes (E7, TOU and RTP). Also, it is appropriate for the houses that operate as a part of a CES.

4.5.1 Structure of the Two-Layer Home Energy Management System

The Two-layer HEMS consists of (a) The upper layer (MPC layer) and, (b) The lower layer (RTC layer) and the two layers are combined together using an interactive control algorithm. The operating algorithms of these layers are explained as follows:

4.5.1.1 The Upper Layer

The upper layer of the hierarchical HEMS comprises an MPC with integrated MILP optimization, as shown in Fig. 4. 15. The upper layer focuses on energy scheduling, ensuring the best economic use of electrical energy in the house, and controlling the operation of the lower layer using an interactive control algorithm.

Every sample time, the upper layer:

1. Requests the forecasted household consumption and PV generation profiles for the next 24 hours. L-PWSD forecasting method for load forecasting and PV-PD forecasting method for PV generation forecasting have been used in this simulation.
2. It also requests the real-time measurements of the HBSS SOC to update the control model.

3. A MILP optimization process is performed to determine the 24-hour profiles with a 15-minute resolution for: (a) the stored energy in the HBSS ' $E_{MPC}(t)$ '; i.e. when using control mode 1, or the reference values of the power at the GCP ' $P_{GCP\ ref}(t)$ '; i.e. when using control mode 2. This profile is sent to the lower layer (RTC layer) to ensure optimal battery operation, see Fig. 4. 15., (b) appliance scheduling for the next 24 hour; the appliance scheduling profiles are used to control the shiftable appliances, i.e. these profiles are sent directly from the upper layer to the specific appliances, see Fig. 4. 15.
4. These steps are repeated every 15 minutes using a rolling horizon approach to update the input variables and obtain new updated settings. These settings will guarantee the best economic use of electrical energy in the home.

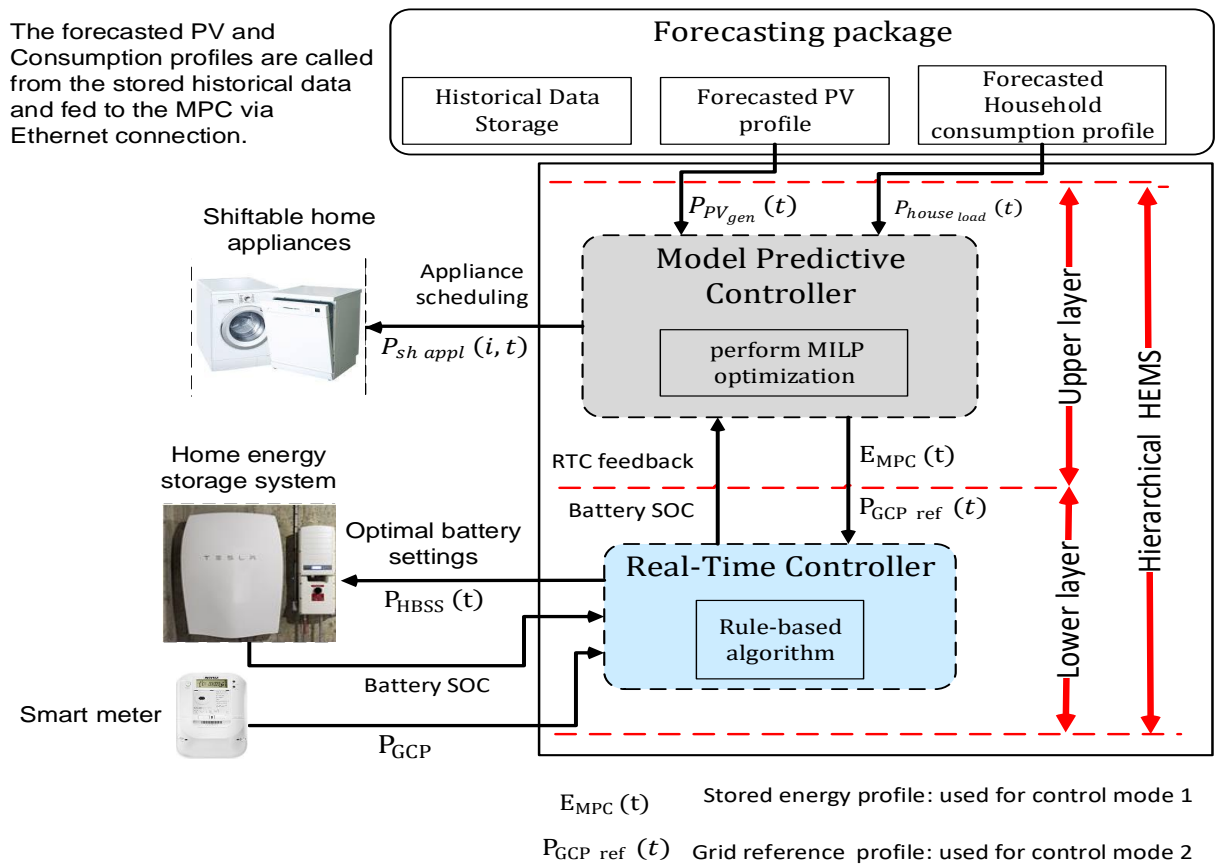


Fig. 4. 15. The hierarchical scheme of the two-layer HEMS.

4.5.1.2 The Lower Layer

The lower layer consists of a RTC, which determines the optimal power settings of the HBSS in real-time every one minute. When using control mode 1, the lower layer receives the stored energy profile for the next 24 hours ' $E_{MPC}(t)$ ' from the upper layer, and uses the rule-based control algorithm (shown in Fig. 4. 16. in the next page) to determine the optimal power settings of the HBSS in real-time. When using control mode 2, the lower layer receives the reference values profile for the power at the GCP ' $P_{GCP\ ref}(t)$ ' for the next 24 hours from the upper layer, and uses the rule-based control algorithm shown in Fig. 4. 17. to determine the optimal power settings of the HBSS in real-time.

The main difference between using control mode 1 and control mode 2 is: control mode 2 determines the reference values for the power at the house's grid connection point and the lower layer tries to follow this reference by charging and discharging the HBSS. However, in control mode 1, the lower layer compares the power at the house's grid connection point with zero and make the HBSS compensate for the difference by charging or discharging the HBSS while considering the stored energy curve received from the upper layer. Control mode 2 is appropriate for all tariff schemes (E7, TOU and RTP), and for the houses that operate as a part of a CES. For example, if the house is being operated as a part of a CES, the house should be able to accurately follow the reference profile for the power that should be shared between the house and the other community members (i.e. this profile is received from the community control centre); in this case control mode 2 is more suitable. Also, if the house is using the RTP tariff, control mode 2 is able to determine the best profile at the GCP (which fits with the used tariff) and force the lower layer to follow this reference with high accuracy, however, control mode 1 could not achieve these tasks.

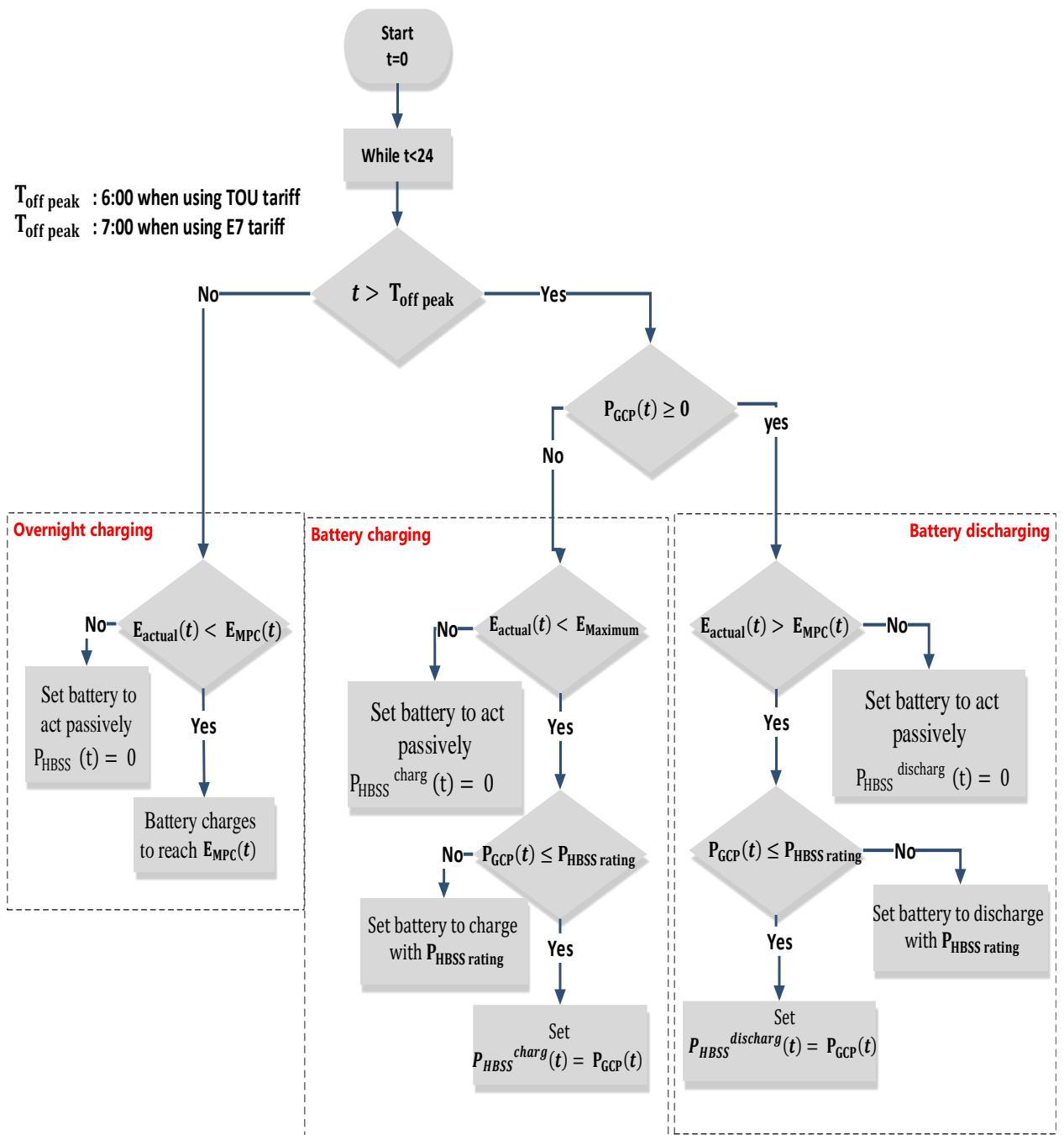


Fig. 4. 16. The rule-based control algorithm when using control mode 1 for the operation of the two layer HEMS.

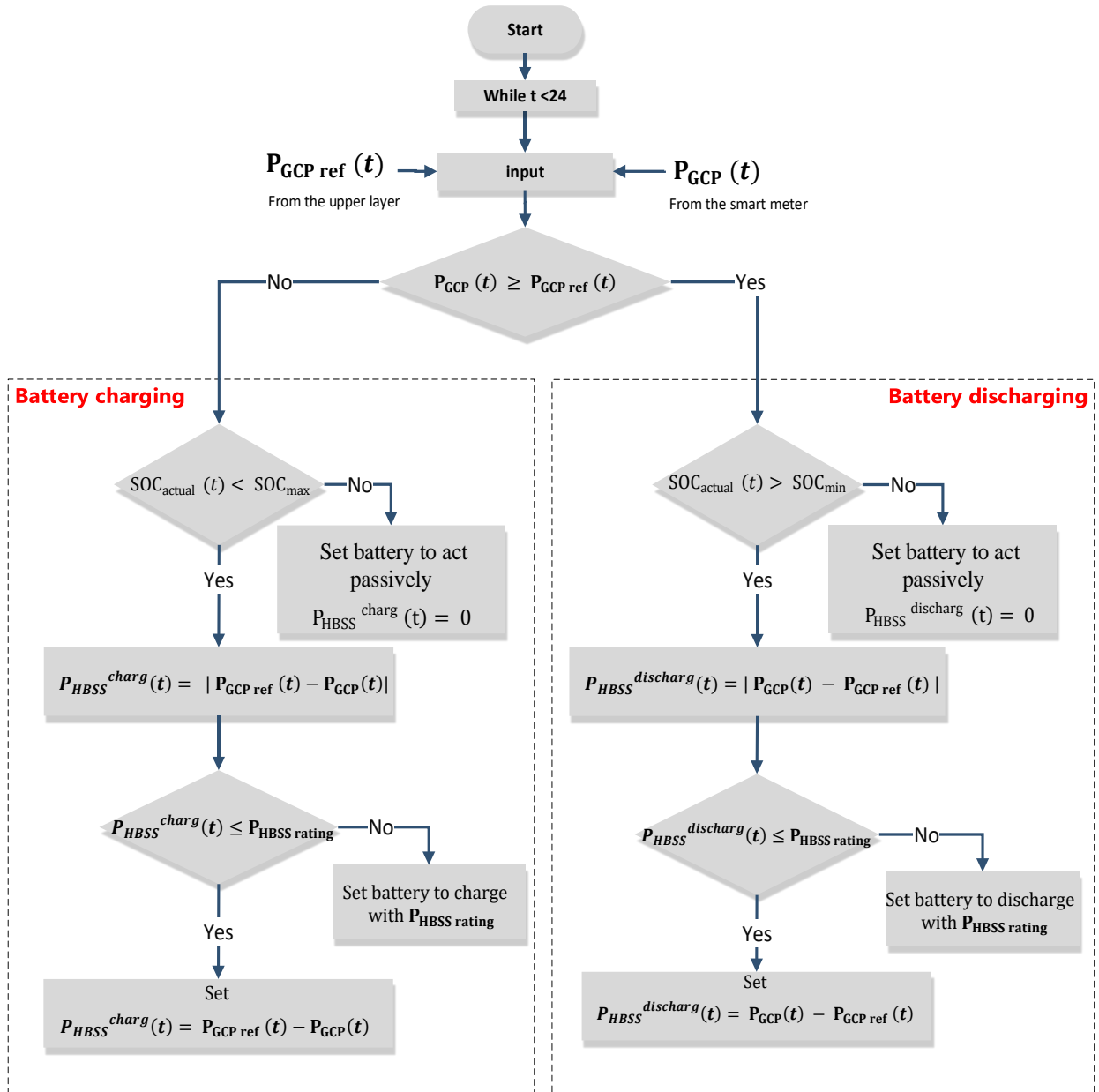


Fig. 4. 17. The rule-based control algorithm when using control mode 2 for the operation of the two-layer HEMS.

4.5.2 Results

The daily operation of the Hierarchical two-layer HEMS (using Control mode 1) has been simulated for one day as shown in Fig.4. 18. For this simulation, the TOU tariff has been used.

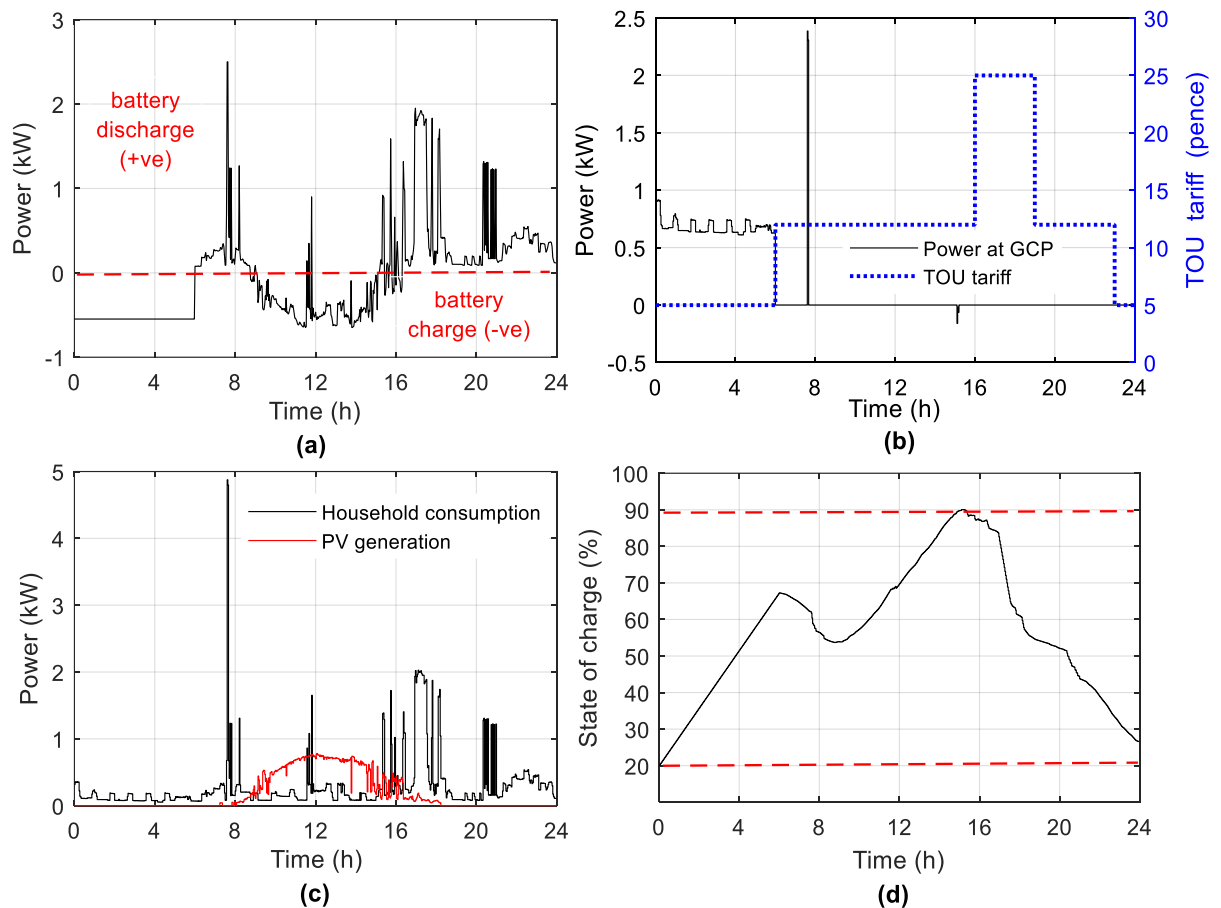


Fig. 4. 18. The daily operation of the household system using the two-layer HEMS (Control mode 1), where (a) the optimal power settings delivered to the HBSS, (b) the actual power measured at the GCP; a positive value means the house is importing power from the utility, and a negative value means exporting, and the corresponding TOU tariff, (c) the actual household demand and PV generation, and (d) the daily SOC of the HBSS.

It can be seen from Fig. 4.18. that the two-layer HEMS, using control mode 1, managed to control the HBSS in a proper way such that it provides improvements over the results shown in Fig. 4. 8. (i.e. the case in which the MPC-based single layer HEMS is used). Using the two-layer HEMS prevents the power spikes that result from forecasting uncertainties, as shown in Fig. 4. 18.b, compared to the results shown in Fig. 4. 8.b using the MPC-based single

layer HEMS. Eliminating power spikes minimizes the energy wastage and the overall energy costs. The reason for the only spike, i.e. the 2.4 kW spike at nearly 8:00 shown in Fig. 4. 18.b, is that the load at that time was 4.9 kW (see Fig. 4. 18.c), and the HBSS discharges using the maximum available power (2.5 kW) (see Fig. 4. 18.a), the remaining power is drawn from the main electricity grid.

The operation of the household system using the two-layer HEMS (as in Fig. 4. 18.) is compared to the case in which the MPC-based single layer HEMS (as in Fig. 4. 8.) is used. The daily household energy costs using the two-layer HEMS is £0.93, compared to £1.13 when using MPC-based single layer HEMS. Also, the energy wastage ratio decreased from 22.3%, when using single layer HEMS, to 0.18% after using the two layer HEMS– a very significant improvement.

Appendix C shows experimental verification for the operation of the two-layer HEMS (Control mode 1) for one day to ensure that the proposed hierarchical two-layer HEMS can be applied in a real system without difficulties. The experimental test has been implemented using the “Smart Home Rig” located at the University of Nottingham’s FlexElec Laboratory.

To consider the effect of the four seasons on the performance of the two-layer HEMS, the household system has been simulated for one year to determine the annual household energy costs and the annual energy wastage ratio, see Table 4. 3. TOU purchasing tariff has been used in this simulation. To consider the effect of forecasting uncertainty, forecasted load demand and PV generation profiles (i.e. using L-PWSD forecasting method for load forecasting, and PV-PD forecasting method for PV generation forecasting) have been used in this simulation. Table 4. 3. is showing also a comparison between the annual results obtained when operating the system using the two-layer HEMS versus using the MPC-based single layer HEMS.

Table 4. 3. The annual results for the household energy costs, energy wastage ratio, and the computation time using the two-layer HEMS versus using single layer HEMS.

	MPC-based single layer HEMS	Two-layer HEMS (mode 1)	Two-layer HEMS (mode 2)
Annual household energy costs	£332.2	£279	£283
Annual energy wastage ratio	18.2 %	7.5%	8.4%
Sample time	2 min.	MPC layer: 15 min. RTC layer: 1 min.	MPC layer: 15 min. RTC layer: 1 min.
Tariff scheme	TOU tariff		
Forecasting method	L-PWSD for load profile, PV-PD for PV profile		
Computing time	104 s	Upper layer: 6 s Lower layer: < 2 s	Upper layer: 6 s Lower layer: < 2 s

The results shown in Table 4. 3. show that using the two-layer HEMS achieves lower annual household energy costs, compared to using the MPC-based single layer HEMS. A household payment reduction of up to 16 % per annum is achieved after using the two-layer HEMS, compared to using a single layer HEMS. The annual energy wastage ratio decreased from 18.2%, when using single layer HEMS, to 7.5 % after using the two-layer HEMS (control mode 1). Overall, it is clear from Table 4. 3. that using two-layer HEMS (control mode 1 or control mode 2) achieves lower household costs, lower energy wastage, and higher PV self-consumption ratio, compared to using MPC-based single layer HEMS with the lowest possible sampling time (2 minutes).

The results in Table 4. 3. show that using control mode 1 achieves lower household energy costs and lower energy wastage and higher PV self-consumption, compared to using control mode 2. This is because control mode 1 gives margin for the HBSS to charge/discharge to compensate for forecasting uncertainty, while minimizing the power at the GCP, compared to control mode 2, which forces the HBSS to charge/discharge with

specific power values to make the household follow the reference values of the power at the GCP, i.e. obtained from the upper level, which conflicts at some stages with the system's constraints and forecasting uncertainty from the upper layer, leads to higher energy costs and lower PV self-consumption ratio.

It is clear from Table 4. 3. that the two-layer HEMS requires less computation time, i.e. 6 seconds for the upper layer and less than 2 seconds for lower layer, compared to MPC-based single layer HEMS which requires a computing time of 104 seconds. The short computing time of the two-layer HEMS means that the controller is able to provide fast responds to small changes in the system that happen in a short time, which achieves lower costs and better performance.

Also, the short computing time enables the two-layer HEMS to be used for a wider system with more complex models and constraints. For example, the upper layer in the current two-layer HEMS needs only 6 s to perform the optimization process, while this layer is executed every 15 minutes, this mean that the HEMS still have a plenty of time, which qualifies the two-layer HEMS to optimize more complex systems with more constraints. However, the MPC-based single layer HEMS requires 1.73 minutes to perform the MILP optimization process of the current system (using two minute sample time), which means that if a more complex system with more constraints is used, the MILP will need more time and hence, it will not be able to execute every two minutes as requested. In this case, a longer sample time will be used, which will result in higher energy costs (see Table 4. 2 for more details about sample time effect).

To show the effect of using the RTP tariff on the performance of the two-layer HEMS, the daily operation of the household system has been tested using the two-layer HEMS (Control mode 2) and the RTP tariff scheme, see Fig. 4. 19.

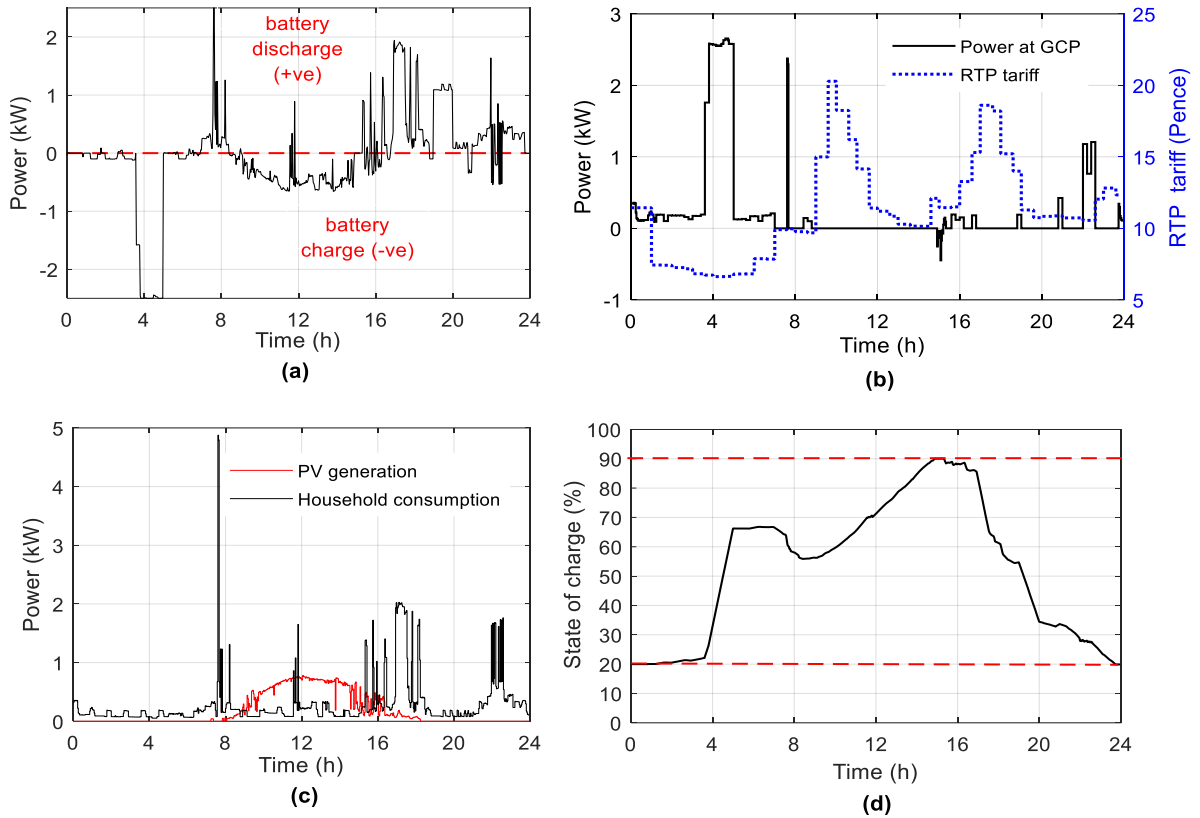


Fig. 4. 19. The daily operation of the household system, using the two-layer HEMS (Control mode 2) and RTP tariff, where (a) the optimal power settings delivered to the HBSS, (b) actual power measured at the GCP; a positive value means the house is importing power from the utility, while a negative value means exporting, and the corresponding RTP tariff, (c) the actual household power demand and PV generation, and (d) the daily SOC of the HBSS.

It can be seen from Fig. 4. 19.a and Fig. 4. 19.b that the two-layer HEM, using control mode 2, managed to control the HBSS in a proper way such that it charges the HBSS from the main electricity grid at the period of the lowest tariff values (3:30 to 5:00) and uses the stored energy to feed the loads at high peak tariff periods (17:00 to 19:00 and 09:00 to 10:30). The HEMS topped up the HBSS with the available excess PV generation between 09:00 and 15:00, as shown in Fig. 4. 19.a, to increase the PV self-consumption ratio and minimizes the energy wastage (i.e. the energy wastage ratio is 1.05 % in this case). The HEMS managed to keep the SOC of the HBSS within limits (20-90%) as shown in Fig. 4. 19.d. The HEMS managed to shift the operation of the shiftable load (washing machine) to operate at the point of the lowest tariff value (at 22:00), instead of operating at 19:30 as requested by the user.

To consider the effect of the four seasons, the operation of the household system has been simulated for one year using the two-layer HEMS (control mode 2) and RTP tariff to determine the annual household energy costs, energy wastage ratio, and PV self-consumption ratio, see Table 4. 4. Furthermore, Table 4. 4. shows a comparison between the operation of the household system using the two-layer HEMS versus using the MPC-based single layer HEMS. Forecasted load demand and PV generation profiles (i.e. using L-PWSD forecasting method for load forecasting, and PV-PD forecasting method for PV generation forecasting) have been used in this simulation.

It can be seen from Table 4. 4. that using the two layer HEMS achieves lower annual household costs and energy wastage ratio, and higher PV self-consumption, compared to using the MPC based single layer HEMS with the lowest possible sampling time (2 minutes). The two-layer HEMS managed to reduce the annual household energy costs from £351.1 (when using single layer HEMS) to £314.2. Also, the using of the two-layer HEMS achieves a lower annual energy wastage ratio (9.2 %), compared to 20.79 % in the case of using MPC based single-layer HEMS.

Furthermore, it is observed that the annual household energy costs in case of using the RTP tariff (i.e. as shown in Table 4.4.) is higher than the annual household energy in case of using the TOU tariff (i.e. as shown in Table 4. 3.), although using the same controller technology. The reason for this is due to the effect of changing purchasing tariff policy, see section 4.4.10.

Table 4. 4. The annual results for household energy costs, energy wastage ratio, and the computation time using the two-layer HEMS (control mode 2) versus using single-layer HEMS, while considering the use of RTP tariff and ideal forecasting.

	MPC-based single layer HEMS	Two-layer HEMS (mode 2)
Annual household energy costs	£351.1	£314.2
Annual energy wastage ratio	20.79 %	9.2 %
Sample time	2 min.	MPC layer: 15 min. RTC layer: 1 min.
Tariff scheme	RTP tariff	
Forecast method	Ideal forecast	
Computing time	104 s	Upper layer: 6 s Lower layer: < 2 s

4.5.3 Limitations of the two-layer HEMS

The limitations of the two-layer HEMS are:

- If the response time of the battery to the real-time controller’s settings is not fast enough, the performance of the controller may be affected.
- The hierarchical two-layer HEMS needs additional control devices (loops) to use it as part of an isolated household systems, i.e. the HBSS should operate in “grid forming” mode when used in an isolated system, compared to operating in “grid following” mode when connected to the grid.

4.6 Summary and Conclusion

The conclusions of this chapter are as follows:

For the RTC based-single layer HEMS:

- The RTC based-single layer HEMS is considered to be a fast controller since it does not require any system modelling or optimization process for its operation. It does not require any load predictions (it depends on instantaneous power measurements), therefore it is less affected by forecasting uncertainties. Furthermore, the use of instantaneous power measurements rather than predicted profiles enables it to respond quickly to the changes in load demand or PV generation. However, it does not guarantee the most cost effective operation of the system.
- Accurate adjustment of the overnight charging level for the HBSS is essential for the operation of the RTC based-single layer HEMS since it helps the controller achieves a significant reduction in the annual household energy costs and improve the PV self-consumption ratio. The best overnight charging level for the summer should be the minimum one to maximize the PV self-consumption ratio, whereas for winter the largest value should be used.
- Accurate adjustment of the overnight charging level for the HBSS using weather prediction for the next day method achieves the lowest annual household energy costs (£310.7) and the highest PV self-consumption ratio (85.7%), compared to all the other methods. However, this methods requires a continuous connection to the internet to download the weather forecast for the next day. Additional costs may be required to make a contract for a proper forecasting package that updates the system with up to date weather prediction data.
- The main drawbacks of the RTC based-single layer HEMS are: there are no predictions, it ignores battery degradation costs, it is not applicable for all tariff policies, it cannot control shiftable appliances, and it needs an accurate adjustment of the overnight charging level.

For the MPC based-single layer HEMS:

- The MPC based-single layer HEMS minimizes the daily household energy costs, maximize the PV self-consumption, while taking into account the battery degradation costs and the possibility of load shifting, compared to using the RTC-based HEMS. The MPC optimizes the system for the current sample while keeping account of changes that will happen in the future, compared to RTC based-single layer HEMS which uses instantaneous power measurements only without taking into account any future changes.
- The MPC based-single layer HEMS was able to manage the shiftable home appliances in an economic way while taking into account the comfort level of householders, compared to the RTC based-single layer HEMS which failed to manage the shiftable home appliances due to the lack of prediction.
- Using a short sample time for MPC operation enables the single-layer HEMS to respond to the changes in load and generation that occur quickly, and this guarantees better performance and a greater reduction in costs for the householders. However, more computational time is required. Using a two minute sample time, for the MPC operation, achieves a 18.8% reduction in the annual household operation costs, and a significant reduction in the energy wastage ratio (from 30.4% to 5.9%) compared to using a long sample time of 60 minutes.
- The MPC based-single layer HEMS guarantees efficient system operation when using any of the tariff policies (E7, TOU, or RTP tariff schemes), compared to the RTC based-single layer HEMS which can be used with E7 tariffs only.

- Using the TOU purchasing tariff with a PV- battery system, achieves a greater reduction in household energy costs, compared to using other purchasing tariffs such as the E7 or the RTP tariff schemes.
- Proper selection of a forecasting method for load demand and PV generation can attain a significant reduction in the energy wastage ratio (up to 20.48%) and reduces home utility bills by up to 34.11%.
- The main drawbacks of using the MPC based-single layer HEMS are that they are affected by forecasting uncertainties and the sample time.

For the two-layer HEMS:

- The two-layer HEMS managed to reduce the daily household energy costs, maximize the PV self-consumption, minimize energy wastage, minimize the effect of RES power fluctuations, and smooth the fluctuations of the electric power exchanges at the point of common coupling with the main electricity grid, while taking into account the battery degradation costs and the possibility of load shifting. The HEMS was simulated using a model of a household system, in which all the constraints that may affect the daily operation are taken into account including the degradation cost model of the battery.
- The hierarchical two-layer HEMS enabled the battery to be controlled in real-time, using RTCs, under the supervision of an MPC. Therefore, it responds to any changes in the system (i.e. changing of loads and PV generation) that happen in a short time which helps in minimizing the daily energy wastage and in compensating for RES power fluctuations.
- The two-layer HEMS is considered an improvement over the MPC-based single-layer HEMS as it compensates for the effect of forecast uncertainties and the effect of long sample times while considering the computational aspects. Using the two-layer HEMS (control mode 1) to control the HBSS through first defining the reference stored energy

profile for the HBSS for the next 24 hours and then allowing the RTC to control the HBSS in real-time, achieved better results compared to directly control the HBSS using the MPC-based single layer HEMS.

- Using the historical data for household consumption and PV generation to forecast the next day load demand and PV generation profiles minimizes the dependence on external forecasting packages that require additional meteorological data. This makes this control hierarchy reasonable for remote areas that suffer from for example a bad internet connection.
- Using the two-layer HEMS (control mode 1) achieves more reduction in the annual operating costs and a higher PV self-consumption ratio, compared to using the two-layer HEMS (control mode 2), and compared to using the MPC based single layer HEMS.
- When applying the RTP tariff, using the two-layer HEMS (control mode 2) achieves lower annual household costs (£314.2), lower annual energy wastage ratio (9.2 %), and higher PV self-consumption ratio (90.8 %) per year, compared to using the MPC based single-layer HEMS with the lowest possible sample time (two minutes) (which achieved £351.1, 20.79 %, 79.2 % for the three indices respectively).
- Using the two-layer HEMS (control mode 2) enables the house to participate in CEMS as it can receive reference values for the power at the GCP and follow it accurately.
- For the same battery size, the use of the two-layer HEMS can achieve a household payment reduction of up to 16% per annum, compared to the use of the MPC-based single layer HEMS. Also, it achieves a PV self-consumption ratio of up to 92.5% per annum, compared to using the single layer HEMS which achieves only 81.8%.
- Experimental test has been implemented to ensure that the proposed hierarchical two-layer HEMS can be applied for a real system without any difficulties and can achieve better results compared to the MPC based-single layer HEMS.

Chapter 4 has investigated energy management for a single residence. The work presented in this chapter has potentially addressed objectives (1) and (2) listed in section 1.3. Chapter 5 will develop the energy management algorithms, but apply them to a community made up of several residences, to determine whether additional advantages can be derived.

Chapter 5

Distributed and Centralized Community Energy Management System

5.1 Introduction

This chapter extends the concept of energy management to a community made up of several domestic residences. The aim here is to demonstrate that a residence can earn greater rewards by operating as a prosumers in a community energy scheme.

Novel centralized and decentralized hierarchical Community Energy Management Systems (CEMSs) are introduced in this chapter. The two CEMSs facilitate energy trading between prosumers in the energy community by coordinating the operation of the distributed HBSSs and the shiftable home appliances (located in each house), either in a centralized or a decentralized way, to achieve a further reduction in the daily household energy costs for each house, compared to being operated individually (not being a part of the CES). The CEMSs maximize the local PV self-consumption, and smooth the fluctuations of the electric power exchanges at the point of common coupling with the main electricity grid, while taking into account battery degradation costs and the possibility of load shifting.

Two types of CEMSs are presented: (a) Distributed CEMS, and (b) Centralized CEMS. The distributed CEMS controls the HBSS and the shiftable appliances located in each house using distributed controllers fitted in each house, while the centralized CEMS controls the HBSS and shiftable appliances located in each house in a centralized way using a community control centre.

5.2 Architecture of the Community Energy System

A CES of four houses has been used as the case study in this chapter. Each house includes common home appliances, a rooftop PV generation system, a HBSS, and shiftable home appliances. Each house can share excess energy with the other neighbour houses in the CES. Also, all the house are connected to the main electricity grid to import/export any required energy. Fig. 5. 1. shows the architecture of the CES. Four houses have been included in this study because this is the minimum number of houses that should be used to clearly show the operation of the energy management algorithm which will be presented in section 5.3 (i.e. distributed peer to peer energy management system).

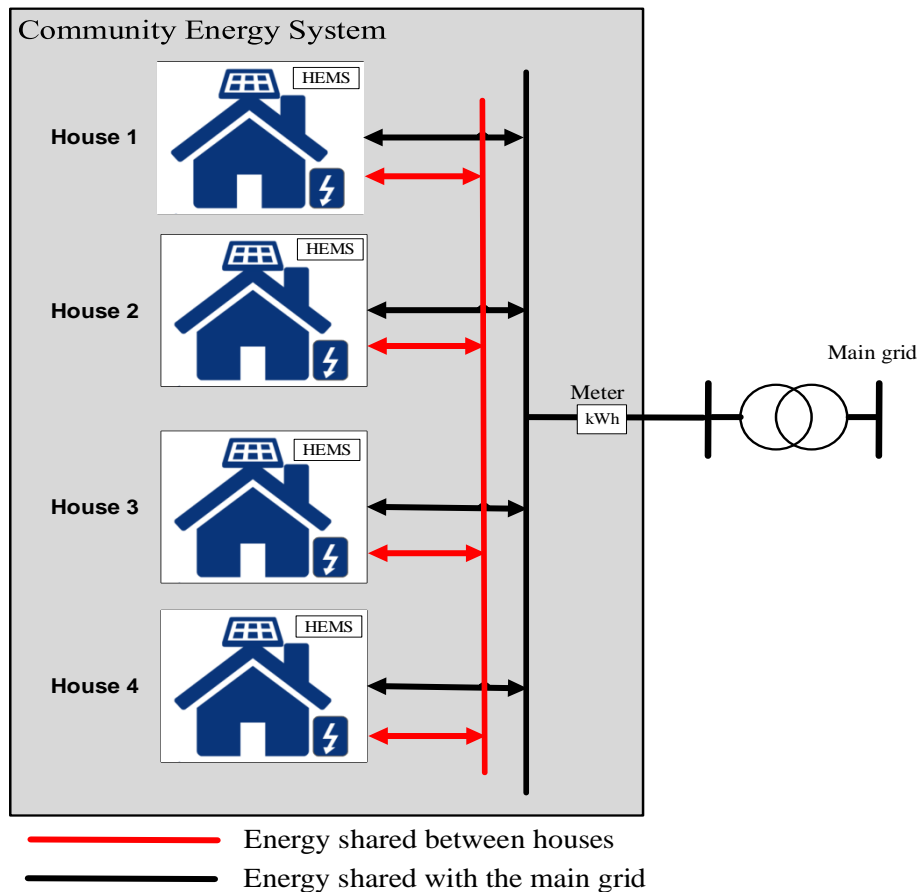


Fig. 5. 1. The architecture of the CES.

Table 5.1 presents more details for the four houses used in the CES. The load consumption data used for each house are based on the real data described in section 3.2. This data was combined with the real PV generation profile described in section 3.3. The PV generation profile was scaled for each house to be equivalent to the PV generation shown in Table 5.1., which was assumed to be suitable for the houses under study. The same PV profile – but with different scale- has been used for each of the four houses, since these houses are assumed to be in the same area (have nearly the same solar radiation). It is important to note that the algorithm which will be introduced in section 5.3 is a general algorithm and can manage different households with different PV profiles.

Table 5. 1. Data and parameters of the four houses

	House 1	House 2	House 3	House 4
Annual Load	4104 kWh	7493 kWh	6689 kWh	4772 kWh
PV generation system	1.4 kW	3.5 kW	2.8 kW	2.1 kW
Annual PV generation	1358 kWh	3395 kWh	2716 kWh	2037 kWh
Battery storage system [42]	6.4 kWh (η_b 95%)	13.5 kWh (η_b 90%)	13.5 kWh (η_b 90%)	6.4 kWh (η_b 95%)
Battery's power converter [167]	2.5 kW (η_{conv} 96%)	5 kW (η_{conv} 96%)	5 kW (η_{conv} 96%)	2.5 kW (η_{conv} 96%)
Shiftable load (Washing machine)	1 kW	1.1 kW	No	0.9 kW
Capital cost of the HBSS system (CC_{bat}) [14], [42]	£3000	£6300	£6300	£3000
Number of life cycles of the battery (N_{cycle}) [42]	5000	5000	5000	5000

5.3 Distributed Community Energy Management System

The distributed CEMS aims to achieve a further reduction in the daily household energy costs for each house in the CES, compared to being operated individually, by coordinating the operation of the distributed HBSSs and shiftable home appliances located in each house using distributed controllers. First, the daily household energy cost of each house is optimized as a single system. Then, the results are further improved through a Peer-to-Peer (P2P) operating mode in which house pairs are selected if they can achieve greater reductions in daily operating cost if they can share their surplus energy rather than importing/exporting energy with the main electric grid. this process is repeated every 15 minutes using a rolling horizon approach to update the input variables and obtain new updated settings.

5.3.1 Structure of the Distributed Community Energy Management System

The distributed CEMS consists of three levels, as shown in Fig 5. 2., (a) the Home Energy Management level (HEML), (b) the Peer-to-Peer Energy Management level (P2PEML), and (c) the Selection level.

5.3.1.1 The Home Energy Management Level

The lowest level of the hierarchical distributed CEMS is the HEML. In this level, each house is optimized alone as a single system, without sharing any energy with neighbouring houses, to determine its own minimum daily energy cost $C_{house}^{single(x)}$. In this stage, the house is only allowed to import/export any required energy with the main electricity grid. At this level, the operation of the house is optimized individually using the upper layer (MPC layer) of the hierarchical two-layer HEMS installed in each house, see Fig 5. 2.a.

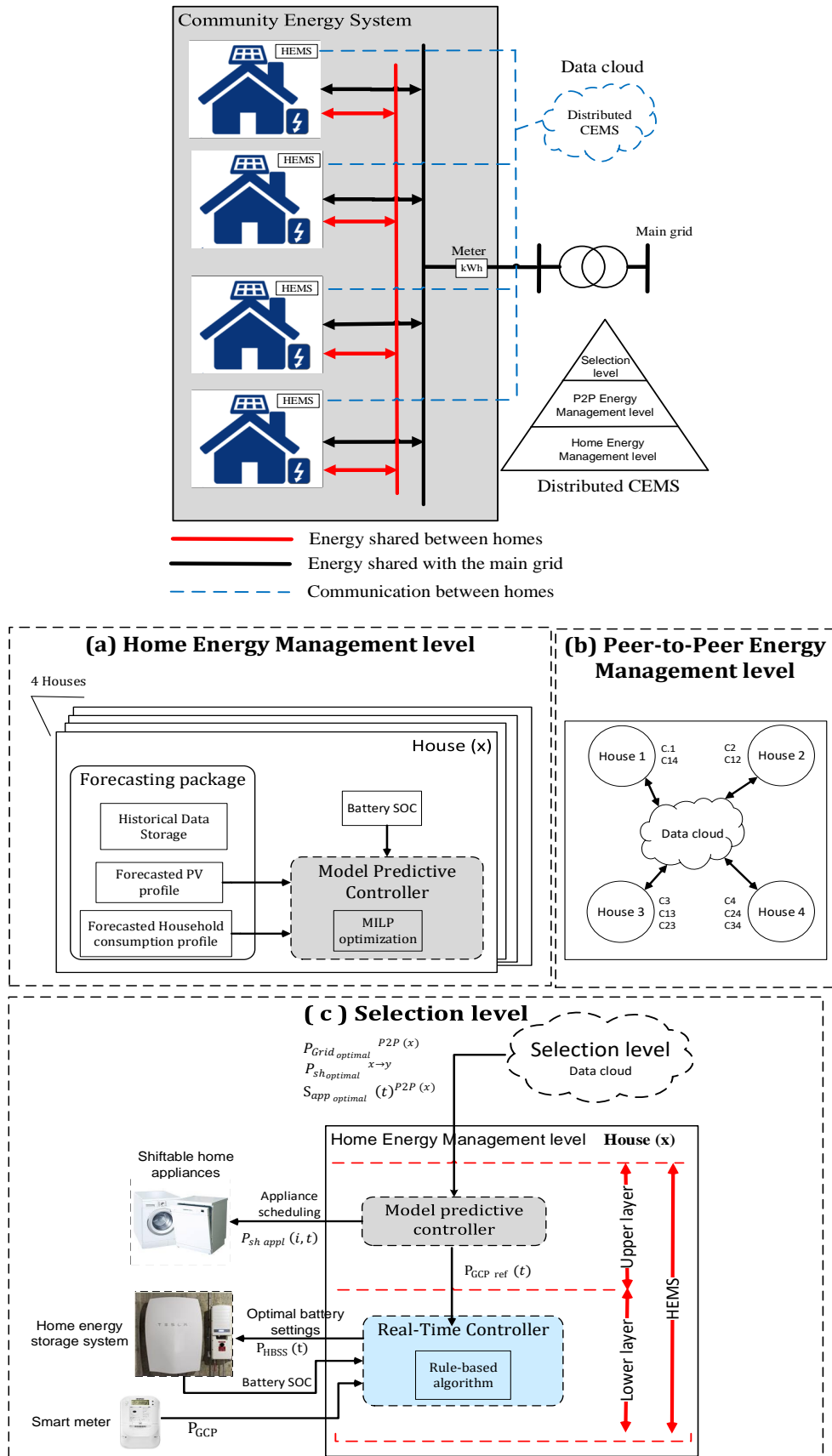


Fig. 5. 2. The hierarchical Distributed CEMS.

Every sample time ΔT (i.e. 15 minutes in this case), the HEML (using the MPC layer of the HEMS):

1. Requests the forecasted household consumption and PV generation profiles for the next 24 hours. It also requests the real-time measurements of the SOC of the HBSS to update the control model.
2. Perform a MILP optimization process to determine: (a) the minimum daily household energy cost for the house as a single system $C_{house}^{single(x)}$, (b) the 24-hour profiles with 15-minute resolutions for the reference values of the power at the GCP between the house and the main electricity grid $P_{Grid}(t)^{single(x)}$, and (c) the 24-hour profiles with 15-minute resolutions for the optimal scheduling of the shiftable appliances in the house $S_{appl}(i, t)^{single(x)}$.
3. Uploads all the results and the settings obtained from the optimization process to a data cloud. Also, it uploads the data of forecasted household consumption and PV generation profiles for the next 24 hours, and the real-time measurements of the SOC of the HBSS.
4. These steps are repeated every 15 minutes using a rolling horizon approach to update the input variables and obtain new updated settings. These settings will guarantee the best economic use of electrical energy in the home.

5.3.1.2 The P2P Energy Management Level

P2PEML is used to optimize the operation of each pair of houses in a sequential way by using a joint optimization process. This level uses the data available in the data cloud, and the MPC layer of the hierarchical two-layer HEMS platform, installed in each house, to optimize the operation of the expected house pairs as follows:

For each pair of houses, i.e. house (x) and house (y), a joint optimization process (will be explained in details in section 5.3.2) is performed to determine: (a) the minimum daily energy cost of each pair C_{P2P} , (b) the 24-hour profiles with 15-minute resolutions for the power shared between the paired houses $P_{sh_{optimal}}^{x \rightarrow y}$, (c) the 24-hour profiles with 15-minute resolutions for the reference values of the power shared between the house (x) and house (y) from one side and the main electricity grid $[P_{Grid_{optimal}}^{P2P(x)} P_{Grid_{optimal}}^{P2P(y)}]$, (d) the 24-hour profiles with 15-minute resolutions for the optimal scheduling of the shiftable appliances in the house (x) and house (y) respectively $[S_{app_{optimal}}(i, t)^{P2P(x)} S_{app_{optimal}}(i, t)^{P2P(y)}]$.

The MPC layer in each house, is responsible for a certain joint optimization process besides one individual optimization process. For example, the MPC layer in house no. 1 is responsible for (a) the joint optimization of the house no. 1 and the house no. 4 (i.e. C14 optimization), and (b) its own individual optimization process (i.e. C1 optimization) which is performed as a part of HEML, see Fig 5. 2.b. The same for the MPC layers in houses no. 2, 3, and 4. It is worth noting that both the joint optimization process and individual optimization process are repeated every 15 minutes using a rolling horizon approach to update the input variables and obtain new updated settings. These settings will guarantee the best economic use of electrical energy in the home. Finally, all the results and the settings obtained from the P2PEML are uploaded to the data cloud.

5.3.1.3 The Selection level

Selection level is used to select the most promising pair of houses in a sequential way as follows:

1. From the solution obtained from P2PEML, only pairs of houses where the value of the C_{P2P} function is lower than the sum of its $C_{house}^{single(x)}$ cost functions are considered (feasible pairs). The number of available pair solutions is $N_{houses} \times (N_{houses} - 1)/2$.
2. Among these feasible pairs, the pair with the highest percentage reduction in household energy cost is selected (e.g. pair i, j).
3. All other solutions that contain one of the pairs that has already been selected in the last step is deleted.
4. From the remaining feasible pairs, after removing pairs selected in step 2, the pair with the second highest percentage reduction in operating cost is selected. A new pair (e.g. pair k, p) is selected. This process is repeated until all pairs are determined.

The selection level determines all promising pairs of houses and prepares the final optimal settings in data arrays to be ready for calling from the HEMS platform fitted in each house; note: the selection process is performed in the data cloud. Finally, the hierarchical HEMS platform fitted in each house extracts the final decision from the selection level (data cloud) and implements the optimal settings as follows, see Fig 5. 2.,c.

1. The 24-hour profiles with 15-minute resolutions for the reference values of the power shared between the house (x) and the main electricity grid $P_{Grid_{optimal}}^{P2P(x)}$, and the 24-hour profiles with 15-minute resolutions for the power shared between the house (x) and the paired house within the community $P_{sh_{optimal}}^{x \rightarrow y}$ are merged into a new profile, see eq. (5.1). This profile is sent to the lower layer of the two-layer HEMS fitted in the house (x). Then, the lower layer of the HEMS determines the optimal power settings for the HBSS using the rule-based controller shown in Fig. 4. 17.

$$P_{GCPref}(t)^{(x)} = P_{Grid_{optimal}}^{P2P(x)} + P_{sh_{optimal}}^{x \rightarrow y} \quad (5.1)$$

2. Appliance scheduling profiles for house (x) $S_{app_{optimal}}(i, t)^{P2P(x)}$, are used to control the shiftable appliances in the house, i.e. these profiles are sent directly to the each appliance.

5.3.2 Formulation of the joint optimization problem

The cost function for a paired house (house (x) and house (y)), which needs to be minimized C_{P2P} , can be formulated as (5.2, 5.3):

$$C_{P2P} = C_{house}^{(x)} + C_{house}^{(y)} \quad (5.2)$$

$$C_{house}^{(x)} = C_{house \text{ import}} + C_{house \text{ export}} + C_{HBSS_d} - C_{house_{sh}} \quad (5.3)$$

$$C_{house \text{ import}} = \sum_{t=t_0}^{t_0+24h} \Delta T \times f_{import}(t) \times P_{Grid}(t) \quad , \text{ at } P_{Grid}(t) > 0 \quad (5.4)$$

$$C_{house \text{ export}} = \sum_{t=t_0}^{t_0+24h} \Delta T \times f_{export}(t) \times P_{Grid}(t) \quad , \text{ at } P_{Grid}(t) < 0 \quad (5.5)$$

$$C_{HBSS_d} = \sum_{t=t_0}^{t_0+24h} \left(\frac{CC_{bat} \times \eta_{Conv} \times \eta_c \times \Delta T \times P_{HBSS}^{charg}(t)}{B_{capacity} \times 2 \times N_{cycle}} + \frac{CC_{bat} \times \Delta T \times P_{HBSS}^{disch}(t)}{B_{capacity} \times \eta_{Conv} \times \eta_d \times 2 \times N_{cycle}} \right) \quad (5.6)$$

$$C_{house_{sh}} = \begin{cases} \Delta T \times \sum_{t=t_0}^{t_0+24h} f_{sh \text{ exp}}(t) \times P_{sh}^{x \rightarrow y}(t) & , P_{sh}^{x \rightarrow y}(t) > 0 \\ \Delta T \times \sum_{t=t_0}^{t_0+24h} f_{sh \text{ imp}}(t) \times P_{sh}^{x \rightarrow y}(t) & , P_{sh}^{x \rightarrow y}(t) < 0 \end{cases} \quad (5.7)$$

where $C_{house}^{(x)}$ is the daily electrical energy cost of the house (x) (£), $C_{house}^{(y)}$ is formulated in the same way as $C_{house}^{(x)}$, $C_{house \text{ import}}$ is the daily cost of the electrical energy purchased from the main electricity grid for house (x) (£), $C_{house \text{ export}}$

is the daily cost of the exported electrical energy from the house (x) to the main electricity grid (£), C_{HBSS_d} is the daily battery degradation cost of the battery located at house (x) (£), $C_{\text{house}_{sh}}$ is the daily cost of the shared energy between the house (x) and the paired house (y) in the community, ΔT is the sample time (h), $P_{\text{grid}}(t)$ is the electrical power imported/exported from the main electricity grid (kW) at a time t, $f_{\text{import}}(t)$ is the electricity purchase tariff from the main electricity grid a time t (£/kWh), $f_{\text{export}}(t)$ is the electricity sale tariff (i.e. feed in tariff) to the main electricity grid at a time t (£/kWh), CC_{bat} is the capital cost of the battery (£). N_{cycle} is the typically number of life cycles of the battery, B_{capacity} is the rated capacity of the battery (kWh), $P_{\text{HBSS}}^{\text{disch}}(t)$ and $P_{\text{HBSS}}^{\text{charg}}(t)$ are respectively the HBSS discharge and charge powers at a time t (kW); $P_{\text{HBSS}}^{\text{disch}}(t)$ is always a positive value while $P_{\text{HBSS}}^{\text{charg}}(t)$ is always a negative value, η_d, η_c are the battery discharging and charging efficiencies respectively (%), η_{conv} is the efficiency of the power converter (%), $f_{\text{sh exp}}(t)$ is the electricity export tariff for the energy shared between the paired houses (£/kWh), $f_{\text{sh imp}}(t)$ is the electricity import tariff for the energy shared between paired houses (£/kWh), $P_{\text{sh}}^{x \rightarrow y}(t)$ is the electric power flow from house (x) to house (y) (kW).

The following constraints (5.8-5.14) are used to introduce the link restrictions between the different houses to ensure that the power shared between houses at each sample time, flows in one direction only.

$$P_{sh}^{x \rightarrow y}(t) + P_{sh}^{y \rightarrow x}(t) = 0 \quad (5.8)$$

$$\sigma_{sh}^{x > y}(t) = \begin{cases} 1 & , P_{sh}^{x > y}(t) > 0 \\ 0 & , P_{sh}^{x > y}(t) \leq 0 \end{cases} \quad (5.9)$$

$$\sigma_{sh}^{y > x}(t) = \begin{cases} 1 & , P_{sh}^{y > x}(t) \geq 0 \\ 0 & , P_{sh}^{y > x}(t) < 0 \end{cases} \quad (5.10)$$

$$\sigma_{sh}^{x > y}(t) + \sigma_{sh}^{y > x}(t) \leq 1 \quad (5.11)$$

$$P_{sh}^{x>y}(t) \leq \delta_{sh}^{x>y}(t) \cdot P_{sh,max}(t) \quad (5.12)$$

$$P_{sh}^{y>x}(t) \leq \delta_{sh}^{y>x}(t) \cdot P_{sh,max}(t) \quad (5.13)$$

$$P_{losses}^{x>y}(t) = \eta_{loss}^{x>y}(t) \cdot P_{sh}^{x>y}(t) \quad (5.14)$$

where $\delta_{sh}^{x>y}(t)$ is a binary variable; i.e. equals 1 if the energy, at a time t, is flowing from the house (x) towards the house (y) and 0 otherwise, $\delta_{sh}^{y>x}(t)$ is a binary variable; i.e. equals 1 if the energy, at a time t, is flowing from the house (y) towards the house (x) and 0 otherwise, $P_{sh,max}(t)$ is the maximum limit for the power shared between house (x) and house (y); this value could be adjusted upon request, otherwise; this value is set to infinity, $\eta_{loss}^{x>y}(t)$ is the transmission efficiency (%); this value is adjusted by the community operators based on the distance between houses in the community.

The interchange of energy between two houses is subject also to transport losses which can be modelled as (5.15).

$$P_{sh}^{x\rightarrow y}(t) = P_{losses}^{x\rightarrow y} + P_{net_sh}^{x\rightarrow y}(t) \quad (5.15)$$

where $P_{losses}^{x\rightarrow y}$ is the power losses (kW) through the power transmission between house (x) and house (y); if the energy is flowing from the house (x) towards the house (y), the absolute value of the energy received by (y) is equal to the energy which leaves the house (x), minus the transport losses.

When the two houses are working as a network, the energy balance equation for each house must be reformulated as follows (5.16-5.18), i.e. instead of (4.30):

For house (x):

$$P_{Grid}^x(t) + P_{HBSS}^x(t) - P_{sh}^{x\rightarrow y}(t) = P_{load}^x(t) + P_{sh\ appl}^x(i, t) - P_{PV}^x(t) \quad (5.16)$$

For house (y):

$$P_{Grid}^y(t) + P_{HBSS}^y(t) - P_{sh}^{y \rightarrow x}(t) = P_{load}^y(t) + P_{sh\ appl}^y(i, t) - P_{PV}^y(t) \quad (5.17)$$

For house (x) and (y):

$$\begin{aligned} \sum_{n=x,y} \{P_{Grid}^n(t) + P_{HBSS}^n(t)\} - P_{losses}^{x>y}(t) - P_{losses}^{y>x}(t) \\ = \sum_{n=x,y} \{P_{load}^n(t) + P_{sh\ appl}^n(i, t) - P_{PV}^n(t)\} \end{aligned} \quad (5.18)$$

To prevent the HBSSs in the houses from exporting energy to the main electricity grid, the following constraint (5.19) is used to introduce link restrictions between the discharging of the HBSS and exporting power to the grid.

$$\delta_{B\ disch}^n(t) + \Phi_{export}^n(t) \leq 1 \quad \text{where } n = x, y \quad (5.19)$$

where $\delta_{B\ disch}(t)$ is a binary variable; i.e. equals 1 if the battery is discharging and equals 0 otherwise. $\Phi_{export}(t)$ is a binary variable; i.e. equals 1 if the house is exporting power to the main electricity grid at a time t and 0 otherwise.

Constraint (5.20) is used to prevent the house (x) from importing energy from the main electricity grid and at the same time exporting energy to the paired house (y). Also, constraint (5.21) is used to prevent the house (x) from exporting energy to the main grid and at the same time importing energy from the paired house (y).

$$\delta_{sh}^{x>y}(t) + \Phi_{import}^x(t) \leq 1 \quad (5.20)$$

$$\delta_{sh}^{y>x}(t) + \Phi_{export}^x(t) \leq 1 \quad (5.21)$$

where $\Phi_{export}(t)$ is a binary variable; i.e. equals 1 if the house is exporting power to the main electricity grid at a time t and 0 otherwise, $\Phi_{import}(t)$ is a binary variable; equals 1 if the house is importing power from the main electricity grid at a time t and equals 0 otherwise.

Also, all the constraints associated with each model in the household system, i.e. the constraints of the HBSS model (4.6-4.15), the constraint of the shiftable loads (4.18-4.23), and the constraints of the imported/exported power (4.24-4.28), are applied for both the house (x) and the house (y) and considered in the joint optimization problem.

The joint optimization problem is solved using the MILP optimization technique. The solution of the optimization problem for a paired houses; generates a set of optimal control variables $[P_{Grid_{optimal}}^{P2P(n)} S_{app_{optimal}}(i,t)^{P2P(n)} P_{sh_{optimal}}^{x \rightarrow y}(t)]$, where n refers to the house (x) and the house (y) respectively. The solution given by the cost function of the P2P operation must provide a more advantageous situation with respect to working as a single house (individually). An agreement is found when the next constraints (5.22, 5.23) are satisfied; i.e. the value of the cost function of house (n) when being operated using P2P algorithm, is less than the value of the cost function when being operated individually (single operation).

$$C_{house}^x ([P_{Grid_{optimal}}^{P2P(x)} P_{sh_{optimal}}^{x \rightarrow y}(t) S_{app_{optimal}}(t)^{P2P(x)}]) \leq C_{house}^x ([P_{Grid_{optimal}}^{single(x)} S_{app_{optimal}}(t)^{single(x)}]) \quad (5.22)$$

$$C_{house}^y ([P_{Grid_{optimal}}^{P2P(y)} P_{sh_{optimal}}^{x \rightarrow y}(t) S_{app_{optimal}}(t)^{P2P(y)}]) \leq C_{house}^y ([P_{Grid_{optimal}}^{single(y)} S_{app_{optimal}}(t)^{single(y)}]) \quad (5.23)$$

5.3.3 Results and Discussion

The distributed CEMS proposed in section 5.3.1 has been implemented for one day (in summer) in a simulation environment using MATLAB software. The load and generation data are based on the real data described in section 3.2 and section 3.3. respectively.

The following assumptions are considered in the simulation process: (a) the TOU tariff is used for purchasing electric energy from the main grid, (b) a fixed tariff is used for selling

electrical energy to the main grid, (c) a zero tariff (zero/kWh) is used for selling and purchasing the surplus energy between the houses, and (d) power losses are neglected. (c) and (d) have been assumed to make a fair comparison between the operation of the community when using the decentralized hierarchical CEMSs and when using the centralized hierarchical CEMSs (will be presented section 5.4.). L-PWSD forecasting method for load forecasting and PV-PD forecasting method for PV generation forecasting have been used in this simulation. In addition, the parameters of the four houses used in the simulation process, including the annual consumption, annual PV generation, and the size of the HBSS of each house, are shown in Table 5.1.

The results obtained from the simulation process are summarized in Table 5. 2. and Table 5. 3. Table 5. 2. shows the results of the selection process of the promising paired houses using the P2P optimization process. From the results obtained, it is observed that the best pair for this day is house no. 1 and house no. 2. The best pair is the pair which achieves the highest reduction in the sum of the daily household energy costs of the paired houses, compared to them being operated individually. The sum of the daily household energy costs of house no. 1 and house no. 2 is reduced by 8.97% after pairing, compared to the case of being operated individually. The second pair is house no. 3 and house no. 4, which achieves a 5.64 % reduction in the sum of the daily household energy costs.

Table 5. 3. shows the daily reduction percent in the household energy costs for each house, after selecting the best pair. It is clear from the table that the daily reduction in the household energy costs for each house varies between 0% and 16.35%. The house no. 1, which is one of the houses of the best pair, has achieved the highest reduction in daily energy cost (16.35%). However, house no. 2 which is also one of the houses of the best pair, achieves 0% reduction in cost. It is worth noting this criteria: first the distributed CEMS tries to make a reduction in the daily household energy cost for both houses (paired houses). If this is not

possible, the distributed CEMS tries to achieve a reduction in the household energy costs of least one house of the paired houses, while keeping the energy costs of the other house as if it is being operated individually, see constraints 5.22-5.23. If this is also not possible, this means that no feasible solution could achieve a further reduction in the daily costs for this pair, compared to being operated individually. The latter choice takes the lowest ranking in the selection table, see section criteria in section 5.3.1.3.

Table 5. 2. Results of the selection process of the promising paired houses using the P2P optimization process.

Pairs	Daily household energy cost (£)						Percent. reduction
	House 1	House 2	House 3	House 4	Individual operation	P2P operation	
House 1,2	0.59	0.58			1.3	1.18	8.97%
House 1,3	0.64		0.74		1.45	1.38	4.60%
House 1,4	0.67			0.51	1.25	1.18	5.65%
House 2,3		0.55	0.74		1.33	1.30	2.08%
House 2,4		0.58		0.45	1.13	1.03	8.18%
House 3,4			0.74	0.47	1.28	1.21	5.64%

Table 5. 3. The daily household energy costs of the four houses when being operated as a part of CES using distributed CEMS (P2P operation), compared to being operated individually.

	Daily energy cost (£) (individual operation)	Daily energy cost (£) (P2P operation)	Reduction percentage
House 1	0.71	0.59	16.35%
House 2	0.58	0.58	0 %
House 3	0.74	0.74	0 %
House 4	0.54	0.47	13.33 %

It is observed from in Table 5. 3. that the distributed CEMS managed to make house no. 2 help house no. 1 achieve a further reduction in the daily energy costs (16%), compared

to being operated individually-without charging house no. 2 any additional costs. It is worth noting that this operating scenario is not fixed every day. For example, the reduction percentage of the daily energy costs for house no. 2 may be higher than house no. 1 during the following days. Generally speaking, the philosophy of participating in a CES is that each house could help the other houses (if possible) to achieve a reduction in their energy costs without being charged any additional costs for its own operation.

Table 5. 3. shows that the house no. 2 and the house no. 3 have not achieved any further improvement in the reduction of the daily energy costs, compared to being operated individually. However, house no. 1, and no. 4 achieves a reduction in daily energy cost of 16% and 13.33% respectively. The reduction percent in the daily energy costs of each house is not a fixed value but it changes every day depending on many factors such as the daily household consumption and generation profiles for each house, the size and the efficiency of the HBSS in each house, and the number of participated houses in the CES.

Fig. 5. 3. shows the optimal settings obtained from the distributed CEMS for the daily operation of the best pair (house no. 1 and house no. 2). For more results, Appendix D shows the optimal settings obtained from the distributed CEMS for the daily operation of the four houses in this CES. It is observed from Fig. 5. 3.(House 1-a) and Fig. 5.3.(House 2-a) that house no. 2 exports the extra energy available from the PV generation (from 11:00 to 16:00) to house no. 1. The distributed CEMS uses the HBSS located in house no. 1 to store the surplus PV energy generated from house no. 2, instead of using the HBSS in house no. 2 to store this energy to minimize the number of operating cycles and the degradation cost of the HBSS in house no. 2, i.e. the HBSS in house no. 2 has higher operating cost and lower efficiency compared to the HBSS in house no. 1.

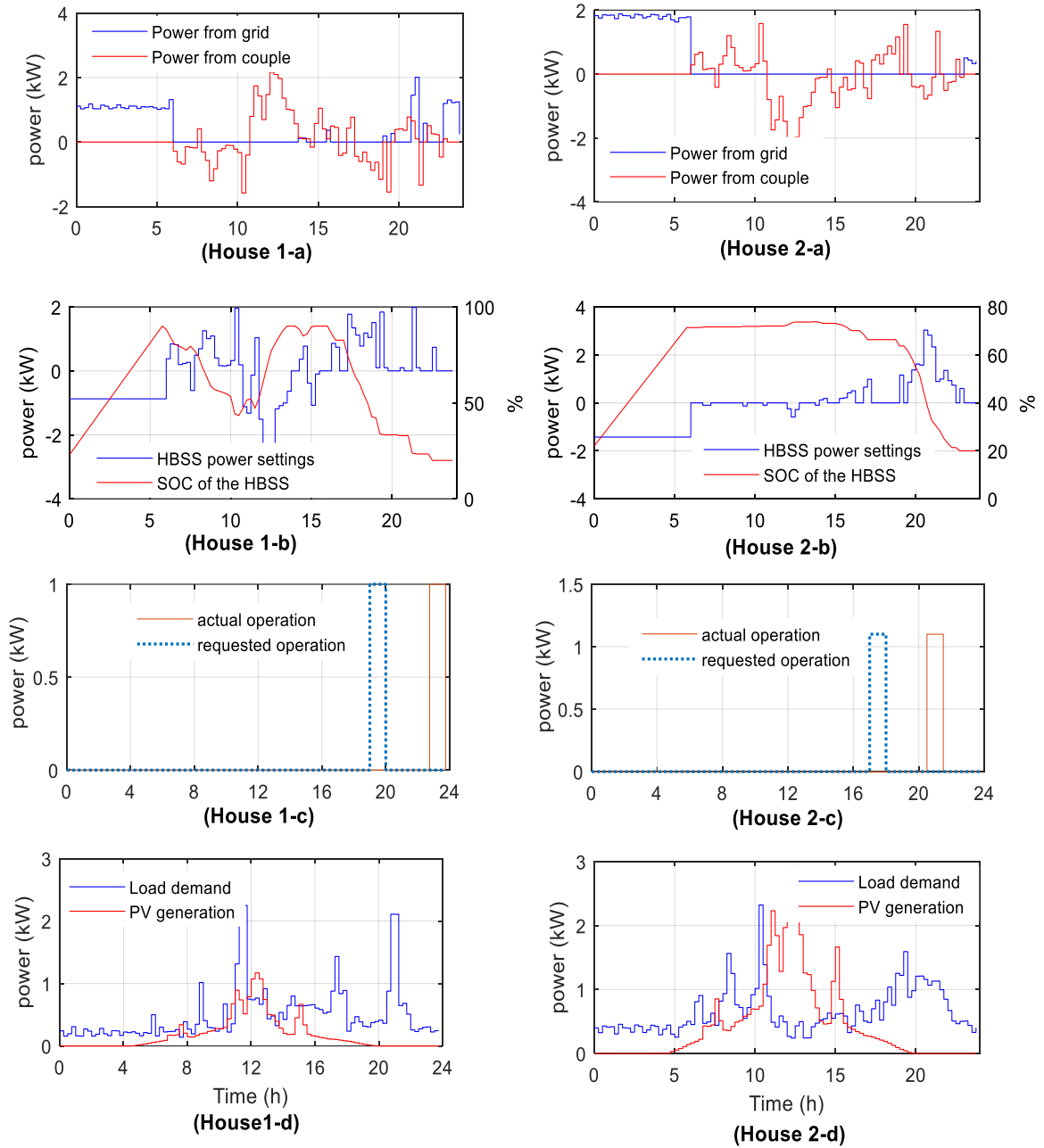


Fig. 5. 3. The optimal settings obtained from the distributed CEMS for the daily operation of the best pair (house no. 1 and house no. 2), where (House 1-a) and (House 2-a) represents the reference values for the power that should be imported from the main electricity grid by each house (i.e. blue settings), and the reference values for the power that should be shared between the paired house (i.e. red settings) for the two houses respectively; a positive value means the house is importing power from the pair house, while a negative value means the house is exporting power to the paired house, (House 1-b) and (House 2-b) represents the operation of the HBSS, (House 1-c) and (House 2-c) represents the shiftable appliance scheduling of each house. (House 1-d) and (House 2-d) represents the daily household consumption and PV generation profiles of each house.

Also, it is clear from Fig. 5. 3.(House 1-b) that the HBSS in house no. 1 worked for the benefits of house no. 2, i.e. it discharged energy to feed the household consumption of the house no. 2 (from 17:30 to 19:30) plus storing the surplus PV energy generated from the house no. 2. This operation leads to a slight increase in the degradation cost of HBSS in the house no. 1. However, the daily reduction in energy cost for house no. 1 compensates for the slight increase in the battery degradation cost.

Fig. 5. 3.(House 2-a) show that house no. 2 imports energy from house no. 1 (from 6:00 to 11:00 and from 16:00 to 19:00) at no charge (zero sharing energy charge) to feed the household consumption of house no. 2 and minimize the imported energy from the main electricity grid at high prices (11.99 pence/kWh and 24.99 pence/kWh). Also, it is clear from Fig. 5. 3.(House 1-a) and Fig. 5. 3.(House 2-a) that there is no imported energy from the main grid when exporting energy to the paired house, see constraints (5.19 - 5.21).

It is clear from the Fig. 5. 3.(House 2-b) that the CEMS managed to decrease the degradation cost of the HBSS in house no. 2 by decreasing the number of discharge and charge cycles, compared to being operated individually (i.e. it has to store the surplus PV energy and feed the morning loads when operating individually). Also, the distributed CEMS managed to provide proper scheduling for the shiftable appliances in both house no. 1 and house no. 2 to work for the benefits of both houses not only one individual house, see Fig. 5. 3.(House 1-c) and Fig. 5. 5.(House 2-c).

Generally speaking, the distributed CEMS managed to coordinate the operation of the HBSS, as well as the shiftable appliances, in house no. 1 and house no. 2 in a way that minimizes the overall degradation cost and also achieves more reduction in household energy costs. In this way, participating in the distributed CEMS as a part of the community helps in

reducing the daily household energy cost of the houses in the community, compared to being operated individually.

Fig. 5. 4. shows a comparison between operation of house no. 1 as a part of the CES using distributed CEMS, versus being operated individually (i.e. no power is shared with other houses). It is observed from Fig. 5. 4.(P2P-a) that house no. 1 imports free of charge energy from the paired house in the period from (11:00 to 15:00) when being operated as a part of the CES, instead of importing the same energy from the main electricity grid at peak prices when being operated individually as in Fig. 5. 4.(single-a).

It is clear from Fig. 5. 4. (P2P-a) that house no. 1 exports energy to the paired house (from 6:00 to 11:00 and from 16:00 to 19:00), after satisfying the load consumptions of the house no. 1. By comparing the results obtained in Fig. 5. 4.(single-b) and Fig. 5. 4.(P2P-b), it is observed that the degradation of the HBSS in house no. 1 slightly increase when being a part of the CES, compared to being operated individually. However, the daily reduction in energy cost compensates for the slight increase in the battery degradation cost. These explanations discuss the main reasons for the reduction of the daily energy cost of house no. 1 when being operated as a part of the community compared to being operated individually.

To consider the effect of all the seasons, the performance of the distributed CEMS has been evaluated for one year as shown in Table 5. 4. Table 5. 4. shows the annual household energy costs of the four houses when being operated as a part of the community using the P2P operating algorithm, compared to being operated individually. Note that the arrangement of the paired houses is changed every day –they are not fixed for the year.

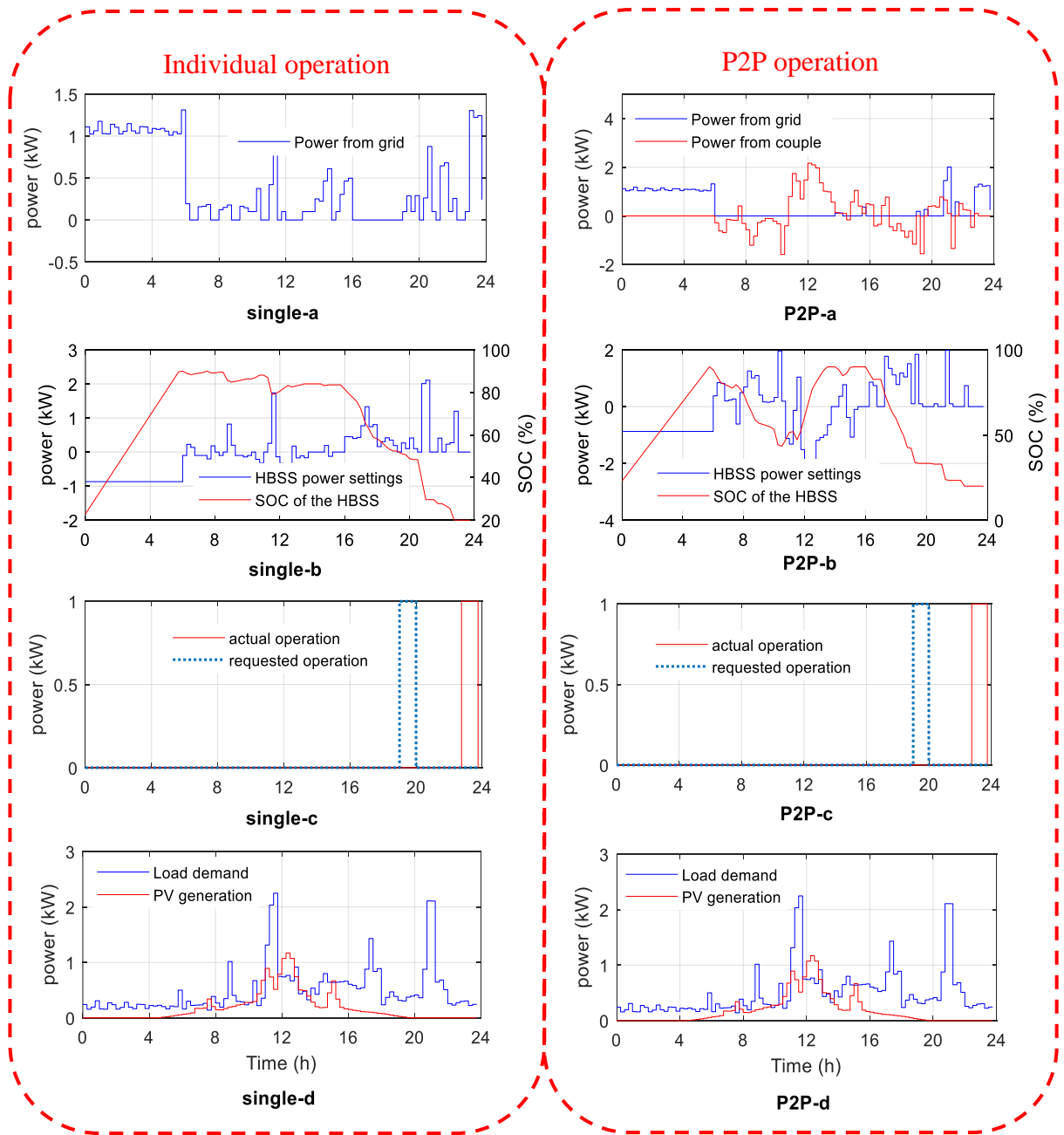


Fig. 5. 4. The operation of the house no. 1 as a part of the community using distributed CEMS (P2P), versus being operated individually (single), where (single-a) the power imported from the main electricity grid by the house. (P2P-a) the reference values for the power that should be imported from the main electricity grid by house no. 1 (blue settings), and the reference values for the power that should be shared between house no. 1 and the paired house (red settings); where a positive value means the house is importing power from the paired house, while a negative value means the house is exporting power to the paired house. (single-b) and (P2P-b) represent the operation of the HBSS in each case. (single-c) and (P2P-c) represent the shiftable appliance scheduling of the house in each case. (single-d) and (P2P-d) represent the daily household consumption and PV generation profiles for the house, i.e. they are the same for both cases.

It is clear from Table 5. 4. that operating the houses as part of a CES (using P2P operation) achieves a reduction in the annual household energy costs for all the participating houses, i.e. the reduction percentage for each house varies from 2.6% -8.96%. The reduction percentage of the household energy costs for each house depends on many reasons such as the yearly household consumption, the yearly PV generation, the size and the efficiency of the HBSS, and the flexibility of shiftable loads.

Table 5. 4. The annual household energy costs of the four houses when being operated as a part of the community using the P2P operating algorithm, compared to being operated individually.

	Energy costs (£) (single operation)	Energy costs (£) (P2P operation)	Reduction percentage
House 1	252.84	235.17	6.98%
House 2	404.27	393.76	2.60%
House 3	378.64	365.71	3.42%
House 4	263.59	240.23	8.86%
Whole community	1299.34	1234.87	4.96%

It is observed that house no. 2 and house no. 3, achieve lower reductions in costs compared to the other two houses. The reason is that both house no. 2 and house no. 3 have a HBSS of 13.5 kWh and 90% efficiency. However, both house no. 1 and house no. 4 have a HBSS of 6.4 kWh and 95% efficiency. The HBSS with larger size and lower efficiency makes the distributed CEMS depend less on these batteries due to their high operating and degradation costs, compared to the smaller HBSS size and higher efficiency, which gives a chance for the houses with smaller HBSS size and high efficiency to achieve a greater reduction in the household energy costs when being operated as a part of the community.

It is clear from It is clear from Table 5. 4. that operating the houses as part of a CES (using P2P operation) achieves a reduction in the annual household energy costs for all the participating houses, i.e. the reduction percentage for each house varies from 2.6% -8.96%.

The reduction percentage of the household energy costs for each house depends on many reasons such as the yearly household consumption, the yearly PV generation, the size and the efficiency of the HBSS, and the flexibility of shiftable loads.

Table 5. 4 that the distributed CEMS managed to achieve a reduction for all houses that participate in the CES, however, some houses achieve greater reduction in cost compared to the others. It is worth noting that the big reduction in the annual household costs for some houses comes from the participation of other houses that have large generation capabilities (HBSS and PV) which share their energy with the other houses to make this reduction. Generally, the variation of the sizes of the HBSS and the PV generation installed in the CES and also the variation of the household consumption of the houses are important for achieving more reduction in the household energy costs when participating in CES. Also, as the number of houses in the community increases, more options for pairs to achieve a higher reduction in annual costs will appear.

The houses with large generation capabilities (e.g. large HBSS or large PV system) are encouraged to participate in the CES since: (a) they could achieve a further reduction in the household energy costs, compared to being operated individually, (b) they could use the HBSS located in the other houses (i.e. houses with lower PV generation or available capacity in the HBSS) to store their own surplus PV energy, when installing large PV generation system, and re-call this (free of charge) energy again during the peak tariff periods, instead of buying the same energy from the main grid at high prices, (c) they could minimize the degradation and operating costs of the large HBSS by depending on the smaller HBSS with high efficiencies and lower operating costs (located in the other houses), (d) the distributed CEMS guarantees that no house is being charged any additional costs while participating in the CES, compared to being operated individually.

It is observed from Table 5. 4. that the annual reduction in the energy cost of the whole community is 4.96 %, compared to being operated individually. This means that participating in the CES using the distributed CEMS achieves a higher reduction in the annual energy costs of all houses while taking into account that no house is being charged any additional cost, compared to being operated individually.

5.3.4 Limitations of the Distributed Community Energy Management System

- The option of sharing energy between the house and the community is restricted to the paired house only, which limits the achievement of greater reduction in costs if the house could share energy with more than one house at the same time.
- The distributed CEMS depends heavily on data measurements and a communication system.
- Controlling the maximum power imported by the whole CES from the main electricity grid using this distributed CEMS will affect the reduction percentage in the household energy costs for each house. This is because this distributed CEMS has to share the capacity of the distribution transformer equally between the houses in the CES, i.e. means adding more constraints on the joint optimization problem. If the distributed CEMS has not controlled the maximum power imported by the whole CES from the main electricity grid, this may lead to more loading on the distribution transformer and feeders at certain time periods.

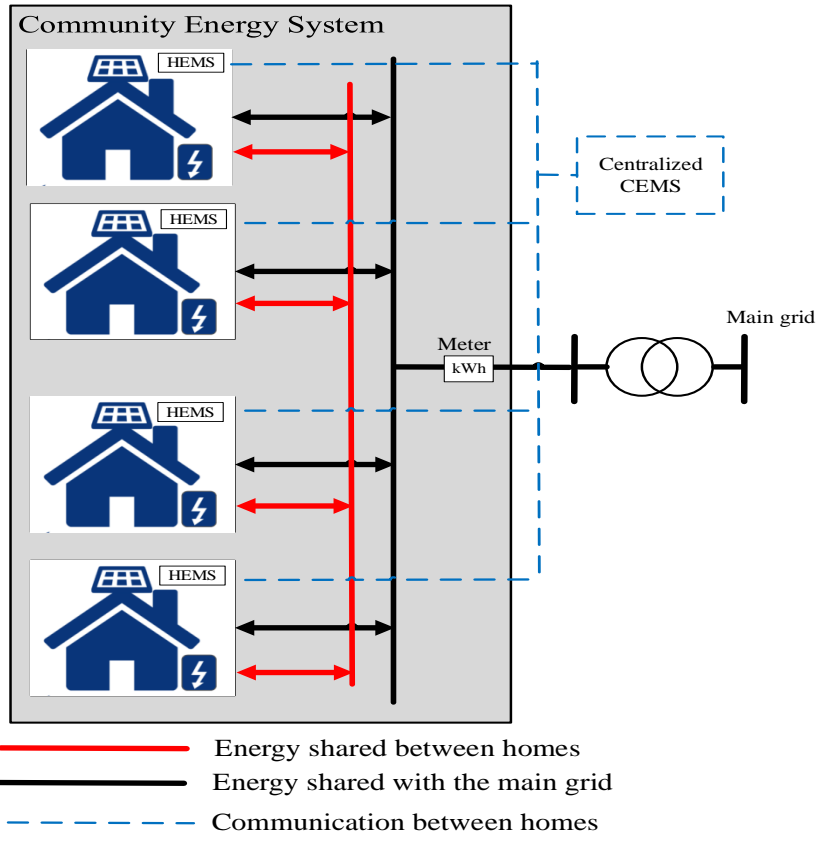
5.4 Centralized Community Energy Management System

The centralized CEMS presented in this section coordinates the operation of the distributed HBSSs (located in each house) and the shiftable home appliances in a centralized way rather than the distributed way presented in section 5.3. The centralized CEMS aims to

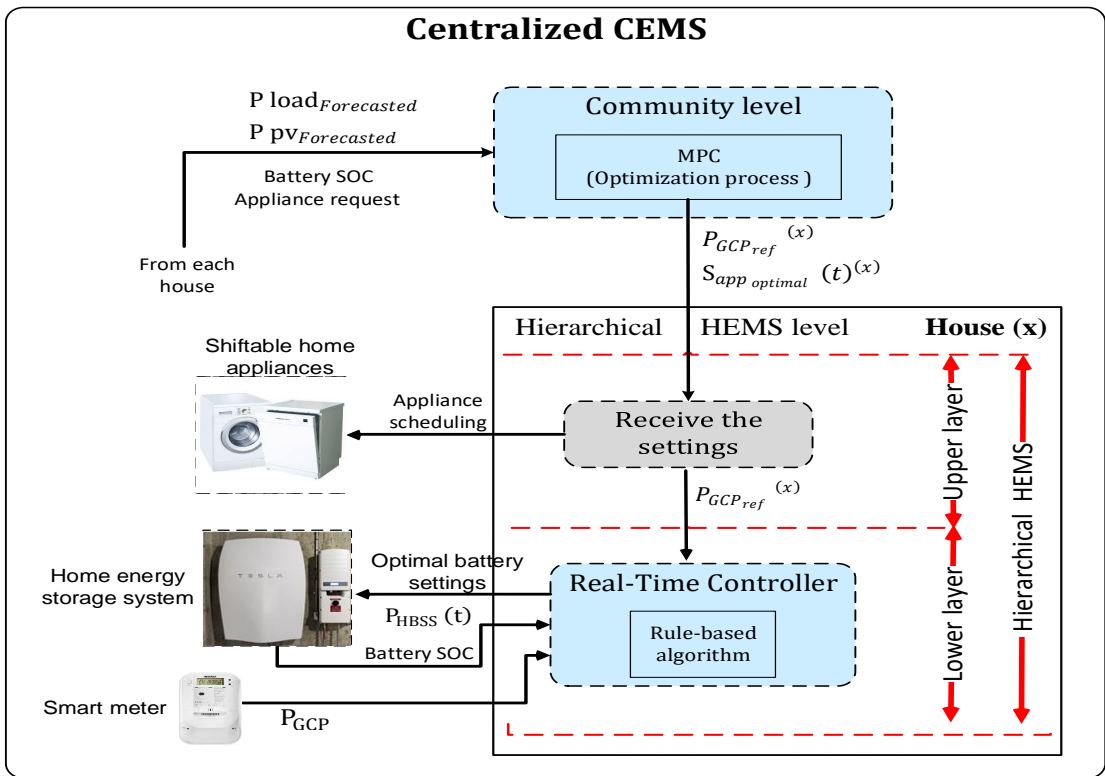
achieve a further reduction in the daily household energy costs of each house in the community, compared to being operated individually. The houses in the centralized CEMS can share energy with each other as well as with the main electricity grid. The architecture of the CES when using the centralized CEMS is shown in Fig 5. 5.

5.4.1 Structure of the Centralized Community Energy Management System

The proposed centralized hierarchical CEMS consists of two levels, see Fig. 5. 5.: (a) the Community level and, (b) the Home Energy Management Level (HEML). The Community level comprises an MPC which optimizes the community energy usage using a Mixed-Integer Linear Programming (MILP) optimization. The Community level determines the reference values of the power at the GCP between each house and the CES $P_{Grid\ ref}(t)^{(n)}$ and the scheduling of the shiftable appliances located in each house $S_{appl\ optimal}(i, t)^{(n)}$. The settings obtained from the community level are then forwarded to the HEMS in each house. The HEMS level applies these settings as shown in Fig. 5. 5.b.



(a)



(b)

Fig. 5. 5. Hierarchical centralized CEMS.

5.4.1.1 The Community level

The community level of the centralized CEMS comprises an MPC which optimizes the community energy usage using MILP optimization as shown in Fig. 5. 5.b. Every sample time, the community level:

1. Requests the forecasted household consumption and the PV generation profiles for the next 24 hours from each house. It also receives the actual SOC of the HBSS and the operation requests of the shiftable appliances (if they exist) in each house.
2. Performs a centralized MILP optimization process (will be explained in section 5.4.2.) to determine (a) the minimum daily operating cost of the community $C_{community}$, (b) the 24-hour profiles with 15-minute resolution for the reference values of the power at the GCP between each house and the community $P_{Grid\ ref}(t)^{(n)}$, and (c) the 24-hour profiles with 15-minute resolution for the shiftable appliances scheduling for each house $S_{appl\ optimal}(i, t)^{(n)}$. These profiles are then forwarded to each house (i.e. to the HEMS in each house). These settings will guarantee the best economic use of electrical energy in the community.
3. These steps are repeated every 15 minutes using a rolling horizon approach to update the input variables and obtain new updated settings.

At the end of the 24 hours, the community level determines the final daily household energy cost C_{house}^n for each house in the CES; i.e. the daily CES cost $C_{community}$ is distributed between the houses based on their daily load consumption and PV generation as in (5.24). The degradation cost of each HBSS is already considered in the optimization function and subsequently in the overall cost. The authors have followed this approach to combine the degradation costs for all batteries together, then distribute this cost to all the

consumers. It is worth noting that as the consumption of house no. (n) increases or it generates less PV energy, the house will pay a higher ratio of the daily community bill $C_{community}$.

$$C_{house}^n = C_{community} \times \frac{\sum_{t=t_0}^{t_0+24h} \{P_{load}^n(t) - P_{PV}^n(t)\}}{\sum_{n=house\ 1}^{house\ 4} \sum_{t=t_0}^{t_0+24h} \{P_{load}^n(t) - P_{PV}^n(t)\}} \quad (5.24)$$

5.4.1.2 The Home Energy Management level

The two-layer HEMS located in each house receives: (a) the 24-hour profile with 15-minute resolution for the reference values of the power at the GCP between the house and the community $P_{Grid\ ref}(t)^{(n)}$; this profile is sent to the lower layer (RTC layer), to determine the best power settings for the HBSS in real-time every one minute using the rule-based algorithm shown in Fig. 4. 17. The HBSS power settings enable the house to follow the reference values of the power at the GCP with high accuracy. (b) the 24-hour profiles with 15-minute resolution for shiftable appliance scheduling $S_{appl\ optimal}(t)^{(n)}$ and forwards them directly to each shiftable appliance in the house, see Fig. 5. 5.b.

5.4.2 Formulation of the optimization problem

The cost function of the whole community (all the four houses), $C_{community}$, that need to be minimized, can be formulated as (5.25, 5.26).

$$C_{community} = \sum_{n=house\ 1}^{house\ 4} C_{house}^n \quad (5.25)$$

$$C_{house}^n = C_{house\ import} + C_{house\ export} + C_{HBSS_d} \quad (5.26)$$

$$C_{house\ import} = \sum_{t=t_0}^{t_0+24h} \Delta T \times f_{buy}(t) \times P_{Grid}(t) \quad , at P_{Grid}(t) > 0 \quad (5.27)$$

$$C_{house\ export} = \sum_{t=t_0}^{t_0+24h} \Delta T \times f_{sell}(t) \times P_{Grid}(t) \quad , at P_{Grid}(t) < 0 \quad (5.28)$$

$$C_{HBSS_d} = \sum_{t=t_0}^{t_0+24h} \left(\frac{CC_{bat} \times \eta_{Conv} \times \eta_c \times \Delta T \times P_{HBSS}^{charg}(t)}{B_{capacity} \times 2 \times N_{cycle}} + \frac{CC_{bat} \times \Delta T \times P_{HBSS}^{disch}(t)}{B_{capacity} \times \eta_{Conv} \times \eta_d \times 2 \times N_{cycle}} \right) \quad (5.29)$$

where C_{house}^n is the daily electrical energy cost of house no. (n) (£), $C_{house import}$ is the daily cost of the electrical energy purchased from the main electricity grid for the house (n) (£), $C_{house export}$ is the daily cost of the exported electrical energy from house no. (n) to the main electricity grid (£), C_{HBSS_d} is the daily battery degradation cost of the battery located at house (n) (£), ΔT is the sample time (h), $P_{grid}(t)$ is the electrical power imported/exported from the main electricity grid (kW) at a time t, $f_{buy}(t)$ is the electricity purchase tariff from the main electricity grid a time t (£/kWh), $f_{sell}(t)$ is the electricity sale tariff (i.e. feed-in tariff) to the main electricity grid at a time t (£/kWh), CC_{bat} is the capital cost of the battery (£), N_{cycle} is the typically number of life cycles of the battery, $B_{capacity}$ is the rated capacity of the battery (kWh), $P_{HBSS}^{disch}(t)$ and $P_{HBSS}^{charg}(t)$ are respectively the HBSS discharge and charge powers at a time t (kW); $P_{HBSS}^{disch}(t)$ is always a positive value while $P_{HBSS}^{charg}(t)$ is always negative, η_d , η_c are the battery discharging and charging efficiencies respectively (%), η_{Conv} is the efficiency of the power converter (%).

When the houses are working as a network, the energy balance equation for the whole community must be reformulated as (5.30).

$$\sum_{n=house\ 1}^{house\ 4} \{P_{grid}^n(t) + P_{HBSS}^n(t)\} = \sum_{n=house\ 1}^{house\ 4} \{P_{load}^n(t) + P_{sh\ appl}(i, t)^n - P_{PV}^n(t)\} \quad (5.30)$$

To prevent the HBSSs in the houses from exporting energy to the main electricity grid, the following constraint (5.31) is used to introduce link restrictions between the discharging of the HBSS and exporting power to the grid.

$$\delta_{B \text{ disch}}^n(t) + \Phi_{\text{export}}(t) \leq 1 \quad (5.31)$$

where $\delta_{B \text{ disch}}(t)$ is a binary variable; i.e. equals 1 if the battery is discharging and equals 0 otherwise. $\Phi_{\text{export}}(t)$ is a binary variable; i.e. equals 1 if the house is exporting power to the main electricity grid at a time t and 0 otherwise.

Also, to prevent the HBSS in the house (x) from discharging energy to charge the HBSS in the house (y) and vice versa, the following constraints (5.32, 5.33) are used to introduce link restrictions between the discharging of the HBSS in the house (x) and the charging of the HBSS in the house (y) at the same time. This constraint is used to avoid the degradation of the HBSSs.

$$\delta_{B \text{ disch}}^x(t) + \delta_{B \text{ charg}}^y(t) \leq 1 \quad (5.32)$$

$$\delta_{B \text{ charg}}^x(t) + \delta_{B \text{ disch}}^y(t) \leq 1 \quad (5.33)$$

where x, y are for example house (x) and house (y), $\delta_{B \text{ disch}}^{x, y}(t)$ is a binary variable; i.e. equals 1 if the battery is discharging and equals 0 otherwise, $\delta_{B \text{ charg}}^{x, y}(t)$ is a binary variable; i.e. equals 1 if the battery is charging and equals 0 otherwise.

Also, all the constraints associated with each model in the household system, i.e. the constraints of the HBSS model (4.6-4.15), the constraint of the shiftable loads (4.18-4.23), and the constraints of the imported/exported power (4.24-4.28) are applied to the centralized MILP optimization process.

The optimization problem of the whole community is solved using the MILP optimization technique. The solution of the optimization problem for the whole community (all the four houses), generates a set of optimal control settings for each house (n) $[P_{GCP \text{ ref}}^{(n)} S_{\text{appoptimal}}(i, t)^{(n)}]$, where $S_{\text{appoptimal}}(i, t)^{(n)}$ is the optimal appliance scheduling for the next 24 hour for the house no. (n) and $P_{GCP \text{ ref}}^{(n)}$ is

reference values of the power at the GCP between the house no. (n) and the community. Finally, these settings are sent to each house in the community.

5.4.3 Results

The centralized CEMS proposed in section 5.4.1 and 5.4.2 has been implemented for one day (in summer) in a simulation environment using MATLAB software. The results obtained are summarized in Table 5.5. TOU tariff for purchasing electric energy from the main grid, a fixed tariff for selling electric energy to the main grid, L-PWSD forecasting method for load forecasting and PV-PD forecasting method for PV generation forecasting have been used in this simulation. The parameters of the four houses used in the simulation process, including the annual consumption and annual PV generation, and the HBSS size for each house, are shown in Table 5.1.

Table 5. 5. shows the daily energy costs of the four houses when being operated as a part of the CES using the centralized CEMS, compared to being operated individually. The results show that the daily operating cost of the whole community when being operated using the centralized CEMS is £2.26. This cost is distributed over the four houses based on their daily load consumption and PV generation, see (5.24). For example, the house no. 1 takes 29.20% of the daily community energy bill $C_{community}$ because the ratio between the daily load consumption and PV generation for the house no. 1, compared to the four houses is 29.20%.

It is clear from Table 5. 5. that the centralized CEMS managed to achieve a daily reduction in the household energy costs (between 8.11% and 20.34%) for all houses. By comparing the results in Table 5. 5. and Table 5. 3., it is observed that using a centralized CEMS achieves a higher reduction in the daily energy costs for houses no. 2, 3, and 4, i.e. 20.34%, 8.11%, 16.67%, compared to using distributed CEMS, which achieves 0%, 0%, 13.33% for the three houses respectively.

Table 5. 5. The daily energy costs of the four houses when being operated as a part of the CES using the centralized CEMS, compared to being operated individually.

	Daily energy cost (£) (single operation)	Daily energy cost (£) (Part of community)	Reduction percentage
House 1	£0.71	£0.66	7.04%
House 2	£0.58	£0.46	20.34%
House 3	£0.74	£0.68	8.11%
House 4	£0.54	£0.45	16.67%
Whole community	£2.57	£2.25	12.40%

It is observed from Table 5. 5. that house no. 2 achieved the highest reduction in daily energy cost (20.34%), compared to the other houses. This is because the rational effect of the generated PV energy to the load consumption of each house; It is observed that the ratio between the generated PV energy to the load consumption of this day was 36.05%, 67.88%, 49.07%, and 56.06% for the four houses respectively. Since house no. 2 has the highest ratio of (PV energy/load consumption), it achieved the highest reduction in cost for this day. Furthermore, it is observed that if that ratio between the generated PV energy to the load consumption for one of the houses increased, the reduction percentage of the household energy cost of the other houses will be affected. This is because a higher ratio of the daily community bill will be distributed over the remaining houses, which increases their energy costs and decreases the reduction percentage for each of them.

Fig. 5. 6. provides more details about the operation of the whole community for one day using the centralized CEMS. It is clear from Fig. 5. 6.a that the centralized CEMS managed to control the energy imported from the grid in a way that minimizes the energy purchased from the grid at peak and mid-peak tariff periods (06:00 to 23:00), which leads to minimizing the whole community bill. It is worth noting that the centralized CEMS could control the

power purchased from the main electricity grid at any period to minimize the overall energy costs and also the peak power, see constraints (4.27, 4.28).

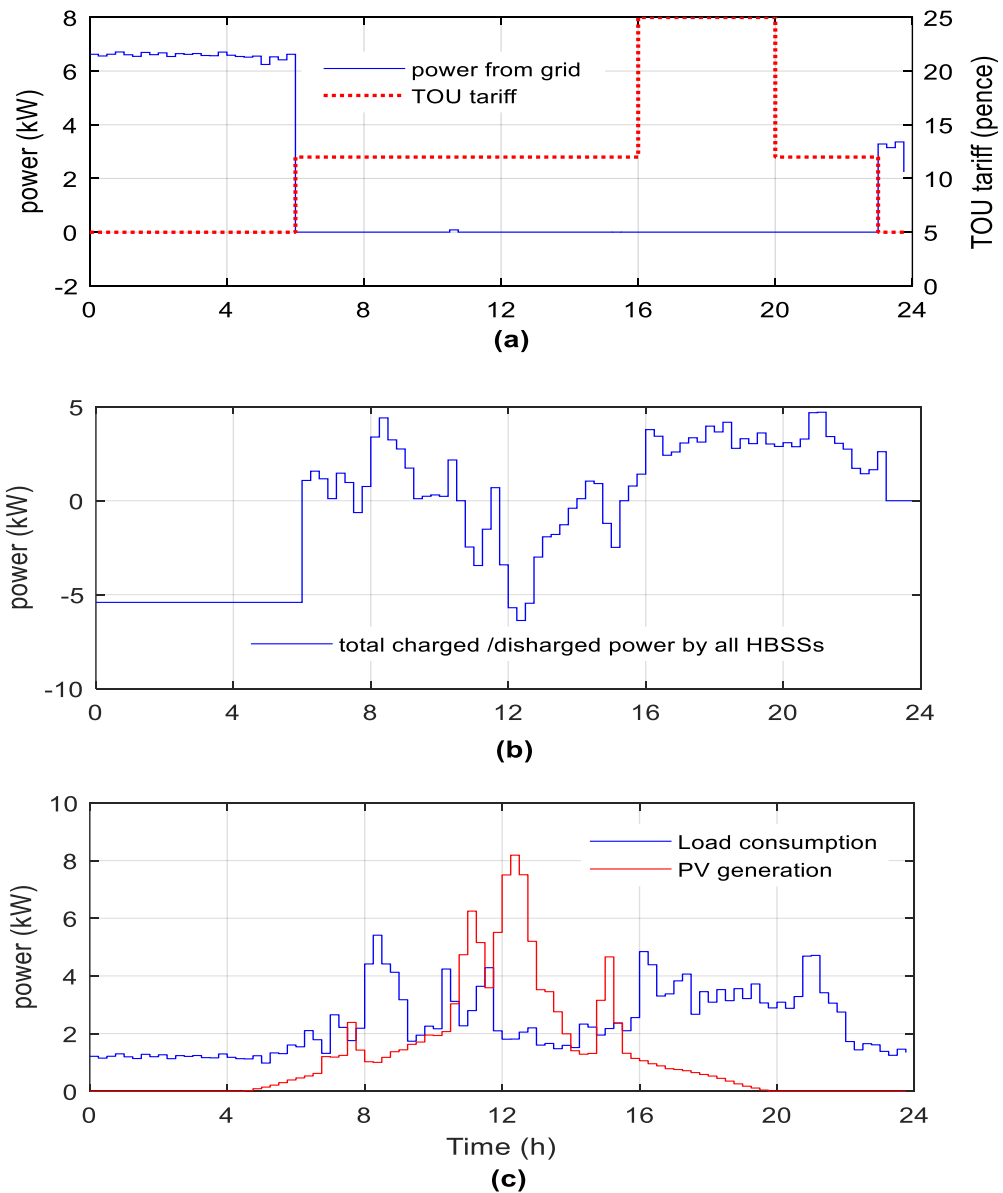


Fig. 5. 6. The operation of the whole community for one day using the centralized CEMS, (a) the overall power drawn by the community from the main electricity grid, and the corresponding TOU tariff, (b) the overall charged /discharged power by all HBSSs at all houses in the community, a positive value means the HBSS is discharging, while a negative value means charging, (c) the total load consumption and PV generation of houses in the community.

Fig. 5. 6.b shows that the centralized CEMS charged all the HBSS in the community using the low-cost energy at night period (00:00 to 06:00). The centralized CEMS coordinates the operation of the HBSS to store all the excess PV energy (from 11:00 to 15:00) to avoid exporting any excess PV energy to the main electricity grid, i.e. clear from Fig. 5. 6.a that the PV self-consumption ratio is 100%. The coordination of HBSSs enhances the self-consumption of the generated PV energy within the community using the same battery sizes, compared to being operated individually which may force the houses to export the excess energy to the grid if the battery size is small or the battery is already charged.

Fig. 5. 7. shows the optimal settings obtained from the centralized CEMS for the operation of the house no. 1 and the house no. 2 (for example) for one day. For more results, Appendix E shows the optimal settings obtained from the centralized CEMS for the daily operation of the four houses in this community. It is observed from Fig. 5. 7 that the centralized CEMS sets the reference values for the operation of house no. 1 and house no. 2 as shown in Fig. 5. 7.(House 1-a) and Fig. 5. 7.(House 2-a) respectively. These settings will minimize the overall energy cost for the community. By adding the reference values for all houses, the overall power drawn by the community from the main electricity grid profile (Fig. 5. 6.a.) will be obtained.

It is clear from the Fig. 5. 7.(House 2-a) that the house no. 2 exports the extra energy available from the PV generation (from 11:00 to 15:00) to the community. The centralized CEMS uses the HBSS located in the house no. 1 to store a part of the surplus PV energy generated from the house no. 2. This is because the HBSS in house no. 1 has lower operating cost and high efficiency compared to the HBSS in the house no. 2. The centralized CEMS managed to provide proper scheduling for the shiftable appliances in both house no. 1 and house no. 2, see Fig. 5. 7. (House 1-c) and Fig. 5. 7.(House 1-c).

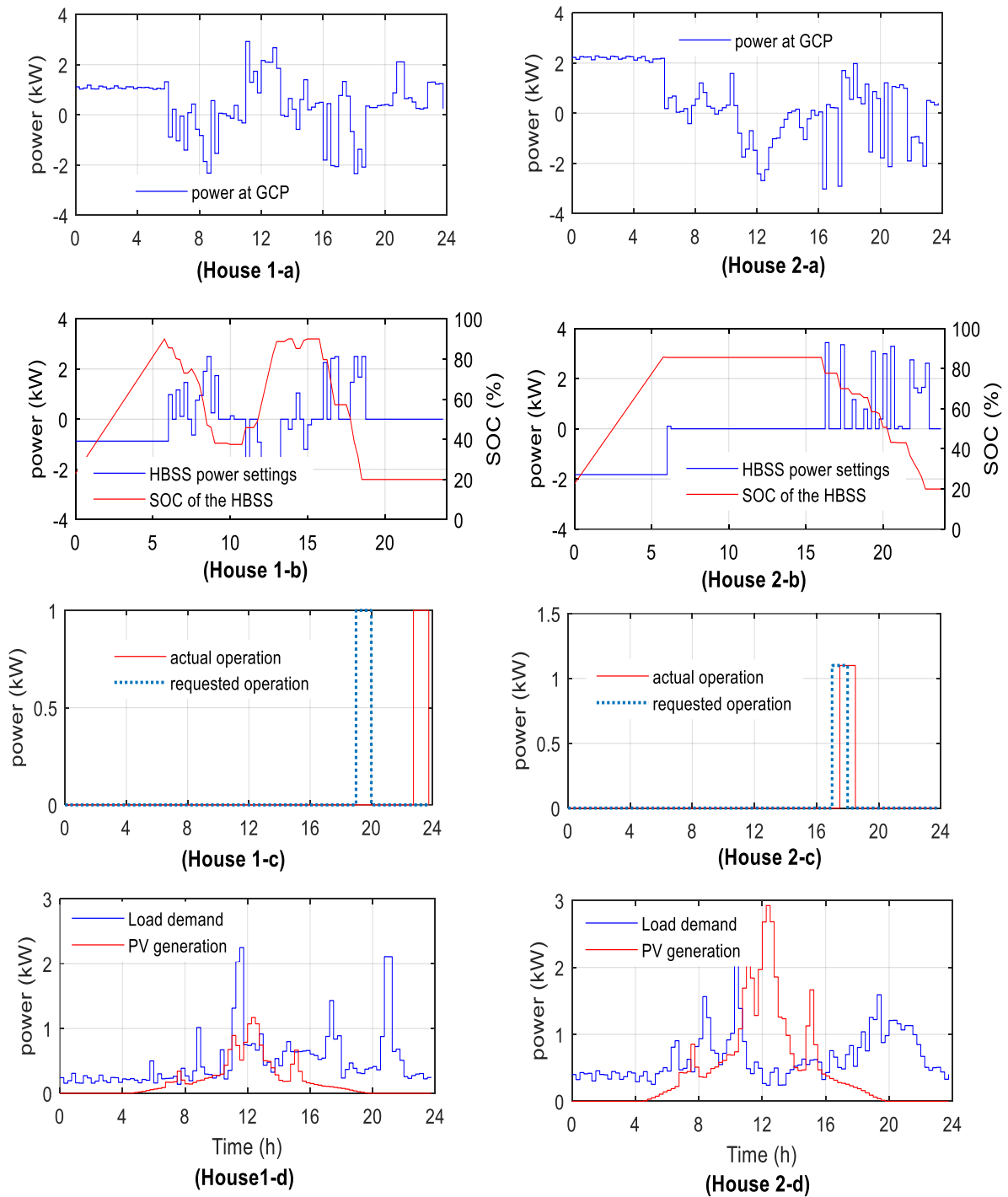


Fig. 5. 7. The optimal settings obtained for the daily operation of house no. 1 and house no. 2 using the centralized CEMS, where (House 1-a) and (House 2-a) represents the reference values for the power that should be shared between the house and the community; a positive value means the house is importing power from the community, while a negative value means exporting. (House 1-b) and (House 2-b) represents the operation of the HBSS, (House 1-c) and (House 2-c) represents the shiftable appliance scheduling for each house, (House 1-d) and (House 2-d) represents the daily household consumption and PV generation profiles of each house.

Generally speaking, the centralized CEMS managed to coordinate the operation of the HBSS in house no. 1 and house no. 2, and also to provide a proper scheduling for the shiftable appliances in both houses in a way that minimizes the overall degradation cost and also achieve more reduction in the household energy costs.

Fig. 5. 8. shows a comparison between the operations of house no. 1 as a part of CES using the centralized CEMS, and being operated individually (i.e. no power is shared with other houses). When being operated individually, it is observed that house no. 1 imports energy from the main electricity grid at high prices, see Fig. 5. 8 (single-a). However, when operating as part of the CES, house no. 1 has followed the reference values for the power at GCP, see. Fig. 5. 8 (central-a). Accurately following this reference will ensure minimizing the household energy costs for all houses.

It is observed from Fig. 5. 8 (central-b) that the degradation cost of the HBSS in house no. 1 slightly increases when operated as part of the community, compared to being operated individually. However, the degradation cost for the HBSS when part of the centralized CEMS is distributed over all houses. Fig. 5. 8 (central-c) and Fig. 5. 8 (central-c) show that there is no change in the shiftable appliance scheduling in the two cases.

The results of the centralized CEMS has been evaluated for one year to take the effect of all seasons. Table 5. 6. shows the annual household energy costs of the four houses when being operated as a part of the community using centralized CEMS, compared to being operated individually. It is clear from the results that operating the houses as a part of the community produces a greater reduction in the household energy costs for all the participating houses. The percentage reduction in the annual household energy cost of each house varies from 6.19 % to 15.89% when being operated as a part of the community.

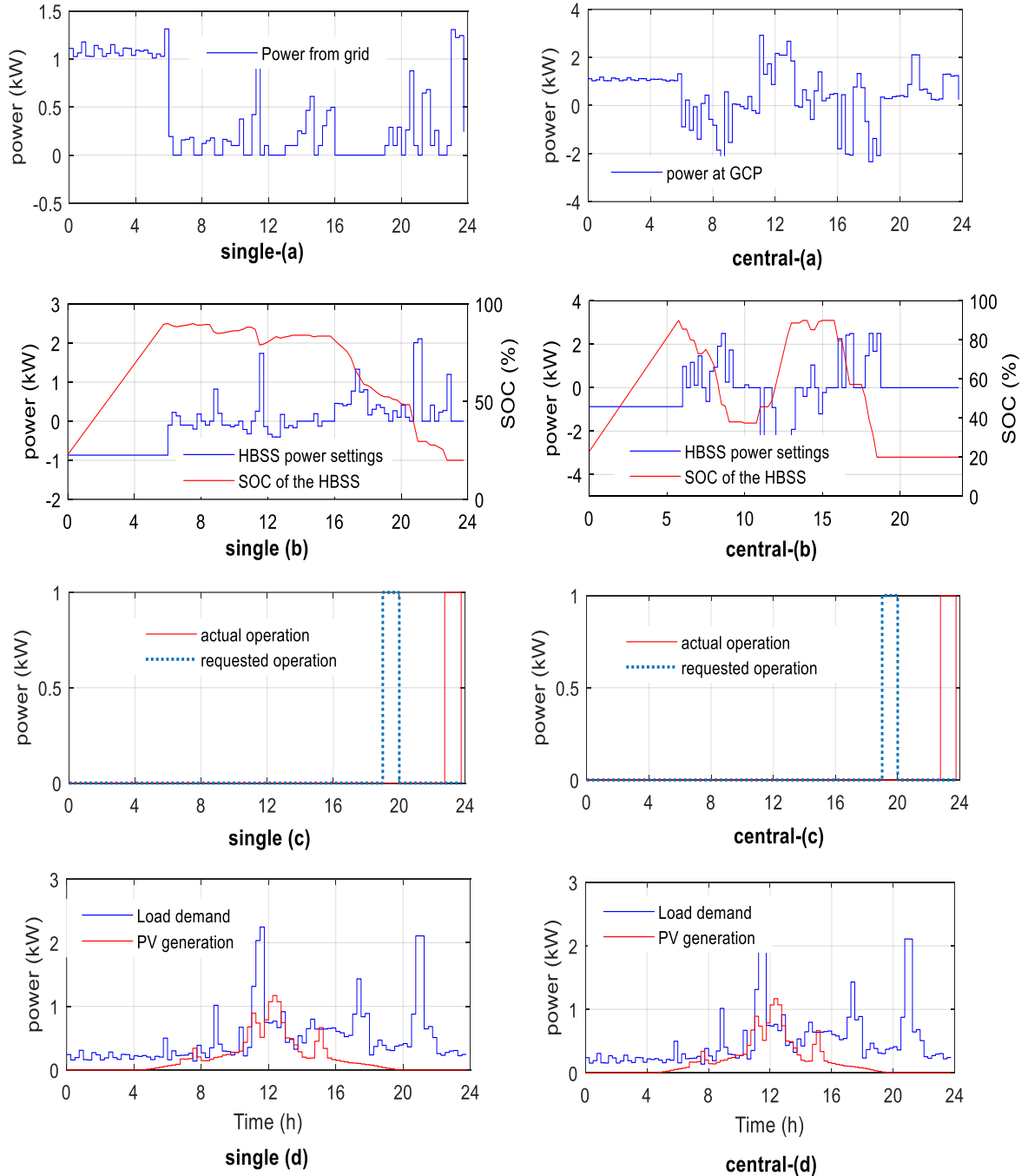


Fig. 5. 8. Operation of house no. 1 as a part of the community using centralized CEMS, versus being individually (single operation), where (single-a) the power imported from the main electricity grid by house. (central -a) the reference values for the power that should be shared between the house and the community; a positive value means the house is importing power from the community, while a negative value means exporting power to the community, (single-b) and (central-b) represent the operation of the HBSS in each case. (single-c) and (central -c) represent the shiftable appliance scheduling in each case. (single-d) and (central -d) represent the daily household consumption and PV generation profiles for the house.

Table 5. 6. The annual household energy costs of the four houses when being operated as a part of the community using centralized CEMS, compared to being operated individually.

	Energy costs (£) (single operation)	Energy costs (£) (Part of community)	Reduction percentage
House 1	252.84	228.23	9.73%
House 2	404.27	379.26	6.19%
House 3	378.64	353.40	6.67%
House 4	263.59	221.71	15.89%
Whole community	1299.34	1182.6	8.98%

By comparing the results in Table 5. 6. and Table 5. 4., it is clear that using a hierarchical centralized CEMS achieves a higher reduction in the daily household energy costs for all houses, i.e. 9.73%, 6.19%, 6.67%, 15.89%, compared to using a hierarchical distributed CEMS which achieves 6.98%, 2.60%, 3.42%, 8.86% for the four houses respectively. This is because the centralized CEMS allows each house to share energy with more than one house, compared to the distributed CEMS which limits the energy sharing between only the paired houses. Also, the degradation cost of each HBSS is shared between the four houses when using the centralized CEMS, which gives the centralized CEMS more options to coordinate the HBSS to minimize the overall energy costs. However, when the community is being operated using the distributed CEMS, the degradation cost of each HBSS is counted only for the house which is fitted in.

It is observed from Table 5. 6. that using the centralized CEMS achieves a total reduction of 8.98 % in the annual community bill (for all houses), compared to being operated individually, and also compared to using distributed CEMS, which achieves only 4.96%, see Table 5. 4.

Generally speaking, participating in the CES using hierarchical centralized CEMS achieves a higher reduction in the annual energy costs for all houses while taking into account

that no house is being charged any additional cost, compared to being operated individually. Also, it is observed that the percentage reduction in the household energy costs for all houses is not fixed, but it depends on the number of houses in the community and the load consumption and PV generation of each house.

5.4.4 Limitations of the Centralized CEMS

- Still depends on data measurements and the availability of communication system.
- No accurate monitoring for the money flow between the houses, and the energy losses in the system.
- The optimization process will take more computational time if more houses with more appliances are included in the CEMS optimization problem.

5.5 Summary and Conclusion

The conclusions of this chapter are as follows:

- The commercial operation of the interconnected houses can be improved if they participate in a CES using the proposed hierarchical decentralized or centralized CEMS. The proposed decentralized or centralized CEMS guarantees a further reduction in the household energy costs for all houses, compared to being operated individually.
- Using the hierarchical centralized CEMS achieves a higher reduction in the annual energy costs for all houses in the CES, i.e. 9.73%, 6.19%, 6.67%, 15.89%, compared to using the distributed CEMS which achieves only 6.98%, 2.60%, 3.42%, 8.86% for the four houses respectively. This is because the distributed CEMS allows each house to share energy with the paired house only, while the centralized CEMS enables the house to share energy with more than one house at the same time, which achieves a greater reduction in

costs, i.e. sharing energy with more than one house at the same time gives more options for control and management.

- The networked operation of houses can improve the economic benefits compared to single mode operation, reduce the need for overly large HBSS, and reduce the exported power to the main electricity grid. It also helps to maximize the HBSS lifetime as the cooperation between houses can decrease the number of cycles each battery performs and limits the need for high values of charging and discharging power, i.e. minimizes the overall degradation costs. Coordinating the operation of the HBSSs enhances the PV self-consumption within the community using the same battery sizes, compared to the single operation of the houses.
- The percentage reduction in the household energy costs for all houses is not fixed, but it depends on the number of the houses in the community, the load consumption and PV generation of each house, and the size and the efficiency of each HBSS. Also, it is observed that the daily percentage reduction in the household energy costs for each house is affected by the operation of the other houses in the community.
- It is expected that a greater reduction in the household energy costs will be achieved when houses with different sources of energy, different load demand profiles, and different tariff schemes are used. Also, a greater reduction in the household energy costs will be achieved as a higher number of houses participate in the CES.
- The hierarchical distributed CEMS provides advantages of monitoring and accurately controlling both the energy flow and the money flow between houses, compared to the centralized CEMS, which enables the houses to share energy with each other for paid charge, and enables the system to observe and consider the power losses of the shared energy, and hence increases the system's efficiency.

- The hierarchical distributed CEMS depends on decentralized agents (multi-agents) to perform the control optimization process, compared to the centralized CEMS which uses a single central controller to perform the optimization process. Distributing the optimization process over the available MPC platforms (agents) in each house, minimizes the overall processing and computing time, and makes the optimization process less affected by the increasing number of controllable devices or system constraints.
- The hierarchical centralized CEMS coordinates the operation of the HBSS and the shiftable loads to minimize energy purchased from the grid at peak times, and to store all the surplus PV energy and avoid exporting any energy to the main electricity grid.
- The hierarchical centralized CEMS controls the maximum power imported from the main electricity grid at any period to minimize the overall community bill and the peak power, i.e. lowering the peak power minimizes the load on the distribution transformers and feeders and provide more room for adding new EV chargers in the system (if required). Also, the centralized CEMS enables the community to respond to any instructions from the main electricity grid using the DSM techniques (load shifting).
- The using of the centralized CEMS provides a fairer distribution of savings between the houses, compared to using distributed CEMS, i.e. the houses with higher consumption and lower generation take a higher ratio of community bill, therefore achieves lower savings. Also, the operation and the degradation costs of all HBSS are added together and distributed between all the houses.

Chapter 5 has investigated energy management for a community made up of several domestic residences. This chapter demonstrated that a residence can earn greater rewards by operating as a prosumers in a community energy scheme, compared to being operated

individually (not being a part of the community). The work presented in this chapter has potentially addressed objectives (3) and (4) listed in section 1.3.

However, the technologies proposed in chapter 5 had drawbacks of being mainly dependent on the community level to take decisions. This makes the optimization process takes more computational time if more houses with more appliances are included in the CEMS optimization problem. Also makes the community level more affected by the communication systems.

Chapter 6 will develop the structure of the hierarchical centralized community energy management algorithm, to provide greater flexibility, ensure that the optimization process is faster and more robust to communications, and be applied to larger communities (with a large number of houses). Also, Chapter 6 will investigate how the networked operation of houses in the community reduces the need for an overly large CBESS and ensures lower investment costs.

Chapter 6

A Hierarchical Community Energy Management System Using a Centralized Battery Store and Demand-Side Management

6.1 Introduction

It was seen in chapter 5 that advantages could be gained in electricity costs for community residences if they were willing to cooperate in a community energy scheme to exchange energy. However, the technologies proposed in chapter 5 had drawbacks. In this chapter, the structure of the centralized CEMS has been modified to provide greater flexibility, ensure that the optimization process is faster and more robust to communications, and be applied to larger communities (with a large number of houses), compared to the CEMS presented in chapter 5. A new level - The Demand-side management level (DSML) - has been created to manage the operation of the shiftable appliances in each house, instead of being managed directly from the central CEMS. Also, the distributed HBSSs-located in each house have been replaced by a single central Community Battery Energy Storage System (CBESS) with the same equivalent size. This simplifies the architecture, and makes it representable of the same real energy community [196].

The hierarchical CEMS minimizes the household energy costs and energy wastage, maximizes PV self-consumption and also considers battery degradation costs and the possibility of load shifting. The hierarchical CEMS coordinates the operation of a central CBESS with the household consumption in a way that achieves a further reduction in the annual household energy costs for each house in the community.

This chapter also investigates how the networked operation of houses in the community reduces the need for an overly large CBESS and ensures lower investment costs. A reduction in the annual energy costs is achieved for the community, and also there are lower demands on the community supply infrastructure at its point of coupling.

The complete hierarchical CEMS has been implemented experimentally in real-time using an emulation MG in the University of Nottingham FlexElec Laboratory, to ensure that the proposed CEMS can work correctly in a real system without any difficulties.

6.2 Structure of the Hierarchical Community Energy Management System

The hierarchical CEMS, presented in this chapter, consists of three levels as seen in Fig. 6. 1. : (a) The community level (MPC level), (b) the CBESS control level, and (c) the Demand-side management level (DSML). The distributed HBSSs-located in each house have been replaced by a single central CBESS with the same equivalent size as seen in Fig. 6.1. This simplifies the architecture, and is representable of the same real energy community such as Trent Basin energy community [196]. The community is a part of the Trent Basin neighbourhood of low energy homes.

Each house can still share the excess energy from its own PV generation with other neighbour houses in the community. Also, the community is still connected to the main electricity grid to import/export any required energy.

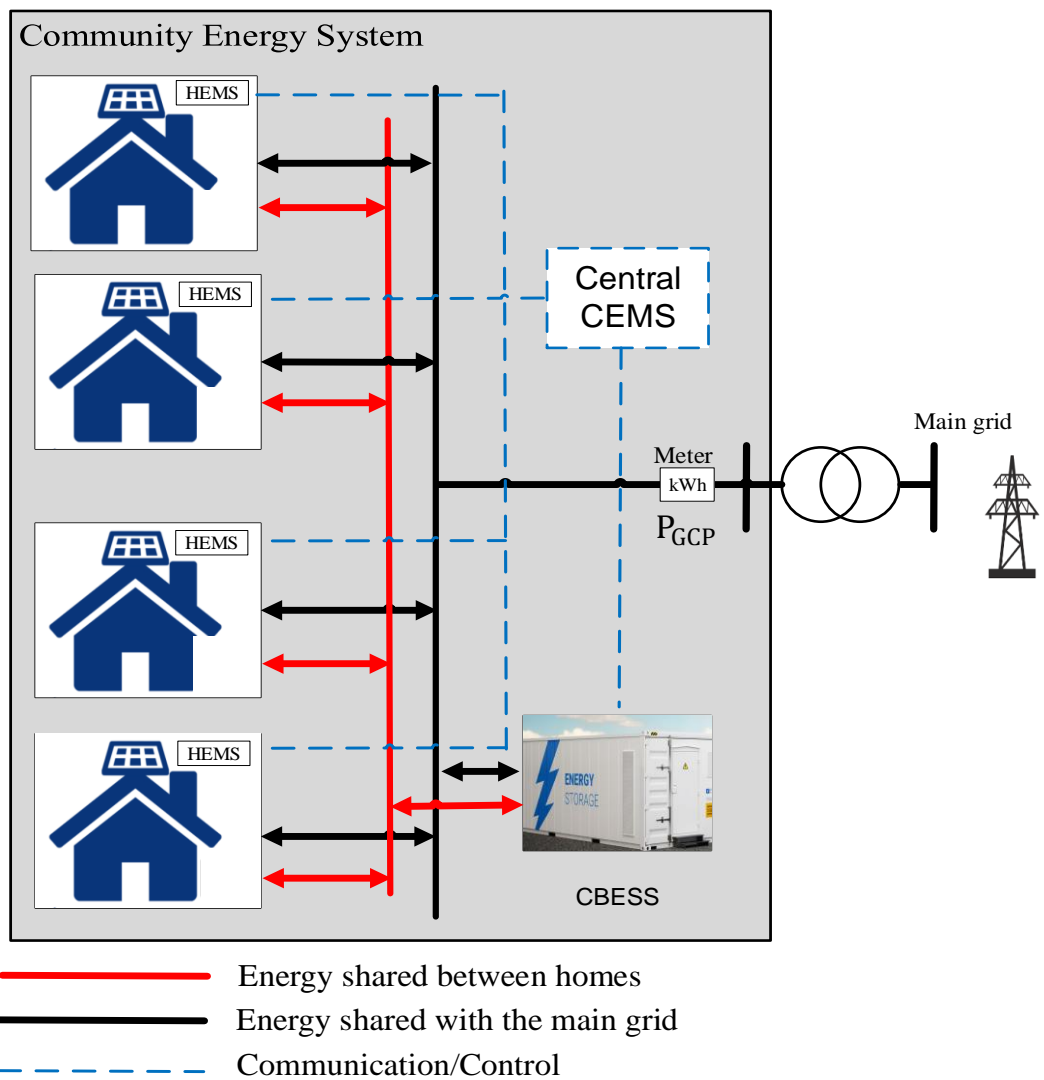
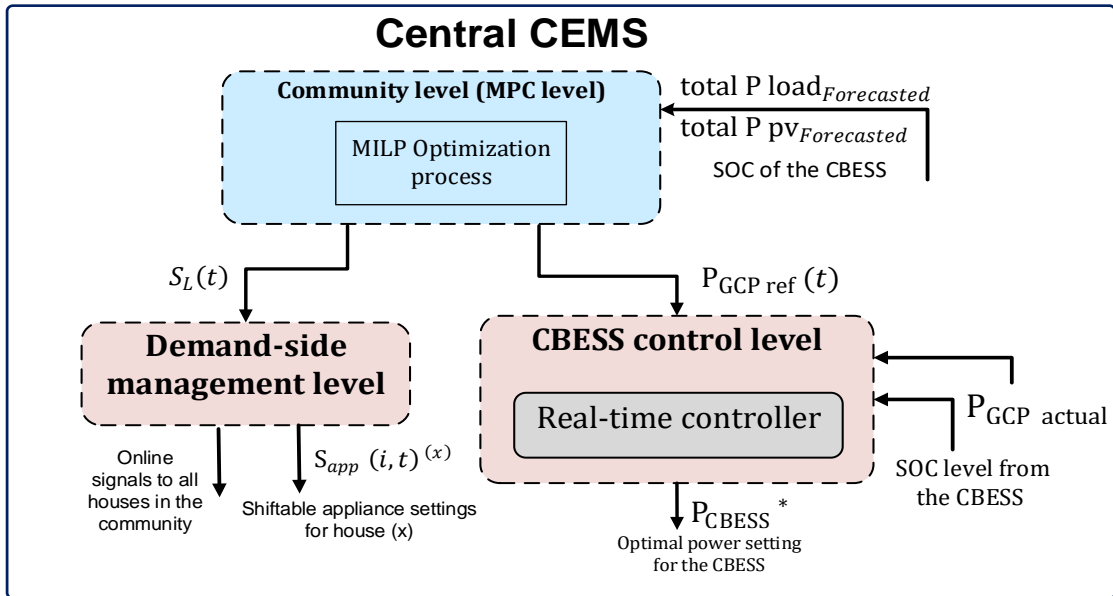


Fig. 6. 1. Architecture of the hierarchical central CES in the presence of a central CBESS.

6.2.1 Community Level

The community level comprises an MPC which optimizes the use of community energy as shown in Fig. 6. 1. Every sample time, the community level:

1. Requests the total forecasted household consumption and PV generation profiles for the next 24 hours. The forecasted household consumption and PV generation profiles of each house is sent regularly from each house to the CEMS.
2. Requests the actual SOC of the central CBESS.
3. A MILP optimization process is performed to determine the 24-hour profiles with 15-minute resolution for: (a) the reference values of the power at the GCP ‘ $P_{GCP\ ref}(t)$ ’ (the connection point between the main electricity grid and the community), (this profile is sent to the CBESS control level), (b) the load shift coefficient profile ‘ $S_L(t)$ ’, i.e. this profile is sent to the DSML.
4. These steps are repeated every 15 minutes using a rolling horizon approach to update the input variables and obtain new updated settings. These settings will guarantee the best economic use of electrical energy in the community.

6.2.2 CBESS Control Level

The central CBESS control level consists of a real-time controller (RTC) as shown in Fig. 6. 1. The central CBESS control level receives the reference values for the power at the GCP ‘ $P_{GCP\ ref}(t)$ ’ for the next 24 hours from the MPC level, and uses the rule-based algorithm shown in Fig. 6. 2. to determine the optimal power settings for the CBESS in real-time every one minute. The RTC compensates for the effect of forecast uncertainties and sample time. The RTC sends regular feedback to update the community level with the actual SOC of the CBESS, as this is essential to perform the following optimization process (new energy scheduling).

6.2.3 Demand-Side Management Level

The DSML is responsible for: (a) managing the operation of the shiftable home appliances in the community, and (b) sending online signals to the consumers to modify their consumption behaviour.

The DSML uses the load shift coefficients-received from the community level, in addition to the switch ON signal request from appliances- It assumed that the user has already sent a switch ON signal to the DSML to enable the start of an appliance 'i' - to determine the 24-hour profiles with 15-minute resolution for the optimal scheduling of the shiftable appliances in each house (n) ' $S_{app}(i, t)^{(n)}$ '. Also, it is supposed that the DSML sends online signals to the consumers to modify their consumption behaviour, to achieve better response to the shifting coefficients. For example, if the load shift coefficient for a certain period 't' is to increase the load demand, the DSML will switch ON the shiftable home appliances which have been requested to operate in that time period. If the load shift coefficient is to decrease the load demand, the DSML will postpone the operation of any shiftable home appliances- which have been requested to operate until a later time and sends an online signal to the community resident to reduce the consumption at that time period.

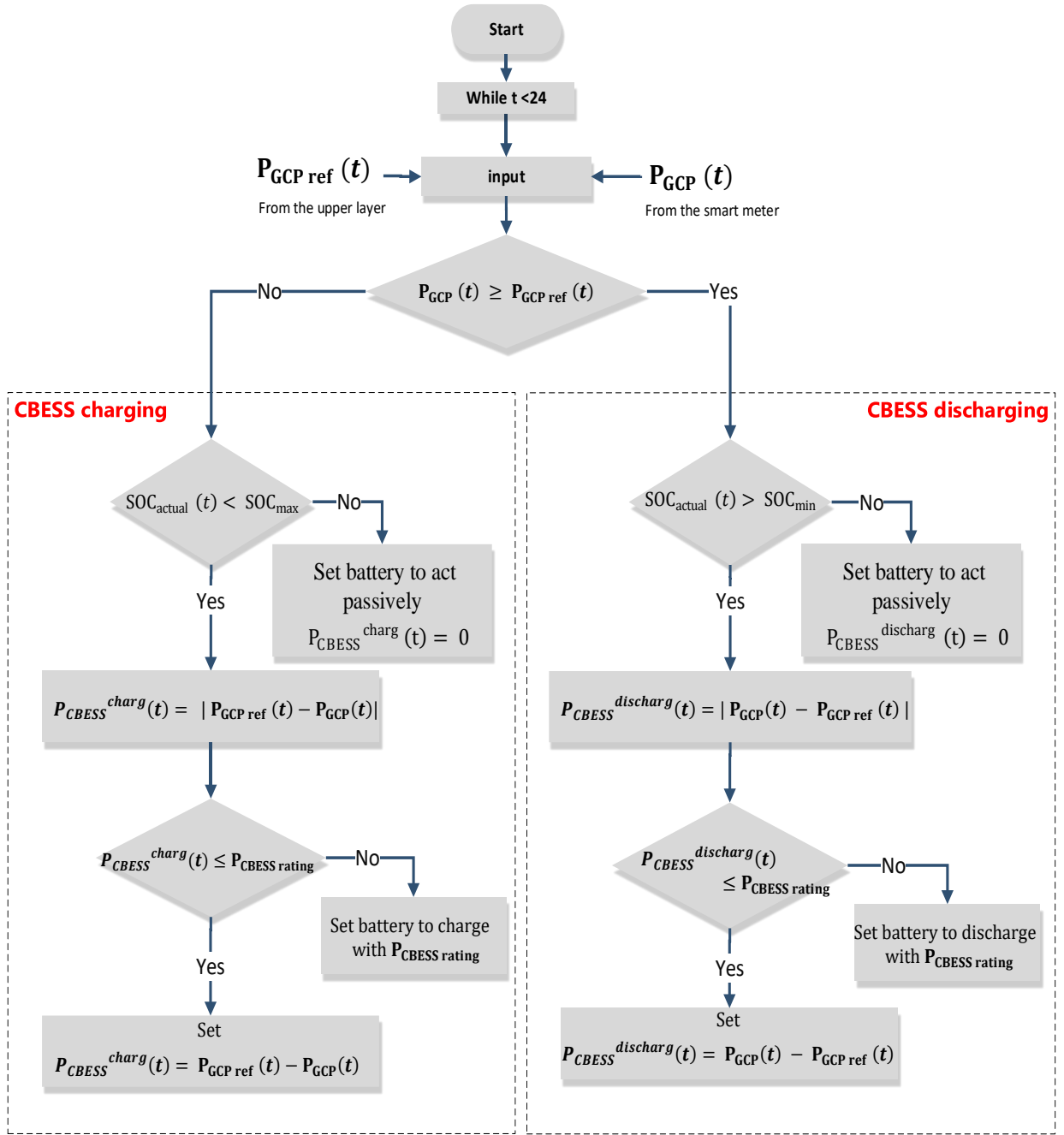


Fig. 6. 2. The rule-based algorithm used in the CBESS control level.

6.3 Formulation of the optimization problem

The cost function for the whole community (all the four houses), that needs to be minimized ‘ $C_{community}$ ’, can be formulated as (6.1, 6.2).

$$C_{community} = C_{CBESS_d} + \sum_{n=house\ 1}^{house\ 4} C_{house}^n \quad (6.1)$$

$$C_{house}^n = C_{house\ import} + C_{house\ export} \quad (6.2)$$

$$C_{house\ import} = \sum_{t=t_0}^{t_0+24h} \Delta T \times f_{import}(t) \times P_{Grid}(t) \quad , at P_{Grid}(t) > 0 \quad (6.3)$$

$$C_{house\ export} = \sum_{t=t_0}^{t_0+24h} \Delta T \times f_{export}(t) \times P_{Grid}(t) \quad , at P_{Grid}(t) < 0 \quad (6.4)$$

$$C_{CBESS_d} = \sum_{t=t_0}^{t_0+24h} \left(\frac{CC_{bat} \times \eta_{Conv} \times \eta_c \times \Delta T \times P_{CBESS}^{charg}(t)}{B_{capacity} \times 2 \times N_{cycle}} + \frac{CC_{bat} \times \Delta T \times P_{CBESS}^{disch}(t)}{B_{capacity} \times \eta_{Conv} \times \eta_d \times 2 \times N_{cycle}} \right) \quad (6.5)$$

where C_{house}^n is the daily electrical energy cost of house no. (n) (£), $C_{house\ import}$ is the daily cost of the electrical energy purchased from the main electricity grid for house no. (n) (£), $C_{house\ export}$ is the daily cost of the exported electrical energy from house no. (n) to the main electricity grid (£), C_{CBESS_d} is the daily degradation cost of the central CBESS (£). ΔT is the sample time (h), $P_{grid}(t)$ is the electrical power imported/exported from the main electricity grid (kW) at a time t, $f_{import}(t)$ is the electricity purchase tariff from the main electricity grid at a time t (£/kWh), $f_{export}(t)$ is the electricity sale tariff (i.e. feed-in tariff) to the main electricity grid at a time t (£/kWh), CC_{bat} is the capital cost of the battery (£), N_{cycle} is the typically number of life cycles of the battery, $B_{capacity}$ is the rated capacity of the battery (kWh), $P_{CBESS}^{disch}(t)$ and $P_{CBESS}^{charg}(t)$ are respectively the CBESS discharge and charge powers at a time t (kW), $P_{CBESS}^{disch}(t)$ is always a positive value while $P_{HSS}^{charg}(t)$ is always a negative value η_d , η_c are the battery discharging and charging efficiencies respectively (%), η_{Conv} is the efficiency of the power converter (%).

When the houses are working as a network, the energy balance equation for the whole community must be reformulated as (6.6).

$$\begin{aligned}
P_{CBESS}(t) + \sum_{n=house\ 1}^{house\ 4} P_{grid}^n(t) \\
= S_L(t) \times \sum_{n=house\ 1}^{house\ 4} P_{load}^n(t) - \sum_{n=house\ 1}^{house\ 4} P_{PV}^n(t)
\end{aligned} \tag{6.6}$$

where $P_{CBESS}(t)$ is the charged/discharged electrical power from the central CBESS at a time t (kW); a negative value means the CBESS is charging, while a positive value means discharging, $\sum_{n=house\ 1}^{house\ 4} P_{load}^n(t)$ is the expected load demand for all houses in the community including the shiftable home appliances for the next 24 hour, $P_{PV}^n(t)$ is the electrical power generated by the PV system in house no. (n) at a time t (kW), $S_L(t)$ is the load shift coefficient at a time t for the next 24 hours; where a value more than one means increasing load, while less than one means loads reduction. $\sum_{n=house\ 1}^{house\ 4} P_{grid}^n(t)$ is the total power imported/exported by the whole community from the main electricity grid

Constraint (6.7) is used to provide boundaries to the load shift coefficient. These boundaries take into account the number of shiftable appliances in the community, the maximum expected consumer response to the shifting signal, and the required comfort level for consumers. Furthermore, constraint (6.8) is used to ensure that the load shifting is only allowed to be scheduled in the allowable time period.

$$S_{Lmin}(t) \times U_{SL}(t) \leq S_L(t) \leq U_{SL}(t) \times S_{Lmax}(t) \tag{6.7}$$

$$U_{SL}(t) = \begin{cases} 1 & , t_{min} < t < T_{max} \\ 0 & otherwise \end{cases} \tag{6.8}$$

where $S_{Lmax}(t)$ is the maximum limit for increasing the loads demand at a time t (%). $S_{Lmin}(t)$ is the maximum limit for decreasing the load demand at a time t (%). $U_{SL}(t)$ is a binary variable used to ensure that the load shifting is only applied in the allowable time set.

The following constraint (6.9 and 6.10) are used to keep the energy balance for each day, i.e. the energy consumption for the whole day should be the same before and after applying the load shift coefficient.

$$\sum_{t=t_0}^{t_0+24h} \sum_{n=house\ 1}^{house\ 4} P_{load}^n(t) = \sum_{t=t_0}^{t_0+24h} \sum_{n=house\ 1}^{house\ 4} P_{\sim load}^n(t) \quad (6.9)$$

$$\sum_{t=t_0}^{t_0+24h} \sum_{n=house\ 1}^{house\ 4} P_{load}^n(t) = \sum_{t=t_0}^{t_0+24h} (S_L(t) \times \sum_{n=house\ 1}^{house\ 4} P_{load}^n(t)) \quad (6.10)$$

where $P_{load}^n(t)$ is the load demand profile before applying load shifting and $P_{\sim load}^n(t)$ is the load demand profile after applying load shift coefficient.

To prevent the central CBESS from exporting energy to the main electricity grid, the following constraint (6.11) is used to introduce link restrictions between the discharging of the central CBESS and exporting power to the grid.

$$\delta_{B\ disch}(t) + \Phi_{export}(t) \leq 1 \quad (6.11)$$

where $\delta_{B\ disch}(t)$ is a binary variable; i.e. equals 1 if the CBESS is discharging and equals 0 otherwise. $\Phi_{export}(t)$ is a binary variable; i.e. equals 1 if the community is exporting power to the main electricity grid at a time t and 0 otherwise.

Also, all the constraints associated with each model in the CES, i.e. the constraints of the central CBESS model (4.6-4.15) and the constraints of the imported/exported power (4.24-4.28) are applied to the MILP optimization process.

The optimization problem for the whole community is solved using the MILP optimization technique. The solution of the optimization problem for the whole community (all the four houses) generates a set of optimal control settings $[P_{GCP\ ref}(t) \ S_L(t)]$, where $P_{GCP\ ref}(t)$ is the reference values of the power at the GCP between the community and

the main electricity grid for the next 24 hours, and $S_L(t)$ is the load shift coefficient for the next 24 hour. These settings will guarantee the best economic use of electrical energy in the community.

At the end of every day, the community level determines the final daily household energy cost for each house in the community. The daily community energy costs ‘ $C_{community}$ ’ is distributed between the houses based on their daily load consumption and PV generation as in (6.12).

$$C_{house}^n = C_{community} \times \frac{\sum_{t=t_0}^{t_0+24h} \{ P_{load}^n(t) - P_{PV}^n(t) \}}{\sum_{n=house\ 1}^{house\ 4} \sum_{t=t_0}^{t_0+24h} \{ P_{load}^n(t) - P_{PV}^n(t) \}} \quad (6.12)$$

This means that as the consumption of house no. (n) increases or if it generates less PV energy, the house will pay a higher ratio of the daily community bill ‘ $C_{community}$ ’. It is worth noticing that the degradation cost of the central CBESS is already considered in the optimization function and sequentially in the overall cost. This cost is distributed between consumers.

6.4 Experimental Test

6.4.1 Laboratory-based Microgrid Rig Architecture

The complete hierarchical CEMS has been implemented in real-time in the University of Nottingham FlexElec Laboratory, using the MG shown in Fig. 6. 3. and Fig. 6. 4. This experiment aimed to: (1) ensure that the proposed CEMS can be applied in a real system without any difficulties; (2) observe the system response while using a real BESS; (3) Ensure that the proposed strategy will operate correctly in the presence of a real communication system which can introduce a time-lag in the control signals.

This MG consists of various pieces of electrical equipment including:

- 2 busbars, 2000A each; One busbar is used as the MG busbar, and the other one represents the main electricity grid.
- 2 Gendrive converters, 10 kW each, used as emulators to emulate the load profile, and PV generation profile.
- 24 kWh Li-ion battery, Nominal battery voltage 400 V.
- 7 kW power converter, is used to connect the battery to the community MG. The converter efficiency is 95%.
- 1 Mbps Controller Area Network (CAN) BUS, is the communication system used in this experiment, it represents the nervous system that enables the communication between all MG's parts.
- A PC: Core i3-7100 CPU, 3.91 GHz was used to run a MATLAB software, which is used to perform the MILP optimization process.
- LABVIEW software, used as a graphical user interface and a control tool to implement the hierarchical CEMS.

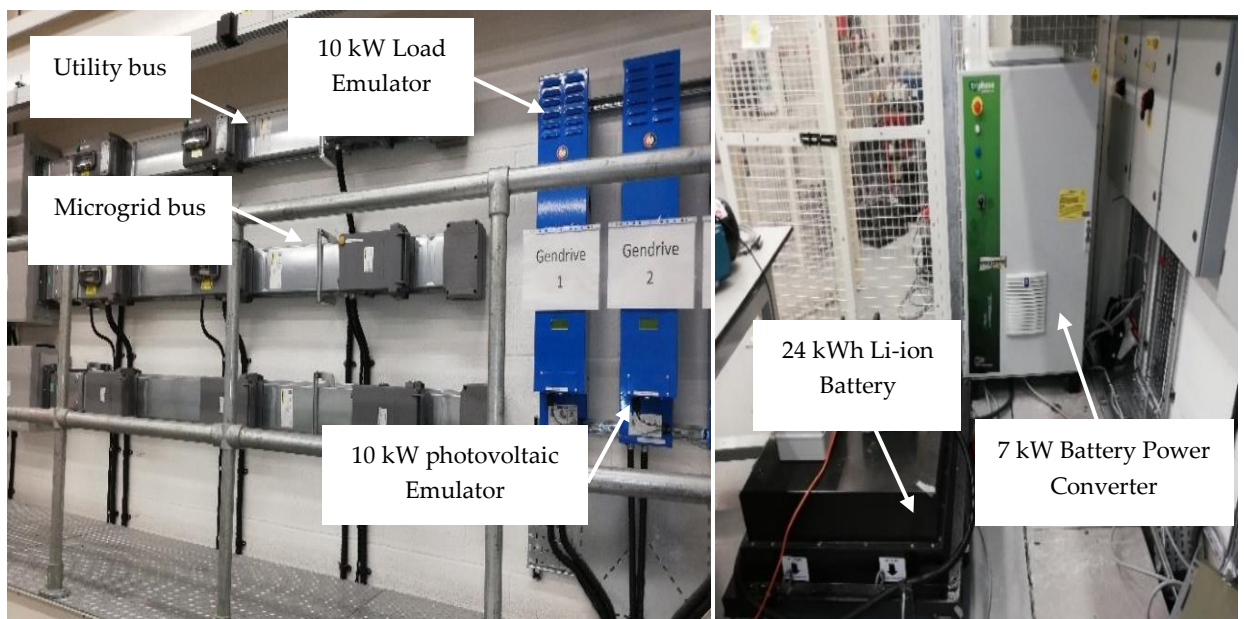


Fig. 6. 3. MG used in the experiment at the University of Nottingham Laboratory.

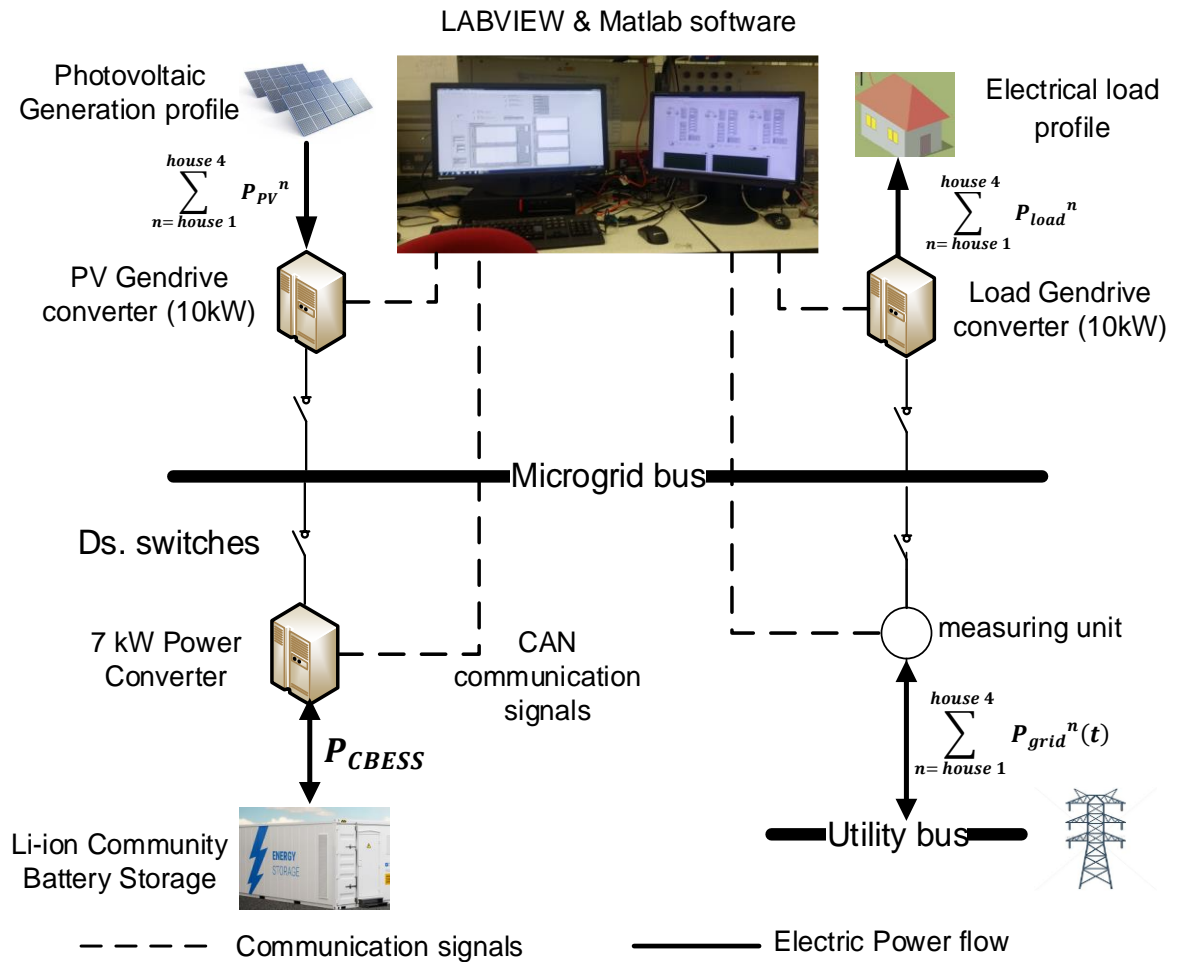


Fig. 6. 4. Architecture of the MG at the University of Nottingham Laboratory.

All the MG components are connected to an isolated busbar (Microgrid Bus). The main source for this MG is a 90 kVA Triphase converter [197] which is a programmable source acting as the main grid connection. Two 10 kW bidirectional Gendrive power converters are connected between the main utility bus and the MG: these inject or absorb active and reactive power into the MG according to references received from a CANBUS communication interface [198]. They are used to emulate the load profiles and PV profiles by following references (generated using the load and PV power profiles described in section 3.2 and section 3.3) sent from the central control platform. The 24 kWh battery system is connected to the MG using a 7kW Triphase power converter.

The hierarchical CEMS is implemented using LABVIEW on a PC and communicates with all the MG elements via a CANBUS interface. The community level is implemented using LABVIEW software which includes embedded MATLAB functions to perform the MILP optimization process. The CBESS level (including the RTC) is implemented using LABVIEW software which includes embedded MATLAB functions to execute the rule-based controller. Also, the DSM level is implemented using LABVIEW software to execute the requested instructions. Appendix F shows the LABVIEW program used in the experiment test of the Hierarchical centralized community energy management system

6.4.2 Experimental procedure

The community level performs the MILP optimization process to determine the best operating scenario for the community for one day ahead. The optimization process minimizes the daily operating cost of the MG and increases the self-consumption of the RES. The reference settings for the power drawn from the main electricity grid, obtained from the optimization process, are updated and passed to the central CBESS level every 15 minutes using a CAN communication system. The optimization process uses a 15 minutes sample time and is repeated every 15 minutes in a rolling horizon manner.

The forecasted daily profiles for the load demand and the PV generation are fed to the optimization process using a sample time of 15 minutes. The forecasted load profile for the next day is obtained from a separate forecasting package (i.e. Adaptive neuro-fuzzy inference system (ANFIS))- this forecasting package is described in more detail in appendix b. The average MAPE of the daily forecasted profiles for the load demand is 8.9%. The forecasted PV generation profile for the next day has been assumed to be the actual PV generation profile for the next day, and Gaussian noise has been added to this profile. This is possible as we are using the historical database. The Gaussian noise represents the forecasting uncertainty

associated with the forecasted PV generation. The function of adding Gaussian noise to a signal - imbedded in Matlab- has been used to create a Gaussian noise waveform profile which is then added to the actual values of the PV generation profiles to represent the forecasted profiles. The values of the signal to noise ratio have been determined using iteration method until the desired value of the MAPE of the daily forecasted PV generation profiles is achieved. The average MAPE of the daily forecasted PV generation profiles is 14%.

The DSM level uses the load shift coefficients-received from the community level every 15 minutes- to shift the actual load demand profile with the required shift coefficient. This is possible because the actual load profiles are known from the historical data.

The CBESS level (including the RTC) makes the MG accurately follow the reference values of the power drawn from the main electricity grid in real-time by defining the optimal power settings of the central CBESS. Every sample time (i.e. one minute), the RTC: (a) receives the reference value for the power drawn by the community MG from the main electricity grid ' $P_{GCP\ ref}(t)$ ', (b) receives the measured SOC of the CBESS using the CAN system, and (c) receives the measured power drawn by the community MG from the main electricity grid (measured using a measuring unit installed at the point of common coupling between the community MG and the main electricity grid- the 90 kVA triphase converter), (d) the RTC determines the power settings for the CBESS every one minute. These settings are sent to the battery's power converter via a CANBUS interface.

6.4.3 Experimental results

Fig. 6. 5. shows the experimental results obtained using the hierarchical CEMS for an emulation over one day (in this case a spring day).

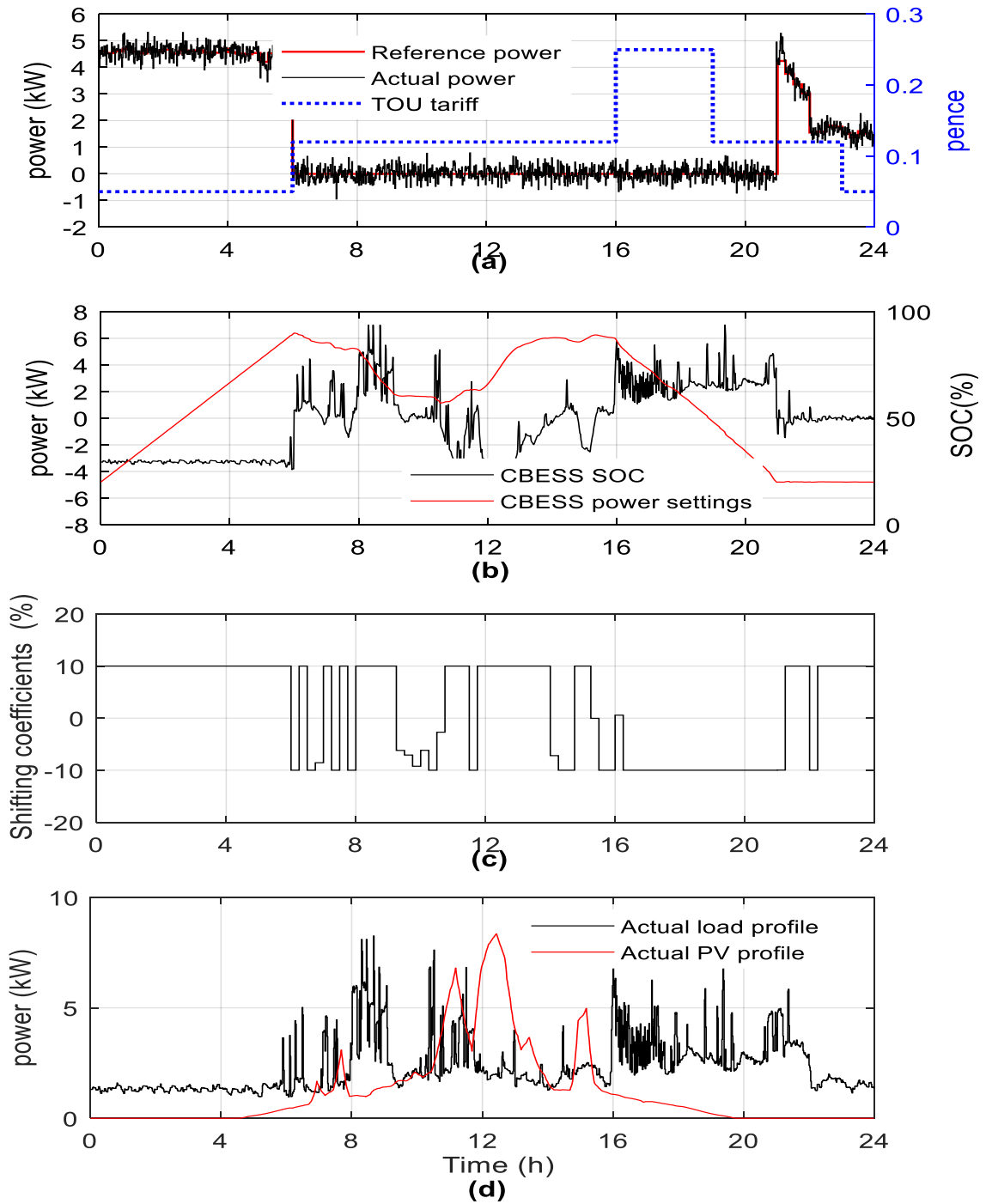


Fig. 6. 5. Experimental results for the daily operation of the community MG using the hierarchical CEMS, where (a) the reference values for the power absorbed by the community MG from the main grid (red settings) - obtained from the MPC level, the measured absorbed power from the main grid through the day (black profile), and the corresponding TOU tariff (blue profile), (b) the optimal power settings of the CBESS (black profile), and the measured SOC of the CBESS during the day (red profile), (c) the load shift coefficient profile during the day-obtained from the MPC level, and (d) the load demand and PV generation profiles.

It is clear from Fig. 6. 5.a that the hierarchical CEMS succeeded in forcing the community MG to follow the reference values for the power drawn from the main electricity grid with high accuracy. There is a very small difference– in the range of 2-4% - between the actual power absorbed by the community MG and the power reference from the MPC level; this value is very small and has a negligible effect on the total operating cost for the whole day. This difference is due to the time delay associated with this being an experimental system, i.e. the actual measurements, computational delays and the delays associated with the battery response as well as measurements noise.

It is clear from Fig. 6. 5.b that the CBESS is charged during the off-peak time (between 00:00 and 06:00) when the cost of purchasing electricity from the main grid is low, and this energy is then used to feed the load during the morning period (from 06:00 to 10:00) and the peak tariff period (from 16:00 to 21:00). Fig. 6. 5.b shows that the central CBESS is charged to 90% of its capacity during the off-peak tariff period when the purchase tariff of the electrical energy from the main grid is low, a part of the stored energy is used to feed the morning load. After this, all of the surplus PV generation (between 10:00 and 16:00) has been used to charge the CBESS. This operating scenario is common when surplus PV generation is expected. Also, it is clear from Fig. 6. 5.b that the proposed CEMS kept the SOC of the central CBESS within limits (between 20 and 90 %).

Fig. 6. 5.c shows the load shift coefficient profile during the day-obtained from the MPC level. The DSML uses this profile to control the shiftable home appliances and send online signals to the consumers to change their consumption behaviour. It is observed from Fig. 6. 5.c that the MPC level sets the load shift coefficient to (-10%)-from 16:00 to 21:00 (peak tariff period), to decrease the load demand during this period. The reduced percentage in the load demand is shifted to another time, e.g. from 00:00 to 06:00, when the CEMS asks to increase the load demand by 10%.

Fig. 6. 6. shows the time consumed for measuring, computing and communicating by each of the MPC level, the DSML and the central CBESS level. It is clear from the Fig. 6. 6.a that the MPC level takes only 14 second for computing and communicating. This time is very short (could be neglected) and does not affect the CEMS results -compared to the time period in which this level is updated (i.e. updated every 15 minutes). Fig. 6. 6.b shows the time required for measuring, computing and communicating through the central CBESS level. It is clear from the results that the CBESS level takes only 4.6 seconds. As this level is repeated every 1 minute, the time taken for measuring, computing and communicating is acceptable. Fig. 6. 6.c shows the time required for the operation of the DSM level. The DSM level uses the shifting coefficient value at each sample time to determine the appliance settings and the online signals for this sample time.

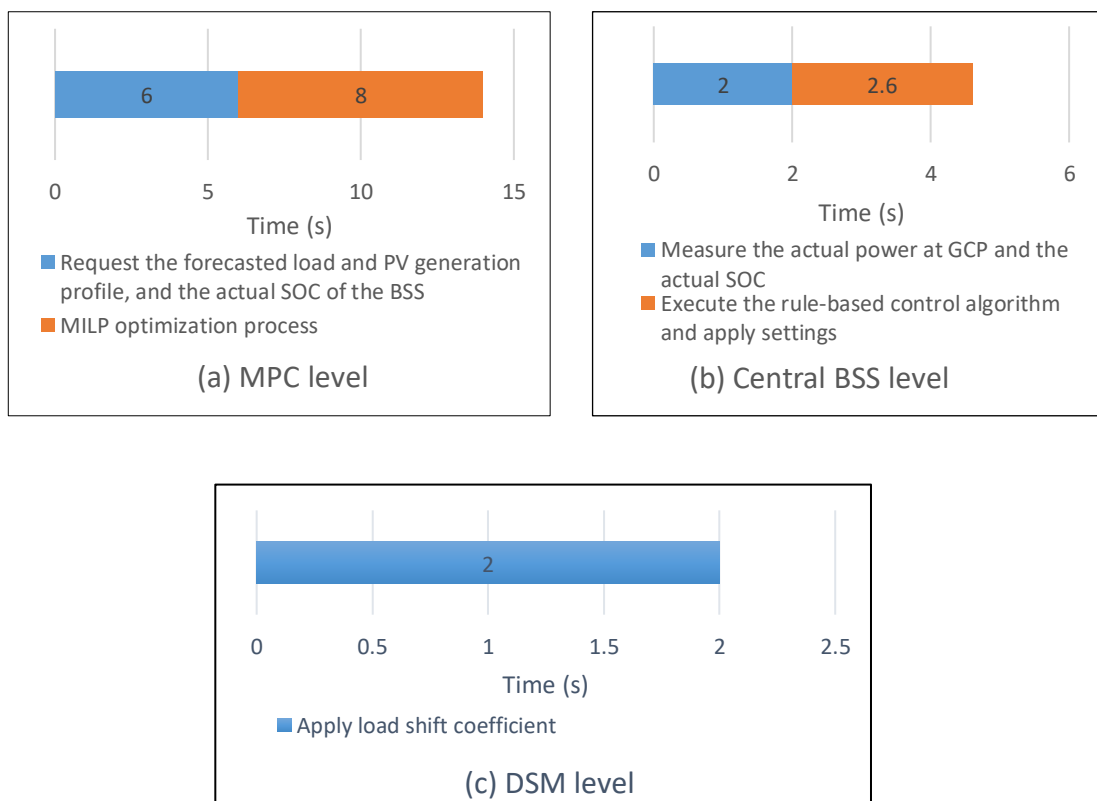


Fig. 6. 6. Time required for measuring, computing and communicating by (a) the MPC level, (b) the central CBESS level, and (c) the DSM level.

6.5 Simulation Results

The operation of the CES has been simulated for one year to consider the effect of all seasons on the operation of the hierarchical CEMS. The load and generation data are based on the real data described in section 3.2 and section 3.3. respectively. L-PWSD forecasting method for load forecasting and PV-PD forecasting method for PV generation forecasting have been used in this simulation.

To clearly compare between the results obtained in this chapter and the results obtained in the previous chapter (chapter 5), it is assumed that a single equivalent central CBESS of 39.8 kWh has been used to replace the combined 6.4 kWh, 13.5 kWh, 13.5 kWh, 6.4 kWh HBSSs located in the four houses. Also, a single power converter of 15 kW has been assumed to replace the 2.5 kW, 5 kW, 5 kW, 2.5 kW power converters used in the four houses.

Table 6. 1. shows a comparison between the annual household energy costs of the four houses when being operated as a part of a CES using the hierarchical CEMS with a 10% load shift coefficient, compared to being operated individually. It is clear from the results that operating the houses as a part of the community produces a greater reduction in the household energy costs of all participating houses (i.e. the percentage reduction in the household energy cost for each house varies from 8.92 % to 17.11%), compared to being operated individually. Also, it is observed that using the hierarchical CEMS achieves 11.11 % reduction in the annual energy costs for the whole community (all houses), compared to being operated individually.

It is observed from Table 6.1. that house no. 4 achieves the highest reduction percent in annual energy cost (17.11%) and house no. 2 achieves the lowest reduction (8.92%), compared to the other houses. The reason is that, according to eq. (6.12), house no. 4 takes the lowest ratio of the community bill as it has the lowest ratio of the daily load consumption and PV generation (18.9%), compared to 19.26%, 31.87%, and 29.54% for the other three

houses respectively. Therefore it achieves the highest reduction in its own household energy costs. However, house no. 2 takes the highest percentage in the community bill, due to having the highest ratio of the daily load consumption and PV generation (31.87%), so it achieves the lowest reduction percentage.

Table 6. 1. Annual household energy costs of the four houses when being operated as a part of a community using the hierarchical CEMS, compared to being operated individually.

	Energy costs (£) (single operation)	Energy costs (£) (Part of community)	Reduction percentage
House 1	252.84	222.57	11.97%
House 2	404.27	368.21	8.92%
House 3	378.64	341.25	9.87%
House 4	263.59	218.5	17.11%
Whole community	1299.34	1155.03	11.11%

By comparing the results in Table 6. 1., Table 5. 4. and Table 5. 6, it is observed that using the hierarchical CEMS with a central CBESS and a DSM technique achieves a higher reduction in the annual energy costs (11.97%, 8.92%, 9.87%, 17.11%) for the four houses respectively, compared to using the centralized hierarchical CEMS with distributed HBSSs which achieves 9.73%, 6.19%, 6.67%, 15.89%, and compared to using the distributed CEMS which achieves 6.98%, 2.60%, 3.42%, 8.86%. The reason is: (a) the hierarchical CEMS with a central CBESS uses a central CBESS of 95% efficiency, compared to using distributed HBSSs of various efficiencies (95%, 90%, 90%, 95%) for the four houses; this means that using a single central CBESS with high efficiency achieves lower reduction in the annual energy costs for the whole community, compared to using multi HBSSs with different efficiencies, (b) the hierarchical CEMS with central CBESS enables each house to share its surplus PV energy with the other houses and also with the central CBESS, compared to the distributed CEMS which limits the energy sharing to be only between the paired houses, and

compared to the central CEMS with distributed HBSSs which suffers from losing energy to storing efficiencies and transmission losses, and (c) the use of a 10% load shift coefficient enables more loads to be shifted in time by controlling the home appliances (with more flexibility) or by modifying the consumer's behaviour, compared to only shifting the home appliances as in chapter 5, which achieves a higher reduction in the annual energy costs

In addition to the reduction achieved in the annual energy costs of each house, the hierarchical CEMS presented in this chapter is considered an improvement over the centralized and distributed CEMSs presented in chapter 5 as: (a) the use of the central CBESS, instead of distributed HBSSs, minimizes the need for complex communication systems to communicate with the large number of HBSSs, which means lower investment costs in the communication system. Also, the probability of the delay or loss of data and the failure of one or more of the HBSSs will be minimized, (b) the use of a central CBESS, instead of multi HBSSs, reduces the size of the optimization problem and the number of constraints, i.e. optimizing the operation of only one CBESS instead of optimizing the operation of multi HBSSs. Therefore, a faster optimization process and more accurate results are guaranteed, (c) the use of the DSML, reduces the size of the optimization problem and the number of constraints, i.e. it is required to determine only the load shift coefficient, instead of determining the optimal operating schedule for each shiftable home appliance. Therefore, the optimization process becomes faster and requires less computing time, (d) the use of a simple communication system and a fast optimization process qualifies the proposed CEMS to be used for managing large communities with a large number of houses, and (e) a smaller size of CBESS and battery power converter could be used instead of using the same equivalent size of the distributed HBSSs (will be discussed in detail in section 6.6). This means potentially a lower investment cost, compared to using multi-HBSSs.

6.6 Sensitivity Analysis and Selection of Key Parameters

This section investigates how the networked operation of houses in the community reduces the need for an overly large CBESS, leaves more transformer and feeder capacity and achieves a further reduction in the annual energy costs for the community. The networked operation of houses using the hierarchical centralized CEMS facilitates the coordination between different factors such as the load shift coefficient, the grid maximum power limit and the size of the battery system (kWh and kW). Coordinating and managing these factors achieve a further reduction in the annual energy costs of the community besides achieving a reduction in the investment costs and leaves more transformer and feeder capacity, e.g. managing the load shift coefficient to shift the loads from high peak periods to lower periods reduces the need for large sizes of transformers besides reducing the need for an overly large CBESS.

6.6.1 Load Shift Coefficient versus Grid Maximum Power Limit

The operation of the community system has been simulated using the hierarchical CEMS and using different load shift coefficients and different grid maximum power limits (the grid maximum power limit is the maximum limit for the power absorbed by the community from the main electricity grid).

Table 6. 2. shows the reduction percentage in the annual energy costs of the whole community using different load shift coefficients and different grid maximum power limit, compared to the case where the rated grid maximum power limit and zero load shift coefficient are used.

Table 6. 2. The reduction percentage in the annual energy costs of the community using different load shift coefficients and different grid maximum power limit, where a positive value means a reduction in the annual energy costs, while a negative value means an increase in the annual energy costs.

		load shift coefficient (S_{Lmin}/S_{Lmax})			
		1.0/1.0	0.9/1.1	0.85/1.15	0.8/1.2
Maximum grid power limit	Rated*	0.00 %	2.58 %	4.18 %	6.21 %
	0.8 rated	0.00 %	2.58 %	4.18 %	6.21 %
	0.65 rated	0.00 %	2.58 %	4.18 %	6.21 %
	0.55 rated	-0.19 %	2.25 %	4.00 %	5.63 %
	0.50 rated	-2.47 %	0.63 %	2.86 %	4.57 %
	0.45 rated	-6.70 %	-4.26 %	-1.86 %	-0.07 %
	0.40 rated	-8.73 %	-4.74 %	-2.10 %	-0.39 %

* The rated limit is assumed to be the rated power of the transformer which feeds the community.

It is clear from Table 6. 2 that the percentage reduction in the annual energy costs increases as the range of the load shift coefficient increases, i.e. the percentage reduction in the annual energy costs reaches more than 6 % by increasing the load shift coefficient range to 20%. This is because more load is shifted from the high tariff period to the low tariff periods as the range of the load shift coefficient increases. This achieves a greater reduction in the annual energy costs. However, this comes over the comfort level of the consumers as a more active response from the users is needed to shift their loads as requested by the CEMS. Also, the wait time of the shiftable appliances will be longer.

It is clear from Table 6. 2 that the percentage reduction in the annual energy costs decreases as the maximum limit of the power absorbed from the main grid decreases. It is observed that the annual energy cost increases by 8.73% when the maximum limit for the power absorbed from grid decreases by 60%, compared to using the rated limit for the power

absorbed from the main grid. This is because decreasing the maximum power limit tightens the limits for the CBESS when changing during the overnight period, which affects the overall costs.

It can be seen from Table 6. 2 that the percentage reduction in the annual energy costs (for each value of the load shift coefficients) does not change as the maximum limit of the power absorbed from the main grid decrease by 20% and 35%. This is because: (a) the overnight charging period of the central CBESS is not affected by this decrease, i.e. the limit of the power absorbed from the main grid is higher than the maximum power needed to charge the central CBESS during the night period, (b) the use of the CBESS reduced the peak power of the load (usually between 16:00 and 20:00) to below the maximum limit of the power absorbed from the main grid. This means that the CES could operate all the year using only a maximum of 65% of the capacity of the transformer and the feeders, leaving 35% of the capacity of the transformer spare. This spare capacity could to be used for additional purposes such as adding EV charging stations or expected future extension in the number of houses at that location.

It can also be seen from Table 6. 2 that there are key operating points for the community (i.e. point 1 and point 2). These key points achieve lower annual energy costs, higher spare capacity in the transformer, and a high comfort level for users. For example, at operating point 1, using a load shift coefficient of 10% and a grid maximum power limit of 55% achieve a 2.25% reduction in the annual energy costs and guarantee 45% spare capacity in the transformer. Furthermore, a greater reduction in the annual energy costs is achieved (4.57%) when a higher load shift coefficient (20%) is used, as in operating point 2. However, this comes with reduction to the user's comfort level. The community users could choose the appropriate operating scenario (point) according to their needs.

Generally speaking, from Table 6. 2., it is important to study the effect of different factors on the operating scenarios of the system to select the best operating point. The best operating point is the point which achieves the lowest reduction in costs, the highest spare capacity for the transformer and a high comfort level for the customers.

6.6.2 Load Shift Coefficient versus Capacity of the Central CBESS

This part shows how the management of the load shift coefficient - to shift the loads from high peak periods to the lower peak periods- reduces the need for a large CBESS and achieves a further reduction in the annual energy costs for the community.

In order to show this part, the operation of the CES has been simulated using different load shift coefficients and different capacities of the central CBESS, see Table 6. 3. It is clear from table 6. 3. that percentage reduction in the annual energy costs (for each value of load shift coefficients) decreases as the battery's size decreases, i.e. the annual energy costs increased by 5.15% when the capacity of the used CBESS decreased to 80% of the rated size, compared to using the rated CBESS size. This is logical because using a lower size of CBESS means that the CBESS is not able to store sufficient energy during the off-peak period to feed the loads during the peak periods, which leads to higher energy costs. Nevertheless, it is observed that increasing the load shift coefficients can compensate for the decrease in CBESS size, to maintain a reduction in the annual energy costs; i.e. the percentage reduction in the annual energy costs reaches 1.36% while using 80% of the rated CBESS size and 20% load shift coefficients.

Table 6. 3. The reduction percentage in the annual energy costs of the community using different load shift coefficients and different capacities of the central CBESS, where a positive value means a reduction in the annual energy costs, while a negative value means an increase in the annual energy costs.

		Load shift coefficient (S_{Lmin}/S_{Lmax})			
		1.0/1.0	0.9/1.1	0.85/1.15	0.8/1.2
Battery capacity	Rated	0.00 %	2.58 %	4.18 %	6.21 %
	0.95 rated	-0.59 %	1.52 %	3.15 %	4.45 %
	0.9 rated	-1.81 %	0.38 %	2.09 %	3.48 %
	0.85 rated	-3.36 %	-0.84 %	1.03 %	2.42 %
	0.80 rated	-5.15 %	-2.22 %	-0.17 %	1.36 %

It is observed from Table 6. 3. that using a load shift coefficient of 15% and 85% of the rated CBESS size, achieves a 1.03% reduction in the annual energy costs, compared to the case where the rated CBESS size and a zero load shift coefficient are used. This point is called the key operating point. The key operating point for this case is the point which achieves a reduction in annual energy costs for the community while using a lower CBESS size. Using a lower size of the CBESS means lower investment costs and higher indirect profits. It is worth noting that this point should be selected accurately since the revenue from the reduction in the CBESS size comes at the expense of the comfort level of the consumers.

6.6.3 Changing the Size of the Battery’s Power Converter

It is observed from section 6.6.1 and section 6.6.2. that a further reduction in the annual energy costs of the community is achieved when the load shift coefficient has been controlled. This is accompanied by a possibility of lowering the limit for the power absorbed by the community from the main electricity grid (as discussed in section 6.6.1) and using a lower

size of the central CBESS (as discussed in section 6.6.2). In this section, changing the size of the battery power converter will be studied to determine if a further reduction in the investment costs can be achieved besides the reduction in the annual operating costs of the community.

The operation of the community has been simulated using the hierarchical CEMS and using different sizes of the battery power converter, a central CBESS with 85% of the rated size, load shift coefficient of 15%, and a grid maximum power limit of 55%. The results of the simulation process are summarized in Table 6. 4.

It is observed from Table 6. 4. that the reduction in the annual energy costs decreases as the converter size decreases, i.e. a 0.42% reduction in the annual energy costs is achieved while using only 60% of the rated size of the power converter. The reduction percentage in the annual energy costs reached 0.90% when the rated size of the battery’s power converter is used in addition to a 85% of the rated size of the CBESS, load shift coefficient of 15%, and grid maximum power limit of 55%. The reduction percentage is compared to the case where the rated battery’s power converter size, the rated CBESS size, the rated grid maximum power limit and zero load shift coefficient are used.

Table 6. 4. The reduction percentage in the annual energy costs for the community using different sizes of the battery’s power converter while using 85% of the rated sized of the CBESS, load shift coefficient of 15%, and grid maximum power limit of 55%, compared to using the rated CBESS size, the rated grids’ power limit and zero load shift coefficient.

	The size of the battery’s power converter			
	Rated	0.75 rated	0.6 rated	0.5 rated
Reduction percentage in the annual energy costs	0.90 %	0.77 %	0.42 %	-0.29 %

Key point



From the results obtained, using the proposed hierarchical CEMS with a central CBESS and DSM techniques achieves a 0.42% reduction in the annual energy costs for the community while using (a) a 85% of the rated size of the CBESS, (b) a load shift coefficient of 15%, (c) a grid maximum power limit of 55%, and (d) a 60% of the rated size of the power converter. Using lower sizes for CBESS and power converter means lower investment costs. Lowering the grid's power limits means more free capacity in the power transformers and feeders, which enables them to be used for additional purposes such as adding EV charging stations or expected future extension in the number of houses.

6.7 Summary and Conclusion

The conclusions of this chapter are as follows:

- This chapter presented a hierarchical centralized CEMS with a central CBESS control level and a Demand-side management level. The hierarchical CEMS minimized the annual household energy costs and maximized the PV self-consumption. A complete model for the community has been built, considering all the constraints that affect the operation of the community. The MILP optimization technique successfully obtained reference values with a low processing time. The hierarchical CEMS coordinates the operation of the central CBESS and the shiftable home appliances (using the DSML) to minimize the energy purchased from the main grid at peak times, store all the excess PV energy, and avoid exporting any energy to the main electricity grid. It has been shown that the commercial operation of the interconnected houses can be improved by their participation in a community using the proposed hierarchical CEMS, compared to being operated individually.
- Optimizing the operation of the community using the hierarchical CEMS with a central CBESS and DSM technique achieves a higher reduction in the annual energy costs

(11.97%, 8.92%, 9.87%, 17.11%) for the four houses respectively, compared to being operated individually, and compared to using the centralized CEMS with distributed HBSSs which achieves 9.73%, 6.19%, 6.67%, 15.89%, and compared to using the distributed CEMS which achieves 6.98%, 2.60%, 3.42%, 8.86%. In addition to the reduction achieved in the annual energy costs of each house, the hierarchical CEMS presented in this chapter is considered an improvement over the centralized and distributed CEMSs presented in chapter 5 due to using simple communication systems, fast optimization process, being less affected by the delay or loss of data and could be used for managing big communities with a large number of houses.

- The experimental results demonstrate the proposed strategy can work in real-time with a real communication system providing an interconnect between the system elements.
- Merging the DSM technique and the proposed hierarchical CEMS achieves a 4.57% reduction in the annual energy costs while using only 50% of the maximum capacity of the distribution transformer and feeder. The remaining capacity (50%) could be used for adding new EV charging stations in the system (if required) or for system extension in the future.
- Using the proposed hierarchical CEMS in addition to a load shift coefficient of 20% achieves a 6.21% reduction in the annual energy costs, compared to the case where a zero load shift coefficient is used.
- A lower size of the central CBESS and a lower size of the power converter could be used in the community (replacing the rated sizes), by merging the DSM techniques and the proposed hierarchical CEMS-while still achieving an acceptable reduction in the annual energy costs. Using a lower size of the CBESS and the power converter means lower investment costs (indirect profits).

- The results show that the networked operation of houses can reduce the need for an overly large CBESS, and leave more transformer and feeder capacity. 0.42% reduction in the annual energy costs for the community could be achieved using only 85% of the rated size of the CBESS, 60% of the rated size of the power converter, 15% load shift coefficient, and grid maximum power limit of 55%. The results obtained encourage the investment in the hierarchical CEMS with a central CBESS and DSM as it ensures a reduction in the annual energy costs and lower investment costs.

Chapter 6 has examined the developed structure of the hierarchical centralized community energy management algorithm to make it applied to larger communities (with a large number of houses). Also, this chapter has investigated how the networked operation of houses in the community reduces the need for an overly large CBESS and ensures lower investment costs. The work presented in this chapter has potentially addressed objective (5) listed in section 1.3.

The next chapter will examine a method to appropriately size the CBESS for a given energy community to ensure that the community is not over-investing in its energy storage assets. Also, will investigate whether additional revenues could be achieved from the participating of the CBESS in ancillary services in the UK market.

Chapter 7

Sizing of a Community Battery to Provide Energy Management Services

7.1 Introduction

This chapter introduces a methodology for selecting the best size for a Community Battery Energy Storage System (CBESS) (in terms of energy and power rating) to provide Community Energy Bill Management (CEBM). The best size of the CBESS to provide CEBM service is the size which minimizes both the investment cost of the CBESS and the operational cost when used to provide the CEBM service. The best size has been determined using a simulation process for the operation of the CBESS for one year. The results obtained are then used in an economic study to obtain the Internal Rate of Return (IRR) of this investment over a 20-year period.

Chapter 6 has shown that using a central large scale CBESS to provide CEBM service for communities can result in significant energy cost savings for members of the community, and therefore achieve a high IRR for investment in this type of technology. However, it is still difficult to receive planning permission from the UK Grid Operators to manage a behind-the-meter large scale CBESS to provide this type of service [199]. Therefore, it is interesting to investigate the use of the same CBESS to provide the services which are currently available in the UK energy market (such as the Capacity Market (CM) service and Dynamic Firm Frequency Response (DFFR) service) so the work on CEBM can be benchmarked. These services potentially offer the best revenues for energy storage from the UK energy market. A comparison has been performed to determine the financial reward if the same CBESS is used

to participate in the UK energy/capacity market services compared to providing the CBEM service.

In addition, it was important to investigate whether the same CBESS could provide services such as CM and DFFR as well as providing a CEBM service and whether providing multiple services could maximize the profits from the investment in the CBESS.

7.2 The Architecture of the Community Energy System

In the sizing optimization problem of the CBESS, it is important to consider a case study of a real community system to clearly show the effect of the battery size on the internal rate of return (IRR) values and to have a realistic indication of the revenue from the investment in the CBESS to provide a CBEM service. Therefore, the community of four houses, used in the previous chapters, will be replaced with a more realistic community size.

The case study used in this chapter is modelled on a real community which includes distributed (rooftop) PV generation systems and a central CBESS. The community is located on the banks of the River Trent, Nottingham, UK. The community is a part of the Trent Basin neighbourhood of low energy homes [196]. The community consists of 114 houses with an average daily demand of 2.1 MWh. The community has 500 kW peak distributed PV panels which generate an average of 1.25 MWh each day. The community is also connected to the main distribution grid [200]. Fig. 7. 1. shows the architecture of the CES. The load profile of the whole community has been created by adding the actual measurements of the load demand of 22 houses based in Milton Keynes, UK (to show the aggregation effect of load profiles), and then scaling up this community load profile to give an equivalent average daily load demand of 2.1 MWh. The community load profile is for one year and has a 15 minute resolution. This data was combined with the real PV generation profile, presented in section 3.3. The PV generation profile is also scaled up to give an equivalent average daily generation of 1.25

MWh, with the assumption that the PV panels are positioned on the 114 co-located houses. There are no HBSS are fitted into any of the houses. There is a central community battery storage system.

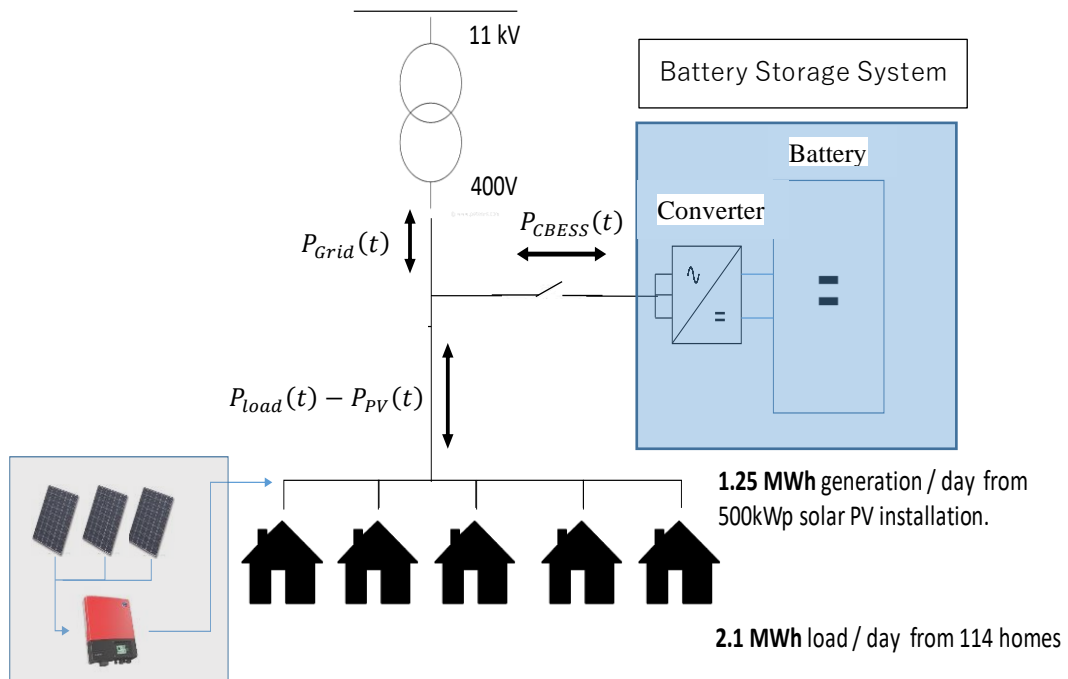


Fig. 7. 1. Architecture of the CES.

7.3 The Techno-Economic Sizing Methodology

Initially, it is assumed that the CBESS is used to provide the CEBM service. The best size of CBESS to provide CEBM has been determined using a simulation process for the operation of the CBESS for one year, described in section 7.4. The results obtained are then used in an economic study to obtain the Internal Rate of Return (IRR) of this investment over a 20-year period. The effect of changing the capacity of the CBESS and the size of the power converter on the IRR are also studied.

The IRR of the investment for using the CBESS for the CEBM service is then compared with other cases where the same CBESS is used instead to provide Capacity Market (CM) service or Dynamic Firm Frequency Response (DFFR) service for the UK energy market.

This comparison is performed to determine the financial reward if the CBESS is used instead to participate in the UK energy/capacity market services.

7.4 CBESS Sizing to Provide a CEBM Service

The central CBESS shown in Fig. 7. 1. is firstly assessed by considering its use for providing a CEBM service to the community. The CBESS is charged at night (low tariff period) to a certain level, then topped up with the surplus PV generation during the day. After that, the stored energy in the CBESS is used to feed the loads during the morning and the peak tariff periods to avoid purchasing energy at high price from the main electricity grid. The central CBESS is used to reduce the annual community energy bill and maximize the PV self-consumption within the community using the same community energy management algorithm as described in section 6.2 but with a modified optimization problem as described in the next section to determine the best size of the CBESS. The optimal CBESS size is the size which minimizes both the investment cost of the CBESS and the operational cost when used to provide the CEBM service, see Fig. 7. 2.

The CBESS investment cost ($CAPEX_{year}$) includes the initial cost of the battery (£350/kWh) and the initial cost of the battery's power converter (£115.5/kW), while the operational costs ($OPEX_{year}$) are mainly the operating costs of the community after using the CBESS - the cost of imported electricity from the main distribution grid to feed the community's load demands and charge the CBESS over a year, plus the revenue of the surplus energy sold to the main grid, i.e. the excess electricity produced by the PV generation after satisfying the community demands and charging the CBESS- in addition to the annual CBESS maintenance costs.

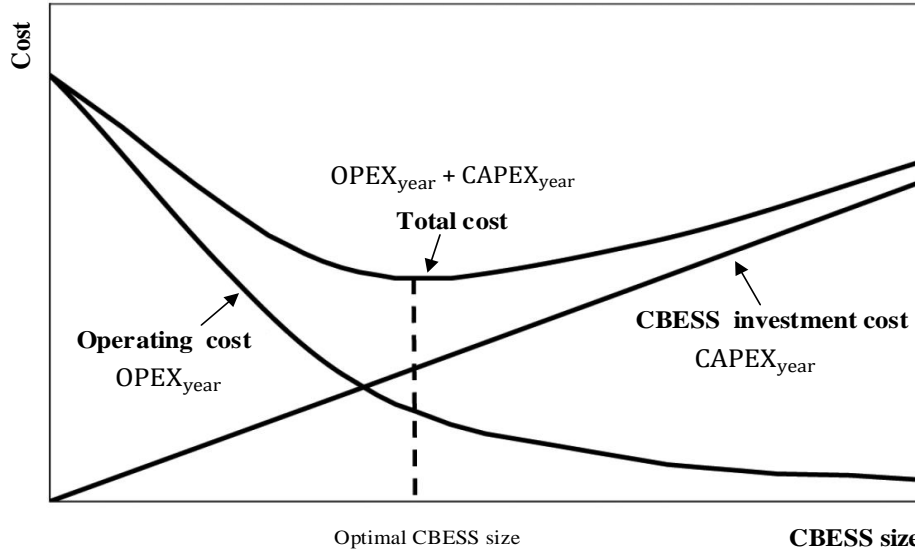


Fig. 7. 2. Effect of changing the CBESS size on the initial investment cost, operating cost, and the total project cost when used to provide CEBM services.

7.4.1 Formulating the Optimization Problem and its Constraints

The objective function described here aims to determine the best size for the battery storage system as well as the best size for the power converter to minimize both the capital investment cost of the CBESS ($CAPEX_{year}$) and the annual operating costs of the community system ($OPEX_{year}$). The objective function, which needs to be minimized, is formulated as a MILP optimization problem as in (7.1). The CBESS investment cost ($CAPEX_{year}$) (7.2) includes the initial cost of the battery and the initial cost of the battery's power converter. It includes also pro-rata installation costs for energy rating (IC_{energy}) and power rating (IC_{power}). The CBESS investment cost is normalized on an annual basis (i.e. distributed over the lifespan of the CBESS). The expected operating costs of the community after using the CBESS ($OPEX_{year}$) (7.3) are: (a) ' C_{buy} ' the cost of imported electricity from the main distribution grid to feed the community's load demands and charge the CBESS over a year, (b) ' C_{sell} ' the revenue of the surplus energy sold to the main grid, i.e. the excess electricity produced by the PV generation after satisfying the community demands and charging the

CBESS [201], (c) ‘ SC ’ the annual standing charge, (d) ‘ Y_{main_cost} ’ (7.6) the annual maintenance cost of the CBESS; this cost is divided into fixed and variable maintenance costs. The fixed maintenance cost is used for regular servicing of the CBESS, whilst the variable cost accounts for on demand related maintenance. The annual maintenance cost is assumed to be 0.45 % of the total investment cost of the CBESS [202].

$$\min (CAPEX_{year} + OPEX_{year}) \quad (7.1)$$

$$CAPEX_{year} = \frac{IC_{energy}}{LF} \times B_{capacity} + \frac{IC_{power}}{LF} \times P_{CBESS \text{ rating}} \quad (7.2)$$

$$OPEX_{year} = C_{import} + C_{export} + SC + Y_{main_cost} \quad (7.3)$$

$$C_{import} = \sum_{day=1}^{365} \sum_{t=t_0}^{t_0+24h} \Delta T \times f_{import}(t) \times P_{Grid}(t) \quad , \text{at } P_{Grid}(t) > 0 \quad , \text{at } P_{Grid}(t) > 0 \quad (7.4)$$

$$C_{export} = \sum_{day=1}^{365} \sum_{t=t_0}^{t_0+24h} \Delta T \times f_{export}(t) \times P_{Grid}(t) \quad , \text{at } P_{Grid}(t) < 0 \quad , \text{at } P_{Grid}(t) < 0 \quad (7.5)$$

$$Y_{main_cost} = 0.45\% \times CAPEX_{year} \times LF \quad (7.6)$$

where IC_{energy} is the CBESS investment cost based on energy rating (£/kWh), IC_{power} is the CBESS investment cost based on power rating (£/kW), $B_{capacity}$ is the rated capacity of the battery (kWh), $P_{CBESS \text{ rating}}$ is the converter rated discharge/charge power (kW), LF is the CBESS Life time (assumed 20 years), SC is the yearly standing charge (£/year), ΔT is the sample time (h), $P_{grid}(t)$ is the electrical power imported/exported from the main electricity grid (kW) at a time (t); a positive value means that the community is importing power from the main electricity grid while a negative value means exporting, $f_{import}(t)$ is the electricity purchase tariff from the main electricity grid a time t (£/kWh), $f_{export}(t)$ is the electricity sale tariff to the main electricity grid at a time t (£/kWh), Y_{main_cost} is the yearly maintenance (£) cost of the CBESS.

Since the number of charging/discharging cycles per day for the CBESS depends on the way in which the battery is operated [203]. Constraint (7.7) has been used to ensure that the total number of life cycles undergone by the battery is lower than the typical life cycles specified by the manufacturer [124]. Constraint (7.7) count for battery degradation from charging and discharging cycles [204].

$$\sum_{day=1}^{365} \sum_{t=t_0}^{t_0+24h} \left(\frac{\sqrt{\eta} \times \Delta T \times P_{CBESS}^{charg}(t)}{C_B \times 2} + \frac{\Delta T \times P_{CBESS}^{disch}(t)}{C_B \times \sqrt{\eta} \times 2} \right) \leq \frac{N_{cycle}}{LF} \quad (7.7)$$

where N_{cycle} is the typical number of life cycles of the battery, $P_{CBESS}^{disch}(t)$ and $P_{CBESS}^{charg}(t)$ are respectively the CBESS discharge and charge powers at a time interval t (kW), $P_{CBESS}^{disch}(t)$ is always a positive value whilst $P_{CBESS}^{charg}(t)$ is always a negative value, and η is the battery full cycle efficiency (%). $\sqrt{\eta}$ is the charging or discharging efficiency of the battery. Charging efficiency or discharging efficiency of the battery can be calculated by taking the square root of the battery full cycle efficiency [205].

The power balance equation constraint of the total active power in the community is formulated as in (7.8):

$$P_{Grid}(t) + P_{CBESS}(t) = P_{load}(t) - P_{PV}(t) \quad (7.8)$$

where $P_{load}(t)$ is the yearly electrical load profile of the community (kW), $P_{PV}(t)$ is the yearly electrical profile of the power generated by the PV systems located in the community (kW), $P_{CBESS}(t)$ is the yearly electrical profile of the discharged/charged power by the CBESS (kW), (i.e. $P_{bat_disch}(t) - P_{bat_charge}$); where a positive value means that the CBESS discharges, and a negative value means that the CBESS charges, $P_{Grid}(t)$ is the yearly electric profile of the power purchased/sold to the main electric grid at the grid connection point between the community and the main electricity grid.

To prevent the CBESS from exporting energy to the main electricity grid, the following constraint (7.9) is used to introduce link restrictions between the discharging of the CBESS and exporting power to the grid.

$$\delta_{B \text{ disch}}(t) + \Phi_{\text{export}}(t) \leq 1 \quad (7.9)$$

where $\delta_{B \text{ disch}}(t)$ is a binary variable; i.e. equals 1 if the battery is discharging and equals 0 otherwise, $\Phi_{\text{export}}(t)$ is a binary variable; i.e. equals 1 if the community is exporting power to the main electricity grid at a time t and 0 otherwise.

Also, all the constraints associated with the CBESS model (4.6-4.15) and the constraints of the imported/exported power from the main electricity grid (4.24-4.28) are applied to the MILP optimization process. The CBESS model feeds into the power calculations of the MILP optimization problem, i.e. $P_{\text{CBESS}}(t)$ in eq. (7.8), and the constraints of the CBESS model are considered as a MILP optimization constraints.

7.4.2 Economic analysis

The optimization problem, described in section 7.4.1, is solved using the MILP optimization technique. The solution to the optimization problem determines the best size of CBESS (rated capacity of the battery and the rated value of the power converter) which minimizes the annual operating costs of the community system together with the capital investment cost. The optimization process is performed using the historical profiles for the load and the PV generation and with the aid of the community energy management algorithm, i.e. described in section 6.2. The optimization problem is implemented using a MATLAB script to determine the best size of the CBESS and also to create power profiles for grid and battery usage which can be allocated to specific charge periods using a TOU tariff. The results obtained from the simulation process are then passed to a Microsoft Excel worksheet to obtain the IRR value of this investment over a 20-year period. The IRR value is calculated using an

embedded function in Microsoft Excel. The IRR is a metric used in capital budgeting to estimate the revenue of potential investment over a fixed time period, see eq. (3.4) in section 3.8. for more details about the IRR formulation. The parameters used in the simulation process are shown in Table 7. 1. (CEBM column).

The economic analysis is performed using a spreadsheet in which the yearly revenue from using the CBESS for CEBM service can be presented in terms of incomes and payments. The incomes include the difference between the annual energy costs before using the CBESS (the cost of the electricity purchased by the community from the supply utility before using the CBESS, assuming a flat rate for the whole day), compared to the annual energy costs when using the CBESS to provide CEBM service. The payments include: (a) the yearly standing charge ‘SC’ for Transmission Network Use of System (TNUOS) and Distribution Use of System (DUOS) - explained in detail in section 3.8., and (b) the annual maintenance cost of the CBESS. The economic analysis considered important factors such as the annual inflation rate, energy tariff increase rate, battery’s round trip efficiency, and capacity fade for the operation of the CBESS (i.e. the annual reduction in the rated capacity of the CBESS until it reaches 80% - the end of lifetime). These factors have a significant effect on the investment in the CBESS to provide the CEBM service for a long period of time.

Table 7. 1. Values used in the simulation process for the participation of the CBESS in the CEBM, CM and DFFR services.

Parameter	Service type		
	CEBM	CM	DFFR
CBESS energy rating investment cost (IC_{energy}) [206] , [168]	£350 /kWh		
CBESS power rating investment cost (IC_{power}) [207]	£115.5 /kW		
Battery full cycle efficiency (η)	90%		
Battery maximum SOC limit (SOC_{max})	90%		
Battery minimum SOC limit (SOC_{min})	20%		
Average annual inflation rate [208]	2 %		
CBESS Capacity fade [209]	80% at the end of lifetime		
Battery lifetime (LF)	20 years		
Energy prices increase rate [210]	5 % p.a.		
Standing charge (SC)	80.2 £/year		
Purchasing electricity tariff [160]	TOU tariff	4.99 pence/kWh	-
Sell electricity price	4.85 pence/kWh	11.99 pence/kWh	-
CM revenue (contract fees) [211]	-	£16.8 /kW/year	-
Energy services company management fee [212]	-	20% of net yearly profit	20% of net yearly profit
Availability fees [213]	-	-	£8 /MW/hour
Response Energy Fee (£/MWh)	-	-	£0/MWh
Guarantee of CBESS response for DFFR [207]	-	-	95%

7.4.3 Results

The optimization problem is solved using the MILP optimization technique. The optimal CBESS size to provide the CEBM service is found to have a capacity of 991 kWh and a power rating of 256 kW. The nearest commercial capacity of 1000 kWh and power rating of 250 kW have been selected. The annual operating cost of the community system with PV generation is reduced from £64,562 (before using the CBESS) -i.e. the cost of the electricity purchased by the community from the supply utility before using the CBESS, assuming a flat rate of 13.15 pence/kWh for the whole day - to £33,872 when using the optimal size of the CBESS with a TOU tariff. The percentage reduction is 47.5. This percentage reduction is considered to be the annual income from the investment in using the CBESS for the CEBM service. Also, the local self-consumption of PV generation within the community increased to 93.5 % when using the CBESS, compared to 53% before using the CBESS.

Fig. 7. 3. shows the cumulative cash flow over 20 years for the investment in the 1000kWh/250kW CBESS to provide the CEBM service. The cumulative cash flow for each year is calculated by adding the yearly income from using the CBESS to the initial investment cost of the CBESS. Appendix G shows the calculations used to obtain these results. The initial investment cost in the CBESS is £378,960, i.e. this value is calculated using the 1000kWh/250kW CBESS and the energy/power rating investment costs shown in Table 7. 1.

It is observed from Fig. 7. 3. that the return on investment in the CBESS to provide the CEBM service over 20 years is £397,882, and the payback period is 12 years. The IRR is calculated to be 7.26%. From the results obtained, An investment in this kind of service needs a long time (more than 10 years) to achieve reasonable profits and therefore the CBESS should have a long lifetime and guarantee a minimum of 8000 cycles. The return on investment is expected to increase as the initial cost of batteries is expected to decrease over the next few

years [14] and more flexible tariffs schemes are likely to be introduced. The results obtained encourage the investment in the CBESS to provide a CEBM service as it provides a high IRR (7.2%) and achieves an average local PV self-consumption of 88.4% over the 20 years.

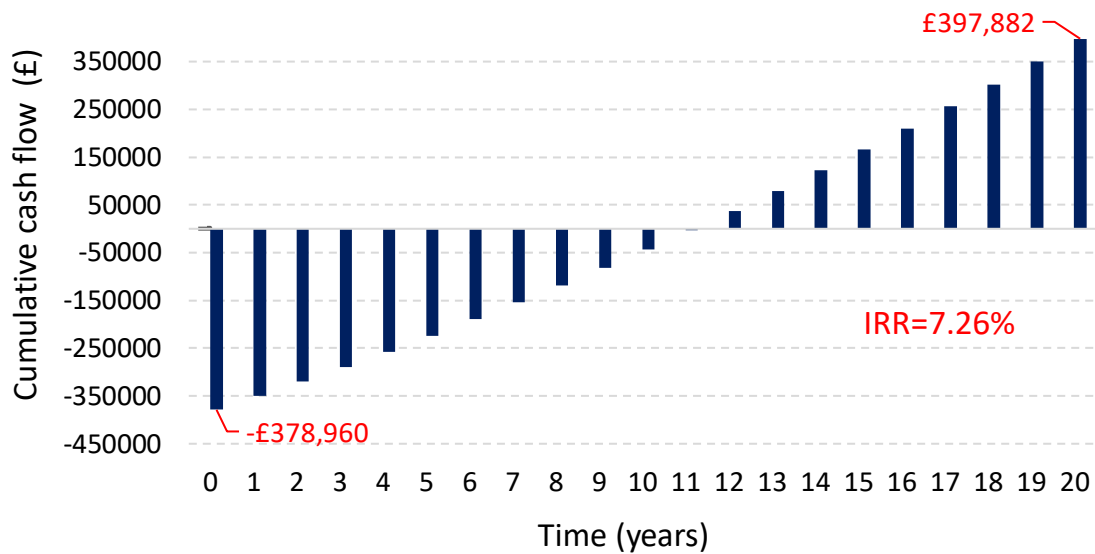


Fig. 7. 3. Cumulative cash flow over 20 years for using a 1000kWh/250kW CBESS to provide CEBM services.

7.4.4 The Effect of the CBESS size on the IRR while Providing a CEBM Service

This section studies the effect of changing the size of the CBESS (the rated capacity and the rated power) on the IRR while providing the CEBM service. The operation of the CBESS has been simulated over a 20 year period and the size of the CBESS has been changed. Fig. 7. 4 shows the effect of using different capacities of CBESS and different sizes of power converter on the IRR while providing a CEBM service. The results show that for each CBESS capacity (kWh), the IRR decreases as the rated power increases. Also, for each value of rated converter power, the IRR decreases as the rated capacity of the CBESS increases. This is because when the capacity or the power of the CBESS increases over a certain limit, the investment cost in this case will be more than the expected reduction in the annual operating cost, as seen in Fig. 7.2, which decrease the overall IRR.

Fig. 7. 4. shows that using a 1000kWh/250kW CBESS to provide the CEBM service achieves an IRR of 7.26% over a 20 year period, whilst using a 2000kWh/1000kW CBESS achieves an IRR of 1.81% over a 20 year period. Note that the capacity of the CBESS used should not be less than 1000kWh to be able to participate in the energy/capacity market as will be discussed later in sections 7.5 and 7.6. The optimal size for the CBESS to provide a CEBM service for this community is 1000kWh/250kW (obtained from the optimization process). Using higher or lower sizes of the CBESS (lower or higher than 1000kWh and 250kW) will achieve lower IRR values for the investment in the CBESS to provide CEBM service.

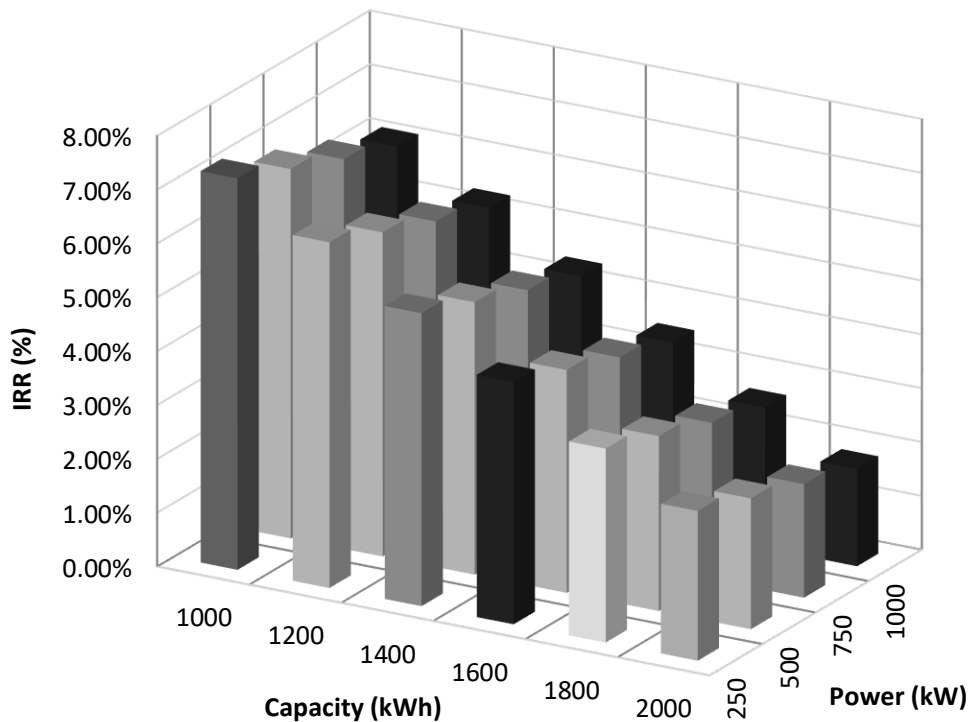


Fig. 7. 4. Effect of changing the size of the CBESS (the rated capacity and the rated power) on the IRR while providing a CEBM service.

7.5 CBESS for Capacity Market Service in the UK

The UK Government introduced the Capacity Market (CM) mechanism to ensure that the supply of electricity continues to meet demand as more renewable generation is introduced [214]. The CM service aims to achieve security of supply for a long-term period. It also provides fixed annual payments to generators within the CM and buys capacity (£/kW/year) ahead of delivery. The CBESS operation within the CM is focused on being directed to discharge over a fixed time period during the day, usually at rated capacity, based on the requirements of the Transmission Network Operators. The CBESS is charged from the surplus PV energy during the day, or from the main supply utility during the night (i.e. using the low purchasing electricity tariff). This operating procedure is repeated daily. The CM service is offered in the form of two auctions: (a) T-1 auction: this auction is performed each year to be delivered one year ahead, and (b) T-4 auction: this auction is performed each year to be delivered four years ahead. This program encourages the building of new power stations.

The National Grid operators notify the providers (i.e. CBESS in this case) that they will be required to deliver the agreed capacity. The Notification includes the start time, the duration period for which the delivery is applicable, and their obligation that providers will deliver [215]. All these requirements should be agreed in advance during the auction process based on provider requests and availability times. If the CBESS is instructed to deliver its CM service, it must guarantee the delivery of the agreed capacity. Failure to deliver the agreed capacity during system stress events will result in penalties [211].

7.5.1 Operating steps and annual revenue calculations

The CBESS operation within the CM is focused on being directed to discharge over a fixed time period during the day, usually at rated capacity, based on the requirements of the National Grid operators. The CBESS is charged from surplus PV energy during the day or at

night (i.e. using the low purchasing electricity tariff). Then the CBESS is biased by the National grid operators to discharge- using the contracted power (250 kW in this case)- for a pre-defined time period during the peak hours (from 4pm to 7pm in this case) using its full capacity. In this simulation, this operating procedure is repeated daily to maximize the revenue from participating in the CM service.

The annual revenue from using the CBESS to provide CM services can be presented in terms of incomes and payments as follows:

The incomes include:

- The CM contract fee (£/KW/year): the CBESS owners provide energy to the National Grid based on a certain contract fee. This fee determines the amount of money that would be paid by the National Grid to the CBESS owners for the contracted power (kW/year); it is assumed that the contract fee is £16.8/KW/year [211]. This value is not fixed for all service providers, but it depends on the size of the generation units and the auction values.
- The cost of the discharged energy to the National Grid, by the CBESS, at a sale price of 11.99 pence/kWh, i.e. when instructed by the National Grid operators [160].

The payments include:

- The yearly standing charge for TNUOS and DUOS.
- Energy Service Company Fee (for project management): it is assumed that 20% of the net yearly profits goes to the Energy Service Company for the management of the project and applying for the auctions.
- Charging the CBESS: the CBESS is charged at night using off-peak energy purchased at a tariff of 4.99 pence/kWh; the CBESS is not fully charged at night so that it can store surplus PV energy during the following day.
- The yearly maintenance cost of the CBESS.

7.5.2 Results

The operation of the CBESS has been simulated for 20 years while providing CM services instead of CEBM. The size of the CBESS used in the simulation process is 1000 kWh/250 kW and has a CAPEX cost of £378,960. Also, the assumptions mentioned in Table 7. 1.(CM column) for the participating of the CBESS in the CM service have been used in this simulation process.

Fig. 7. 5. shows the cumulative cash flow over 20 years for using a 1000kWh/250kW CBESS to provide CM services in the UK market. It is clear that the return on investment is £279,130 over 20 years. Also, the payback period is 14 years. The IRR is calculated to be 5.07%. Appendix H shows all the calculations used to obtain these results. The return on investment in using the CBESS to provide the CM service could be increased by obtaining a higher contract fee from the auctions, or by increasing the tariff for selling energy to the National Grid. Higher contract fees could be secured by aggregating a number of suppliers (CBESS) and apply for auctions using a total higher value of power and capacity; the Energy Service Company could undertake this task.

By comparing the results shown in Fig. 7. 5. and Fig. 7. 3., it is observed that the payback period when using the CBESS to provide a CEBM service is shorter than using the same CBESS to provide a CM service: the payback period is 14 years for CM service compared to 12 years for CEBM service. Shorter payback period means more attractive investment while longer payback periods are less desirable. Also, it is observed that the IRR when using the CBESS to provide a CEBM service is higher than using the same CBESS to provide a CM service.

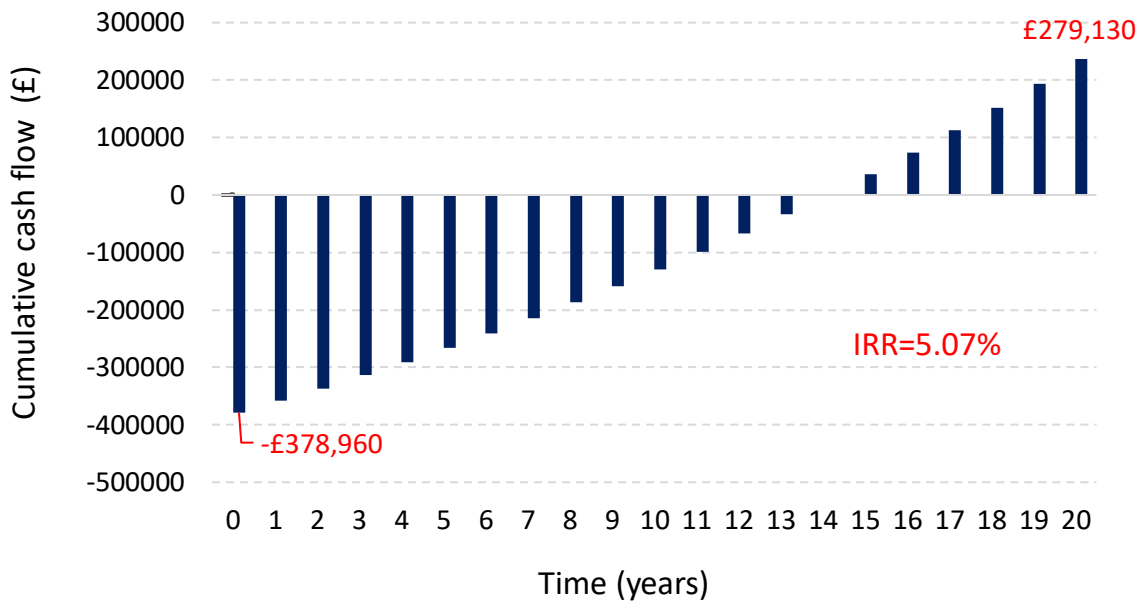


Fig. 7. 5. Cumulative cash flow over 20 years for using a 1000kWh/250kW CBESS to provide CM services.

7.5.3 The Effect of the CBESS Size on the IRR while Providing a CM Service

This section studies the effect of changing the size of the CBESS (the rated capacity and the rated power) on the IRR over 20 years while providing a CM service, see Fig. 7. 6. It is clear from Fig. 7. 6. that, for each value of the CBESS capacity, the IRR increases as the power inverter rating increases. Also, for each value of the power rating, the IRR decreases as the rated capacity of the CBESS increases. It is clear that power delivery is extremely important for CM services since the incomes are directly proportional to the rated power of the CBESS. The maximum IRR (8.56%) is achieved using a CBESS with a power rating of 1000kW and a capacity rating of 1000kWh, i.e. the CBESS provides a CM service for a minimum of half an hour each day using the rated battery power (1000kW), so the minimum net battery capacity required should be 500kWh. Therefore, the overall battery capacity should be 1000kWh after including the SOC limits and capacity fade over years. Using a CBESS of rating 2000kWh/250kW for CM services achieves the minimum IRR (1.91%) over a 20 year period. Note that a CBESS with a capacity lower than 1000kWh is not appropriate

in the UK capacity market at the moment since low capacity units face challenges in achieving successful bids.

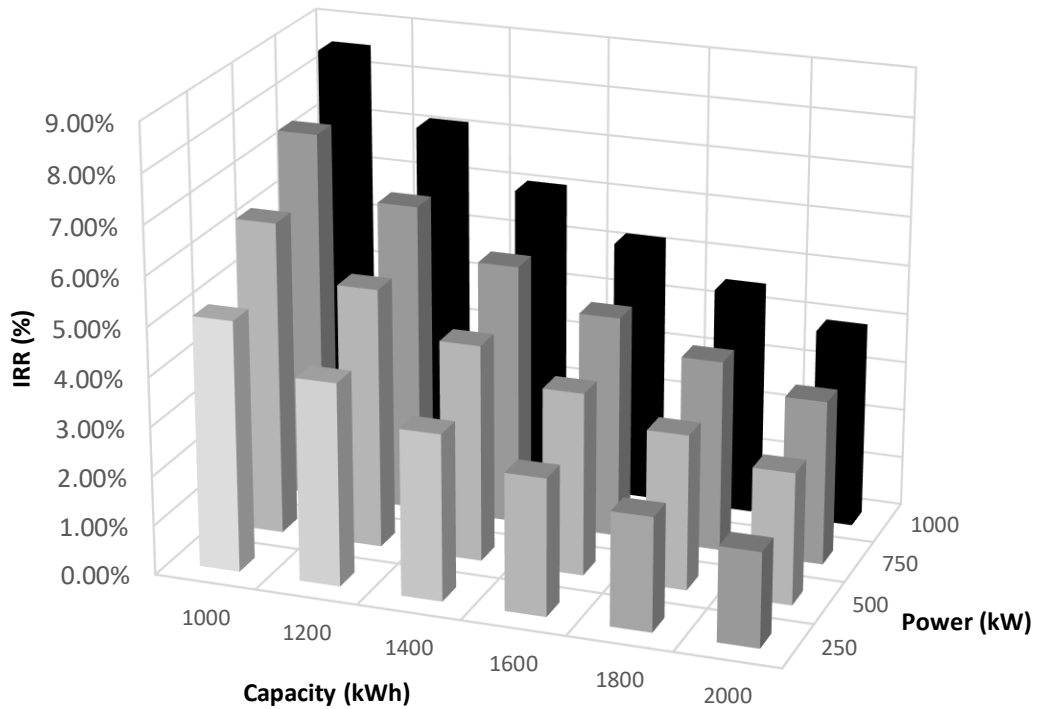


Fig. 7. 6. Effect of changing the size of the CBESS (the rated capacity and the rated power) on the IRR over 20 years while providing a CM service.

7.6 CBESS for Dynamic Firm Frequency Response Service in the UK

The UK National Grid needs energy users to provide frequency response services, where they are expected to act quickly and increase/decrease or shift demand, or switch back-up generation to help stabilize the grid. The Dynamic Firm Frequency Response (DFFR) services enable energy providers to provide a service that can reduce demand or increase generation when instructed by the UK National Grid [216]. DFFR is one of the UK National Grid's most valuable balancing services on a £/MW hour basis, see Fig. 7. 7. [217]. The UK National Grid buys DFFR services through a monthly electronic tendering process. Service providers can

participate in the tendering process once they have passed the pre-qualification assessment and can tender either for a single month or for several months.

There are three sub-services embedded in the DFFR service as shown in Fig. 7. 8. [218]: (a) Primary response: the provider should ensure the response is provided within 10 seconds of an event, which can then continue for another 20 seconds; (b) Secondary response: response provided within 30 seconds of an event, which may be sustained for another 30 minutes; (c) High frequency response: response provided within 10 seconds of an event, which can be sustained indefinitely. Providers may only offer one of these or a combination of different response times. Note that the electronic tenders are evaluated based on the ability to provide all three services together (i.e. the providers get a higher revenue for the tender if they can participate in all three services).

	Scheme	Minimum size*	Notice period	Duration	Regularity**	Value***	Contract
FREQUENCY RESPONSE SERVICES	Static Firm Frequency Response (FFR)	10 MW	30 sec	Max 30 min Typically 5 min	10-30	££	Monthly electronic tender
	Dynamic FFR	10 MW	2 sec	Max 30 min Typically 3-4 min	Daily	£££	Monthly electronic tender
	FFR Bridging	< 10 MW	30 sec	30 min	10-30	££	Bilateral contract of 12-24 months to transition in to the FFR market (either Static or Dynamic).
	Frequency Control by Demand Management (FCDM)	3 MW	2 sec	30 min	~10	££	Bilateral contracts for 1-2 yrs. Week ahead notification of daily load able to shed

Fig. 7. 7. Available frequency response services by the UK National Grid [217].

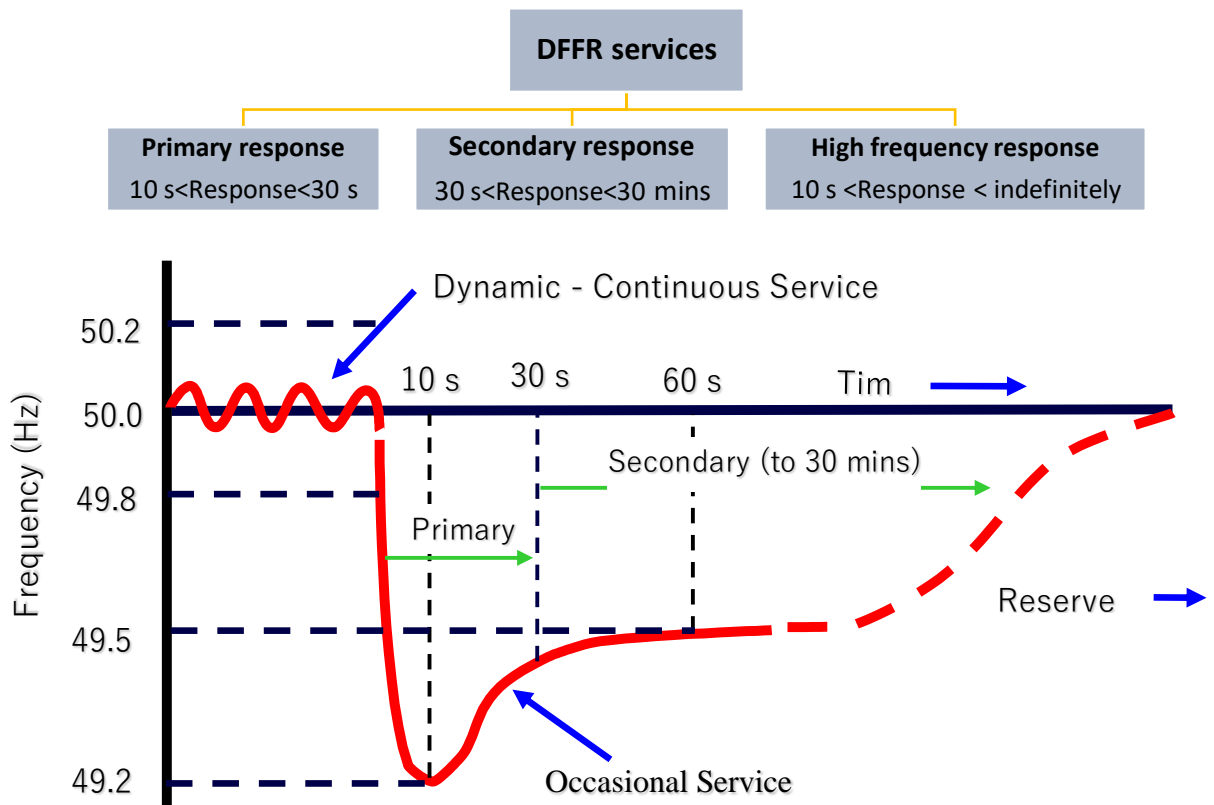


Fig. 7. 8. Dynamic Firm Frequency Response sub-services [219] .

7.6.1 Operating algorithm and annual revenue calculations

The operation of the CBESS to provide the DFFR service is based on being ordered to discharge or charge, usually at rated power, for a certain event (i.e. typically the event lasts for 3-4 minutes, maximum 30 minutes). The CBESS should be capable of discharging/charging at rated power for up to 30 minutes as one of the requirements of the National Grid. Also, the state of charge of the CBESS, while providing a DFFR service, should normally be 50 % in order to be able to respond to any discharging or charging events.

The yearly revenue from using the CBESS to provide the DFFR service can be presented in terms of incomes and payments as follows:

The incomes include:

- Availability Fee (£/MW/hr) [219] – related to the number of hours of availability from the provider. In this research, the Availability Fee is assumed (£8/MW/hour) [213]. Also, it is assumed that the CBESS is available 24 hours per day all the year with a guaranteed response of 95%.
- Response Energy Fee (£/MWh) [219]– based upon the actual response energy provided. Actually, the National Grid usually offers a zero value for the Response Energy Fee since the purchasing and the selling electricity tariff from/to the main grid, while providing a DFFR service, have the same value [220].

The payments include:

- The yearly standing charge for TNUOS and DUOS.
- Energy Service Company Fee for project management, i.e. it is assumed that the Energy Service Company takes 20% of the net annual profits for the project management.
- The annual maintenance cost of the CBESS.

7.6.2 Results

The operation of the CBESS has been simulated for 20 years while providing DFFR services instead of CEBM. The size of the CBESS used in the simulation is 1000 kWh/250 kW and has a CAPEX cost of £378,960. The assumptions mentioned in Table 7. 1. (DFFR column) for the participating of the CBESS in the DFFR service have been used in this simulation process. The daily DFFR events have been simulated by ordering the CBESS to discharge or charge at the rated power (once only per day) for up to 30 minutes. The charge or discharge signal is generated randomly each day, i.e. in any time during the availability period of the CBESS (availability period is 24 hours in this simulation). This operating procedure is repeated daily.

Fig. 7. 9. shows the cumulative cash flow over 20 years for using a 1000kWh/250kW CBESS to provide DFFR services. It is clear from Fig. 7. 9. that the return on investment is £26,051 over a 20 year period. Also, it is clear that the payback period is 20 years. The IRR is calculated to be 0.53%. Appendix I shows all the calculations used to obtain these results. It is observed that the payback period for using a 1000kWh/250kW CBESS to provide DFFR service is too long (20 years), and the IRR is too low 0.53%. This is because the DFFR service depends mainly on the power delivery (kW) as the income, i.e. Availability Fee is paid for the rated power (kW) and the availability period (usually 24 hours). Therefore, as the contracted power increases, the Availability Fee increases and consequently the IRR increases.

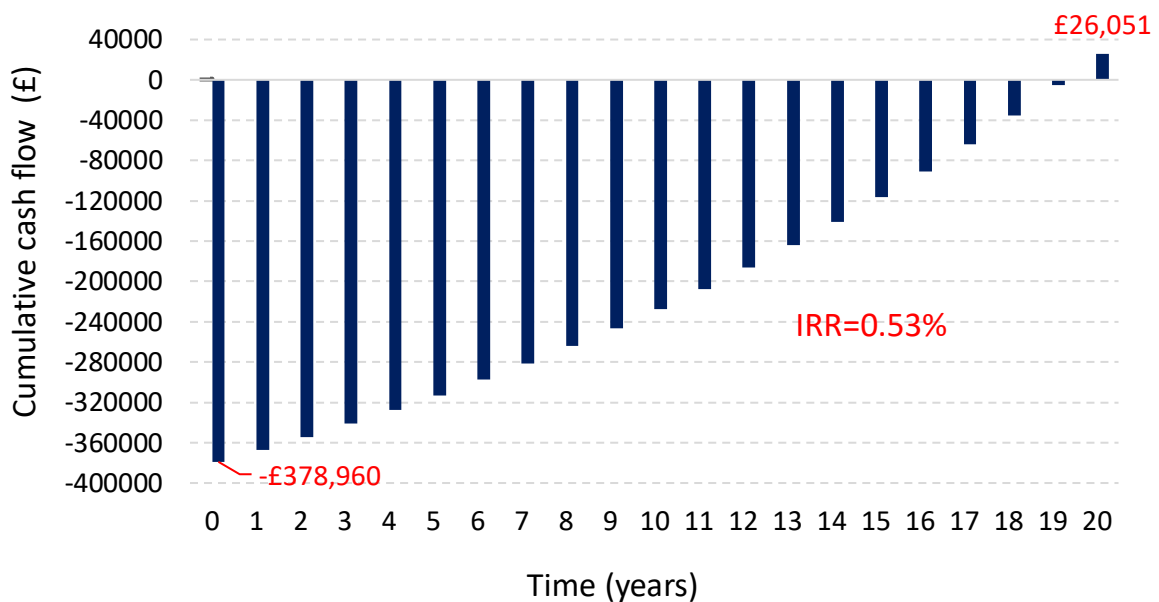


Fig. 7. 9. Cumulative cash flow over 20 years for using a 1000kWh/250kW CBESS to provide DFFR services.

By comparing the results obtained from Fig. 7. 3., Fig. 7. 5. and Fig. 7. 9., it is observed that using the 1000kWh/250kW CBESS to provide a CEBM service achieves the highest value for IRR (7.26%) and also the fastest payback period (12 years), compared to using the same CBESS to provide the CM service which achieves 5.07% IRR and 14 year payback

period, or to provide the DFFR service which achieves 0.53% IRR and 20 year payback period. The results obtained encourage the investment in the 1000kWh/250kW CBESS to provide CEBM services.

It is worth noting that the CBESS should guarantee a certain relation between the rated power and the rated capacity to agree with the requirements of the National Grid in the UK. For example, to be eligible to participate in the DFFR, it is required to deliver a minimum of 1 MW. This value can be from a single unit or aggregated from several smaller units (needing an Aggregator). Also, the unit should guarantee the full contracted kW rating for 30 minutes (secondary response): this means that, for a rated power of 250 kW, a CBESS of 250 kWh net capacity should be used (allowing ± 125 kWh from the event bias point), and this capacity should be guaranteed after considering the maximum and minimum SOC limits of the CBESS and annual capacity degradation. Also, it is worth noting that the CBESS has to keep its SOC near 50%, while providing a DFFR service, to be able to respond to charging or discharging events.

7.6.3 The effect of the CBESS size on the IRR while providing a DFFR service

The operation of the CBESS has been simulated over a period of 20 years while changing the size of the CBESS (the rated capacity and the rated power). Fig. 7. 10. shows the effect of changing the size of the CBESS (the rated capacity and the rated power) on the IRR over a 20 year period while providing DFFR services.

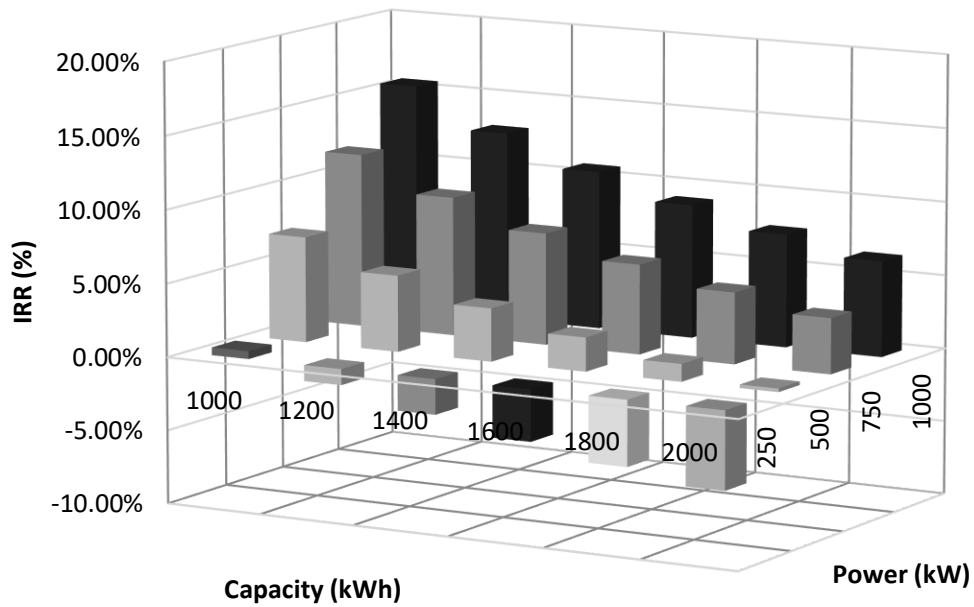


Fig. 7. 10. Effect of changing the size of the CBESS (the rated capacity and the rated power) on the IRR over a 20 year period while providing a DFFR service.

It is clear from Fig. 7. 10. that, for each value of the CBESS capacity, the IRR value increases as the power inverter rating increases. Also, for each value of the power rating, the IRR decreases as the rated capacity of the CBESS increases. It is observed from the figure that using a 1000kWh/1000kW CBESS to provide DFFR service achieves a 15.61 % IRR over a 20 year period. This value is high compared to using the same size of the CBESS to provide other services such as CEBM or CM. However, using a 1000kWh/1000kW CBESS to provide the DFFR service is not applicable since the CBESS need to guarantee a net capacity of 1000kWh (allowing ± 500 kWh from the bias point). Therefore, the overall battery capacity should be higher than 1000kWh to include the SOC limits and capacity fade over the years.

It is interesting to note from Fig. 7. 10. that using a CBESS with a large energy and a low power rating achieves investment losses. Power delivery is extremely important for the participation of the CBESS in DFFR services, since the main income from participation in the DFFR service is the Availability Fee (£/MW/hr), and this value is directly proportional to the rated power of the CBESS. Also, it is worth noting that the return on investment in using the CBESS to provide the DFFR service could also be increased by providing a DFFR service for a longer number of hours per day, i.e. the main income (i.e. Availability Fee (£/MW/hr)) is directly proportional to the number of hours per day that the CBESS is used.

7.7 CBESS Sizing to Provide Multiple Services

To improve the income from the investment in the CBESS, the size of the CBESS should be selected accurately to enable the CBESS to provide more than one service instead of providing only one service. This section studies the selection process for the best size of CBESS and the extra income that could be achieved.

The importance of selecting the best CBESS size to provide more than one service is: (a) the CBESS could achieve higher IRR values if it is able to provide more than one service, compared to using the same CBESS to provide only one service for the whole year, (b) the CBESS will have alternatives (services) to participate in if the contract fees and/or revenue fees for any of the services decrease below the estimated values used at the design period, i.e. the IRR of the investment in the CBESS to participate in the CM and DFFR services is directly proportion to the changes in the contract fees and revenue fees. The values of these fees are not fixed as they depend on auctions, i.e. can vary every month for the DFFR service or every year for the CM service, (c) the CBESS could participate in alternative services if for example there is no requirement for additional capacities for the capacity market, or no more assistance is required for DFFR service in a particular year, and (d) the investment in the CBESS

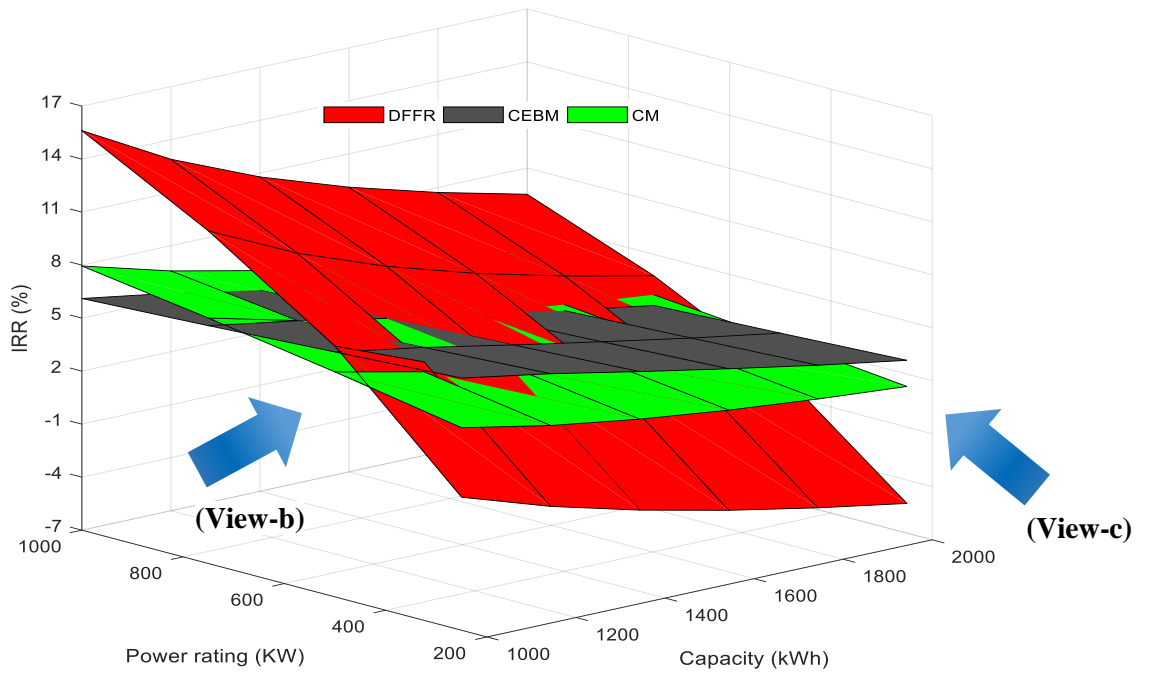
becomes more robust and less affected by changes in the electricity market; this encourages investors to participate in this investment, especially when a guaranteed fixed value of IRR is expected (as opposed to a range of IRR values).

Fig. 7. 11.a shows the effect of changing the size of the CBESS on the IRR while providing CEBM, CM and DFFR services over a 20 year period. It is observed from Fig. 7. 11.a that the values of the IRR of the investment in the CBESS to provide the CEBM, CM, and DFFR services are convergent when using a particular value for the rated power and the rated capacity of the CBESS. This means that the CBESS could be used to provide any of the three services (DFFR, CM, and CEBM) with almost the same IRR value while using the same CBESS size.

It is clear from Fig. 7. 11. (view-b) that using a CBESS with a rated power of 500kW provides a close IRR values for all services (DFFR, CM, and CEBM). From the results, the 500kW is selected as the best size of the power converter which enables the CBESS to provide more than one service with similar IRR values because the investment in the CBESS becomes more robust and more attractive for investors when a guaranteed fixed value of IRR is expected (as opposed to a range of IRR values which depend on market situation).

It can be observed from Fig. 7. 11. (view-b) that the IRR of the investment in the CBESS to provide DFFR service is greatly affected by increasing the rated power of the CBESS, compared to the other two services (CEBM and CM) in which a slight changed in the IRR is observed as the rated power of the CBESS increases. Furthermore, It is can be seen from Fig. 7. 11. (view-c) that using a CBESS capacity of 1000kWh achieves the highest IRR value for all services while using a 500kW power converter. Also, it is observed that, for each CBESS capacity, the change in the IRR value is in the range of (0.2-2%) if the CBESS is used for any

of the three services. Also, it is clear that, for the same power converter size (500kW), increasing the capacity of the CBESS decreases the IRR for all services.



(a)

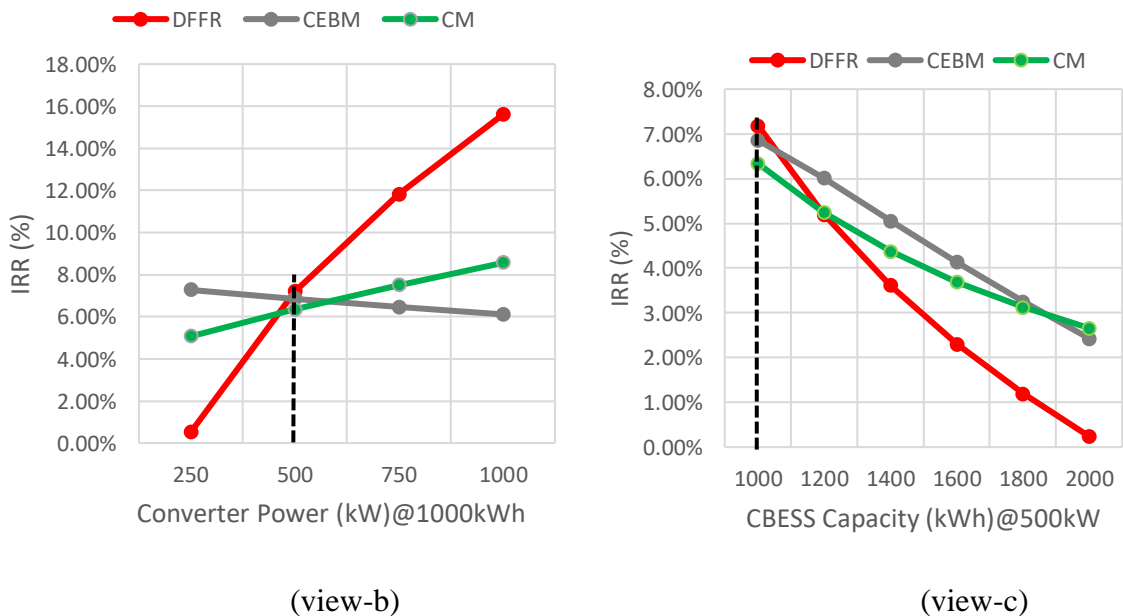


Fig. 7. 11. (a) Effect of changing the size of the CBESS (the rated capacity and the rated power) on the IRR while providing CEBM, CM and DFFR services over a 20 year period, (view-b) 2D view to show only the variation of the IRR as the size of the power converter changes when using a 1000 kWh CBESS. (view-c) 2D view to show only the variation of the IRR as the capacity of the CBESS changes when using a 500kW power converter.

From the results, the best size for the central CBESS which enables it to provide more than one service with almost the same IRR value is 1000kWh/500kW. It is important to select the CBESS size, which enables the CBESS to provide more than one service with similar IRR values, so that the average IRR value if the CBESS is used to provide more than one service over the 20 year period is close to the IRR value obtained from providing only one service over the 20 year period.

Table 7. 2. shows the revenue of the investment in a 1000 kWh/500 kW CBESS if used to provide one of the three services (CEBM, CM, and DFFR) over a 20 year period. It is observed from the results that using the 1000 kWh/500 kW CBESS achieves convergent IRR values if used to provide any of the three services. The payback period for all services is in the range of 10-13 years. The results obtained encourage the investment in the 1000 kWh/500 kW CBESS as it achieves a high IRR value and is capable of providing more than one service.

Table 7. 2. Economic revenue over a 20 year period of the investment in a 1000 kWh/500 kW CBESS if used to provide any of the CEBM, CM, or DFFR services.

	CEBM	CM	DFFR
Initial investment	£393,000	£393,000	£393,000
IRR (20 years)	6.82 %	6.23 %	7.19 %
Return on investment over 20 years	£393,976	£368,470	£451,062
Payback period	12 year	13 year	10 year

7.7.1 Providing multiple services with only one service per year

If the CBESS is used to provide multiple services over the 20 year period, and it is assumed that it will provide only one service each year, then it is important to select the best service (most profitable) in which the CBESS should participate in each year. The flow chart

shown in Fig. 7. 12. shows the annual selection criteria for the most profitable service in which the 1000 kWh/500 kW CBESS should participate in each year. The selection criteria creates a relation between the service provided and the minimum value of the annual or monthly electronic tender which must be secured to ensure the highest economic revenue from this service compared to the other services.

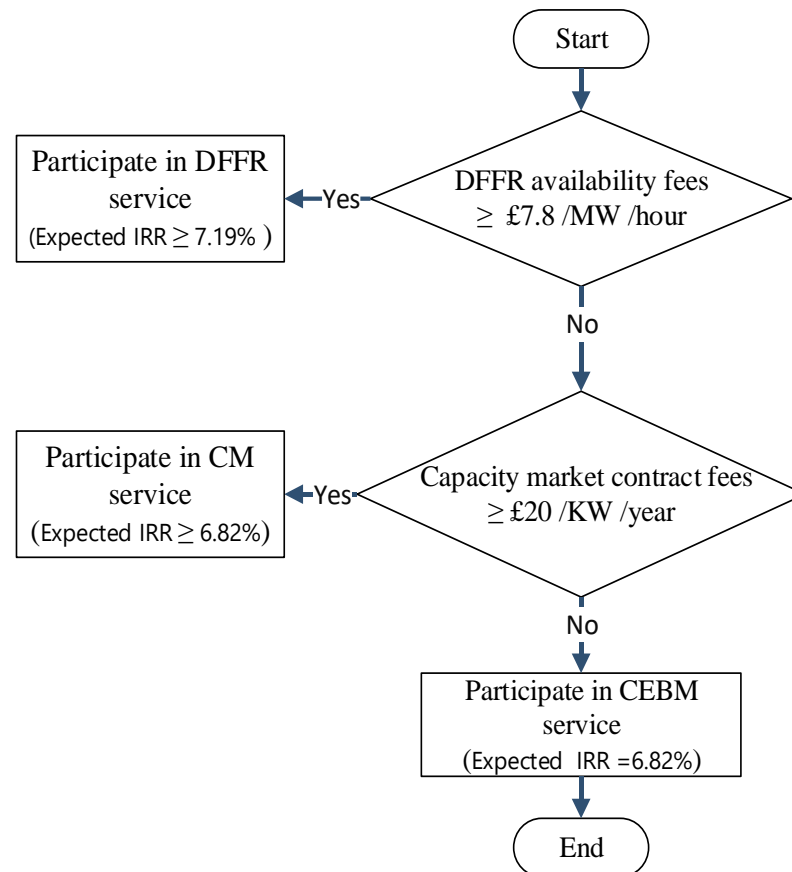


Fig. 7. 12. Selection criteria of the most profitable service in which the 1000 kWh/500 kW CBESS should participate in each year.

It has been observed from Table 7.2. that the best service for the 1000 kWh/500 kW CBESS to provide for a certain year is the DFFR service (which achieves the highest IRR). Providing DFFR service can achieve 7.19% IRR only if the Energy Service Company were successful in obtaining an annual or monthly electronic tender of a minimum of £7.8/MW/hour for the DFFR availability fees. Higher IRR values could be achieved if the

company obtained higher DFFR availability fees. If the Energy Service Company fails to secure a suitable tender then the CBESS should participate in other services. The next-best service for the CBESS is the CM service. The CBESS can achieve 6.82% IRR from providing the CM service only if a minimum capacity market contract fee of £20/kW/year is secured at the annual auction- note that higher IRR values could be achieved if higher contract fees are obtained. If neither of these contracts is obtained, then the CBESS should participate in the CEBM service where it can achieve 6.82% IRR.

7.7.2 Providing multiple services with more than one service per day

The CBESS could be used to provide more than one service per day, instead of providing only one service for the whole day. In this section, The CBESS has been used to provide both the CEBM and DFFR services on the same day instead of providing only one of these for the whole day. This is achieved by providing the DFFR service for a certain number of hours (usually night times) whilst providing the CEBM service during the rest of the day. A simulation process is performed to show the results of providing both the DFFR and the CEBM in the same day. In the simulation process, the CBESS has been used to provide the DFFR during the night time (e.g. from 00: to 07:00)- DFFR events have been created as explained before in section 7.6.2. Then the CBESS has been used to provide the CEBM service starting from 07:00 until the end of the day. The results obtained are then compared to the case when the CBESS is used to provide only DFFR or CEBM services for the whole day, as shown in Table 7.3.

Table 7. 3. IRR of the investment in the 1000 kWh/500 kW CBESS if used to provide both DFFR and CEBM services in the same day, compared to being used to provide only DFFR or CEBM service for the whole day.

Case	Daily service	IRR (%)
1	DFFR only (all the day)	7.19
2	CEBM only (all the day)	6.82
3	DFFR (from 1:00 to 5:00) plus CEBM in the rest of day	9.27
4	DFFR (from 00:00 to 5:00) plus CEBM in the rest of day	10.15
5	DFFR (from 00:00 to 7:00) plus CEBM in the rest of day	8.71

Table 7.3. shows the IRR if the 1000kWh/500kW CBESS is used to provide both DFFR and CEBM services during the same day (as in cases 3, 4, and 5), compared to being used to provide only DFFR or CEBM for the whole day (as in case 1 and case 2). Table 7. 3. shows that using the 1000 kWh/500 kW CBESS to provide both CEBM and DFFR services on the same day achieves higher IRR values compared to using the same CBESS to provide only one service for the whole day. Using the CBESS to provide a DFFR service from 00:00 to 05:00 and a CEBM service for the rest of day achieves the highest IRR value (10.15%), compared to all other cases.

When using the CBESS to provide both services in the same day (cases 3-5), the value of the IRR changes as the number of hours of providing the DFFR service is changed. The highest IRR is achieved when the DFFR service is provided for 5 hours (case 4), compared to case 3 in which the DFFR service is provided for only 4 hours, and case 5 in which the DFFR service is provided for 7 hours. The duration of the participation of the CBESS in the DFFR service per day should not be long as in case 5, to enable the CBESS to store sufficient energy during the night (at low tariff period) to provide the CEBM service for the rest of the day. Also, the duration of the participation in the DFFR service should not be short as in case

3, to maximize the benefits of providing a DFFR service (income from providing a DFFR service increases proportionally with the number of hours).

To maximize the benefits from providing both the DFFR and CEBM services, the CBESS should provide the DFFR service only during the overnight period (23:00 to 6:00) and avoid providing this service during the daytime. During the daytime, it is important to participate in the CEBM service to achieve sufficient income for the community members. Note that selecting the time period in which the CBESS could provide DFFR service to the National Grid is an available option for the DFFR service providers in the UK [221]. However, selecting the overnight period for providing DFFR service may affect negatively the tender price (MW/hour) for providing the DFFR service.

Comparing the results obtained in Table 7. 2. and in Table 7. 3., it is observed that using the 1000kWh/500kW CBESS to provide more than one service in the same day achieves higher IRR values (from 8.71% to 10.15%), compared to using the same CBESS to provide only one service for the whole day for the 20-year period, i.e. IRR in the range of 6.82%-7.19%. The results obtained encourage the investment in the CBESS to provide more than one service in the same day.

7.8 Conclusion

The conclusions of this chapter are as follows:

- Using the 1000 kWh/250 kW CBESS to provide CEBM service achieves a high value for IRR (7.26%) and also a fast payback period (12 years), compared to using the same CBESS to provide the CM service which achieves 5.07% IRR and a 14 year payback period, or to provide the DFFR service which achieves 0.53% IRR and a 20 year payback period.

- The sizing methodology for a CBESS presented in this chapter, reduces the annual community energy bill by 47.5% and increases the PV self-consumption within the community to 93.5%, compared to the case where no CBESS is used.
- The results show that using a CBESS with high rated power and low capacity size achieves more income when providing CM and DFFR services. Power delivery is extremely important for the participation of the CBESS in DFFR or CM services. The lifetime of the CBESS should be long as possible to obtain a high IRR for the investment. Furthermore, the capacity of the CBESS should not be less than 1000kWh to be qualified to participate in the capacity/energy market.
- The participation of the CBESS in DFFR, CM, and CEBM services achieves an IRR of up to 15.61 %, 8.56 % and 7.26% for the three services respectively, depending on the battery's size. Also, the return on investment in the CBESS to provide any service is expected to increase as the initial cost of the CBESS decreases.
- Using the 1000 kWh/500 kW CBESS to provide more than one service in the same day achieves the highest IRR value (10.15%), compared to using the same CBESS to provide only one service for the whole day for 20 years, and compared to using the same CBESS to provide multiple services over the 20 year period (assume providing only one service each year). The results obtained encourage the investment in the 1000 kWh/500 kW CBESS as it achieves a high IRR value, capable of providing more than one service each day, and guarantees the estimated IRR. The size of the CBESS should be selected accurately to enable the CBESS to provide more than one service instead of providing only one service.
- The concept of the CBESS and CEBM is scalable. The results presented in this chapter show that community members can receive benefits by operating as part of an energy community of a reasonable size -144 houses in this case.

Chapter 7 has examined a method to appropriately size the CBESS for a given energy community to ensure that the community is not over-investing in its energy storage assets. Also, chapter 7 demonstrated that additional revenues could be achieved from the participating of the CBESS in ancillary services in the UK market as well as providing a CEBM service. The work presented in this chapter has potentially addressed objective (6) listed in section 1.3.

The next chapter will presents the overall conclusions and recommendations drawn based on the completed work.

Chapter 8

Overall Conclusions, Recommendations and Future Work

8.1 Overall Conclusion

The aim of this project is to investigate how the cooperation between the prosumers in a Community Energy System (CES) can help in achieving greater benefits using integrating control, short-term management strategies, optimal planning/scheduling and appropriate equipment sizing procedures. The project's aims and objectives have been achieved through a series of design and management steps as presented in this thesis.

This chapter presents the conclusions drawn based on the completed work. For instance, **Chapter 2** pointed out the importance of EMSs in modern communities and presented a review of the available EMS and control techniques at both household and community levels, and highlighted also the sizing requirements for a Community Battery Energy Storage System (CBESS) for it to be able to participate in the capacity and energy markets.

Chapter 3 presented all the data resources and the performance indices that have been used to evaluate the performance of the proposed EMSs.

In **Chapter 4**, three main types of real-time interactive Home Energy Management Systems (HEMS) have been presented and examined to be used as a benchmark for making comparisons between the end-users acting individually or as members of a community energy system.

These were (a) the RTC based-single layer HEMS: a fast controller where no system modelling or optimization processes are required for its operation, and it does not require any forecasting, therefore it is less affected by forecasting uncertainties. However, its performance

suffers from lack of prediction, it ignores battery degradation costs, it is not applicable for all tariff policies, it cannot control the shiftable appliances, and it needs an accurate adjustment of the overnight charging level.

(b) The MPC based single layer HEMS: an optimization-based real-time interactive HEMS, which has been created to economically exploit HBSS and DSM techniques for the household level. The MPC based-single layer HEMS minimizes the daily household energy costs, maximizes the PV self-consumption, and manages all the shiftable appliances while taking into account the battery degradation costs and the flexibility of tariff policies. However, its performance is affected by forecasting uncertainties and the sample time.

(c) The hierarchal HEMS: a HEMS which combines the optimization layer and control layer and points out the gap between the planned scheme and the real operation through an interactive control algorithm. The hierarchal HEMS reduced the daily household energy costs by 16% per annum, maximized PV self-consumption to 92.5%, minimized energy wastage ratio to 7.5%, minimized the effect of RES power fluctuations, and smoothed the fluctuations of the electric power exchanges at the point of common coupling with the main electricity grid compared to using MPC-based single layer HEMS.

The results obtained showed that the hierarchical HEMS enables the house to participate in the CEMS because it is able to receive reference values for the power at the GCP and follow it accurately.

Also, **Chapter 4** has shown the effect of different factors such as the overnight charging level, forecasting uncertainty, control sample time and tariff policy on the performance of the home energy management system and on the systems efficiency. This study can be considered an aid for decision makers to select an appropriate controller for each PV-battery system. The

work presented in chapter 4 has potentially addressed objectives (1) and (2) listed in section 1.3.

Chapter 5 introduced two types of community energy management systems: Distributed CEMS and Centralized CEMS, which coordinate the operation of the distributed HBSSs and the shiftable home appliances (located in each house) within the CES either in a centralized or a decentralized way. **Chapter 5** demonstrated that additional financial benefits could be achieved for prosumers cooperating together in a CES, compared to operating individually. For instance, coordinating the operations of prosumers in a CES using a centralized CEMS can achieve an additional reduction in the annual energy costs of up to 15.89% for each house, compared to being operated individually, and an overall reduction in the annual energy costs of the whole community by 8.98%. Also, the use of decentralized CEMS to coordinate the operation of the prosumers could achieve an annual reduction in the energy costs of up to 8.86% for each house, compared to being operated individually, and an overall reduction in the annual energy costs of the whole community by 4.96%. It is expected that a greater reduction in the household energy costs can be achieved if houses with different sources of energy, different load demand profiles, different tariff schemes, and a higher number of houses participating in the CES are used. The work presented in chapter 5 has potentially addressed objectives (3) and (4) listed in section 1.3.

In Chapter 6, the structure of the centralized CEMS has been modified to provide greater flexibility, ensure that the optimization process is faster and more robust to communications, and be applied to larger communities (with a large number of houses), compared to CEMS presented in chapter 5. The results show that using the centralized CEMS with a central CBESS, presented in chapter 6, achieved the highest reduction in the annual energy costs for each house (up to 17.11%), compared to using the CEMS with distributed HBSSs which achieved an annual reduction of 15.89%, and compared to using the distributed CEMS which

achieved an annual reduction of maximum 8.96% only. Furthermore, **Chapter 6** demonstrated that using the hierarchical CEMS, in addition to only 85% of the rated size of the CBESS, and 60% of the rated size of the power converter, together with a load shift coefficient of 15%, and a maximum grid power limit of 55% could still achieve a 0.42% reduction in the annual energy costs of the CES, compared to the case when the rated values are used. This means that an additional reduction in the investment cost can be achieved as well as achieving a reduction in the annual energy costs. The results demonstrate that the networked operation of the houses can reduce the need for an overly large CBESS, and leave unused transformer capacity which could be used for additional services. The results obtained encourage the investment in the hierarchical CEMS with a central CBESS and DSM as it ensures a reduction in the annual energy costs and also lower investment costs. The work presented in chapter 6 has potentially addressed objective (5) listed in section 1.3.

Finally, **Chapter 7** presented a methodology for sizing a CBESS (either aggregated or centralized) in terms of energy and power rating to either provide the CEBM service, or to participate in the UK capacity/energy markets. The results show that the optimal sizing of the CBESS reduces the annual community bill by 47.5% and maximizes the PV self-consumption within the CES to 93.5%, compared to the case where no CBESS is used. Also, the results encourage the investment in the 1000 kWh/500 kW CBESS as it is capable of providing CEBM service as well as additional ancillary service and guarantees a higher IRR value of up to 10.15%. The work presented in chapter 7 has potentially addressed objective (6) listed in section 1.3.

8.2 Recommendations

As an overall conclusion of this thesis, a few recommendations are now presented:

- It is recommended to use the hierarchical two-layer HEMS for the household energy management as it enables the battery to be controlled in real-time, using RTCs, under the supervision of an MPC. Therefore, it can respond to any changes in the system (i.e. changing of loads and PV generation) that happen over a short time which helps in minimizing the daily energy wastage and compensating for RES power fluctuations. Also, it is considered an improvement over the MPC-based single-layer HEMS as it compensates for the effect of forecast uncertainties and the effect of sample time while having low computational requirements. Furthermore, the two-layer HEMS enables the house to participate in the CEMS as it is able to receive reference values for the power at the grid connection point and follow it accurately.
- It is recommended for the householders to participate in the CEMS because the networked operation of the houses - using the proposed hierarchical CEMS in addition to the DSM techniques - can reduce the cost of electricity, reduce the need for overly large storage systems, ensure a larger spare capacity in the transformer which could be used for adding for example new EV charging stations (if required) or for future system's extension, and reduce the exported power to the main electricity grid, compared to the houses being operated individually.
- It is recommended to use the centralized CEMS because it achieves a higher reduction in the annual energy costs for all houses in the community and provides a fairer distribution of savings between the houses, compared to using distributed CEMS. However, it is recommended to use the hierarchical distributed CEMS when the following features are required: (a) accurately controlling both the energy flow and the money flow between

houses, (b) monitoring of the energy flow between houses, (c) considering the power losses of the shared energy, (d) enabling the houses to share energy with others for a paid charge, and (e) minimizing the overall processing and computing time.

- It is recommended that a large number of householders with different sources of energy, different load demand profiles, and different tariff schemes (such as E7, TOU, or RTP tariff schemes) participate in the CEMS because a greater reduction in the household energy costs will be achieved. Furthermore, the houses with large generation capabilities (e.g. large HBSS and large PV system) are encouraged to participate in the CES since they could achieve a further reduction in the household energy costs, compared to being operated individually.
- It is recommended that the community householders participate in the electricity market services such as DFFR and/or CM – using aggregated or centralized CBESS- to achieve additional economic revenue. The size of the CBESS should be selected accurately to enable the CBESS to provide more than one service instead of providing only one service because this achieves the highest revenue compared to the other services.

8.3 Future work

The authors would like to suggest a few areas which could form the basis of the future research.

- 1) There is a strong move towards decarbonizing heating and cooling systems, it would be very beneficial to study the integration of these systems with the electrical system at both the household and the community levels. The CES should be studied as a multi-vector energy system in which electricity, heat, and cooling systems and also electrical transport vehicles interact with each other at various levels. The CEMS can be then developed to enhance the technical and the economic performance of the overall multi-vector system.

Different types of heat energy generation such as ground source heat pumps and hot water tanks should be considered in addition to conventional direct heating systems. We should study the effect of integrating these items on the performance of the household system and also investigate how these items will interact in a virtual energy trading environment between houses in the CES. Also, the integration of EVs at a household level or a community level should be further studied; for example, merging EVs with a vehicle to home option stills need better understanding.

- 2) A more effective sensitivity analysis for the P2P operation of houses in the CES is required. This analysis should take into account the effect of changing the size of the HBSS, the PV generation system and the average annual household consumption, not only on the economic performance of the household itself but also on the other houses in the CES. Furthermore, additional P2P energy trading techniques, i.e. such as the auction trading or game theory trading technique should be studied.
- 3) A techno-economic study of the participation of the CBESS in the Reactive Power Market with the UK National Grid should be presented, whereby the CBESS (i.e. central or aggregated) will be contracted to deliver Enhanced Reactive Power Service [222].
- 4) The CES considered in this work is assumed to be a system connected to a strong grid, and could be a virtual rather than a physical co-located community. However, it is worth investigating the performance of the CES using for example an IEEE distribution feeder system, to clearly understand the effect of different variables such as voltage, power losses and voltage drop when implementing the proposed CEMS on a large physically co-located system. This could be extended to working with microgrids, where there is the possibility of the system having to work as an island.

References

- [1] R. Fu, T. W. Remo, and R. M. Margolis, 2018 US utility-scale photovoltaics-plus-energy storage system costs benchmark, National Renewable Energy Lab.(NREL), Golden, CO (United States), 2018.
- [2] M. Xie, X. Ji, X. Hu, P. Cheng, Y. Du, and M. Liu, "Autonomous optimized economic dispatch of active distribution system with multi-microgrids," *Energy*, vol. 153, pp. 479-489, 2018.
- [3] The Committee of Climate Change, "Climate Change Act 2008 ", available at: <https://www.legislation.gov.uk/ukpga/2008/27/contents>
- [4] European Commission, "Factsheet on the Commission's proposal on binding greenhouse gas emission reductions for Member States (2021-2030) ", available at: https://ec.europa.eu/commission/presscorner/detail/pl/MEMO_16_2499
- [5] Climate Change Committee, "Reducing UK emissions 2018 Progress Report to Parliament ", available at: <https://www.theccc.org.uk/publication/reducing-uk-emissions-2018-progress-report-to-parliament/>
- [6] "P Gardner, " UK Generation and Demand Scenarios for 2030 " 2011, available at: http://assets.wwf.org.uk/downloads/positive_energy_glgh_technical_report.pdf
- [7] Department of Energy and Climate Change, "Updated energy and emissions projections 2015 ", available at: <https://www.gov.uk/government/publications/updated-energy-and-emissions-projections-2015>
- [8] European Parliament, "Fact Sheets on the European Union ", available at: <https://www.europarl.europa.eu/factsheets/en/sheet/70/renewable-energy>
- [9] Mirzania, P., D. Andrews, A. Ford, and G. G. Maidment. "Community Energy in the UK: The End or the Beginning of a Brighter Future?." In *Energy for Society: 1st international conference on Energy Research & Social Science*. 2017.
- [10] Green alliance, "Community Energy 2.0: the future role of local energy ownership in the UK ", available at: https://www.green-alliance.org.uk/community_energy_2.0.php#:~:text=Community%20Energy%202.0%3A%20the%20future,with%20only%2067%2C000%20homes%20benefiting.
- [11] B. P. Koirala, E. Koliou, J. Friege, R. A. Hakvoort, and P. M. Herder, "Energetic communities for community energy: A review of key issues and trends shaping integrated community energy systems," *Renewable and Sustainable Energy Reviews*, vol. 56, pp. 722-744, 2016.
- [12] Department of Energy & Climate Change, "Community Energy Strategy: Full Report," Crown copyright 2014, London," Available at: https://assets.publishing.service.gov.uk/government/uploads/system/uploads/attachment_data/file/275169/20140126Community_Energy_Strategy.pdf
- [13] C. N. Truong, M. Naumann, R. C. Karl, M. Müller, A. Jossen, and H. C. Hesse, "Economics of residential photovoltaic battery systems in Germany: The case of Tesla's Powerwall," *Batteries*, vol. 2, no. 2, pp. 14, 2016.
- [14] BloombergNEF. "A Behind the Scenes Take on Lithium-ion Battery Prices," Available at: <https://about.bnef.com/blog/behind-scenes-take-lithium-ion-battery-prices/>.

- [15] BloombergNEF, "Battery Pack Prices Cited Below \$100/kWh for the First Time in 2020, While Market Average Sits at \$137/kWh", December 2020, Available at: <https://about.bnef.com/blog/battery-pack-prices-cited-below-100-kwh-for-the-first-time-in-2020-while-market-average-sits-at-137-kwh/>
- [16] Ofgem, " Feed-In Tariff (FIT) rates in UK," Available at: <https://www.ofgem.gov.uk/environmental-programmes/fit/fit-tariff-rates>
- [17] Vox Media, "Millions of used electric car batteries will help store energy for the grid. Maybe" Available at: <https://www.vox.com/2016/8/29/12614344/electric-car-batteries-grid-storage>
- [18] Mckinsey&Company, "Breathing new life into used electric vehicle batteries," Available at: <https://www.mckinsey.com/business-functions/sustainability/our-insights/sustainability-blog/breathing-new-life-into-used-electric-vehicle-batteries#>
- [19] A. Pfeifer, V. Dobravec, L. Pavlinek, G. Krajačić, and N. Duić, "Integration of renewable energy and demand response technologies in interconnected energy systems," *Energy*, vol. 161, pp. 447-455, 2018.
- [20] S. Milčiuvienė, J. Kiršienė, E. Doheijo, R. Urbonas, and D. Milčius, "The role of renewable energy prosumers in implementing energy justice theory," *Sustainability*, vol. 11, no. 19, pp. 5286, 2019.
- [21] UK Department Of Energy And Climate Change , " Annual Energy Statement 2014", available at: https://assets.publishing.service.gov.uk/government/uploads/system/uploads/attachment_data/file/371387/43586_Cm_8945_accessible.pdf
- [22] Good Energy , "Good Energy Progress Report 2016," Available at: <https://www.goodenergy.co.uk/blog/2016/06/06/2016-progress-report/>
- [23] Institute of Public Policy Research (IPPR), " COMMUNITY AND LOCAL ENERGY CHALLENGES AND OPPORTUNITIES", available at: https://www.ippr.org/files/publications/pdf/community-energy_June2016.pdf
- [24] Uk Department Of Energy And Climate Change, "Solar photovoltaics deployment ", available at: <https://www.gov.uk/government/statistics/solar-photovoltaics-deployment>.
- [25] G. Seyfang, J. J. Park, and A. Smith, "A thousand flowers blooming? An examination of community energy in the UK," *Energy policy*, vol. 61, pp. 977-989, 2013.
- [26] B. J. Kalkbrenner, and J. Roosen, "Citizens' willingness to participate in local renewable energy projects: The role of community and trust in Germany," *Energy Research & Social Science*, vol. 13, pp. 60-70, 2016.
- [27] T. Van Der Schoor, and B. Scholtens, "Power to the people: Local community initiatives and the transition to sustainable energy," *Renewable and Sustainable Energy Reviews*, vol. 43, pp. 666-675, 2015.
- [28] Y. Zhou, Z. Wei, G. Sun, K. W. Cheung, H. Zang, and S. Chen, "A robust optimization approach for integrated community energy system in energy and ancillary service markets," *Energy*, vol. 148, pp. 1-15, 2018.
- [29] K. Shi, D. Li, T. Gong, M. Dong, F. Gong, and Y. Sun, "Smart Community Energy Cost Optimization Taking User Comfort Level and Renewable Energy Consumption Rate into Consideration," *Processes*, vol. 7, no. 2, pp. 63, 2019.

- [30] X. Xu, X. Jin, H. Jia, X. Yu, and K. Li, "Hierarchical management for integrated community energy systems," *Applied Energy*, vol. 160, pp. 231-243, 2015.
- [31] D. Parra, S. A. Norman, G. S. Walker, and M. Gillott, "Optimum community energy storage for renewable energy and demand load management," *Applied energy*, vol. 200, pp. 358-369, 2017.
- [32] Alex Eller, Dexter Gauntlett, "Energy Storage Trends and Opportunities in Emerging Markets," Available at : <https://www.esmap.org/sites/default/files/esmap-files/7151-IFC-EnergyStorage-report.pdf>
- [33] A. S. Bedi, M. W. Ahmad, S. Swapnil, K. Rajawat, and S. Anand, "Online algorithms for storage utilization under real-time pricing in smart grid," *International Journal of Electrical Power & Energy Systems*, vol. 101, pp. 50-59, 2018.
- [34] J. Chodkowska-Miszczuk, "Small-scale renewable energy systems in the development of distributed generation in Poland," *Moravian Geographical Reports*, vol. 22, no. 2, pp. 34-43, 2014.
- [35] Ofgem, "Ofgem's Annual Report and Accounts 2010-11," Available at : <https://www.ofgem.gov.uk/publications-and-updates/ofgem%E2%80%99s-annual-report-and-accounts-2010-11>
- [36] Weniger, Johannes, Tjarko Tjaden, and Volker Quaschnig. "Sizing and grid integration of residential PV battery systems." In 8th International Renewable Energy Storage Conference and Exhibition (IRES 2013), Berlin. 2013.
- [37] Rabiee, Abdorreza, Hossein Khorramdel, and Jamshid Aghaei. "RETRACTED: A review of energy storage systems in microgrids with wind turbines." *Renewable and Sustainable Energy Reviews* 18 (2013): 316-326.
- [38] Garrett Fitzgerald, James Mandel, Jesse Morris, Hervé Touati "THE ECONOMICS OF BATTERY ENERGY STORAGE," Available at: <https://rmi.org/wp-content/uploads/2017/03/RMI-TheEconomicsOfBatteryEnergyStorage-FullReport-FINAL.pdf>.
- [39] K. Divya, and J. Østergaard, "Battery energy storage technology for power systems—An overview," *Electric power systems research*, vol. 79, no. 4, pp. 511-520, 2009.
- [40] H. Moradi, M. Esfahanian, A. Abtahi, and A. Zilouchian, "Optimization and energy management of a standalone hybrid microgrid in the presence of battery storage system," *Energy*, vol. 147, pp. 226-238, 2018.
- [41] LGChem Ltd. website, " LG Chem RESU ESS Energy Storage Systems ", Available at: <https://www.solarelectricsupply.com/energy-storage-systems/lg-chem-ess/lg-chem-resu-ess-energy-storage-battery-systems>
- [42] Wikipedia, "Tesla Powerwall and Powerpack ", Available at: https://en.wikipedia.org/wiki/Tesla_Powerwall.
- [43] Moixa Energy Holdings Ltd. ," MOIXA Smart Battery ", Available at: <https://www.moixa.com/solar-battery/>.
- [44] J. Linssen, P. Stenzel, and J. Fleer, "Techno-economic analysis of photovoltaic battery systems and the influence of different consumer load profiles," *Applied Energy*, vol. 185, pp. 2019-2025, 2017.
- [45] Zakeri, Behnam, Sanna Syri, and Friedrich Wagner. "Economics of energy storage in the German electricity and reserve markets." In 2017 14th International Conference on the European Energy Market (EEM), pp. 1-6. IEEE, 2017.

- [46] UTILITYDIVE, "Greater than the sum: How aggregation is making storage into a software business", Available at: <https://www.utilitydive.com/news/greater-than-the-sum-how-aggregation-is-making-storage-into-a-software-bus/420753/>.
- [47] IRENA, "BEHIND-THE-METER BATTERIES INNOVATION LANDSCAPE BRIEF", Available at: https://www.irena.org/-/media/Files/IRENA/Agency/Publication/2019/Sep/IRENA_BTMBatteries_2019.pdf.
- [48] A. Azarpour, S. Suhaimi, G. Zahedi, and A. Bahadori, "A review on the drawbacks of renewable energy as a promising energy source of the future," *Arabian Journal for Science and Engineering*, vol. 38, no. 2, pp. 317-328, 2013.
- [49] H. C. Hesse, M. Schimpe, D. Kucevic, and A. Jossen, "Lithium-Ion Battery Storage for the Grid—A Review of Stationary Battery Storage System Design Tailored for Applications in Modern Power Grids," *Energies*, vol. 10, no. 12, pp. 2107, 2017.
- [50] O. P. Mahela, and A. G. Shaik, "Power quality improvement in distribution network using DSTATCOM with battery energy storage system," *International Journal of Electrical Power & Energy Systems*, vol. 83, pp. 229-240, 2016.
- [51] U. Datta, A. Kalam, and J. Shi, "Battery Energy Storage System for Aggregated Inertia-Droop Control and a Novel Frequency Dependent State-of-Charge Recovery," *Energies*, vol. 13, no. 8, pp. 2003, 2020.
- [52] R. Kempener, and E. Borden, "Battery storage for renewables: Market status and technology outlook," International Renewable Energy Agency, Abu Dhabi, 2015.
- [53] Kowalczyk, Albert, Adrian Włodarczyk, and Jarosław Tarnawski. "Microgrid energy management system." In 2016 21st International Conference on Methods and Models in Automation and Robotics (MMAR), pp. 157-162. IEEE, 2016.
- [54] J. Klaimi, R. Rahim-Amoud, L. Merghem-Boulahia, and A. Jrad, "Energy management algorithms in smart grids: state of the art and emerging trends," *International Journal of Artificial Intelligence and Applications*, vol. 7, no. 4, pp. 25-45, 2016.
- [55] W. Zhang, Y. Xu, W. Liu, C. Zang, and H. Yu, "Distributed online optimal energy management for smart grids," *IEEE Transactions on Industrial Informatics*, vol. 11, no. 3, pp. 717-727, 2015.
- [56] P. H. Shaikh, N. B. M. Nor, P. Nallagownden, I. Elamvazuthi, and T. Ibrahim, "A review on optimized control systems for building energy and comfort management of smart sustainable buildings," *Renewable and Sustainable Energy Reviews*, vol. 34, pp. 409-429, 2014.
- [57] J. Pascual, P. Sanchis, and L. Marroyo, "Implementation and control of a residential electrothermal microgrid based on renewable energies, a hybrid storage system and demand side management," *Energies*, vol. 7, no. 1, pp. 210-237, 2014.
- [58] W. Su, and J. Wang, "Energy management systems in microgrid operations," *The Electricity Journal*, vol. 25, no. 8, pp. 45-60, 2012.
- [59] D. E. Olivares, A. Mehrizi-Sani, A. H. Etemadi, C. A. Cañizares, R. Iravani, M. Kazerani, A. H. Hajimiragha, O. Gomis-Bellmunt, M. Saeedifard, and R. Palma-Behnke, "Trends in microgrid control," *IEEE Transactions on smart grid*, vol. 5, no. 4, pp. 1905-1919, 2014.

- [60] M. Elkazaz, M. Sumner, E. Naghiyev, S. Pholboon, R. Davies, and D. Thomas, "A hierarchical two-stage energy management for a home microgrid using model predictive and real-time controllers," *Applied Energy*, vol. 269, pp. 115118, 2020.
- [61] Y. Zhang, R. Wang, T. Zhang, Y. Liu, and B. Guo, "Model predictive control-based operation management for a residential microgrid with considering forecast uncertainties and demand response strategies," *IET Generation, Transmission & Distribution*, vol. 10, no. 10, pp. 2367-2378, 2016.
- [62] A. Fazeli, M. Sumner, M. C. Johnson, and E. Christopher, "Real-time deterministic power flow control through dispatch of distributed energy resources," *IET Generation, Transmission & Distribution*, vol. 9, no. 16, pp. 2724-2735, 2015.
- [63] Y. Zhang, P. E. Campana, A. Lundblad, and J. Yan, "Comparative study of hydrogen storage and battery storage in grid connected photovoltaic system: Storage sizing and rule-based operation," *Applied energy*, vol. 201, pp. 397-411, 2017.
- [64] Kawakami, Tomoya, Tomoki Yoshihisa, Naotaka Fujita, and Masahiko Tsukamoto. "A rule-based home energy management system using the Rete algorithm." In 2013 IEEE 2nd Global Conference on Consumer Electronics (GCCE), pp. 162-163. IEEE, 2013.
- [65] S. Teleke, M. E. Baran, S. Bhattacharya, and A. Q. Huang, "Rule-based control of battery energy storage for dispatching intermittent renewable sources," *IEEE Transactions on Sustainable Energy*, vol. 1, no. 3, pp. 117-124, 2010.
- [66] A. H. Fathima, and K. Palanisamy, "Optimization in microgrids with hybrid energy systems—A review," *Renewable and Sustainable Energy Reviews*, vol. 45, pp. 431-446, 2015.
- [67] C. Suchetha, and J. Ramprabhakar, "Optimization Techniques for Operation and Control of Microgrids—Review," *Journal of Green Engineering*, vol. 8, no. 4, pp. 621-644, 2018.
- [68] D. Tenfen, and E. C. Finardi, "A mixed integer linear programming model for the energy management problem of microgrids," *Electric Power Systems Research*, vol. 122, pp. 19-28, 2015.
- [69] Koutsopoulos, Iordanis, and Leandros Tassioulas. "Control and optimization meet the smart power grid: Scheduling of power demands for optimal energy management." In *Proceedings of the 2nd International Conference on Energy-efficient Computing and Networking*, pp. 41-50. 2011.
- [70] C. Roldán-Blay, G. Escrivá-Escrivá, C. Roldán-Porta, and C. Álvarez-Bel, "An optimisation algorithm for distributed energy resources management in micro-scale energy hubs," *Energy*, vol. 132, pp. 126-135, 2017.
- [71] R. Shipman, and M. Gillott, "SCENe Things: IoT-based Monitoring of a Community Energy Scheme," *Future Cities and Environment*, vol. 5, no. 1, 2019.
- [72] D. Arcos-Aviles, J. Pascual, F. Guinjoan, L. Marroyo, P. Sanchis, and M. P. Marietta, "Low complexity energy management strategy for grid profile smoothing of a residential grid-connected microgrid using generation and demand forecasting," *Applied energy*, vol. 205, pp. 69-84, 2017.
- [73] Y. Wang, S. Mao, and R. M. Nelms, "Distributed online algorithm for optimal real-time energy distribution in the smart grid," *IEEE Internet of Things Journal*, vol. 1, no. 1, pp. 70-80, 2014.

- [74] A. Parisio, E. Rikos, G. Tzamalīs, and L. Glielmo, "Use of model predictive control for experimental microgrid optimization," *Applied Energy*, vol. 115, pp. 37-46, 2014.
- [75] M. Nemati, M. Braun, and S. Tenbohlen, "Optimization of unit commitment and economic dispatch in microgrids based on genetic algorithm and mixed integer linear programming," *Applied Energy*, vol. 210, pp. 944-963, 2018.
- [76] U. Berardi, E. Tomassoni, and K. Khaled, "A Smart Hybrid Energy System Grid for Energy Efficiency in Remote Areas for the Army," *Energies*, vol. 13, no. 9, pp. 2279, 2020.
- [77] Borghetti, A., M. Bosetti, C. Bossi, S. Massucco, E. Micolano, A. Morini, C. A. Nucci, M. Paolone, and F. Silvestro. "An energy resource scheduler implemented in the automatic management system of a microgrid test facility." In 2007 International Conference on Clean Electrical Power, pp. 94-100. IEEE, 2007.
- [78] A. Omu, R. Choudhary, and A. Boies, "Distributed energy resource system optimisation using mixed integer linear programming," *Energy Policy*, vol. 61, pp. 249-266, 2013.
- [79] J. Silvente, G. M. Kopanos, E. N. Pistikopoulos, and A. Espuña, "A rolling horizon optimization framework for the simultaneous energy supply and demand planning in microgrids," *Applied Energy*, vol. 155, pp. 485-501, 2015.
- [80] Marietta, Martin P., Moisés Graells, and Josep M. Guerrero. "A rolling horizon rescheduling strategy for flexible energy in a microgrid." In 2014 IEEE International Energy Conference (ENERGYCON), pp. 1297-1303. IEEE, 2014.
- [81] M. Elsied, A. Oukaour, T. Youssef, H. Gualous, and O. Mohammed, "An advanced real time energy management system for microgrids," *Energy*, vol. 114, pp. 742-752, 2016.
- [82] A. C. Luna, L. Meng, N. L. Diaz, M. Graells, J. C. Vasquez, and J. M. Guerrero, "Online energy management systems for microgrids: experimental validation and assessment framework," *IEEE Transactions on Power Electronics*, vol. 33, no. 3, pp. 2201-2215, 2018.
- [83] Y. Riffonneau, S. Bacha, F. Barruel, and S. Ploix, "Optimal power flow management for grid connected PV systems with batteries," *IEEE Transactions on sustainable energy*, vol. 2, no. 3, pp. 309-320, 2011.
- [84] A. Purvins, and M. Sumner, "Optimal management of stationary lithium-ion battery system in electricity distribution grids," *Journal of Power Sources*, vol. 242, pp. 742-755, 2013.
- [85] P. M. van de Ven, N. Hegde, L. Massoulié, and T. Salonidis, "Optimal control of end-user energy storage," *IEEE Transactions on Smart Grid*, vol. 4, no. 2, pp. 789-797, 2013.
- [86] Mehdi, Laraki, Yassine Ouallou, Oussa Mohamed, and Aawatif Hayar. "New Smart Home's energy management system design and implementation for frugal smart cities." In 2018 International Conference on Selected Topics in Mobile and Wireless Networking (MoWNeT), pp. 149-153. IEEE, 2018.
- [87] M. Beaudin, and H. Zareipour, "Home energy management systems: A review of modelling and complexity," *Renewable and sustainable energy reviews*, vol. 45, pp. 318-335, 2015.

- [88] Chandra, Lokesh, and Saurabh Chanana. "Energy management of smart homes with energy storage, rooftop PV and electric vehicle." In 2018 IEEE International Students' Conference on Electrical, Electronics and Computer Science (SCEECS), pp. 1-6. IEEE, 2018.
- [89] Lebrón, Christopher, Fabio Andrade, Efraín O'Neill, and Agustín Irizarry. "An intelligent Battery management system for home Microgrids." In 2016 IEEE Power & Energy Society Innovative Smart Grid Technologies Conference (ISGT), pp. 1-5. IEEE, 2016.
- [90] S. Van Der Stelt, T. AlSkaif, and W. van Sark, "Techno-economic analysis of household and community energy storage for residential prosumers with smart appliances," *Applied Energy*, vol. 209, pp. 266-276, 2018.
- [91] H. Tazvinga, B. Zhu, and X. Xia, "Optimal power flow management for distributed energy resources with batteries," *Energy Conversion and Management*, vol. 102, pp. 104-110, 2015.
- [92] Kumar, PTVB Narasimha, Sajja Suryateja, Ganivada Naveen, Mukesh Singh, and Praveen Kumar. "Smart home energy management with integration of PV and storage facilities providing grid support." In 2013 IEEE Power & Energy Society General Meeting, pp. 1-5. IEEE, 2013.
- [93] S. Ikeda, and R. Ooka, "Metaheuristic optimization methods for a comprehensive operating schedule of battery, thermal energy storage, and heat source in a building energy system," *Applied energy*, vol. 151, pp. 192-205, 2015.
- [94] O. Erdinc, N. G. Paterakis, T. D. Mendes, A. G. Bakirtzis, and J. P. Catalão, "Smart household operation considering bi-directional EV and ESS utilization by real-time pricing-based DR," *IEEE Transactions on Smart Grid*, vol. 6, no. 3, pp. 1281-1291, 2014.
- [95] C. Sun, F. Sun, and S. J. Moura, "Nonlinear predictive energy management of residential buildings with photovoltaics & batteries," *Journal of Power Sources*, vol. 325, pp. 723-731, 2016.
- [96] M. Muratori, and G. Rizzoni, "Residential demand response: Dynamic energy management and time-varying electricity pricing," *IEEE Transactions on Power systems*, vol. 31, no. 2, pp. 1108-1117, 2015.
- [97] O. Erdinc, "Economic impacts of small-scale own generating and storage units, and electric vehicles under different demand response strategies for smart households," *Applied Energy*, vol. 126, pp. 142-150, 2014.
- [98] N. G. Paterakis, A. Taşçıkaraoğlu, O. Erdinc, A. G. Bakirtzis, and J. P. Catalao, "Assessment of demand-response-driven load pattern elasticity using a combined approach for smart households," *IEEE Transactions on Industrial Informatics*, vol. 12, no. 4, pp. 1529-1539, 2016.
- [99] K. M. Tsui, and S.-C. Chan, "Demand response optimization for smart home scheduling under real-time pricing," *IEEE Transactions on Smart Grid*, vol. 3, no. 4, pp. 1812-1821, 2012.
- [100] F. Y. Melhem, O. Grunder, Z. Hammoudan, and N. Moubayed, "Optimization and energy management in smart home considering photovoltaic, wind, and battery

- storage system with integration of electric vehicles,” *Canadian Journal of Electrical and Computer Engineering*, vol. 40, no. 2, pp. 128-138, 2017.
- [101] X. Jin, J. Wu, Y. Mu, M. Wang, X. Xu, and H. Jia, “Hierarchical microgrid energy management in an office building,” *Applied energy*, vol. 208, pp. 480-494, 2017.
- [102] L. Sun, G. Wu, Y. Xue, J. Shen, D. Li, and K. Y. Lee, “Coordinated control strategies for fuel cell power plant in a microgrid,” *IEEE Transactions on Energy Conversion*, vol. 33, no. 1, pp. 1-9, 2017.
- [103] Marietta, Martin P., Moisés Graells, and Josep M. Guerrero. "A rolling horizon rescheduling strategy for flexible energy in a microgrid." In 2014 IEEE International Energy Conference (ENERGYCON), pp. 1297-1303. IEEE, 2014.
- [104] A. Parisio, E. Rikos, and L. Glielmo, “A model predictive control approach to microgrid operation optimization,” *IEEE Transactions on Control Systems Technology*, vol. 22, no. 5, pp. 1813-1827, 2014.
- [105] T. Terlouw, T. AlSkaif, C. Bauer, and W. van Sark, “Optimal energy management in all-electric residential energy systems with heat and electricity storage,” *Applied Energy*, vol. 254, pp. 113580, 2019.
- [106] Schweppe, Fred C., and Sanjoy K. Mitter. "Hierarchical system theory and electric power systems." In *Proceedings Symposium on Real Time Control of Electric Power Systems*, pp. 259-277. Elsevier Publishing Company, 1972.
- [107] E. Unamuno, and J. A. Barrena, “Hybrid ac/dc microgrids—Part II: Review and classification of control strategies,” *Renewable and Sustainable Energy Reviews*, vol. 52, pp. 1123-1134, 2015.
- [108] Bidram, Ali, and Ali Davoudi. "Hierarchical structure of microgrids control system." *IEEE Transactions on Smart Grid* 3, no. 4 (2012): 1963-1976.
- [109] A. S. Farsangi, S. Hadayeghparast, M. Mehdinejad, and H. Shayanfar, “A novel stochastic energy management of a microgrid with various types of distributed energy resources in presence of demand response programs,” *Energy*, vol. 160, pp. 257-274, 2018.
- [110] Fazeli, Amir, Mark Sumner, C. Mark Johnson, and Edward Christopher. "Coordinated optimal dispatch of distributed energy resources within a smart energy community cell." In 2012 3rd IEEE PES Innovative Smart Grid Technologies Europe (ISGT Europe), pp. 1-10. IEEE, 2012.
- [111] B. Dupont, K. Dietrich, C. De Jonghe, A. Ramos, and R. Belmans, “Impact of residential demand response on power system operation: A Belgian case study,” *Applied Energy*, vol. 122, pp. 1-10, 2014.
- [112] R. Palma-Behnke, C. Benavides, F. Lanas, B. Severino, L. Reyes, J. Llanos, and D. Sáez, “A microgrid energy management system based on the rolling horizon strategy,” *IEEE Transactions on smart grid*, vol. 4, no. 2, pp. 996-1006, 2013.
- [113] Xiaoping, Liu, Ding Ming, Han Jianghong, Han Pingping, and Peng Yali. "Dynamic economic dispatch for microgrids including battery energy storage." In *The 2nd international symposium on power electronics for distributed generation systems*, pp. 914-917. IEEE, 2010.
- [114] Tsikalakis, Antonis G., and Nikos D. Hatziargyriou. "Centralized control for optimizing microgrids operation." In 2011 IEEE power and energy society general meeting, pp. 1-8. IEEE, 2011.

- [115] C.-S. Karavas, G. Kyriakarakos, K. G. Arvanitis, and G. Papadakis, "A multi-agent decentralized energy management system based on distributed intelligence for the design and control of autonomous polygeneration microgrids," *Energy Conversion and Management*, vol. 103, pp. 166-179, 2015.
- [116] D. D. Siljak, *Decentralized control of complex systems*: Courier Corporation, 2011.
- [117] B. Shi, and J. Liu, "Decentralized control and fair load-shedding compensations to prevent cascading failures in a smart grid," *International Journal of Electrical Power & Energy Systems*, vol. 67, pp. 582-590, 2015.
- [118] H. K. Nunna, and S. Doolla, "Multiagent-based distributed-energy-resource management for intelligent microgrids," *IEEE Transactions on Industrial Electronics*, vol. 60, no. 4, pp. 1678-1687, 2012.
- [119] C. M. Colson, and M. H. Nehrir, "Comprehensive real-time microgrid power management and control with distributed agents," *IEEE Transactions on Smart Grid*, vol. 4, no. 1, pp. 617-627, 2013.
- [120] Z. Wang, and R. Paranjape, "Optimal residential demand response for multiple heterogeneous homes with real-time price prediction in a multiagent framework," *IEEE transactions on smart grid*, vol. 8, no. 3, pp. 1173-1184, 2015.
- [121] M. Bragard, N. Soltau, S. Thomas, and R. W. De Doncker, "The balance of renewable sources and user demands in grids: Power electronics for modular battery energy storage systems," *IEEE Transactions on Power Electronics*, vol. 25, no. 12, pp. 3049-3056, 2010.
- [122] Lacey, Stephen. "How distributed battery storage will surpass grid-scale storage in the US by 2020." Report in *Greentech media 10* (2016), available at : <https://www.greentechmedia.com/articles/read/how-distributed-battery-storage-will-surpass-grid-scale-storage-in-the-us-b>
- [123] R. Hiremath, S. Shikha, and N. Ravindranath, "Decentralized energy planning; modeling and application—a review," *Renewable and Sustainable Energy Reviews*, vol. 11, no. 5, pp. 729-752, 2007.
- [124] G. Carpinelli, F. Mottola, and D. Proto, "Probabilistic sizing of battery energy storage when time-of-use pricing is applied," *Electric Power Systems Research*, vol. 141, pp. 73-83, 2016.
- [125] J. Sardi, N. Mithulananthan, M. Gallagher, and D. Q. Hung, "Multiple community energy storage planning in distribution networks using a cost-benefit analysis," *Applied energy*, vol. 190, pp. 453-463, 2017.
- [126] B. Bahmani-Firouzi, and R. Azizipanah-Abarghooee, "Optimal sizing of battery energy storage for micro-grid operation management using a new improved bat algorithm," *International Journal of Electrical Power & Energy Systems*, vol. 56, pp. 42-54, 2014.
- [127] Ekoh, Solomon, Ibrahim Unsal, and Alireza Maheri. "Optimal sizing of wind-PV-pumped hydro energy storage systems." In *2016 4th International Symposium on Environmental Friendly Energies and Applications (EFEA)*, pp. 1-6. IEEE, 2016.
- [128] Kazempour, S. Jalal, and Mohsen Parsa Moghaddam. "Economic viability of NaS battery plant in a competitive electricity market." In *2009 International conference on clean electrical power*, pp. 453-459. IEEE, 2009.

- [129] Starke, M., P. Irminger, B. Ollis, G. Andrews, O. Onar, P. Karlson, S. Thambiappah et al. "Community energy storage with secondary use ev/phev batteries." ORNL, Oak Ridge, TN, USA, DEAC05-00OR22725 (2014).
- [130] O. Erdinc, and M. Uzunoglu, "Optimum design of hybrid renewable energy systems: Overview of different approaches," *Renewable and Sustainable Energy Reviews*, vol. 16, no. 3, pp. 1412-1425, 2012.
- [131] G. Mulder, F. De Ridder, and D. Six, "Electricity storage for grid-connected household dwellings with PV panels," *Solar energy*, vol. 84, no. 7, pp. 1284-1293, 2010.
- [132] L. Xu, X. Ruan, C. Mao, B. Zhang, and Y. Luo, "An improved optimal sizing method for wind-solar-battery hybrid power system," *IEEE transactions on Sustainable Energy*, vol. 4, no. 3, pp. 774-785, 2013.
- [133] M. Bortolini, M. Gamberi, and A. Graziani, "Technical and economic design of photovoltaic and battery energy storage system," *Energy Conversion and Management*, vol. 86, pp. 81-92, 2014.
- [134] N. Zhou, N. Liu, J. Zhang, and J. Lei, "Multi-objective optimal sizing for battery storage of PV-based microgrid with demand response," *Energies*, vol. 9, no. 8, pp. 591, 2016.
- [135] M. Cheng, S. S. Sami, and J. Wu, "Benefits of using virtual energy storage system for power system frequency response," *Applied energy*, vol. 194, pp. 376-385, 2017.
- [136] H. Guozhen, D. Shanxu, C. Tao, and C. Changsong, "Sizing and cost analysis of photovoltaic generation system based on vanadium redox battery," *Transactions of China electrotechnical society*, vol. 27, no. 5, pp. 260-267, 2012.
- [137] J. Mitra, "Reliability-based sizing of backup storage," *IEEE Transactions on Power Systems*, vol. 25, no. 2, pp. 1198-1199, 2010.
- [138] Ross, Michael, Rodrigo Hidalgo, Chad Abbey, and Géza Joós. "Analysis of energy storage sizing and technologies." In 2010 IEEE Electrical Power & Energy Conference, pp. 1-6. IEEE, 2010.
- [139] M. Gitizadeh, and H. Fakharzadegan, "Battery capacity determination with respect to optimized energy dispatch schedule in grid-connected photovoltaic (PV) systems," *Energy*, vol. 65, pp. 665-674, 2014.
- [140] D. Parra, M. Gillott, S. A. Norman, and G. S. Walker, "Optimum community energy storage system for PV energy time-shift," *Applied Energy*, vol. 137, pp. 576-587, 2015.
- [141] Dunn, Bruce, Haresh Kamath, and Jean-Marie Tarascon. "Electrical energy storage for the grid: a battery of choices." *Science* 334, no. 6058 (2011): 928-935.
- [142] M. Kazemi, H. Zareipour, N. Amjady, W. D. Rosehart, and M. Ehsan, "Operation scheduling of battery storage systems in joint energy and ancillary services markets," *IEEE Transactions on Sustainable Energy*, vol. 8, no. 4, pp. 1726-1735, 2017.
- [143] K. Bradbury, L. Pratson, and D. Patiño-Echeverri, "Economic viability of energy storage systems based on price arbitrage potential in real-time US electricity markets," *Applied Energy*, vol. 114, pp. 512-519, 2014.
- [144] Zakeri, Behnam, and Sanna Syri. "Value of energy storage in the Nordic Power market-benefits from price arbitrage and ancillary services." In 2016 13th International Conference on the European Energy Market (EEM), pp. 1-5. IEEE, 2016.

- [145] Pandurangan, Vivek, Hamidreza Zareipour, and Om Malik. "Frequency regulation services: A comparative study of select North American and European reserve markets." In 2012 North American Power Symposium (NAPS), pp. 1-8. IEEE, 2012.
- [146] Strassheim, A., J. E. S. De Haan, M. Gibescu, and W. L. Kling. "Provision of frequency restoration reserves by possible energy storage systems in Germany and the Netherlands." In 11th international conference on the European energy market (EEM14), pp. 1-5. IEEE, 2014.
- [147] V. Knap, S. K. Chaudhary, D.-I. Stroe, M. Swierczynski, B.-I. Craciun, and R. Teodorescu, "Sizing of an energy storage system for grid inertial response and primary frequency reserve," IEEE Transactions on Power Systems, vol. 31, no. 5, pp. 3447-3456, 2015.
- [148] A. M. Adil, and Y. Ko, "Socio-technical evolution of Decentralized Energy Systems: A critical review and implications for urban planning and policy," Renewable and Sustainable Energy Reviews, vol. 57, pp. 1025-1037, 2016.
- [149] Mercurio, Andrea, Alessandro Di Giorgio, and Alessandra Quaresima. "Distributed control approach for community energy management systems." In 2012 20th Mediterranean Conference on Control & Automation (MED), pp. 1265-1271. IEEE, 2012.
- [150] Choi, Soojeong, Sunju Park, Dong-Joo Kang, Seung-jae Han, and Hak-Man Kim. "A microgrid energy management system for inducing optimal demand response." In 2011 IEEE international conference on smart grid communications (SmartGridComm), pp. 19-24. IEEE, 2011.
- [151] Strickland, Dani, M. Abedi Varnosfederani, J. Scott, P. Quintela, A. Duran, R. Bravery, A. Corliss, K. Ashworth, and S. Blois-Brooke. "A review of community electrical energy systems." In 2016 IEEE International Conference on Renewable Energy Research and Applications (ICRERA), pp. 49-54. IEEE, 2016.
- [152] P. Yilmaz, M. H. Hocaoglu, and A. E. S. Konukman, "A pre-feasibility case study on integrated resource planning including renewables," Energy Policy, vol. 36, no. 3, pp. 1223-1232, 2008.
- [153] Richardson, I., Thomson, M. (2010). "One-Minute Resolution Domestic Electricity Use Data ". UK Data Service. SN: 6583, available at: <http://doi.org/10.5255/UKDA-SN-6583-1>.
- [154] PVOutput, "Generation profiles for a 3.8 kW PV station located in Nottingham ", available at: <https://pvoutput.org/>.
- [155] The Greenage, "What is the Economy 7 tariff? " available at: <https://www.thegreenage.co.uk/what-is-economy-7-tariff/#:~:text=Economy%20is%20simply%20a,energy%20at%20off%20peak%20times.&text=As%20a%20result%20Economy%20,find%20a%20use%20for%20it>
- [156] M. Nicolson, G. Huebner, and D. Shipworth, "Are consumers willing to switch to smart time of use electricity tariffs? The importance of loss-aversion and electric vehicle ownership," Energy research & social science, vol. 23, pp. 82-96, 2017.
- [157] M. J. Fell, M. Nicolson, G. M. Huebner, and D. Shipworth, "Is it time? Consumers and time of use tariffs", UCL Energy Institute, pp. 27, 2015.
- [158] Power Compare, "RobinHood energy Economy 7 Tariff ", available at: <https://powercompare.co.uk/robin-hood-energy/>

- [159] Simply Switch, "Innovative 'Time of Day' Tariff Launched by Green Energy UK," available at: <https://www.simplyswitch.com/innovative-time-of-day-tariff-launched-by-green-energy-uk/>.
- [160] Moneysavingexpert, "time-of-day purchasing tariff in UK," available at: <https://www.moneysavingexpert.com/news/2017/01/green-energy-launches-time-of-day-tariff---electricity-savings-available-but-gas-remains-pricey/>.
- [161] Department of Energy and Climate Change, "Domestic energy price statistics 2019 ", available at: <https://www.gov.uk/government/collections/domestic-energy-prices>.
- [162] ERNEST ORLANDO LAWRENCE BERKELEY NATIONAL LABORATORY, "A Survey of Utility Experience with Real Time Pricing," available at: <https://www.osti.gov/servlets/purl/836966>
- [163] ELEXON Ltd, "The New Electricity Trading Arrangements for the Imbalance Market in UK " ELEXON Ltd, UK," available at: <https://www.bmreports.com/bmrs/?q=balancing/systemsellbuyprices/historic>.
- [164] Power Compare, "Robin Hood Energy Reviews & Tariffs ", available at: <https://powercompare.co.uk/robin-hood-energy/>.
- [165] Ofgem. " Feed-In Tariff (FIT) rates in UK ", available at: <https://www.ofgem.gov.uk/environmental-programmes/fit/fit-tariff-rates;2020>
- [166] Tesla co."tesla Powerwall battery," available at: https://www.tesla.com/en_GB/powerwall.
- [167] ALMASOALR co. , "SMA power inverters prices list", 2020 ", available at: <https://www.alma-solarshop.com/131-sma-inverter#/>.
- [168] Tesla co. "POWERPACK Utility and Business Energy Storage," available at: https://www.tesla.com/en_GB/powerpack?redirect=no.
- [169] A.-L. Klingler, and L. Teichtmann, "Impacts of a forecast-based operation strategy for grid-connected PV storage systems on profitability and the energy system," *Solar Energy*, vol. 158, pp. 861-868, 2017.
- [170] Iwafune, Yumiko, Yoshie Yagita, Takashi Ikegami, and Kazuhiko Ogimoto. "Short-term forecasting of residential building load for distributed energy management." In 2014 IEEE international energy conference (ENERGYCON), pp. 1197-1204. IEEE, 2014.
- [171] J. Antonanzas, N. Osorio, R. Escobar, R. Urraca, F. J. Martinez-de-Pison, and F. Antonanzas-Torres, "Review of photovoltaic power forecasting," *Solar Energy*, vol. 136, pp. 78-111, 2016.
- [172] O. Elena Dragomir, F. Dragomir, V. Stefan, and E. Minca, "Adaptive Neuro-Fuzzy Inference Systems as a strategy for predicting and controlling the energy produced from renewable sources," *Energies*, vol. 8, no. 11, pp. 13047-13061, 2015.
- [173] M., Muhammad Asim, et al. "Solar PV Generation Forecast Model Based on the Most Effective Weather Parameters." 2019 International Conference on Electrical, Communication, and Computer Engineering (ICECCE). IEEE, 2019.
- [174] Kreifels, N., S. Killinger, D. Fischer, and B. Wille-Hausmann. "Uncertainty and error analysis of calculation procedures for PV self-consumption and its significance to investment decisions." In 2016 13th International Conference on the European Energy Market (EEM), pp. 1-5. IEEE, 2016.

- [175] G. Litjens, E. Worrell, and W. van Sark, "Assessment of forecasting methods on performance of photovoltaic-battery systems," *Applied Energy*, vol. 221, pp. 358-373, 2018.
- [176] wikipedia "Internal rate of return defination and calculation", available at: https://en.wikipedia.org/wiki/Internal_rate_of_return.
- [177] Investopedia " Internal Rate of Return – IRR ", available at: <https://www.investopedia.com/terms/i/irr.asp>
- [178] Forecast Pro. website, " A Guide to Forecast Error Measurement Statistics and How to Use Them ", available at: <https://www.forecastpro.com/Trends/forecasting101August2011.html>
- [179] UK power, "Average gas and electric usage for UK households " , available at:https://www.ukpower.co.uk/home_energy/average-household-gas-and-electricity-usage
- [180] Innovatio Uk, Project Sensible, available at: " <https://www.projectsensible.eu/>.
- [181] T. Terlouw, X. Zhang, C. Bauer, and T. Alskaiif, "Towards the determination of metal criticality in home-based battery systems using a Life Cycle Assessment approach," *Journal of Cleaner Production*, 2019.
- [182] I. S. ASSOCIATION, "IEEE Guide for the Characterization and Evaluation of Lithium-Based Batteries in Stationary Applications," 2017.
- [183] Barnes, Arthur K., Juan Carlos Balda, Scott O. Geurin, and Andrés Escobar-Mejía. "Optimal battery chemistry, capacity selection, charge/discharge schedule, and lifetime of energy storage under time-of-use pricing." In 2011 2nd IEEE PES International Conference and Exhibition on Innovative Smart Grid Technologies, pp. 1-7. IEEE, 2011.
- [184] K. Holkar, and L. Waghmare, "An overview of model predictive control," *International Journal of Control and Automation*, vol. 3, no. 4, pp. 47-63, 2010.
- [185] X. Xing, L. Xie, and H. Meng, "Cooperative energy management optimization based on distributed MPC in grid-connected microgrids community," *International Journal of Electrical Power & Energy Systems*, vol. 107, pp. 186-199, 2019.
- [186] Y. Wang, and S. Boyd, "Fast model predictive control using online optimization" *IEEE Transactions on control systems technology*, vol. 18, no. 2, pp. 267-278, 2010.
- [187] Camacho, Eduardo F., and Carlos Bordons Alba. "Model predictive control". Springer science & business media, 2013.
- [188] Hoke, Anderson, Alexander Brissette, Dragan Maksimović, Annabelle Pratt, and Kandler Smith. "Electric vehicle charge optimization including effects of lithium-ion battery degradation." In 2011 IEEE Vehicle Power and Propulsion Conference, pp. 1-8. IEEE, 2011.
- [189] Y. Sun, H. Yue, J. Zhang, and C. Booth, "Minimization of residential energy cost considering energy storage system and EV with driving usage probabilities," *IEEE Transactions on Sustainable Energy*, vol. 10, no. 4, pp. 1752-1763, 2018.
- [190] S. Chalise, J. Sternhagen, T. M. Hansen, and R. Tonkoski, "Energy management of remote microgrids considering battery lifetime," *The Electricity Journal*, vol. 29, no. 6, pp. 1-10, 2016.

- [191] F. Garcia-Torres, and C. Bordons, "Optimal economical schedule of hydrogen-based microgrids with hybrid storage using model predictive control," *IEEE Transactions on Industrial Electronics*, vol. 62, no. 8, pp. 5195-5207, 2015.
- [192] Y. Chen, R. P. Liu, C. Wang, M. De Groot, and Z. Zeng, "Consumer operational comfort level based power demand management in the smart grid." pp. 1-6.
- [193] M. Jünger, T. M. Liebling, D. Naddef, G. L. Nemhauser, W. R. Pulleyblank, G. Reinelt, G. Rinaldi, and L. A. Wolsey, "50 Years of Integer Programming 1958-2008: From the Early Years to the State-of-the-art": Springer Science & Business Media, 2009.
- [194] J. P. Vielma, "Mixed integer linear programming formulation techniques," *SIAM Review*, vol. 57, no. 1, pp. 3-57, 2015.
- [195] J. C. Smith, and Z. C. Taskin, "A tutorial guide to mixed-integer programming models and solution techniques," *Optimization in Medicine and Biology*, pp. 521-548, 2008.
- [196] Sustainable Community Energy Networks, "trent basin community", Available at: <https://www.projectscene.uk/trentbasin/>.
- [197] Triphase Ltd., "Microgrid's Converter Data". Available at: <https://triphase.com/microgrid-converters/>
- [198] GenDrive Ltd. "CAN (Controller Area Network) bus specification", available at: [https://www.avrfreaks.net/sites/default/files/CAN%20BUS%20specification%20Rev S.pdf](https://www.avrfreaks.net/sites/default/files/CAN%20BUS%20specification%20Rev%20S.pdf)
- [199] ClientEarth, "Recommendations for improving grid connections for community energy projects in the UK", Available at: <https://www.documents.clientearth.org/wp-content/uploads/library/2015-03-19-recommendations-for-improving-grid-connections-for-community-energy-projects-in-the-uk-ce-en.pdf>
- [200] L. Rodrigues, M. Gillott, J. A. Waldron, L. Cameron, R. Tubelo, and R. Shipman, "Community Energy Networks in the Making: Project SCENe, Nottingham.", *PLEA 2018 : Smart and Healthy within the 2-degree Limit*.
- [201] Elkazaz, Mahmoud, Mark Sumner, Seksak Pholboon, and David Thomas. "Microgrid Energy Management Using a Two Stage Rolling Horizon Technique for Controlling an Energy Storage System." In 2018 7th International Conference on Renewable Energy Research and Applications (ICRERA), pp. 324-329. IEEE, 2018.
- [202] Cole, Wesley J., and Allister Frazier. Cost projections for utility-scale battery storage. No. NREL/TP-6A20-73222. National Renewable Energy Lab.(NREL), Golden, CO (United States), 2019.
- [203] M. Kazemi, and H. Zareipour, "Long-term scheduling of battery storage systems in energy and regulation markets considering battery's lifespan," *IEEE Transactions on Smart Grid*, vol. 9, no. 6, pp. 6840-6849, 2017.
- [204] F. Garcia-Torres, C. Bordons, and M. A. Ridao, "Optimal economic schedule for a network of microgrids with hybrid energy storage system using distributed model predictive control," *IEEE transactions on industrial electronics*, vol. 66, no. 3, pp. 1919-1929, 2018.

- [205] CleanTechnica, "Tesla Megapack, Powerpack, & Powerwall Battery Storage Prices Per KWh — Exclusive," available at: <https://cleantechnica.com/2020/10/05/tesla-megapack-powerpack-powerwall-battery-storage-prices/>.
- [206] U.S. Department of Energy, "Energy Storage Technology and Cost Characterization Report," available at: https://www.energy.gov/sites/prod/files/2019/07/f65/Storage%20Cost%20and%20Performance%20Characterization%20Report_Final.pdf.
- [207] Macrotrends. "UK Inflation Rate 1960-2020", available at: <https://www.macrotrends.net/countries/GBR/united-kingdom/inflation-rate-cpi#:~:text=U.K.%20inflation%20rate%20for%202019,a%200.64%25%20increase%20from%202015>.
- [208] T. Ashwin, Y. M. Chung, and J. Wang, "Capacity fade modelling of lithium-ion battery under cyclic loading conditions," *Journal of Power Sources*, vol. 328, pp. 586-598, 2016.
- [209] Statista, "Electricity prices for households in the United Kingdom (UK) from 2010 to 2020, semi-annually," available at: <https://www.statista.com/statistics/418126/electricity-prices-for-households-in-the-uk/>.
- [210] UK energy security, "Capacity Market auction parameters: letters from BEIS to National Grid ESO, July 2019," available at: <https://www.gov.uk/government/publications/capacity-market-auction-parameters-letter-from-beis-to-national-grid-eso-july-2019>
- [211] Nolden, Colin, and Steve Sorrell. "The UK market for energy service contracts in 2014–2015." *Energy efficiency* 9.6 (2016): 1405-1420.
- [212] Limejump co., "Limejump secures the majority of the fully Dynamic Volume awarded in the January month ahead tender", available at: <https://limejump.com/limejump-secures-57-of-january-ffr-auction/#more-7518>.
- [213] Ofgem. "Capacity Market (CM) Rules", available at: <https://www.ofgem.gov.uk/electricity/wholesale-market/market-efficiency-review-and-reform/electricity-market-reform/capacity-market-cm-rules>.
- [214] UK. power. "CAPACITY MARKET, Five-year Review (2014 – 2019)", available at: https://assets.publishing.service.gov.uk/government/uploads/system/uploads/attachment_data/file/819760/cm-five-year-review-report.pdf.
- [215] UK National Grid, "Profiting from Demand Side Response," available at: http://powerresponsive.com/wp-content/uploads/2016/11/ng_meuc-dsr-book.pdf.
- [216] UK National Grid, "A short guide to how your business can profit from Demand Side Response", available at: <http://powerresponsive.com/wp-content/uploads/pdf/Power%20Responsive%20Guide%20-%20v8.pdf>.
- [217] Yana, Syiska, Anthony Florida James, Abdullah Emhemed, and Graeme Burt. "Decentralised control of dc microgrid based on virtual admittance to enhance dc voltage and grid frequency support." In 2018 53rd International Universities Power Engineering Conference (UPEC), pp. 1-6. IEEE, 2018.
- [218] National Grid ESO, "Getting paid for Firm frequency response (FFR)," available at: <https://www.nationalgrideso.com/balancing-services/frequency-response-services/firm-frequency-response-ffr?market-information>.

- [219] Bmreports, "System Sell & System Buy Prices for participation in DFFR services," , available at: <https://www.bmreports.com/bmrs/?q=balancing/systemsellbuyprices>.
- [220] National Grid ESO, "DFFR tender report -July 2019," , available at: <https://www.nationalgrideso.com/balancing-services/frequency-response-services/firm-frequency-response-ffr?market-information=&page=4>.
- [221] UK National Grid, "Balancing Principles Statement , published in accordance with Standard Condition C16 of National Grid Electricity Transmission Licence, Warwick, 2017", available at: <https://www.nationalgrid.com/sites/default/files/documents/Balancing%20Principles%20Statement%20v15%20Effective%20from%201%20April%202017.pdf>.
- [222] Yuill, W., R. Kgokong, S. Chowdhury, and S. P. Chowdhury. "Application of Adaptive Neuro Fuzzy Inference System (ANFIS) based short term load forecasting in South African power networks." In 45th International Universities Power Engineering Conference UPEC2010, pp. 1-5. IEEE, 2010.
- [223] Akarslan, Emre, and Fatih Onur Hocaoglu. "A novel short-term load forecasting approach using Adaptive Neuro-Fuzzy Inference System." In 2018 6th International Istanbul Smart Grids and Cities Congress and Fair (ICSG), pp. 160-163. IEEE, 2018.
- [224] K. Amber, R. Ahmad, M. Aslam, A. Kousar, M. Usman, and M. Khan, "Intelligent techniques for forecasting electricity consumption of buildings," *Energy*, vol. 157, pp. 886-893, 2018.
- [225] M. Q. Raza, and A. Khosravi, "A review on artificial intelligence based load demand forecasting techniques for smart grid and buildings," *Renewable and Sustainable Energy Reviews*, vol. 50, pp. 1352-1372, 2015.
- [226] J.-S. Jang, "ANFIS: adaptive-network-based fuzzy inference system," *IEEE transactions on systems, man, and cybernetics*, vol. 23, no. 3, pp. 665-685, 1993.
- [227] A. Al-Mayyahi, W. Wang, and P. Birch, "Adaptive neuro-fuzzy technique for autonomous ground vehicle navigation," *Robotics*, vol. 3, no. 4, pp. 349-370, 2014.
- [228] Solar radiation Data website, "weather data archive", Available at : <http://www.soda-pro.com/help/helioclim/helioclim-3-overview>.
- [229] L. Hernández, C. Baladrón, J. M. Aguiar, B. Carro, A. Sánchez-Esguevillas, and J. Lloret, "Artificial neural networks for short-term load forecasting in microgrids environment," *Energy*, vol. 75, pp. 252-264, 2014.
- [230] CCL Components Ltd, "BYD B-BOX HV - LITHIUM BATTERY PACK ", available at: [file:///C:/Users/eexme11/Downloads/BYD%20Battery-Box%20Datasheet%20V1-6%20EN%20\(1\).pdf](file:///C:/Users/eexme11/Downloads/BYD%20Battery-Box%20Datasheet%20V1-6%20EN%20(1).pdf)
- [231] SMA solar technology, "SUNNY BOY STORAGE 2.5 power inverter data sheet" , available at: https://www.sma.de/fileadmin/user_upload/SBS25-DEN1604-V10web.pdf
- [232] SMA solar technology, "SMA INTEGRATED STORAGE SYSTEM SB 3600 SMART ENERGY INVERTER," available at: https://www.off-grid-europe.com/sma-integrated-storage-system-sb-3600-smart-energy-inverter?gclid=CjwKCAjw5fzrBRASEiwAD2OSV8QTkNn5Es4NLxChBekDTGV1-Qt1HfModDjrFphFK49LY05ftgj1cRoCWhkQAvD_BwE.
- [233] CALTEST Instrumnts Ltd. "ZSAC Series – AC Loads – Hoecherl & hackl", available at: <https://www.caltest.co.uk/product/zsac-series/>

- [234] NATIONAL INSTRUMENTS. "CompactRIO Systems", available at: <https://www.ni.com/en-gb/shop/compactrio.html>
- [235] smartprocess Ltd, "SMARTRAIL X835-MID DIN Rail Multifunction Power Meter," available at: https://www.smartprocess.co.uk/PDF/Smart-Process_SMARTRAIL-X835-MID_Datasheet.pdf

Appendices

Appendix A - Details of the four houses used in this study

HOUSE_NUM	HOUSE 1	HOUSE 2	HOUSE 3	HOUSE 4
HOUSE_TYPE	SEMI DETACHED	DETACHED	DETACHED	SEMI DETACHED
NUM_RES	2	5	4	3
Central heating	YES	NO	YES	YES
WATER_HEAT	YES	YES	YES	YES
ELEC_SHOWER	NO	YES	YES	YES
ELEC_HEAT	NO	YES	NO	NO
HAVE_Double glazing	1	1	1	0
HAVE_Cavity wall insulation	1	0	0	0
CFL_PERC	100	50	85	100
HALG_BULB	4	14	10	0
FLOODLIGHT	NO	NO	YES	YES
FRIDGE	1	1	2	1
FRIDGE_FREEZER	0	0	1	0
UPR_FREEZER	1	1	0	1
TV_PLASMA	1	2	2	1
COMP	2	3	1	2
ELEC_HOB	0	1	0	0
ELEC_OVEN	1	1	1	1
GAS_HOB	1	0	1	1
GAS_OVEN	0	0	0	0
Microwave	1	1	1	0
KETTLE	1	1	1	1
TOASTER	1	0	1	1
STEAMER	0	0	1	0
DISH_WASH	0	1	1	1
WASHING	1	1	1	1
WASHER_DRYER	0	0	0	0
AIR_CON	0	0	0	0

Appendix B -Load forecasting using Adaptive Neuro-Fuzzy Inference System (ANFIS) technique

I. Introduction

The short-term load forecasting (STLF) techniques used for EMS of the local communities should be characterized by using an adaptive approach -this is due to the nature of the loads in the local community systems, which change over time with the installation of new equipment such as EVs chargers, heating and other devices [223]; adaptive forecasting techniques (compared to non-adaptive techniques), can produce better results if the system changes [224].

AI techniques have received increasing attention as a powerful computational tool for STLF forecasting since 1980. These techniques cover ANN, Adaptive ANFIS, Fuzzy Systems, Evolutionary Computation, and Swarm Intelligence [225]. AI techniques are able to solve nonlinear problems, and complex relationships, and can be used for adaptive control and decision making under uncertainty [226]. In this research, the ANFIS forecasting technique has been used to forecast the next day load demand for L-FP forecasting method [172].

ANFIS is a type of ANN that is based on the Takagi–Sugeno fuzzy inference system [227]. ANFIS is an adaptive network, which allows the implementation of a neural network topology together with fuzzy logic and utilizes the characteristics of both methods. This method uses a combination of least squares estimation and backpropagation for parameter estimation for the membership functions [224], and can deal with linear, nonlinear and complex problems [228].

II. Structure of ANFIS

ANFIS is used for STLF as a method for tuning an existing rule base of a fuzzy system, with a learning algorithm based on a collection of training data found in an ANN. As the parameters are of a fuzzy system rather than a conventional ANN, the ANFIS is trained faster and more accurately than conventional ANNs. An ANFIS corresponding to a Sugeno type fuzzy model with two inputs and a single output is shown in Figure B. [228]. It is clear from the figure that the ANFIS structure is multi-layer. The function of each layer is described in Table B.

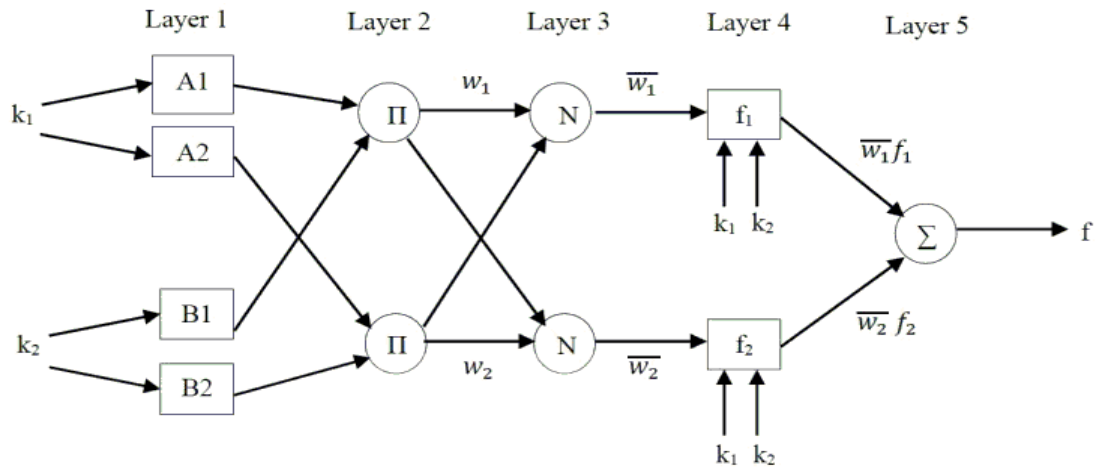


Fig. B-1. Adaptive Neuro-Fuzzy Inference system structure

The common rule set of two fuzzy ‘if-then’ rules used for a Sugeno fuzzy model is as follows:

Rule 1: If k_1 is A_1 and k_2 is B_1 , then $F_1 = p_1 k_1 + q_1 k_2 + r_1$

Rule 2: If k_1 is A_2 and k_2 is B_2 , then $F_2 = p_2 k_1 + q_2 k_2 + r_2$

Table B-1. ANFIS layer description

Layer	Known as	Function
Layer 1	The fuzzification layer	The input data are fuzzified and neuron values are represented by parameterized membership functions.
Layer 2	The rule layer	Each node in this layer represents the number of rules generated by the Sugeno fuzzy logic inference system.
Layer 3	The normalization layer	Each node accepts all nodes coming from the rule layer as input values and calculates the normalized value of each rule.
Layer 4	The defuzzification layer	The weighted result values of a given rule are calculated at each node. The consequent part is obtained via linear regression or multiplication between the normalized level and the output of the respective rule.
Layer 5	The summing layer	The real value of the ANFIS is produced by an algebraic sum over all rules outputs.

III. Load forecasting using ANFIS

The historical load profiles used for ANFIS forecasting are for the period of one year and of 15 minute resolution. The consumption load profile of the CES has been created by adding the actual measurements of the load demand of the houses, see chapter 3. The weather data used (i.e. temperature and humidity) is actual data obtained from the SODA site for solar energy services [229].

The ANFIS model used for load forecasting consists of seven input variables:

- Time of the day (i.e. every quarter hour).
- Weather data (temperature °C).
- Weather data (humidity %).
- Day of the year: used for differentiating between different seasons.
- Type of the day: working day, weekend or a public holiday.

- Previous day same time load (kW).
- Previous week same day same time load (kW).

Each input variable has three membership functions. The membership functions are defined by training the ANFIS using a large set of data for historical load profiles. Also, 10 epochs are used for each training phase. The ANFIS model is trained with 11 months of data, and tested for one month of data. All the data have a 15 minute sample time.

IV. Results

The sharpness of the load profiles for small communities, in addition to using a short sample time to reflect the actual load changes that occur, make STLF for this type of load a great challenge. Fig B-2.a shows both the forecasted and the actual load for one month. Fig B-2.b shows the difference between the actual and the forecasted load demand. The average MAPE of the forecasted loads over this month is 8.9 %. this value is acceptable for this type of kW load profile (for local communities), compared to MAPE values obtained when forecasting MW loads for large grids [230].

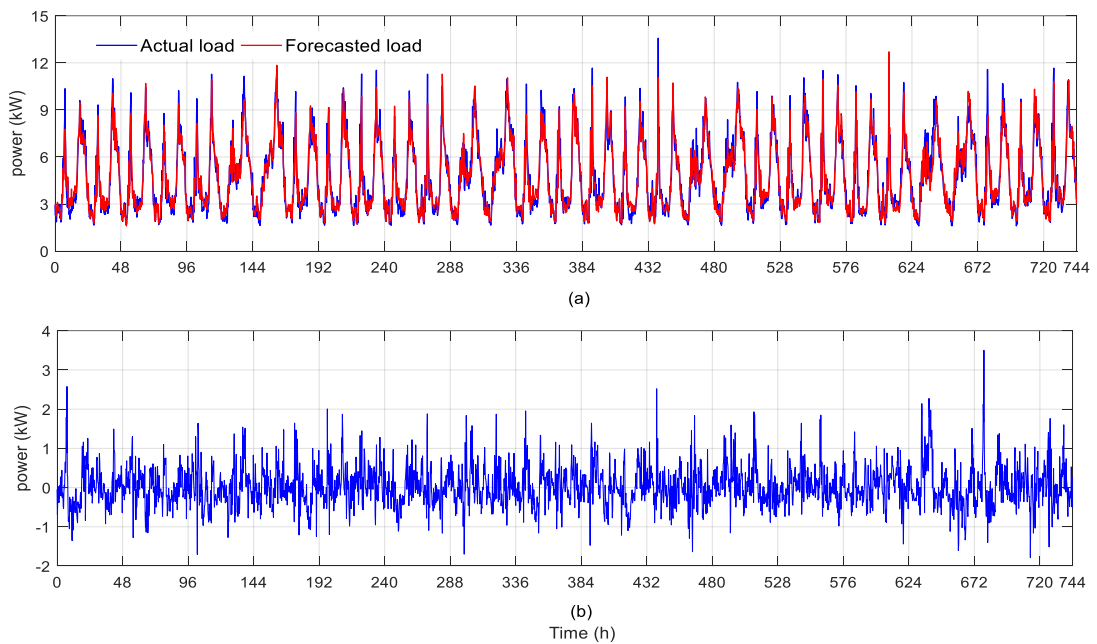


Fig B-2. (a) The actual and the forecasted load demand for one month, (b) the difference between the actual and the forecasted load demand

Fig B-3. shows both the forecasted and the actual load demand for a working day using a sample time of 15 minutes. The MAPE for the forecasted load is 8.03 %. The results obtained demonstrate the capability of the proposed ANFIS in achieving good results for STLF for local communities.

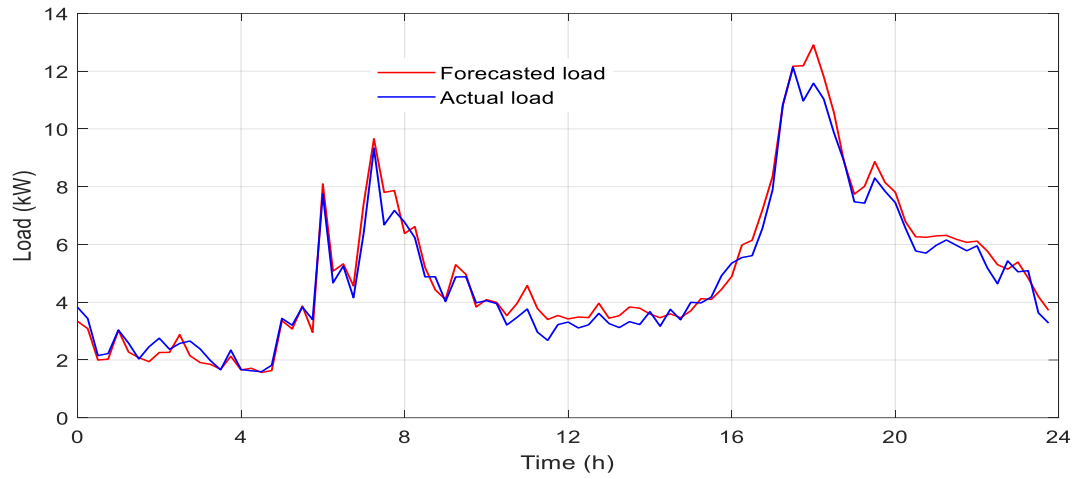


Fig B-3. The forecasted and the actual load demand for a day ahead using a sample time of 15 minutes

Appendix C- Experimental Verification for the Hierarchical Two-Layer HEMS

The hierarchical two-layer HEMS (control mode 1) is tested experimentally for one day at the University of Nottingham's FlexElec Laboratory, using the "Smart Home Rig" (SHR) shown in shown in Fig. C1 and Fig. C2.

I. Laboratory-Based Smart Home Rig Architecture

This SHR consists of various electrical equipment including:

- HBSS: consists of a 6.4 kWh BYD lithium-ion battery pack, and a 2.5 kW SMA bidirectional power converter. The efficiency of the battery and the power converter are 95.3% and 96.7% respectively [231], [232].
- 1.4 kWp PV panels connected to a 3.68 kW SMA power converter and connected to the SHR switchboard [233].
- 5.6 kW ZSAC Electronic AC load emulator [234], which received the digital daily load demand profile from LabVIEW software, and converted it to actual current absorbed from one of the appliance connection sockets in the SHR. A NI compact Rio controller [235] and LabVIEW software were used to move the digital load profiles from the database to the Electronic AC load emulator as a control signal.
- A 3 phase smart meter was used to measure the power at the grid connection point and the PV generation power [236].
- A Raspberry Pi used the Modbus protocol to transmit the measured data from the smart meter to the HEMS, and to transmit the measured SOC of the battery to the HEMS regularly. Also, the Raspberry Pi was used to transmit the optimal battery power settings to the battery power converter.

- A PC: Core i3-7100 CPU, 3.91 GHz was used to run MATLAB software, which in turn runs the HEMS and performs the MILP optimization process.

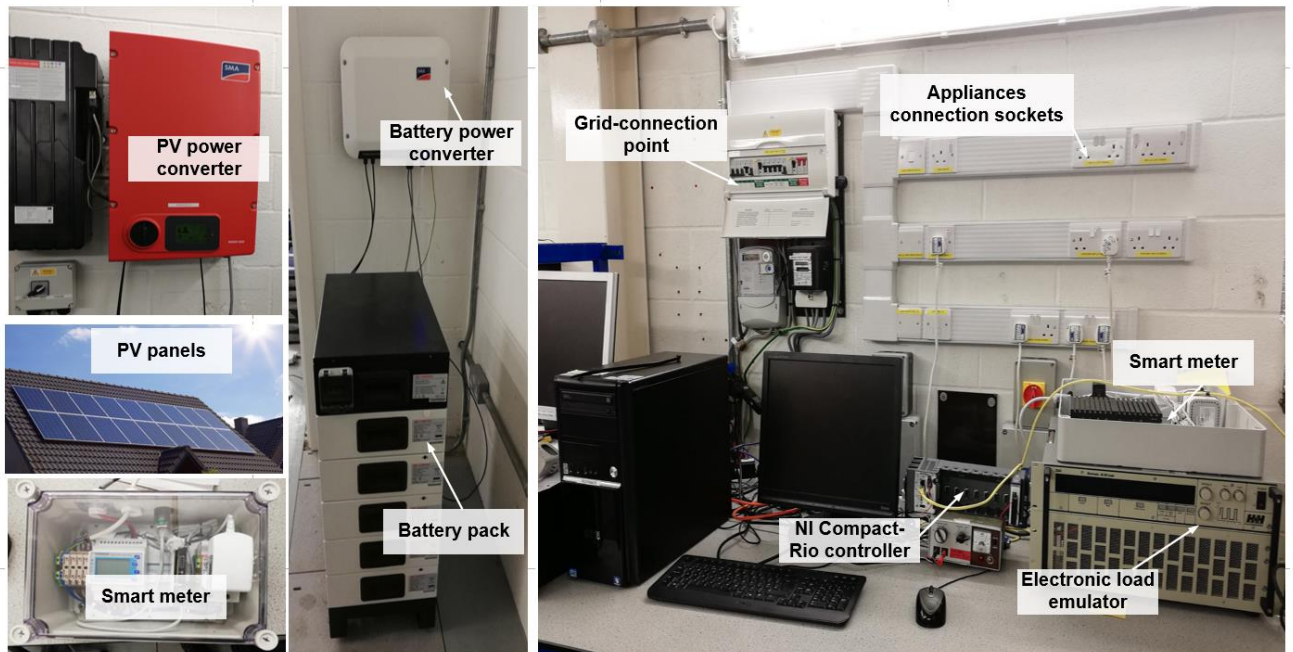


Fig. C1. Architecture of the SHR, used in the experiment, at the FlexElec Laboratory, University of Nottingham.

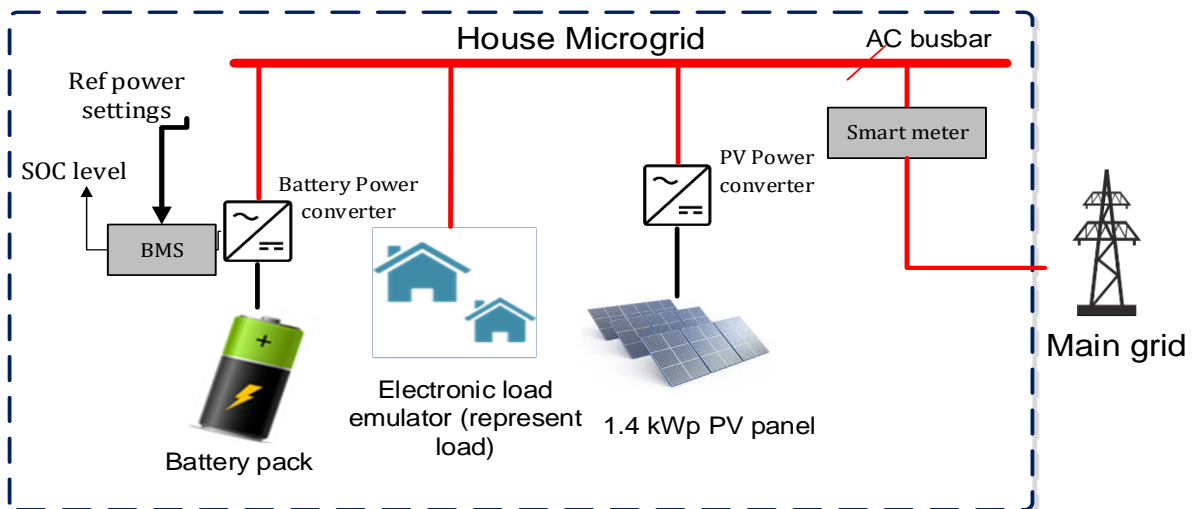


Fig. C2. Connection diagram of the SHR at the FlexElec Laboratory, University of Nottingham.

II. Test procedure

The following procedure has been followed to perform this experiment:

- A. **The upper layer (MPC layer)**, every sample time (i.e. 15 minute in this case), (1) asks for the forecasted household consumption profile, as well as the forecasted PV generation profile for the next 24 hours from the historical data, (2) the values of the actual SOC level of the HBSS are measured from the battery power converter, (3) the MILP optimization process is performed using a MATLAB script, (3) the stored energy profile for the next 24 hours ' $E_{MPC}(t)$ ' (i.e. the profile uses 15 minute sample time), required for optimal battery operation, is obtained and passed to the RTC layer; only the stored energy profile obtained for the next sample time $(t+1)$ is sent to the RTC layer, (4) the previous steps are repeated every 15 minutes.
- B. **The lower layer (RTC layer)**: (1) receives the stored energy profile for the next 24 hours ' $E_{MPC}(t)$ ' from the MPC layer, (2) receives the measured SOC of the battery and the measured power at the GCP and uses the rule-based control algorithm (shown in Fig. 4. 16.) to determine the optimal power settings of the HBSS in real-time, (3) the optimal power settings of the HBSS in real-time are sent directly to the battery power converter. This layer is executed in real-time every one minute.

III. Results

The results obtained from this test are shown in Fig C3. It can be seen from this figure that the two-layer HEMS, using control mode 1, managed to control the HBSS in a proper way. Using the two-layer HEMS minimizes the power spikes that result from forecasting uncertainties, as shown in Fig C3.b. Eliminating power spikes minimizes the energy wastage and the overall energy costs. The reason for the spike, i.e. the 2.4 kW spike at nearly 20:00 shown in Fig C3.b., is that the load at that time was 3.3 kW (see Fig C3.d.), and the HBSS

discharges using the maximum available power (2.5 kW) (see Fig C3.a.), the remaining power is drawn from the main electricity grid.

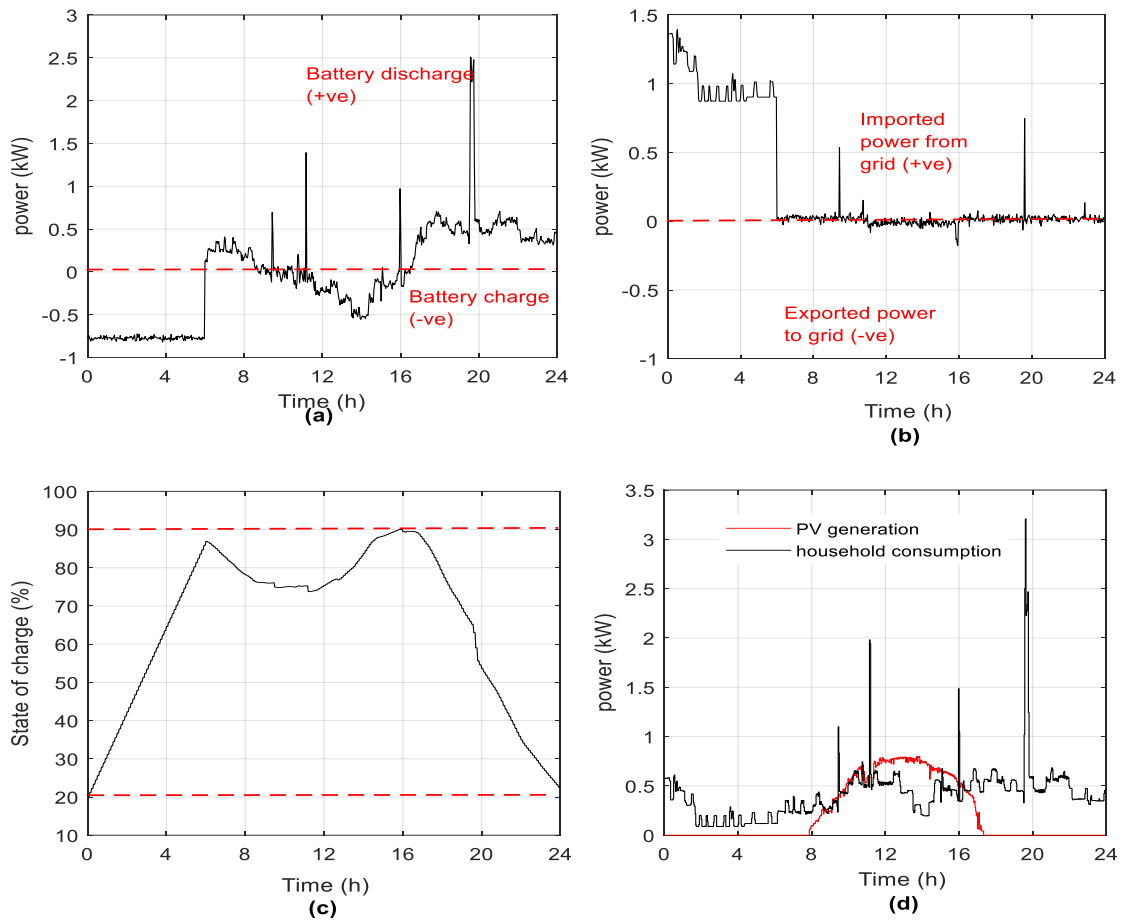


Fig. C3. Emulated House results using the two-layer HEMS (control mode 1) for one day

(a) the optimal power settings of the HBSS (a positive value means that the HBSS is discharging, while a negative value means that the HBSS is charging), (b) actual power measured at the grid connection point (a positive value means the house is importing power from the utility, and a negative value means exporting), (c) the actual measured state of charge (SOC) of the HBSS, (d) the actual household power demand and PV generation.

Appendix D- The daily operation of the four houses using the distributed CEMS

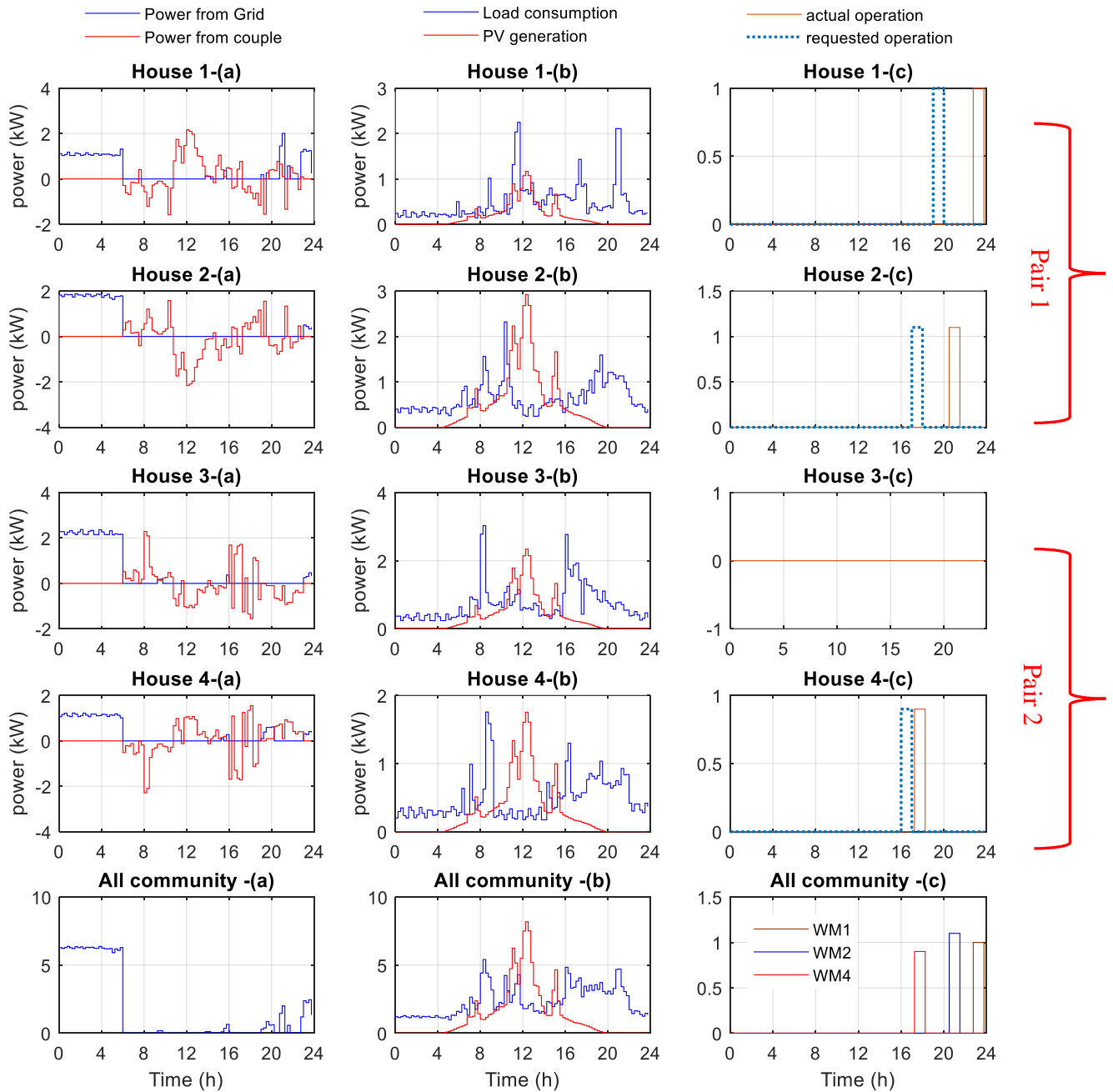


Fig. D. The optimal settings obtained from the Distributed CEMS for the operation of the community system for one day, where (a) the reference values for the power that should be imported from the main electricity grid by each house (i.e. blue settings), and reference values for the power that should be shared between each paired houses within the community (i.e. red settings), the positive value means the house is importing power from the pair house, while a negative value means the house is exporting power to the paired house, (b) the daily household energy consumption and PV generation profiles for each house, and (c) the shiftable appliance scheduling for each house.

Appendix E- The daily operation of the four houses using centralized CEMS

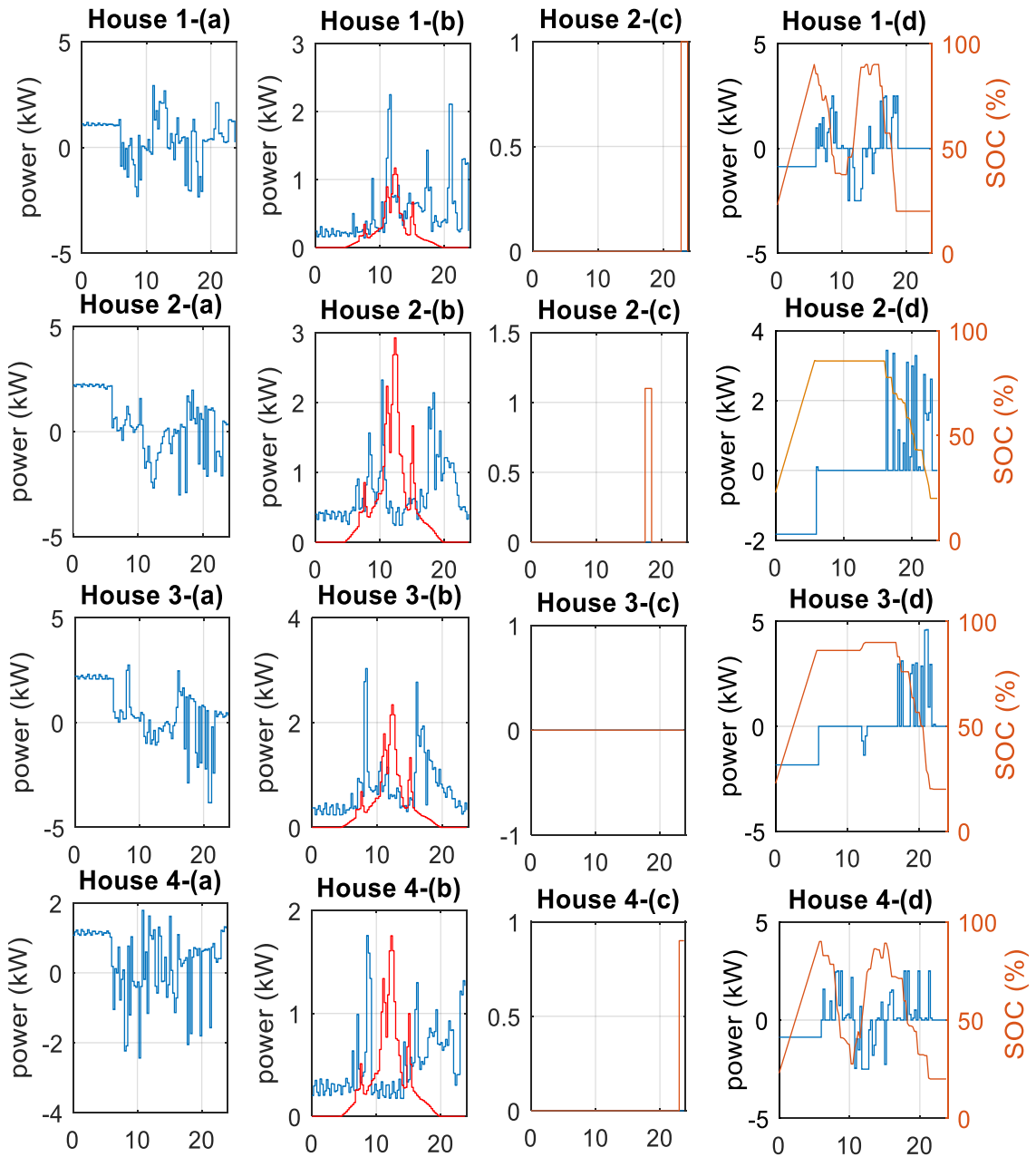
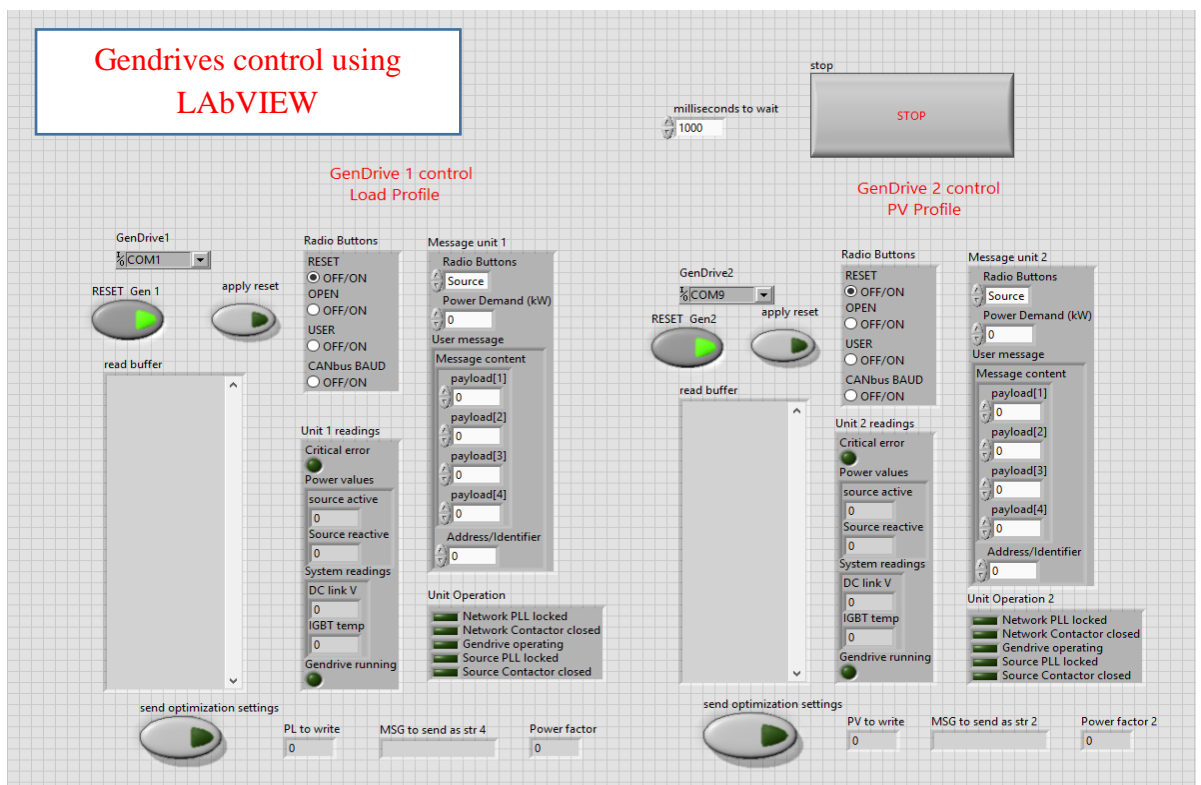
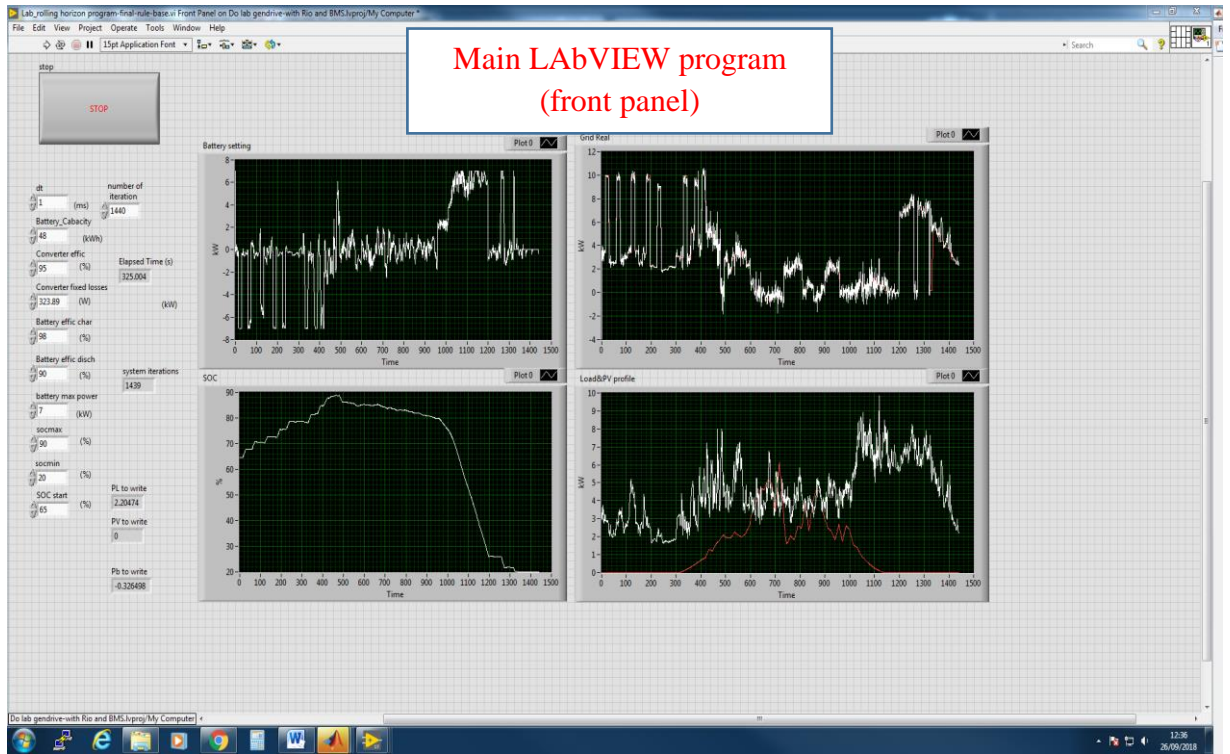
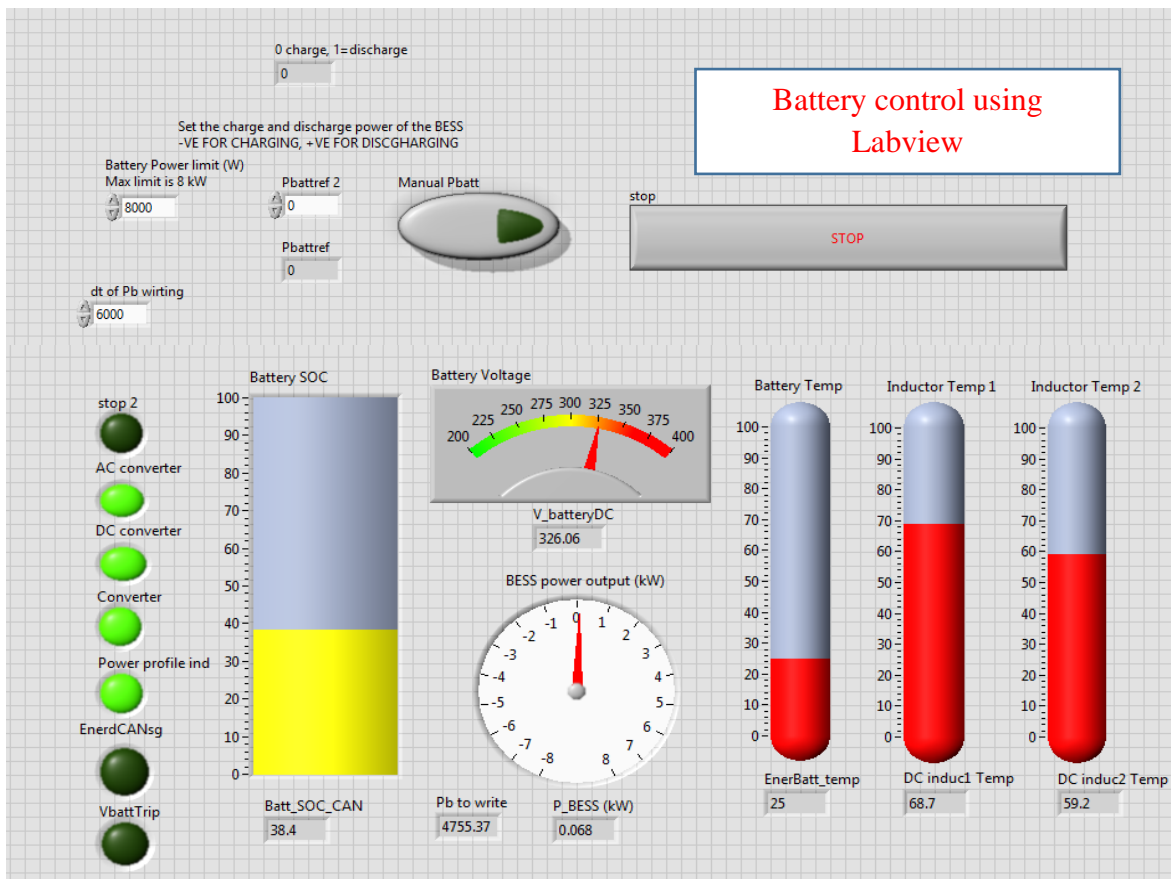


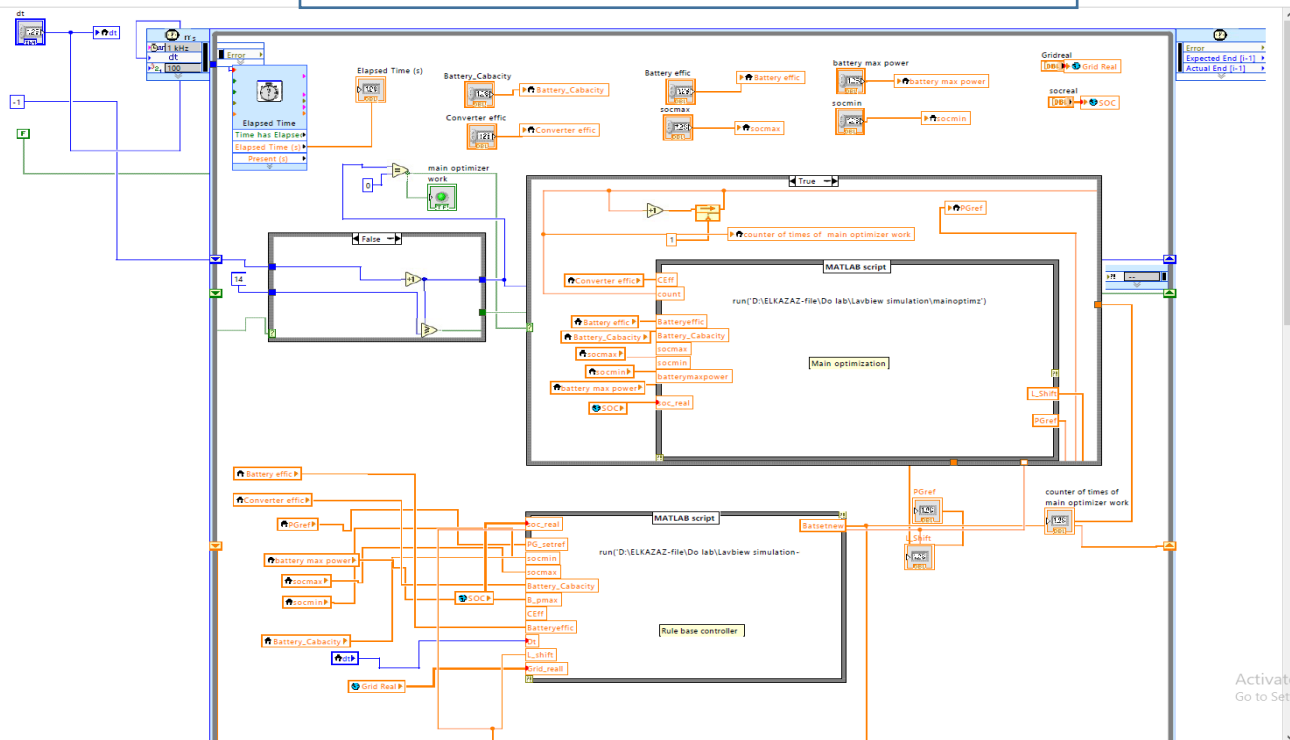
Fig. E. The optimal settings obtained from the centralized CEMS for the operation of the community system for one day, where (a) represents the reference values for the power that should be shared between the house and the community; a positive value means the house is absorbing power from the community, while a negative value means injecting, (b) represents the daily household consumption and PV generation profiles of each house, (c) represents the shiftable appliance scheduling for each house, and (d) represents the operation of the HBSS (i.e. the daily power profile (blue profile), and the daily SOC profile (red profile)).

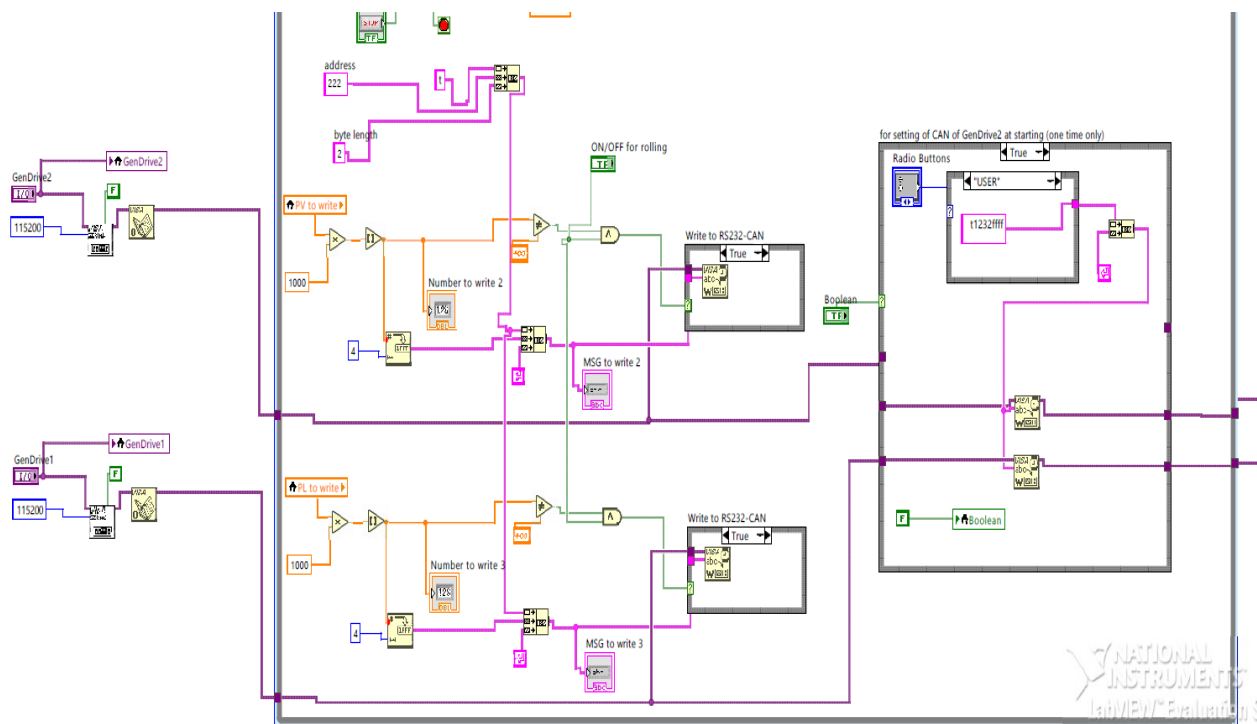
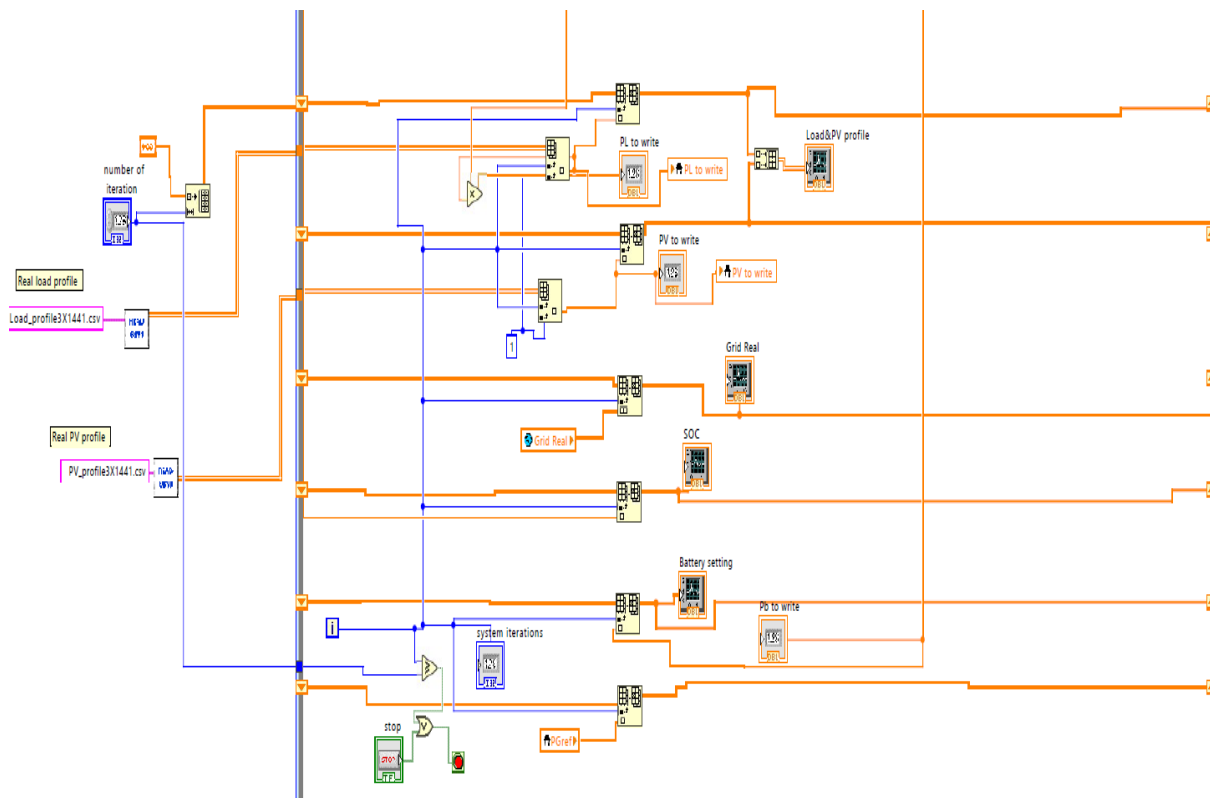
Appendix F- The LABVIEW program used in the experiment test of the Hierarchical centralized community energy management system





LABVIEW block diagram of Hierarchical centralized community energy management system





NATIONAL
INSTRUMENTS
LabVIEW™ Evaluation Kit

Appendix G - Calculations used to obtain the cumulative cash flow results from providing Community Bill Management service

year	standing charge	OP. cost with CBESS ¹	Maintenance cost (Y_{main_cost}) ²	OP. cost without CBESS ³	Percentage reduction in OP. cost ⁴	Total income ⁵	Cashflow ⁶	PV self-consumption
0						-£378,960	-£378,960	
1	£80	£33,872	£1,705	£64,562	47.5%	£28,985	-£349,975	93.5%
2	£84	£36,074	£1,739	£67,790	46.8%	£29,977	-£319,998	92.9%
3	£88	£38,418	£1,774	£71,180	46.0%	£30,987	-£289,011	92.4%
4	£93	£40,916	£1,810	£74,739	45.3%	£32,013	-£256,998	91.8%
5	£97	£43,575	£1,846	£78,476	44.5%	£33,054	-£223,944	91.3%
6	£102	£46,408	£1,883	£82,399	43.7%	£34,109	-£189,835	90.7%
7	£107	£49,424	£1,920	£86,519	42.9%	£35,175	-£154,660	90.2%
8	£113	£52,637	£1,959	£90,845	42.1%	£36,250	-£118,410	89.6%
9	£118	£56,058	£1,998	£95,387	41.2%	£37,331	-£81,079	89.1%
10	£124	£59,660	£2,038	£100,157	40.4%	£38,459	-£42,620	88.6%
11	£131	£63,562	£2,079	£105,165	39.6%	£39,524	-£3,096	88.0%
12	£137	£67,719	£2,120	£110,423	38.7%	£40,584	£37,488	87.5%
13	£144	£72,148	£2,163	£115,944	37.8%	£41,634	£79,122	87.0%
14	£151	£76,866	£2,206	£121,741	36.9%	£42,669	£121,791	86.5%
15	£159	£81,893	£2,250	£127,828	35.9%	£43,685	£165,476	85.9%
16	£167	£87,249	£2,295	£134,220	35.0%	£44,676	£210,152	85.4%
17	£175	£92,955	£2,341	£140,931	34.0%	£45,635	£255,787	84.9%
18	£184	£99,034	£2,388	£147,977	33.1%	£46,555	£302,342	84.4%
19	£193	£105,511	£2,436	£155,376	32.1%	£47,430	£349,772	83.9%
20	£203	£112,550	£2,484	£163,145	31.0%	£48,111	£397,882	83.5%

¹ 'OP. cost with CBESS' is calculated using the annual community load profile, the annual PV generation profile, the TOU tariff and the other operating terms as shown in equation (7.3).

² Annual 'Maintenance cost' is calculated using equation (7.6).

³ 'OP. cost without CBESS' is calculated using the annual community load profile and the annual PV generation profile, using a flat purchasing tariff of 13.15 pence/kWh and an export tariff of 4.85 pence/kWh for selling the surplus PV generation to the main electricity grid.

⁴ 'Percentage reduction in OP. cost' is the annual reduction in the total operating cost of the community after using the CBESS and providing CEBM services, compared to the case without using the CBESS.

⁵ 'Total income' is the difference between the annual operating costs of the community before and after using the CBESS.

⁶ 'Cashflow' is the cumulative cash and asset values resulting from the investment in the CBESS; this value is calculated by adding the total income each year to the initial capital cost of the CBESS.

Appendix H- Calculations used to obtain the cumulative cash flow results from providing Capacity Market service

year	Maintenance cost	standing charge	Night ¹ charging cost	Income ² from the discharged energy to ESCO	Income ³ from CM contract fee	Annual ⁴ total income	Aggregator cost ⁵	Annual ⁶ total revenue	Cash ⁷ flow
0								-£378,960	-£378,960
1	£1,705	£80	£3,643	£27,265	£4,200	£26,036	£5,207	£20,829	-£358,131
2	£1,739	£84	£3,691	£28,342	£4,410	£27,237	£5,447	£21,790	-£336,341
3	£1,774	£88	£3,735	£29,458	£4,631	£28,491	£5,698	£22,793	-£313,548
4	£1,810	£93	£3,774	£30,615	£4,862	£29,801	£5,960	£23,841	-£289,708
5	£1,846	£97	£3,808	£31,815	£5,105	£31,169	£6,234	£24,935	-£264,773
6	£1,883	£102	£3,836	£33,058	£5,360	£32,597	£6,519	£26,078	-£238,695
7	£1,920	£107	£3,856	£34,345	£5,628	£34,089	£6,818	£27,271	-£211,424
8	£1,959	£113	£3,870	£35,679	£5,910	£35,647	£7,129	£28,517	-£182,906
9	£1,998	£118	£3,875	£37,060	£6,205	£37,274	£7,455	£29,819	-£153,088
10	£2,038	£124	£3,871	£38,490	£6,516	£38,972	£7,794	£31,178	-£121,910
11	£2,079	£131	£3,857	£39,970	£6,841	£40,745	£8,149	£32,596	-£89,314
12	£2,120	£137	£3,832	£41,502	£7,183	£42,597	£8,519	£34,077	-£55,236
13	£2,163	£144	£3,794	£43,088	£7,543	£44,529	£8,906	£35,624	-£19,613
14	£2,206	£151	£3,744	£44,728	£7,920	£46,547	£9,309	£37,238	£17,625
15	£2,250	£159	£3,678	£46,425	£8,316	£48,653	£9,731	£38,923	£56,547
16	£2,295	£167	£3,597	£48,179	£8,731	£50,852	£10,170	£40,681	£97,229
17	£2,341	£175	£3,499	£49,993	£9,168	£53,146	£10,629	£42,517	£139,746
18	£2,388	£184	£3,381	£51,868	£9,626	£55,541	£11,108	£44,433	£184,178
19	£2,436	£193	£3,244	£53,805	£10,108	£58,040	£11,608	£46,432	£230,611
20	£2,484	£203	£3,084	£55,806	£10,613	£60,649	£12,130	£48,519	£279,130

¹ 'Night charging cost': the cost of the energy used to charge the battery during the night. The battery is charged during the night up to a certain percentage to keep spare capacity for the battery to be charged with free PV energy during the day. The electricity used during night time charging is purchased at 4.99 pence /kWh.

² 'Income from the discharged energy to ESCO': the income from selling electricity to the ESCO at 11.99 pence/kWh. It is assumed that the battery discharges the rated energy when instructed to deliver energy to the ESCO.

³ 'Income from CM contract fee': this value is calculated using the CM contract fees available in Table 7.1. and the rated CBESS power of 250 kW.

⁴ 'Total income' is the net income from the participation of the CBESS in CM services. This value is calculated using the income from the discharged energy to the ESCO, the income from CM contract fees and the payments for the night time energy supply, the standing charge and the maintenance costs.

⁵ 'Aggregator cost': it is assumed that 20% of annual total income goes to the ESCO for their project management services.

⁶ 'Total revenue': is the net revenue from the participation of the CBESS in CM services. This value is calculated using the 'annual total income' minus the annual 'aggregator cost'.

⁷ 'Cashflow': is the cumulative cash and asset values resulting from the investment in the CBESS; this value is calculated by adding the total income each year to the initial capital cost of the CBESS.

Appendix I- Calculations used to obtain the cumulative cash flow results from providing Dynamic Firm Frequency Response service

year	Maintenance cost	standing charge	DFFR ¹ availability income	Annual ² total income	Aggregator ³ cost	Annual ⁴ total revenue	Cash ⁵ flow
0						-£378,960	-£378,960
1	£1,705	£80	£16,644	£14,858	£2,972	£11,887	-£367,073
2	£1,739	£84	£17,476	£15,653	£3,131	£12,522	-£354,551
3	£1,774	£88	£18,350	£16,487	£3,297	£13,190	-£341,361
4	£1,810	£93	£19,268	£17,365	£3,473	£13,892	-£327,469
5	£1,846	£97	£20,231	£18,288	£3,658	£14,630	-£312,839
6	£1,883	£102	£21,242	£19,257	£3,851	£15,406	-£297,433
7	£1,920	£107	£22,305	£20,277	£4,055	£16,221	-£281,212
8	£1,959	£113	£23,420	£21,348	£4,270	£17,078	-£264,134
9	£1,998	£118	£24,591	£22,474	£4,495	£17,979	-£246,154
10	£2,038	£124	£25,820	£23,658	£4,732	£18,926	-£227,228
11	£2,079	£131	£27,111	£24,902	£4,980	£19,922	-£207,306
12	£2,120	£137	£28,467	£26,209	£5,242	£20,968	-£186,339
13	£2,163	£144	£29,890	£27,583	£5,517	£22,067	-£164,272
14	£2,206	£151	£31,385	£29,028	£5,806	£23,222	-£141,050
15	£2,250	£159	£32,954	£30,545	£6,109	£24,436	-£116,614
16	£2,295	£167	£34,602	£32,140	£6,428	£25,712	-£90,902
17	£2,341	£175	£36,332	£33,816	£6,763	£27,053	-£63,850
18	£2,388	£184	£38,148	£35,577	£7,115	£28,461	-£35,388
19	£2,436	£193	£40,056	£37,427	£7,485	£29,942	-£5,447
20	£2,484	£203	£42,059	£39,372	£7,874	£31,497	£26,051

¹ 'DFFR availability income': this value is calculated by multiplying the DFFR availability fees available in Table 7.1. by the availability period (i.e. 365 day * 24 hour) and by the CBESS guaranteed response (0.95).

² 'Annual total income' is the net income from the participation of the CBESS in DFFR services. This value is calculated using the availability income minus the payment for the standing charge and maintenance costs.

³ 'Aggregator cost': it is assumed that 20% of annual total income is paid to the ESCO for their project management services.

⁴ 'Annual total revenue': is the net revenue from the CBESS participation in DFFR services. This value is calculated using the 'annual total income' minus the annual 'aggregator cost'.

⁵ 'Cashflow': is the cumulative cash and asset values results from the investment in the CBESS; this value is calculated by adding the total income each year to the initial capital cost of the CBESS.